AD-A226 750

DTIC
S ELECTE D
SEP 27 1990
D CO

Twelfth
NASTRAN®
Users'
Colloquium

Proceedings of a colloquium held in
Orlando, Florida
May 7-11, 1984

NASA SCIENTIFIC AND TECHNICAL INFORMATION FACILITY

P.O. BOX 8757 BALTIMORE WASHINGTON INTERNATIONAL AIRPORT MD. 21240, (301) 859-5300

ATTN: JOYCECHIRAS(OKPERPATT)
DATE OF REQUEST: 09/19/90
USER ID: 02672
ORDER CONTROL NUMBER: 900919103040
USER SECURITY LEVEL: SECRET RESTRICTED

ENCLOSED IS YOUR ORDER FOR 0001 STOCK COPY   **OF NASA ACCESSION**
NUMBER N84-32864
TITLE: Twelfth NASTRAN (R) Users' Colloquium
REPORT NUMBER: NASA-CP-2328

DOCUMENT CLASSIFICATION: UNCLASSIFIED
DISTRIBUTION LIMITATION STATEMENT: UNLIMITED

QUESTIONS CONCERNING THIS ORDER SHOULD BE DIRECTED TO DOCUMENT REQUEST SERVICES, NASA STI FACILITY (301) 621-0147.
PLEASE INCLUDE YOUR ORDER CONTROL NUMBER WITH YOUR INQUIRY.

02672-900919103040
DEPT OF DEFENSE
DEFENSE TECHNICAL INFORMATION CENTER
ATTN: DTIC-FDAC
CAMERON STATION BLDG 5
ALEXANDRIA VA   22304

02672-900919103040
DEPT OF DEFENSE
DEFENSE TECHNICAL INFORMATION CENTER
ATTN: DTIC-FDAC
CAMERON STATION BLDG 5
ALEXANDRIA VA   22304

Twelfth NASTRAN® Users' Colloquium

Proceedings of a colloquium held in
Orlando, Florida
May 7-11, 1984

NASA

National Aeronautics
and Space Administration

**Scientific and Technical
Information Branch**

1984

FOREWORD

NASTRAN® (NASA STRUCTURAL ANALYSIS) is a large, comprehensive, nonproprietary, general purpose finite element computer code for structural analysis which was developed under NASA sponsorship and became available to the public in late 1970. It can be obtained through COSMIC (Computer Software Management and Information Center), Athens, Georgia, and is widely used by NASA, other government agencies, and industry.

NASA currently provides continuing maintenance of NASTRAN® through COSMIC. Because of the widespread interest in NASTRAN®, and finite element methods in general, the Twelfth NASTRAN® Users' Colloquium was organized and held at the Harley Hotel, Orlando, Florida, May 7-11, 1984. (Papers from previous colloquia held in 1971, 1972, 1973, 1975, 1977, 1978, 1979, 1980, 1982 and 1983, are published in NASA Technical Memorandums X-2378, X-2637, X-2378, X-2893, X-3278, X-3428, and NASA Conference Publications 2018, 2062, 2131, 2151, 2249 and 2284.) The Twelfth Colloquium provides some comprehensive general papers on the application of finite element methods in engineering, comparisons with other approaches, unique applications, pre- and post-processing or auxiliary programs, and new methods of analysis with NASTRAN®.

Individuals actively engaged in the use of finite elements or NASTRAN® were invited to prepare papers for presentation at the Colloquium. These papers are included in this volume. No editorial review was provided by NASA or COSMIC, however, detailed instructions were provided each author to achieve reasonably consistent paper format and content. The opinions and data presented are the sole responsibility of the authors and their respective organizations.

CONTENTS.

COSMIC/NASTRAN FREE-FIELD INPUT

by

GORDON C. CHAN
Sperry Systems Management
Huntsville, Alabama

ABSTRACT

This paper serves as a user's guide to the COSMIC/NASTRAN free-field input for the Bulk Data section of the NASTRAN program. The free-field input is designed to be user-friendly and under no circumstances snould the user be forced out of the computer system due to input errors. It is easy to use, with only a few simple rules to follow. A stand-alone version of the COSMIC/NASTRAN free-field input is also available. The use of free-field input is illustrated by a number of examples.

INTRODUCTION

With the advance of real-time terminal usage in computer applications, the need for COSMIC/NASTRAN free-field input for the Bulk Data section is long overdue. Beginning in the April '84 COSMIC/NASTRAN release, free-field input becomes available in all four machines (CDC, IBM, UNIVAC, and VAX). The relaxation of the rigid 8-column input format will not only benefit all real-time terminal users, but also the batch-job users will find it helpful in reducing possible fatal errors due to mis-punching data in the wrong columns. In addition, another long sought feature is also available – that is, the ability to duplicate similar input cards with minor changes in one or more selected fields automatically. The COSMIC/NASTRAN free-field input offers several options that can be invoked at any time during a free-field input session – options to make terminal keyboard data entry easier, to allow a user to execute NASTRAN LINK 1 only, and to punch out generated card images.

1

This work was originally developed for the Sperry version of NAS-TRAN. It is now available to the COSMIC/NASTRAN with improved capabilities.

FREE-FIELD CAPABILITY

The free-field capability is best understood by stating the following rules and program features:

1. Free-field input is available only after a 'BEGIN BULK' card is read, and is disabled automatically when 'ENDDATA' is entered.

2. Free-field input is activated by one or more commas (,) or an equal sign (=) in the first 10 columns of the input card.

3. Only small-field cards can be created.

4. Data items must be separated with a comma, one or more blanks, or the combination of a comma and blanks.

5. Duplication of fields from the preceding card is accomplished by coding an equal sign (=) in the appropriate field.

6. Two equal signs (==) indicate duplication of all the trailing fields from the preceding card.

7. Increment of a value from the previous input card is indicated by coding *(i), where i is the value of the increment (integer or floating point number) and * is the increment character. This feature is field dependent in the input card.

8. Increment of a value from the previous input card to an ending value is indicated by coding %(E), where E is the ending value (integer or floating point number) in the last card to be generated, and % is the ending character. This feature is also field dependent.

9. Repeated duplication is indicated by coding =(N), where N is the number of card images to be generated using the value of the increment on the preceding card (or current card) by *(i), or the computed incremental value on the preceding card by %(E). The last generated card is also displayed on the terminal screen if the prompt option (see 17 below) has been turned on.

10. A field index and value can be coded by n)X, where n is the field index and X the value.

11. The symbol)+ is equivalent to 10)+, where 10 is the tenth field of the input card, which is normally the continuation ID field.

12. A right bracket) in column 1 indicates the duplication of the tenth field of the preceding card into the first field of the current card being generated.

13. Continuation ID (in field 1 or 10) is automatically increased (by 1) in the repeated-duplication operation. The ID must be in the form of +A-X, where A is one or more alphanumeric characters preceded by a plus, and followed by a minus sign. X is an unsigned integer to be used as the initial value for increment. A maximum of eight characters (including signs) is allowed, with no embedded blank(s). An '=(1)' in the first input field is needed for single card duplication.

14. Data in field 10, not in the form of +A-X, is replaced by blanks during repeated-duplication operation.

15. The ECHO card (described in the Case Control section of the Users' Manual) can be input (or re-defined) at any time during the free-field input session.

16. A new option, 'ECHO=LINK1', can be entered at any time to alter the NASTRAN execution sequence to that of 'link-one-only', and to skip BANDIT grid-point resequencing.

17. A prompt command, PROMPT=ON, PROMPT=OFF, PROMPT=YES, can be entered any time during the free-field input session so that the computer will display (or not display) on the terminal screen a prompt symbol (either a '>' or 'ENTER:') when it is ready to receive input data. The PROMPT=YES option will also display the generated card image on screen in addition to the prompt symbol.

18. Floating-point numbers in the forms of 1.23E+04, 1.23+4, or 12300. are acceptable.

19. Both upper-case and lower-case letters are acceptable. (NASTRAN, not in free-field input mode, accepts only upper-case input cards. If lower-case letters are used in the Executive and the Case Control sections of NASTRAN, the first 8 columns of an input card must contain at least one lower-case letter, that would trigger the free-field routine to convert all lower-case letters in the current input card to upper-case automatically. This requirement is not needed in the Bulk Data input section).

20. Both BCD and EBCDIC character sets are acceptable. This is required for some EBCDIC machines (e.g. IBM) with BCD input cards.

21. The dollar sign ($) can be used freely as described in NASTRAN Users' Manual.

22. Embedded blank(s) are not allowed in all double-character free-field input commands such as: =(, *(, %(,)+, and ==.

23. A stand-alone version of NASTRAN free-field input is available to the user by executing NASTRAN LINKFF.

24. Two additional commands are available only in the stand-alone version. They are:

(a) SCALE/8 or SCALE/10 – to display a scale based on 8-column format, or 10-column format, on screen to aid input spacing.

(b) CANCEL=n – to cancel n previously generated cards.

25. The ECHO command is not available in the stand-alone version.

26. The punch option and catalog file (to save generated card images) are set at the beginning of the stand-alone version.

27. A 'NASTRAN TITLEOPT=-2' card is recommended to be the very first line of input for all terminal users executing NASTRAN LINK1 (not the stand-alone version of LINKFF). It suppresses the printout of the NASTRAN title pages on screen. This card is required for UNIVAC terminal users executing LINK1, which also reassigns the alternate print file (the log-message file) to avoid system crashing.

The following examples illustrate the use of free-field input.

Example 1.

```
GRID,  2,  3,   1.0  2.0,,  4,316
=,   *(1),  =,  *(.2),  == $
=(3)
```


The above free-field cards will generate the following bulk data cards in NASTRAN 8-column-field format:

1	2	3	4	5	6	7	8
GRID	2	3	1.0	2.0		4	316
GRID	3	3	1.2	2.0		4	316
GRID	4	3	1.4	2.0		4	316
GRID	5	3	1.6	2.0		4	316
GRID	6	3	1.8	2.0		4	316

Example 2:

```
grid,2,3,1.0,2.0,,4,316
=(4),*(1),=,%(1.8),==
```


The above cards will generate the same bulk data cards as in Example 1.

Example 3:

```
Grid, 2 3 1.0 2.0, 7) 4,  316
```

This example will generate the same first card as in Example 1.

Example 4:

```
Tabled3,62, 126.9, 30.0   10)+abc
),  1.23e+4,  5.67+8, 1234567.  endt
```

This example will generate the following bulk data cards:

```
   1       2       3       4       5       6       7            10
--------+++++++--------+++++++--------+++++++-------- ~ ~ ~+++++
TABLED3 62      126.9   30.0                                   +ABC
+ABC    1.23E+4 5.67+8  1234567.ENDT
```

Example 5:

```
taBLed3,  62    126.9  30.0    )+aBc
```

This example will generate the same first card as in Example 4.

Example 6:

```
This  is only a te;t
THIS  IS only a test
This, is only a test
```

The different results of the above 3 input lines are shown by the generated card images below:

```
   1       2       3       4       5       6       7
--------+++·++++--------+++++++--------+++++++---------~ ~
THIS  IS ONLY A TEST
THIS  IS only a test
THIS    IS      ONLY   A       TEST
```

Example 7:

```
PBAR, 3, 4, 5.0 , 6.0, )+ABC-1
= , *(1), =, *(2.)   ==
=(2)
+ABC-1, 7.7  8.8  9  )+DEF-22
=(3),==
```

This example will generate the following 8 cards with continuation ID fields automatically increased by 1.

1	2	3	4	5	6	9	10
PBAR	3	4	5.0	6.0			+ABC-1
PBAR	4	4	7.0	6.0			+ABC-2
PBAR	5	4	9.0	6.0			+ABC-3
PBAR	6	4	11.0	6.0			+ABC-4
+ABC-1	7.7	8.8	9				+DEF-22
+ABC-2	7.7	8.8	9				+DEF-23
+ABC-3	7.7	8.8	9				+DEF-24
+ABC-4	7.7	8.8	9				+DEF-25

Example 8:

```
CQUAD2, 101 1       11 12 16 15
CQUAD2, 102 1       12 13 17 16
CQUAD2, 103 1       13 14 18 17
```

This example shows the combination of tree-field and tabulation input. The requirement of 8-columns per field does not apply here.

Example 9:

This example is the actual input cards used in COSMIC/NASTRAN demonstration problem No. 1-6-1b. It gives the same sorted input data as Problem No. 1-6-1a, which uses the regular fixed-field input format.

```
ID      D01061,BNASTRAN
APP     DISP
SOL     1,1
TIME    5
CEND
TITLE = SOLID DISC WITH RADIALLY VARYING THERMAL LOAD
        (FREE-FIELD INPUT)
SUBTITLE = NASTRAN DEMONSTRATION PROBLEM NO. 1-6-1B
LABEL = TRAPEZOIDAL RING ELEMENTS
ECHO  = BOTH
SPC   = 16
TEMPERATURE(LOAD) = 16
    OUTPUT
    SET 1 = 1,3,5,7,9,11,13,15,17,19,21,23,25,26
    DISP  = 1
    ELSTRESS = ALL
BEGIN BULK
CTRAPRG, 1,1,3,4,2,.0,12
=(11), *(1) *(2) *(2) *(2) *(2), ==
GRDSET, 8)2456
GRID,1,,.0
=(3),*(2),,*(.005)
GRID,2,,.0,,.01
=(3),*(2),,*(.005),==
GRID,9,,.02
=(8),*(2),,%(.10)
GRID,10,,.02,,.01
=(8),*(2),,%(.10),==
MAT1,12,1.0+7,,.3,.2587-3,1.0-7,.0
SPC,16,1,13,.0,2,1,.0
TEMP,16,1,100.,2,100.,3,99.75
=,=,4,99.75,5,99.0,6,99.0
=,=,7,97.75,8,97.75,9,96.0
=,=,10,96.0,11,91.0,12,91.0
=,=,13,84.0,14,84.0,15,75.0
=,=,16,75.0,17,64.0,18,64.0
=,=,19,51.0,20,51.0,21,36.0
=,=,22,36.0,23,19.0,24,19.0
=,=,25,.0,26,.0
ENDDATA
```

LIMITATION

Embedded blank(s) are not allowed in field 10, which is sometimes used as a comment field.

The ability to duplicate generated cards repeatedly as shown in Example 1 is indeed only one dimensional. Presently, there is no intention to expand this useful feature into two- or three-dimensional duplications, which would undoubtedly require more complicated input rules and procedures.

CONCLUSION

COSMIC/NASTRAN free-field input is accomplished by replacing one simple subroutine (XREAD) with a new routine that handles free-field input logic. It is designed to be simple to use, and user-friendly. It is intended only to be an instrument to aid NASTRAN bulk data input, and to avoid possible fatal errors. It is not intended to become a mesh-generation and modeling tool.

THE DESIGN AND USAGE OF THE NEW DATA MANAGEMENT FEATURES IN NASTRAN©

P. R. Pamidi and W. K. Brown
RPK Corporation

SUMMARY

Two new data management features have been installed in the April 1984 release of NASTRAN. These two features are the Rigid Format Data Base and the "READFILE" capability. The Rigid Format Data Base is stored on external files in card-image format and can be easily maintained and expanded by the use of standard text editors. This data base provides the user and the NASTRAN maintenance contractor with an easy means for making changes to a Rigid Format or for generating new Rigid Formats without unnecessary compilations and link editing of NASTRAN. Each Rigid Format entry in the data base contains the Direct Matrix Abstraction Program (DMAP), along with the associated restart, DMAP sequence subset and substructure control flags. NASTRAN reads a specific entry in the data base directly in every NASTRAN run and performs the necessary transformations to allow the DMAP to be processed and compiled by the NASTRAN executive.

The "READFILE" capability allows an user to reference an external secondary file from the NASTRAN primary input file and to read data from this secondary file. There is no limit to the number of external secondary files that may be referenced and read. The "READFILE" capability may be invoked anywhere in the Executive Control, Substructure Control, Case Control and Bulk Data Decks.

INTRODUCTION

The April 1984 release of NASTRAN has been enhanced by the addition of two new features. These are the Rigid Format Data Base and the "READFILE" capability. Both of these features greatly add to the flexibility and versatility of NASTRAN. They are described in detail in the following sections.

RIGID FORMAT DATA BASE

The new Rigid Format Data Base allows for convenient maintenance of the existing Rigid Formats and the addition of new Rigid Formats. Editing of the data base may be done by using standard text editors provided on the host computer systems. The basic rationale and the advantages of the data base have been discussed in an earlier paper (Reference 1).

Design of the Data Base

The Rigid Format Data Base is a collection of all Rigid Formats available to the user in NASTRAN. Each Rigid Format is maintained as a separate card-image entry within the data base. The entry for each Rigid Format consists of three parts. The first part is the DMAP part. It contains the DMAP sequence for the Rigid Format, the DMAP sequence subset flags, the restart flags (card name, file name and Rigid Format switch restart flags) and the substructure DMAP ALTER control flags. The second part contains the card name table and the third part contains the file name table. The restart flags in the first part and the name tables comprising the second and third parts are not processed by NASTRAN in non-restart runs. Similarly, the substructure control flags in the first part are not processed in non-substructure runs.

The format of the data base is free field. Each of the three parts in a Rigid Format entry is separated from the other parts by a "$*" card. The following fictitious example illustrates a Rigid Format entry in the data base.

```
      APR.84
      $$$$ THIS IS A COMMENT
      $$$$ ****************************************************
      MODULE1   IN1,IN2,/OUT1,OUT2//*PARM1* $
      ****SBST  1,3,9-12
      ****RFMT  188,200-201
      ****CARD  1-20,30,44
      ****FILE  100-104,110
      ****PHS1  I1
      ****PHS2  DB5
      ****PHS3  D7
      $$$$ ****************************************************
      MODULE2   IN3,IN4/OUT3/*PARM2* $
      ****CARD  1-40,45
      ****FILE  101,102
      ****PHS2  DE5
      $$$$ ****************************************************
```

```
          .
          .
          .
$$$$
$*CARD NAME TABLE
$$$$
1         AXIC    AXIF    CELAS1     CELAS2
2         ADUM1   CDUM1   CROD
          .
          .
          .

$$$$
$*FILE NAME TABLE
$$$$
94        SLT     GPTT
95        KGGX    GPST
          .
          .
          .

$*
```

The very first card of an entry identifies the release of NASTRAN with which the Rigid Format is associated. In this example, the Rigid Format is associated with the April 1984 release.

The "$*CARD" card separates the card name table from the DMAP part of the entry and the "$*FILE" card separates the file name table from the card name table. A "$*" card terminates the file name table and the Rigid Format entry.

Comment cards are identified in the data base by the "$$$$" identification in the first four columns of the field and control cards are identified by the "****" identification in the first four columns of the field.

Comment cards may be placed anywhere in the card name or file name tables (the second and third parts of a Rigid Format entry). However, comment cards have a required usage and serve a specific purpose in the DMAP part of a Rigid Format entry. In this part, a comment card is used to distinguish and separate a DMAP entry (that is, a DMAP statement and its associated control cards) from another DMAP entry. Hence, there must be at least one comment card separating a DMAP entry from the next DMAP entry. In the data base supplied with NASTRAN, a comment card with a trailing string of "*" is used for this purpose to serve as a cosmetic delineation between successive DMAP entries.

All DMAP statements must conform to the rules as specified in the NASTRAN User's Manual (Reference 2). Any card in the DMAP part of a Rigid Format entry that does not begin with "$$$$" or "****" in the first four columns of the field is considered to be a DMAP statement or part of a DMAP statement.

13

Comment and control cards in a Rigid Format entry can extend up to 80 columns. However, DMAP cards can only extend up to 72 columns.

Control cards (that is, cards that begin with "****" in the first four columns of the field) are permitted only in the DMAP part of a Rigid Format entry. A control card must have any one of seven four-character names in columns five through eight. The permissible names are: SBST, RFMT, CARD, FILE, PHS1, PHS2 and PHS3. Control cards follow the corresponding DMAP statement in the entry and may be specified in any order.

The "SBST", "RFMT", "CARD" and "FILE" control cards contain sequences of numbers and/or ranges of numbers in ascending order represented by the use of a dash. A comma is required after each number in a sequence or after a range of numbers, if an additional number or range of numbers is to follow. There may be multiple cards for any one of these control cards for a specific DMAP statement.

The "SBST" control card provides DMAP sequence subset controls. If a user requests a given subset on the "SOL" card of a NASTRAN run and that number is in the sequence of numbers given on the "SBST" card, then the associated DMAP statement is deleted. The range of subset numbers is from 1 to 9 and each number is documented in the NASTRAN User's Manual (Reference 2).

The "RFMT" control card is processed in restart runs and is applicable to cases where a Rigid Format switch has occurred. Each Rigid Format has a unique number assigned to it. For APPROACH DISP, Rigid Formats 1 through 15 are assigned numbers 187 through 201. For APPROACH HEAT, Rigid Formats 1, 3 and 9 are assigned numbers 207, 208 and 209. For APPROACH AERO, Rigid Formats 10 and 11 are assigned numbers 214 and 215. A DMAP statement is flagged for execution in a modified restart if the number associated with the Rigid Format that was used in the checkpointed run is listed in the sequence of numbers given on the "RFMT" card provided with the DMAP statement.

The "CARD" and "FILE" control cards provide restart information for changes that involve input data or files within the DMAP. For a given Rigid Format, every type of effective change in the Case Control and Bulk Data Decks and each output file (or data block) in the DMAP is assigned a number as defined in the card name and file name tables in the second and third parts of a Rigid Format entry. In a modified restart, if the number associated with an input data change or an affected file appears in the sequence of numbers given on the "CARD" or "FILE" cards, then the corresponding DMAP statement is flagged for execution in the restart run.

The "PHS1", "PHS2" and "PHS3" control cards are used to indicate where substructure DMAP ALTERs are to be generated. The number following the "PHS" refers to the substructure phase

14

number. These cards must have one of the following flags: "In", "Dn", "DBn" or "DEn". The "n" in these flags is an integer that refers to the subroutine governing the substructure run (subroutine ASCM01, ASCM05, ASCM07 or ASCM08) and must have the value "1" for Phase 1 cards, either the value "5" or "8" for Phase 2 cards, and either the value "1" or "7" for Phase 3 cards. The "I" in the "In" flag indicates that a DMAP ALTER is to be inserted after this DMAP statement. The "D" in the "Dn" flag indicates that this DMAP statement is to be deleted and possibly replaced by a DMAP ALTER. The "DB" in the "DBn" flag and the "DE" in the "DEn" flag indicate the beginning and the end of a group of contiguous DMAP statements that are to be deleted and possibly replaced by a DMAP ALTER. Users are cautioned to be very careful in making any changes to these substructure control cards because of their impact on the DMAP ALTERs automatically generated in substructure analyses. (The substructure capability is currently implemented only in Rigid Formats 1, 2, 3, 8 and 9, APPROACH DISP.)

The card name and file name tables assign numbers to every type of effective change in the Case Control and Bulk Data Decks and to every output file (or data block) in the DMAP. Numbers 1 through 93 are assigned to card names and numbers 94 through 186 are assigned to file names. This information is used subsequently to determine the DMAP statements to be flagged for execution in modified restarts. The format of these tables is free field. Each entry in these tables must have an integer number in the first field and a list of names in the remaining fields of the entry. All names are to be alphanumeric and may contain up to a maximum of eight characters. No name should appear twice in these tables. Comment cards may be freely used in these tables to facilitate readability.

Implementation of the Data Base

The Rigid Format Data Base is implemented differently on the CDC, DEC VAX, IBM and UNIVAC versions. On the CDC and DEC VAX versions, each Rigid Format entry is stored as a separate file. The local names of these files during a NASTRAN execution are: DISP1 through DISP15 for APPROACH DISP; HEAT1, HEAT3 and HEAT9 for APPROACH HEAT; and AERO10 and AERO11 for APPROACH AERO. These same files are stored as members of a partitioned data set (PDS) on the IBM version and as elements of the *NASTRAN file on the UNIVAC version. The member and element names are exactly the same as the local file names on the CDC and DEC VAX versions. On the IBM version, the PDS containing the Rigid Format Data Base must be referred to by a Data Definition card, "DD", with the DDname of RFDATA. On the UNIVAC version, the *NASTRAN file is the file containing the NASTRAN program absolutes. (See References 3 and 4 for the formats of file names for the CDC and DEC VAX versions, respectively. See Reference 5 for the formats of DDnames and member names for the IBM version. See Reference 6 for the format of UNIVAC file names.)

Usage of the Data Base

The following examples illustrate the manner in which the Rigid Format Data Base is accessed and used on all of the four versions of NASTRAN.

CDC VERSION

```
/JOB.
.
.
GET,DISP1,DISP2,DISP3,DISP4,DISP5.
GET,DISP6,DISP7,DISP8,DISP9,DISP10.
GET,DISP11,DISP12,DISP13,DISP14,DISP15.
GET,HEAT1,HEAT3,HEAT9,AERO10,AERO11.
RFL,220000.
REDUCE,-.
LINK1,INPUT,OUTPUT,PUNCH,UT1.
/EOR
ID ....
.
.
ENDDATA
/EOF
```


DEC VAX VERSION

```
ASSIGN   DDB1:[NASDIR]DISP1.DT DISP1.
ASSIGN   DDB1:[NASDIR]DISP2.DT DISP2.
          .
          .
ASSIGN   DDB1:[NASDIR]HEAT1.DT HEAT1.
          .
          .
ASSIGN   DDB1:[NASDIR]AERO11.DT AERO11.
@DDB1:[NASDIR]NASTRAN    DEMO.DT
```


IBM VERSION

```
//    EXEC    NASTRAN
//NS.RFDATA   DD   DSN=RIGID.FORMAT.DATA,DISP=SHR
//NS.SYSIN    DD   *
ID ....
.
.
ENDDATA
//
```

UNIVAC VERSION

```
@ASG,A    *NASTRAN.
@XQT      *NASTRAN.LINK1
```

Development of User Rigid Formats

In addition to using COSMIC-supplied Rigid Formats, users may develop their own Rigid Formats, with restart capabilities included. Rigid Formats developed by users must conform to the rules explained earlier and must be similar in content and structure to the COSMIC-supplied Rigid Formats. Each user-developed Rigid Format must reside as a separate file on the CDC and DEC VAX versions, as a member of a PDS on the IBM version and as a file or file.element on the UNIVAC version.

Before developing their own Rigid Formats, users are strongly advised to carefully study and examine the COSMIC-supplied Rigid Formats, particularly with regard to their use of the control cards. The following important guidelines should help users in developing their own Rigid Formats.

1. The DMAP sequence of the user Rigid Format must be tested for its correctness and logic. This testing may be done either in a DMAP environment or in the environment of an existing Rigid Format by use of ALTERs.

2. The card name table (the second part of a Rigid Format entry) must be constructed by assigning numbers 1 through 93 for all types of Case Control and Bulk Data Deck changes that will affect the logic of the Rigid Format. Normally, those input data changes that have the same effect on the logic of the Rigid Format are assigned the same number.

3. The file name table (the third part of a Rigid Format entry) must be constructed by assigning numbers 94 through 186 for all files (or data blocks) that are output by the functional modules in the Rigid Format. Normally, all files (or data blocks) output from a given functional module are assigned the same number.

4. The DMAP part (the first part of a Rigid Format entry) must be constructed by following each statement in the DMAP sequence by the appropriate control cards and by ensuring that each DMAP entry (that is, a DMAP statement and its associated control cards) is separated from the next DMAP entry by at least one comment card.

5. A given DMAP statement must be followed by a "SBST" control card if that DMAP statement belongs to one or

17

more of the DMAP subsets. These subset numbers must be specified on the "SBST" card. The acceptable subset numbers and their meanings are documented under the description of the SOL Executive Control card in the NASTRAN User's Manual (Reference 2).

6. A "RFMT" control card must follow a DMAP statement if that DMAP instruction is to be flagged for execution on restart from a checkpoint of one of the COSMIC-supplied Rigid Formats. (It is not possible to have a restart in a COSMIC-supplied Rigid Format from a checkpoint of an user-developed Rigid Format.) This will be so if this DMAP instruction is not part of the DMAP sequence of the Rigid Format that was used in the checkpoint run. The "RFMT" control card must list the numbers of the appropriate COSMIC-supplied Rigid Formats (187 through 201 for Rigid Formats 1 through 15 for APPROACH DISP, 207, 208 and 209 for Rigid Formats 1, 3 and 9 for APPROACH HEAT and 214 and 215 for Rigid Formats 10 and 11 for APPROACH AERO).

7. A DMAP statement must be followed by one or more "CARD" control cards indicating the effective input data changes that require that DMAP instruction to be flagged for execution on restart. Any effective input data change will affect one or more files (or data blocks) or parameters in the DMAP sequence. Therefore, for a given data change, all DMAP instructions that use the affected files (or data blocks) or parameters as input are potential candidates to be flagged for execution on restart. However, the logic of these individual DMAP instructions must be checked further (see Reference 7) to see if they are really impacted by the given data change. This procedure must be applied in turn to those DMAP instructions that use the output of the affected DMAP instructions as input. This procedure must be repeated until the entire DMAP sequence has been considered.

8. A DMAP statement must be followed by one or more "FILE" control cards indicating the DMAP files (or data blocks) whose generation requires the execution flag for that DMAP statement to be turned on during restart. Normally, for a given DMAP file (or data block) that is required on restart but is not available from the checkpoint run, the DMAP instruction that generated it must be flagged for execution. However, in practice, additional DMAP instructions like PURGE and EQUIV that manipulate the given file (or data block) must also be flagged for execution.

9. The restart flags for a COND DMAP instruction must include the restart flags for those DMAP instructions whose execution it controls.

18

10. "PHS1", "PHS2" and "PHS3" control cards must not be used as the substructure capability is not applicable to user Rigid Formats.

Usage of User-Developed Rigid Formats

An user-developed Rigid Format is referenced through the use of the "SOL" card in the Executive Control Deck. However, instead of specifying the solution number or the name of the COSMIC-supplied Rigid Format on this card, the name of the user-developed Rigid Format is specified. This name is a file name on the CDC and DEC VAX versions, a member name of a PDS on the IBM version and a file or file.element name on the UNIVAC version. The member name given on the IBM version must be in the file referenced on the RFDATA DD statement. The manner in which an user-developed Rigid Format is accessed and used is similar to that of a COSMIC-supplied Rigid Format, as explained in the examples given above. Thus, for instance, an user-developed Rigid Format can be accessed and used on the CDC version in the following manner.

```
/JOB.
.
.
GET,NEWRF.
RFL,220000.
REDUCE,-.
LINK1,INPUT,OUTPUT,PUNCH,UT1.
/EOR
ID ....
SOL NEWRF
.
.
/EOF
```

User Advantages

The advantages of the Rigid Format Data Base are readily apparent and are discussed in detail in Reference 1. Users can now very easily update the data base to incorporate corrections due to Software Problem Reports (SPRs) relating to Rigid Formats and their associated restart and subset tables. This ease also benefits the maintenance contractor in the maintenance of the Rigid Formats. Further, users can now generate their own Rigid Formats with restart capabilities or modify existing Rigid Formats permanently for their own use. Previously, changes to Rigid Formats required the use of temporary DMAP ALTERs or Fortran compilations and the link editing of NASTRAN. Elimination of these compilations and link edits benefits both the user and the maintenance contractor.

THE "READFILE" CAPABILITY

The "READFILE" capability allows a user to logically read data from one or more external, secondary, card-image files by referencing these files from the NASTRAN primary input file. The primary input file is the file that is assigned to Fortran unit 5 from which NASTRAN normally reads the input data.

Description of the Capability

The format of the "READFILE" card is as follows:

        READFILE   name

where "name" refers to an external, secondary, card-image file.

When a "READFILE" card is encountered in the primary input file, NASTRAN reads all subsequent input data from the specified secondary file until an end-of-file condition or an ENDDATA card is encountered on that file, whichever occurs earlier. If an end-of-file condition is encountered on the secondary file before an ENDDATA card is detected, the program resumes reading of the input data from the primary input file and the process continues. If an ENDDATA card is encountered on the secondary file before an end-of-file condition is detected, obviously the program will not read any more input data from either the secondary file or the primary file, unless the INPUT module is being used in which case the data required for the INPUT module will be read from the primary input file (see Item 6 in the following discussion).

The following important points about the usage of the "READFILE" capability must be noted by the user:

1. The format of the "READFILE" card is free-field. The only restrictions are that there should be at least one space between the word "READFILE" and the "name" of the secondary file and that the card cannot extend beyond one card image (80 columns).

2. "READFILE" cards are permitted only in the NASTRAN primary input file and are not allowed in secondary input files. In other words, all references to secondary input files must be made from the primary input file and no secondary file can reference another secondary file.

3. As a corollary to the above, since a SOL card in the Executive Control Deck references an external, secondary file (either implicitly or explicitly), it must appear on the primary input file and is not permitted on a secondary file.

4. Any number of "READFILE" cards may be used, but each such card must reference an unique secondary file name.

5. "READFILE" cards may be used anywhere in the Executive Control, Substructure Control, Case Control and Bulk Data Decks. (The NASTRAN card can also be specified on a secondary file.)

6. If the INPUT module is used, the data required for that module must appear on the primary input file.

7. On the CDC and DEC VAX versions, "name" may be any valid file name (see Examples 1 and 2 below). On the IBM version, "name" may be either a sequential file name (see Example 3) or a member name of a PDS (see Example 4). On the UNIVAC, "name" may be any file name (see Example 5) or file.element name (see Example 6).

Examples of "READFILE" Capability Usage

The following examples illustrate several ways in which the "READFILE" capability can be used. These examples also illustrate the usage of this capability on all four versions of NASTRAN.

Example 1

This example illustrates the usage of the "READFILE" capability for reading in the restart dictionary in a checkpoint/restart run on the CDC version. (This example assumes that the output on the punch file in the checkpoint run contains only the restart dictionary.)

```
/JOB
.
.
COPYBR,INPUT,INPUT1.
COPYBR,INPUT,INPUT2.
REWIND,INPUT1,INPUT2.
* RUN CHECKPOINT JOB
LINK1,INPUT1,OUTPUT,PUNCH1,UT1.
* MANIPULATE FILES
PACK,PUNCH1.
REWIND,PUNCH1.
RETURN,POOL.
RENAME,OPTP=NPTP.
* RUN RESTART JOB
LINK1,INPUT2,OUTPUT,PUNCH2,UT1.
/EOR
NASTRAN  FILES=NPTP
.
. (DATA FOR CHECKPOINT JOB)
.
```

21

```
      /EOR
      NASTRAN   FILES=OPTP

      .
      $ READ THE RESTART DICTIONARY
      READFILE PUNCH1

      .
      CEND

      .
      .   (DATA FOR RESTART JOB)
      .
      /EOF
```

Example 2

This example illustrates the use of multiple "READFILE" cards on the DEC VAX version.

```
      ID ....
      .

      .
      BEGIN BULK
      READFILE DDB1:[NASDIR]FUSELAGE.DT
      READFILE DDB1:[NASDIR]WINGS.DT
      READFILE DDB1:[NASDIR]TAIL.DT
      ENDDATA
```

The directory and device names need not be specified if default values are to be used.

Example 3

In this example, the "READFILE" capability is used to access a sequential file on the IBM version. The format for reading a sequential file is to include the DDname of the file on the "READFILE" card as shown below.

```
      //   EXEC NASTRAN
      //NS.CARDS   DD    DSN=USER.JOB1EXEC.DATA,DISP=SHR
      //NS.SYSIN   DD    *
      ID ....
      .

      .
      READFILE    CARDS
      /*
```

An ENDDATA card is not used in the Bulk Data Deck here as it is assumed to be included in the data on the sequential file.

22

Example 4

In this example, the "READFILE" capability is used to read a member of a PDS on the IBM version. The format for reading a member of a PDS is to include the DDname of the PDS with the member name in parentheses immediately following it as shown below.

```
//   EXEC NASTRAN
//NS.CARDS   DD    DSN=USER.PDS.DATA,DISP=SHR
//NS.SYSIN   DD    *
ID ....
   .
   .
READFILE     CARDS(JOB2EXEC)
   .
   .
/*
```

The member JOB2EXEC is read from the PDS USER.PDS.DATA.

Example 5

In this example, a file name on the UNIVAC is referenced by a "READFILE" card.

```
@ASG,A CARDS*UN1EXEC.
@XQT    *NASTRAN.LINK1
ID ....
READFILE     CARDS*UN1EXEC.
   .
   .
```

The file UN1EXEC with the qualifier CARDS will be read immediately after the ID card.

Example 6

In this example, a file.element name on the UNIVAC is referenced by a "READFILE" card.

```
@ASG,A CARDS*UN2.
@XQT    *NASTRAN.LINK1
ID ....
READFILE     CARDS*UN2.EXEC
   .
   .
```

The element EXEC of file UN2 with the qualifier CARDS is read immediately after the ID card.

CONCLUDING REMARKS

The Rigid Format Data Base and the "READFILE" capability will be welcomed by both the NASTRAN user community and the maintenance contractor. The Rigid Format Data Base is easily maintained and allows users the freedom of updating and modifying existing Rigid Formats as well as generating their own Rigid Formats, without having to compile and link edit NASTRAN. The "READFILE" capability will also prove to be extremely helpful and convenient to users. Both features will greatly enhance the flexibility, generality and attractiveness of NASTRAN.

REFERENCES

1. Pamidi, P. R., and Brown, K. B., "A New Method for Generating and Maintaining Rigid Formats in NASTRAN," NASA Conference Publication 2284, Eleventh NASTRAN Users' Colloquium, San Francisco, California, May 5-6, 1983, pp. 249-254.

2. The NASTRAN User's Manual, NASA SP-222(06), September 1983.

3. Control Data Corporation NOS 1.0 Reference Manual, Document No. 60435400.

4. VAX/VMS Command Language User's Guide, Digital Equipment Corporation, Order No. AA-D023C-TE.

5. IBM OS/VS2 MVS JCL, Document No. GC28-0692-4.

6. Sperry UNIVAC 1100 Series Executive System EXEC Programmer Reference, Volume 2, Document No. UP-4144.2.

7. The NASTRAN Programmer's Manual, NASA SP-223(05), December 1978.

ACCURACY OF THREE DIMENSIONAL SOLID FINITE ELEMENTS

W. R. Case and R. E. Vandegrift
NASA/Goddard Space Flight Center

SUMMARY

This paper presents the results of a study to determine the accuracy of the three dimensional solid elements available in NASTRAN for predicting displacements. Of particular interest in the study is determining how to effectively use solid elements in analyzing thick optical mirrors, as might exist in a large telescope. Surface deformations due to thermal and gravity loading can be significant contributors to the determination of the overall optical quality of a telescope. The study investigates most of the solid elements currently available in either COSMIC or MSC NASTRAN. Error bounds as a function of mesh refinement and element aspect ratios are addressed. It is shown that the MSC solid elements are, in general, more accurate than their COSMIC NASTRAN counterparts due to the specialized numerical integration used. In addition, the MSC elements appear to be more economical to use on the DEC VAX 11/780 computer.

INTRODUCTION

Optical mirrors for spaceborne telescopes often have thicknesses which are as much as 10 percent of their diameter. Because of this, and also due to the need to obtain accurate predictions of optical surface deformations in the presence of temperature gradients that are often nonlinear, these mirrors are modeled with three dimensional, solid, finite elements. In addition to thermal deformation being a significant design driver for these mirrors, deformation due to "gravity release" must also be considered. When fabricated and tested, the mirror is in a 1-g environment which is "released" once the telescope reaches the 0-g environment in orbit.

A common design practice is to fabricate these mirrors from low coefficient of thermal expansion (CTE) materials but to mount them to conventional metal housings with much larger CTE's. In order to avoid stressing the mirror when it is subject to simple bulk temperature changes, the mirror is often mounted to its housing through the use of (nearly) kinematic mounts that may connect to the mirror in only three locations.

The purpose of this study is to determine how to effectively model such mirrors for thermal and gravity loading using the available solid elements in NASTRAN. In a study such as this there are three significant questions to consider.

1. How fine a mesh must be used to obtain displacements of the optical surface within a certain error range?

2. Do the individual solid finite elements exhibit sensitivity to aspect ratios significantly different than 1.0?

26

3. Which of the available elements are the most economical to use (accuracy vs cost in computer resources)?

Questions 1 and 2 above can best be answered in an investigation that completely separates the two effects. That is, the mesh refinement studies should be done using elements with an aspect ratio of 1.0. Then, once a fine enough mesh has been reached such that the errors are small, the effects of aspect ratio can be investigated by keeping the mesh size constant and varying the overall dimensions of the problem, thus resulting in each element aspect ratio changing. Obviously, in order to accomplish this latter step there must be a theoretical (or some other good comparison) solution to the problem with which to compare the finite element model results since at each step a problem of different dimensions (and therefore different theoretical solution) is being modeled. This technique has been used in previous studies for two dimensional membrane elements, [1], [2].

With the above considerations in mind, the sample problem used in the study (described in more detail below) is a cubic slab of equal dimension in the X-Y plane and whose thickness varies between one-twentieth and one-half of the X-Y plane dimensions (see Figure 1). The slabs were constrained in a kinematic fashion simulating the type of restraint often used in actual practice. For the thick slab, a mesh refinement can be made of elements having aspect ratios of 1.0 without requiring an exorbitant number of elements in the X-Y plane when a reasonable number is used through the thickness. For a linear temperature gradient through the slab there exist theoretical solutions. Thus the thick slab, although it does not look much like a mirror, is a good candidate for the mesh refinement studies when the temperature gradient loading is used. Also, since the theoretical solution exists for arbitrary thickness of the slab, the sample problem is also suitable for an element aspect ratio study. Keeping the mesh refinement constant (that is the number of elements in the model), simply by varying the slab thickness, the element aspect ratios must change.

For the gravity loading the situation is not as good. There is no theoretical solution to compare to so it is not practical to attempt the aspect ratio study with this loading. However, if the various elements used in the study show a trend toward convergence to an answer as the mesh is refined, the mesh refinement studies can provide useful information with this loading.

PROBLEM DETERMINATION

Figure 1 shows the geometry, coordinate system, boundary conditions, and basic material information used in this study. The constraints are kinematic and the problem is symmetric about the x=0 plane. That is, the x displacement is zero along the x=0 plane. Using this constraint, only half the slab was modeled for the study.

Both COSMIC and MSC elements were tested in this study. This included hexahedral elements with up to two midside nodes and wedge shaped elements with up to one midside node. Figure 2 displays the different types examined.

The mesh geometry is shown in Figure 3. All models had half the number of elements through the thickness as in the other two dimensions. Only the diamond pattern shown in Figure 3 was used for wedge shaped elements and the triangular shape was always in the x-y plane as recommended in [4]. When an element aspect ratio was desired, the value of t was changed while the number of elements through the thickness remained unchanged. This created shorter or squat elements.

Temperature Gradient Loading

The temperatures applied to the test model varied only in the z direction. A linear gradient was created which ranged from $+\frac{1}{2}$ to $-\frac{1}{2}$ degrees centigrade. The equation for this gradient is:

$$T = \tfrac{1}{2}\left(1 - \tfrac{z}{t}\right)$$

$$T = \text{temperature}, \quad t = \text{thickness}$$

An exact theoretical solution exists for a linear temperature gradient [3] and in this case the equations are:

$$u = \bar{u} + u_0 - y\Theta_{z_0} + z\Theta_{y_0}$$
$$v = \bar{v} + v_0 - z\Theta_{x_0} + x\Theta_{z_0}$$
$$w = \bar{w} + w_0 - x\Theta_{y_0} + y\Theta_{x_0}$$

where

$$u, v, w = \text{displacements}, \quad \alpha = \text{CTE}$$

$$\bar{u} = \alpha\left(\tfrac{1}{2} - \tfrac{z}{t}\right)x$$

$$\bar{v} = \alpha\left(\tfrac{1}{2} - \tfrac{z}{t}\right)y$$

$$\bar{w} = \alpha\left[\left(\tfrac{1}{2} - \tfrac{z}{t}\right)z + \tfrac{1}{2t}\left(x^2 + y^2 + z^2\right)\right]$$

Using the boundary conditions as shown in Figure 1 we get:

$$u = \alpha\left(\tfrac{1}{2} - \tfrac{z}{t}\right)x$$

$$v = \alpha\left(\tfrac{1}{2} - \tfrac{z}{t}\right)y$$

$$w = \alpha\left[\left(\tfrac{1}{2} - \tfrac{z}{t}\right)z + \tfrac{1}{2t}\left(x^2 + y^2 + z^2\right)\right]$$

Gravity Loading

Since many telescopes operate in a zero gravity environment, surface deformations due to their original one G environment are important in evaluating their optical quality. The load used in this study was

28

applied in the -z direction with the supports at the bottom surface. No theoretical solution is available for this case.

A thin slab (i.e. t=.0504M (2")) model was used for the gravity loading. Since this created elements with aspect ratios of 5, only elements which showed no susceptibility to aspect ratio errors in the temperature load case were used.

RESULTS

Temperature Gradient Loading

For the linear temperature gradient loading the results of the mesh refinement and aspect ratios studies are shown in Figures 4 and 5. Figure 4 shows the error in displacement at point A as a function of mesh size (N) for each of the nine solid elements in the study. The number of elements in any one model is N x N x N/2 in the x, y, z directions, respectively, for the complete problem and are half this amount for the one-half of the slab actually modeled due to symmetry. In order to keep the element aspect ratio 1.0 for this part of the study, the slab dimensions were chosen to be .508 x .508 x .254M (20 x 20 x 10").

The linear temperature gradient, coupled with the stress-free mounting used in the problem, produces a linear strain variation through the thickness of the slab. It is to be expected, therefore, that isoparametric elements of high enough order, when integrated using Gauss quadratur with a sufficient number of points, will yield exact results (even when the problem contains only one element through the thickness). This is true for the COSMIC quadratic and cubic elements, CIHEX2 and CIHEX3. In addition, it should also be true for the MSC elements CHEXA (20 node) and CPENTA (15 node) which are also quadratic isoparametric elements but which use reduced integration for selected terms in the stiffness matrix. Reduced integration is used in conjunction with many isoparametric elements in an effort to improve on the overly stiff behavior of some of the lower order of these elements [5]-[8]. When used in situations in which there is primarily bending behavior, the lower order isoparametric elements have a "parasitic" shear introduced due to the allowable modes of deformation as defined by the polynomial displacement field. This parasitic shear can be removed by selectively reducing the order of numerical integration used in generating the element stiffness matrices. The result is an element which no longer demonstrates interelement displacement compatibility but which, paradoxically, often performs better. Table 1 lists the order of the numerical integration used for the isoparametric elements used in this study. The exact details of the reduced integration for the MSC elements is not made clear in their documentation but is believed to be such that the shear terms are represented by only one point for the linear displacement polynomial elements.

Figure 4 shows that the MSC linear isoparametric elements give exact behavior as well as the higher order elements which were expected to be exact. The linear elements, like their COSMIC counterpart CIHEX1, are based on products of linear shape functions which are capable of

29

representing all constant states of strain and some linear states as well. However, the linear normal strains in the x, y directions are not represented by these elements so that the exact behavior of the 8 node CHEXA MSC element is not fully understood. It should be anticipated however, that the 8 node CHEXA would be better for this temperature loading than the COSMIC CIHEX1 due to the reduced integration used.

In order to determine the sensitivity of these elements to element aspect ratios different than 1.0, only the finest mesh for each element was run with the slab thickness decreasing in successive runs from .254 M (10") to .0254 M (1"). This resulted in element aspect ratios changing from 1.0 to 10 (that is, the element dimensions in the x-y plane, in ratio to its thickness changed from 1.0 to 10). Figure 5 shows how the displacement errors are affected by these changes in element aspect ratio. The only isoparametric element which shows sensitivity to aspect ratio is the COSMIC linear element CIHEX1.

Since the slab thickness has decreased from .254 M (10") to .0254 M (1") while the element aspect ratio increased from 1 to 10, the slab deflections are due more to bending now than they were when the thickness was .254 M (10"). As mentioned previously, the CIHEX1 has a parasitic shear due to bending so that it might be expected that the deflection errors would worsen as the slab exhibits more bending. The other isoparametric elements avoid this problem, to some degree or another, by either having higher order displacement polynomials and/or reduced integration.

Gravity Loading

As with the temperature loading study, the gravity loading study began with the thick slab in order to preserve the 1.0 element aspect ratio during the mesh refinement portion of the study. As mentioned previously, there is no theoretical solution to a thick slab loaded by a body force when constrained in the kinematic fashion used in this study. Thus, Figure 6, which shows the mesh refinement results, has actual displacement (rather than displacement error) plotted versus mesh size. The results shown on Figure 6 indicate no convergence has taken place for the range of mesh sizes used. Apparently, the reason for no convergence is due to the concentrated loads at the support points (along either side of the slab). The mesh for this kind of a problem really needs to be more refined in these areas rather than just using a uniform mesh for the whole problem. In addition, the "point" support must be distributed over a finite surface area to avoid the singularity (in displacement and stress) that exists, in the limit, as the mesh size (N) becomes infinitely large. However, in a three dimensional problem, this mesh refinement is very difficult to do without the aid of some automatic mesh generation program (which was not available for a this study).

The difficulty in convergence evidenced by the results in Figure 6 was thought to be compounded by the fact that the slab is quite thick (one half of the in-plane dimensions). Since the overall study is really aimed at how to model moderately thick mirrors it was decided to change

30

the slab to one that had a thickness of one-tenth the in-plane dimensions but keeping the element mesh arrangement the same (N x N x N/2). Since this would result in elements with aspect ratios of 5, only those elements that exhibited no aspect ratio sensitivity in the thermal load study were used. This included the 1 and 2 mid-side node COSMIC isoparametric elements and all of the MSC isoparametric elements.

Figure 7 shows the results of the mesh refinement study using the thin slab (.504 x .504 x .0504 M (20 x 80 x 2")). Again it is obvious that convergence has not been reached by any of the element types even though the finest mesh for the MSC 20 node hexahedral was 10 x 10 x 5 and contained 4064 degrees of freedom for the half model. This run took nearly six hours of CPU time on the VAX 11/780. An attempt to run this element for the 12 x 12 x 6 mesh failed due to the size of a matrix multiply requiring more memory than was available. Table 3 shows how large these problems can become (for the half model) using the N x N x N/2 uniform mesh. The run that failed contained nearly 6700 degrees of freedom.

From the lack of convergence for this more practical problem it is obvious that a uniform mesh size is very impractical to use for a loading and constraint system like those encountered for some large mirrors. The local deformation in the vicinity of the support points requires refinement. Figure 8 illustrates this by showing the displacement at point B which is directly above one of the support points (which carries one half the weight of the slab). These displacements obviously are much smaller than those at point A, however, they are still growing significantly as the mesh is refined. In an effort to see if the convergence problem is really associated with the concentrated loading at the support points, the relative deflection between points A and B was determined. Figure 9 shows this relative displacement and it appears to be converging indicating that the front surface (i.e. the z = t surface) shape is defined but that the whole slab is still "sinking" over the point support under B (and its symmetric counterpart at y = z = 0 and x = 1/2). Figure 9 is really only useful in demonstrating that the mesh really needs refining (and the point support needs to be distributed over a finite area) in the vicinity of the supports in order to obtain useful information about the deflections of the slab.

Timing Study

Table 2 shows all of the elements tested and the computer time required to generate their stiffness matrices on the DEC VAX 11/780. The COSMIC isoparametric elements with one and two midside nodes take an appreciable amount of time and limit the practical problem sizes which can be run.

In reality, it is the total computer costs for a given accuracy that is of most importance. One of the original goals of this study was to address this issue. However, due to the difficulty with obtaining convergence for the gravity loading, a "comparison" answer was not able to be found with which to guage the absolute accuracy of the

31

gravity loading results. This precluded obtaining a plot of accuracy versus cost for this loading. However, based on the solution times for the data of Figures 7-9, it appears that the MSC hexahedra with one midside node is the best element in terms of accuracy versus cost.

Conclusions

Most of the available isoparametric solid elements in both COSMIC and MSC NASTRAN appear to be well suited for thermal deformation analyses of kinematically supported mirror-type structures. An exception to this is the COSMIC 8 noded hex element (CIHEX1) which exhibits large errors when the element aspect ratio deviates from 1.0; the element should not be used for aspect ratios above 2.0.

For gravity loading, the situation is much less clear. Use of a uniform mesh in three dimensional problems is an attractive choice due to the complexity of envisioning nonuniform meshes in more than two dimensions. However, the study indicates that with point supports, an extremely fine mesh would have to be used to get convergence for any of the elements used and the "point" support must be distributed over some fixed finite area as the mesh becomes more and more refined. It appears that mesh refinement in the vicinity of the supports is the only realistic way to model these structures and use of some automatic mesh generation program to accomplish this is a necessity.

From the standpoint of economy, the MSC 20 node hex element (CHEXA) appears to be by far the best of all of the available elements.

References

[1] Guidelines for Finite Element Idealization, ASCE National Structural Engineering Convention, New Orleans, April 1975, Preprint 2504.

[2] W. R. Case and J. B. Mason, "NASTRAN Finite Element Idealization Study," Sixth NASTRAN Users' Colloquium, Cleveland, Ohio, October 1977, pp. 383-404.

[3] B. A. Boley and J. H. Weiner, Theory of Thermal Stresses, John Wiley and Sons, Inc., London, 1960, pp. 272-275.

[4] MSC/NASTRAN Applications Manual, Section 5.13, The MacNeal-Schwendler Corp., Los Angeles, CA (1978).

[5] O. C. Zienkiewicz, R. L. Taylor and J. M. Too, "Reduced Integration Techniques in General Analysis of Plates and Shells," Int. J. Num. Meth. Engng. 3, 275-290 (1971).

[6] S. F. Pawsey and R. W. Claugh, "Improved Numerical Integration of Thick Shell Finite Elements," Int. J. Num. Meth. Engng. 3, 575-586 (1971).

[7] B. M. R. Irons and T. K. Hellen, "On Reduced Integration in Solid Isoparametric Elements When Used in Shells with Membrane Modes," Int. J. Num. Meth. Engng. 1179-1182 (1975).

[8] MacNeal, R. H., "A Simple Quadrilateral Shell Element," Computers and Structures, Vol. 8, pp. 175-183, 1978.

Table 1

Gauss Quadrature Numerical

Integration Mesh Used For

Isoparametric Elements

NASTRAN Version	Isoparametric Element	Number of Nodes	Displacement Polynomial	Gauss Quadrative Mesh Points
COSMIC	CIHEX1	8	linear	2x2x2 = 8
	CIHEX2	20	quadratic	3x3x3 = 27
	CIHEX3	32	cubic	3x3x3 = 27
MSC	CHEXA	8	linear	2x2x2 = 8 [1]
	CHEXA	20	quadratic	3x3x3 = 27 [1]
	CPENTA	6	linear	6 [1]
	CPENTA	15	quadratic	9 [1]

(1) All MSC elements use a numerical integration for selected terms (shear) at a number of Gauss points reduced from those indicated.

34

Table 2

Element Generation

NASTRAN Version	Element	EMG + EMA time per element (C.P.U. sec)[2]
COSMIC		
	CHEXA2	2.1
	CWEDGE	1.0
	CIHEX1	1.2
	CIHEX2	10-13
	CIHEX3	23-29
MSC		
	CHEXA (8 nodes)	.8
	CHEXA (20 nodes)	4.5
	CPENTA (6 nodes)	.4
	CPENTA (15 nodes)	1.8

*These times were taken from models run on a VAX 11/780 using COSMIC versions 17.6 and April 1983 and MSC version 63.

Table 3

Number of Degrees of Freedom for Specific Model Sizes

N	HEX or WEDGE 0 midside nodes	HEX 1 midside node	WEDGE 1 midside node	HEX 2 midside nodes
2	27	80	92	133
4	117	383	455	649
6	305	1052	1268	1799
8	627	2231	2711	3835
10	1119	4064	4964	7009
12	1817	6695	8207	11,573

APPENDIX – NOTATION

AR_e = ELEMENT ASPECT RATIO (le/te)

ℓ = PROBLEM SLAB LENGTH

ℓ_e = ELEMENT LENGTH

E = YOUNGS MODULUS

t = PROBLEM SLAB THICKNESS

t_e = ELEMENT THICKNESS

u, v, ω = DISPLACEMENTS

a, α = COEFFICIENT OF EXPANSION

ρ = DENSITY

ν = POISSON RATIO

FIG. 1
TEST PROBLEM
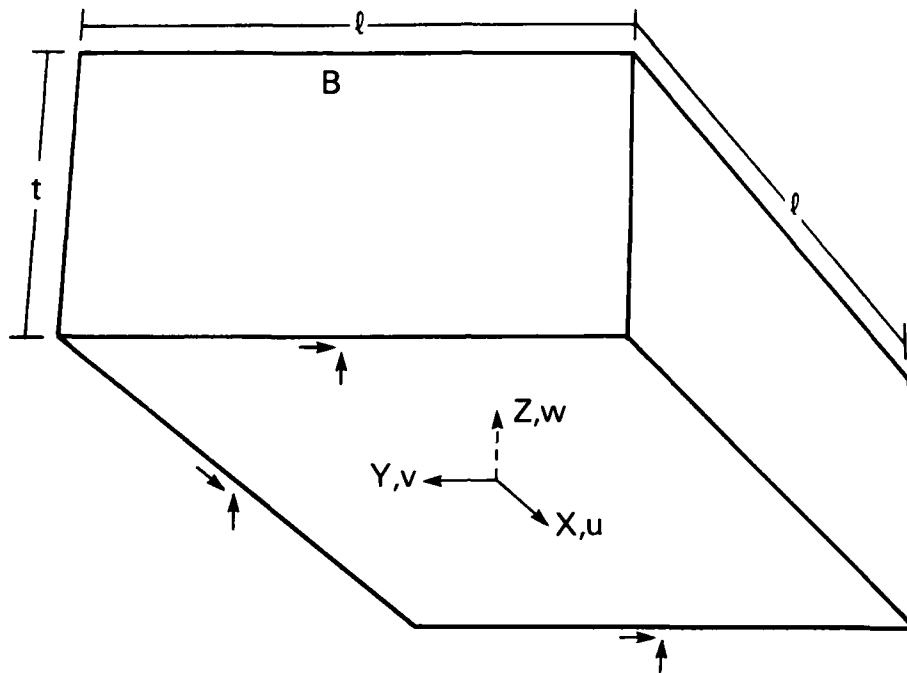
↑ INDICATES DEGREE OF FREEDOM CONSTRAINED FOR KINEMATIC MOUNTS

$v = w = 0$ AT $Y = Z = 0$, $X = \pm \ell/2$

$u = w = 0$ AT $X = Z = 0$, $Y = \ell/2$

$A = (0., 0., t)$

$B = (\ell/2, 0., t)$

MATERIAL INFORMATION (ALUMINUM)

$E = 6.89 \times 10^{10}$ N/M^2 $(10 \times 10^6$ LB/IN$^2)$

$\rho = 2.71 \times 10^3$ KG/M^3 $(.098$ LB/IN$^3)$

$a = 22.7 \times 10^{-6}$ /K
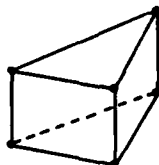
$\upsilon = .33$

FIG. 2

ELEMENT TYPES
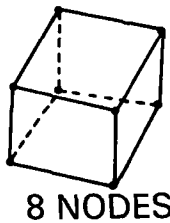
CHEXA2 10 TETRAHEDRA (COSMIC)
CIHEX1 LINEAR ISOPARAMETRIC (COSMIC)
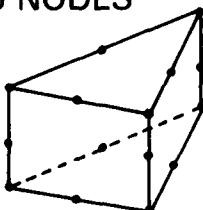8 NODES   CHEXA LINEAR ISOPARAMETRIC (MSC)
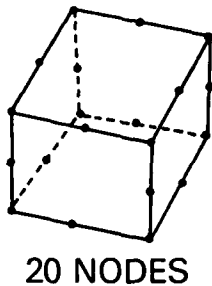
CIHEX2 QUADRATIC ISOPARAMETRIC (COSMIC)
20 NODES   CHEXA QUADRATIC ISOPARAMETRIC (MSC)
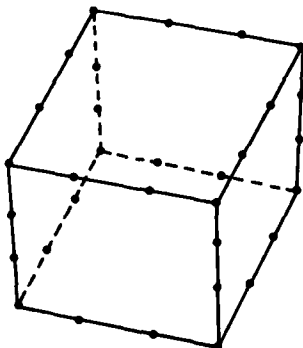
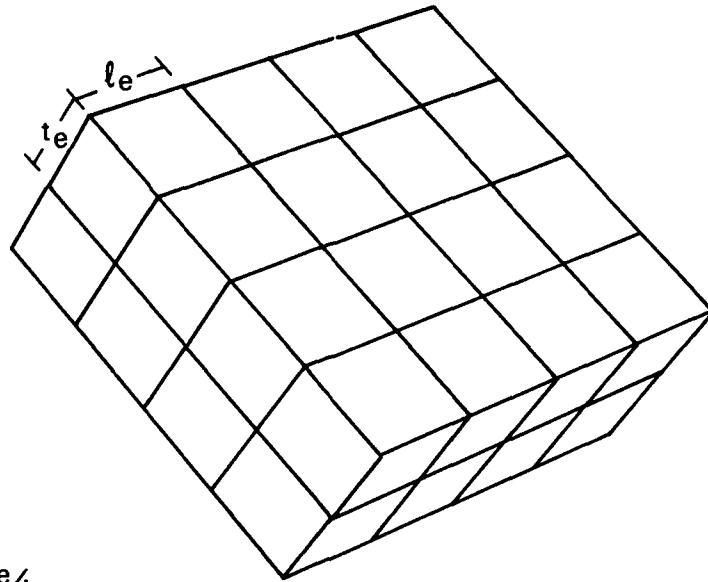32 NODES   CIHEX3 CUBIC ISOPARAMETRIC (COSMIC)

CWEDGE 3 TETRAHEDRA (COSMIC)

6 NODES   CPENTA LINEAR ISOPARAMETRIC (MSC)

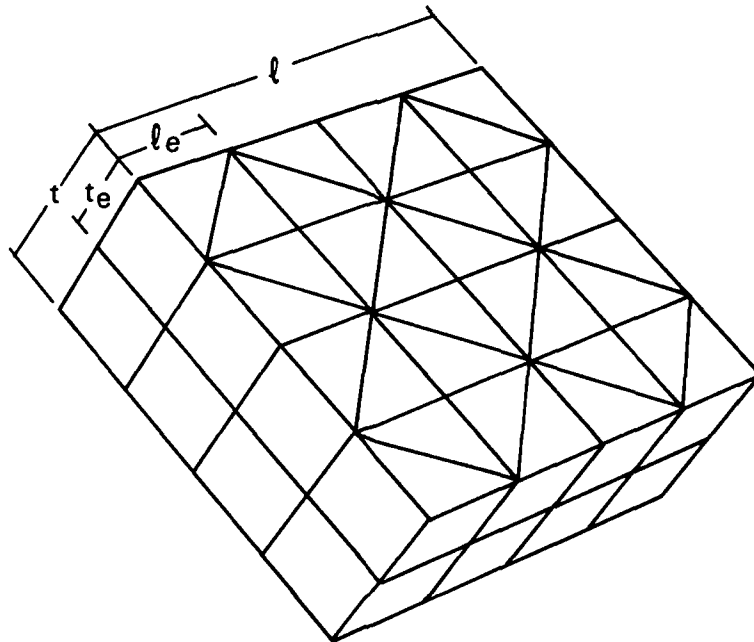15 NODES   CPENTA QUADRATIC ISOPARAMETRIC (MSC)

FIG. 3

MESH GEOMETRY

$$AR_e = {}^{\ell_e}/_{t_e}$$

$$N = {}^{\ell}/_{\ell_e}$$

HEXAHEDRAL PATTERN

WEDGE PATTERN

FIG. 4

Z DISPLACEMENT ERROR AT (A)
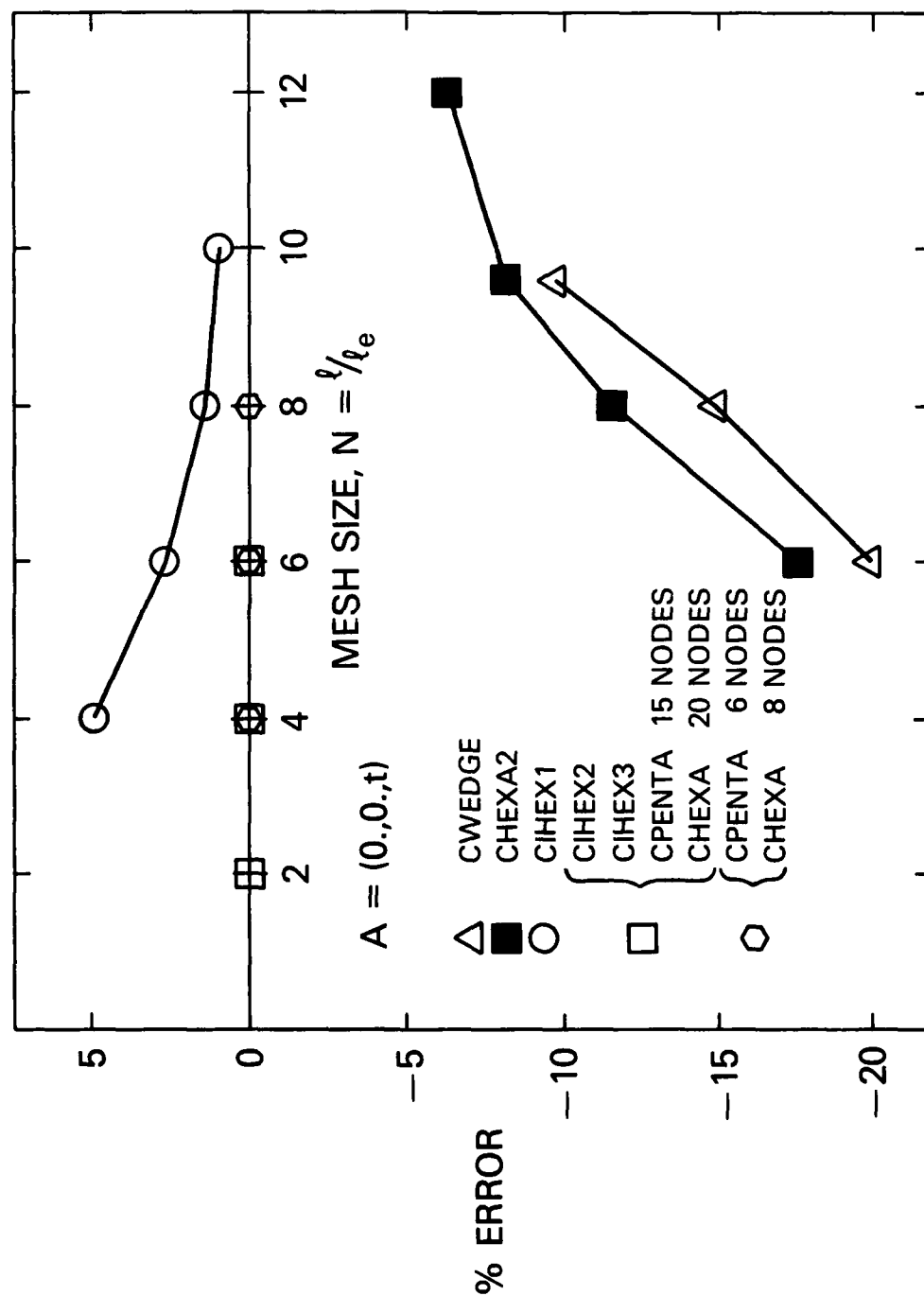## THICK SLAB—LINEAR TEMPERATURE GRADIENT
(MESH SIZE STUDY)

41

FIG. 5
Z DISPLACEMENT ERROR AT (A)
LINEAR TEMPERATURE GRADIENT
(ASPECT RATIO STUDY)

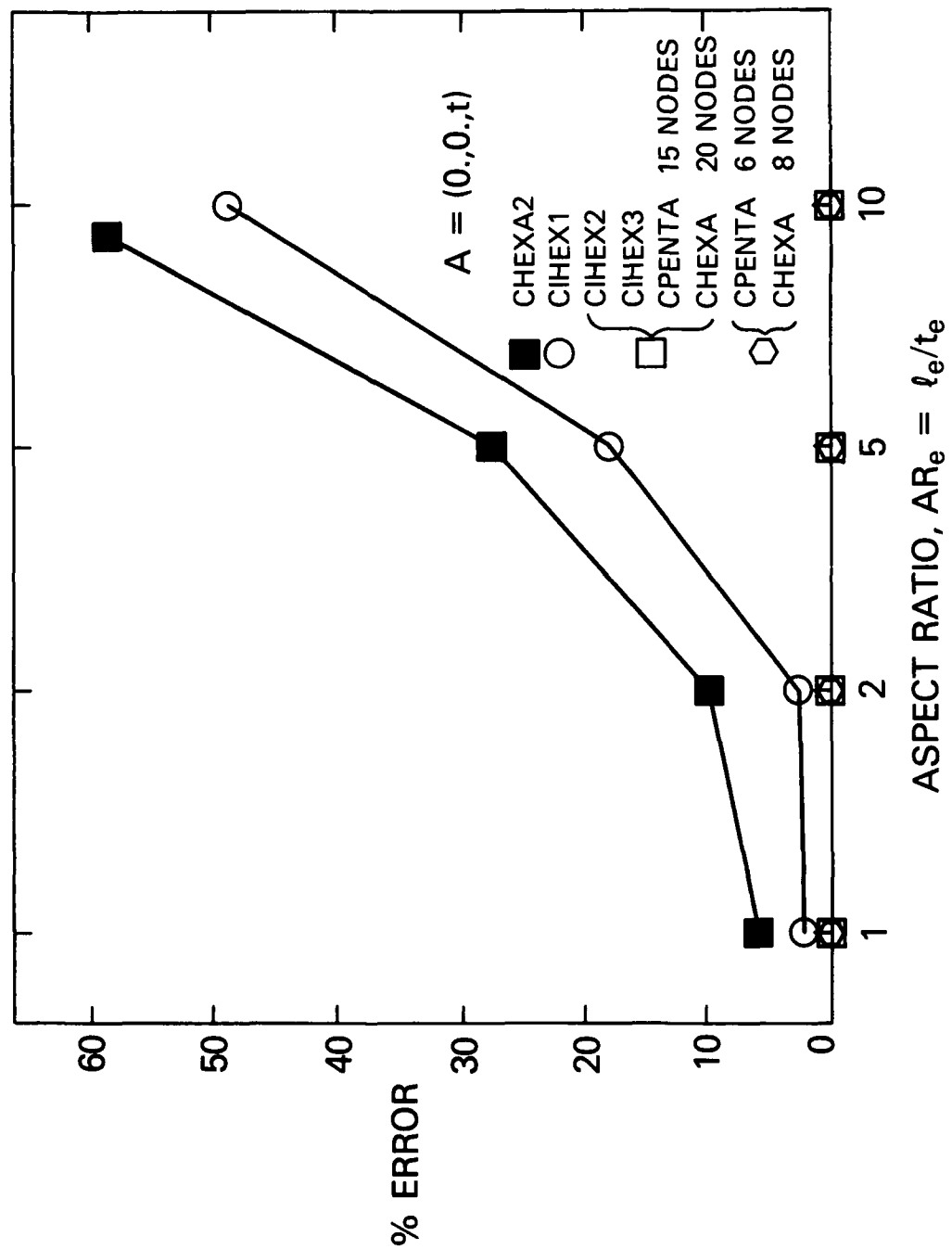FIG. 6

Z DISPLACEMENT AT (A)
THICK SLAB — GRAVITY

$\times 10^{-7}$

A = (0.,0.,t)

CIHEX2
CIHEX3
CHEXA 8 NODES
CHEXA 20 NODES
CPENTA 6 NODES
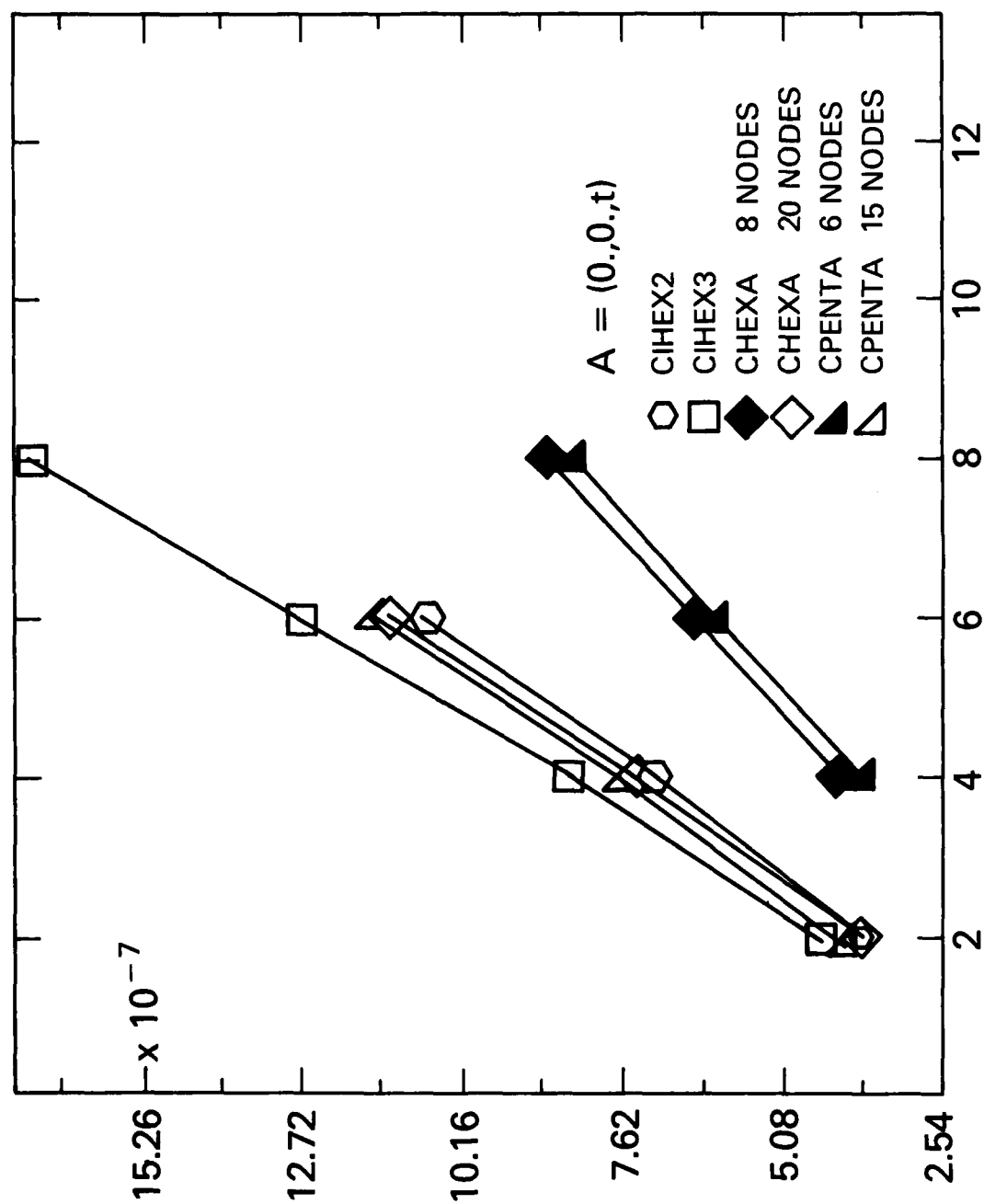CPENTA 15 NODES

FIG. 7
Z DISPLACEMENT AT (A)
THIN SLAB—GRAVITY LOADING
(MESH SIZE STUDY)

44
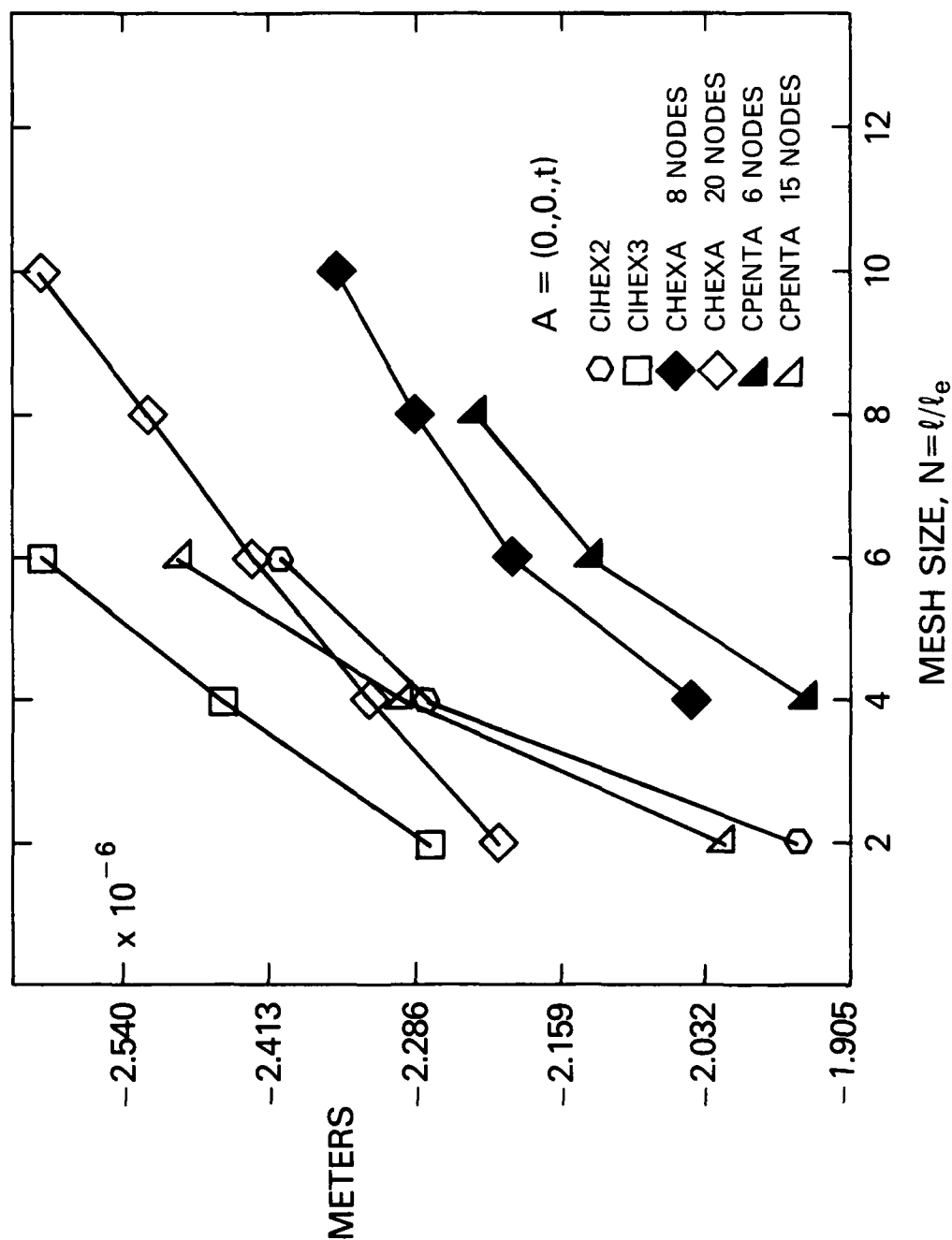
FIG. 8

Z DISPLACEMENT AT (B)
THIN SLAB – GRAVITY LOADING
(MESH SIZE STUDY)

$B = (-10., 0., t)$

◇ CIHEX2
□ CIHEX3
◇ CHEXA   20 NODES
△ CPENTA 15 NODES
⟨ CHEXA   8 NODES
⟨ CPENTA 6 NODES

MESH SIZE, $N = \ell / \ell_e$
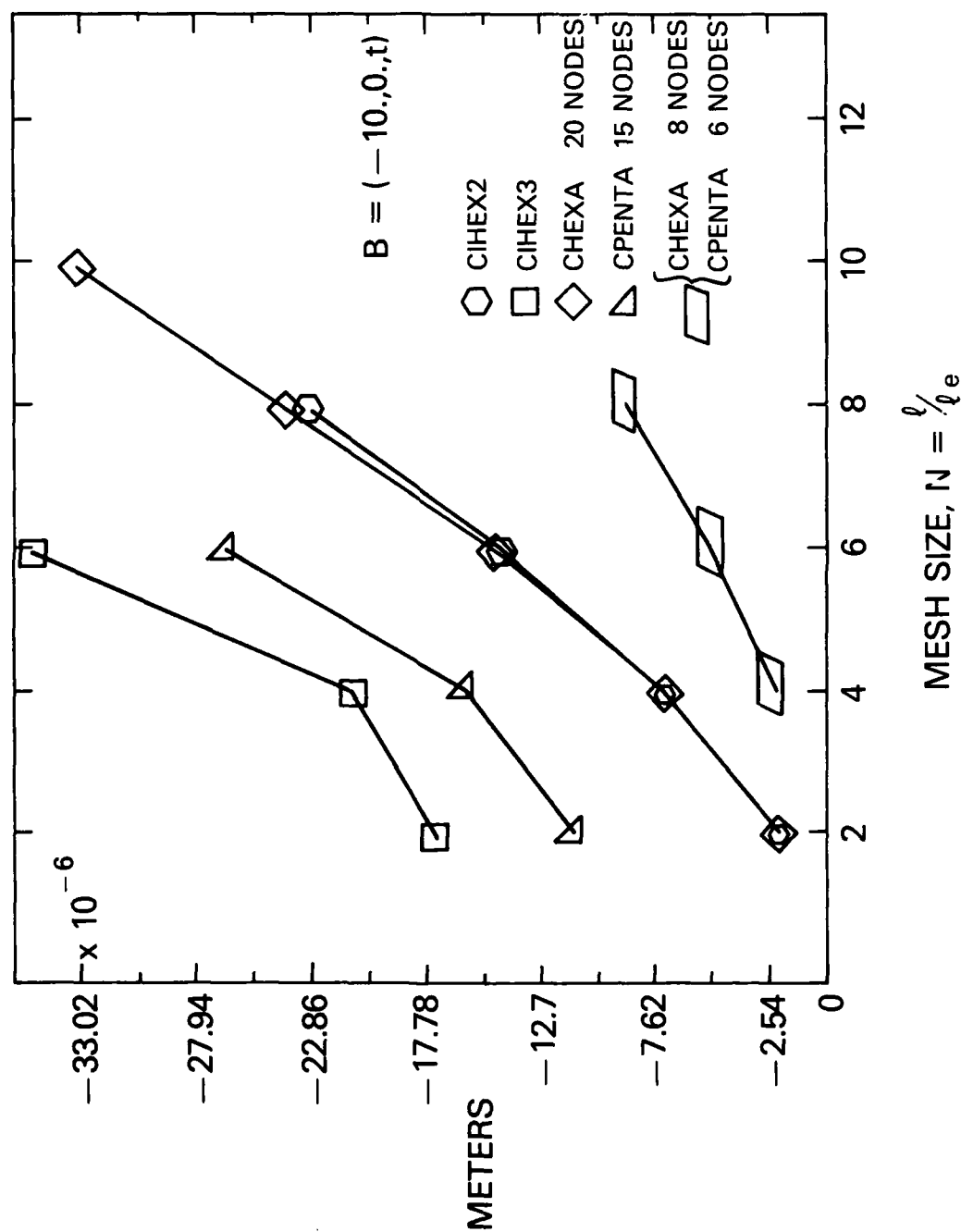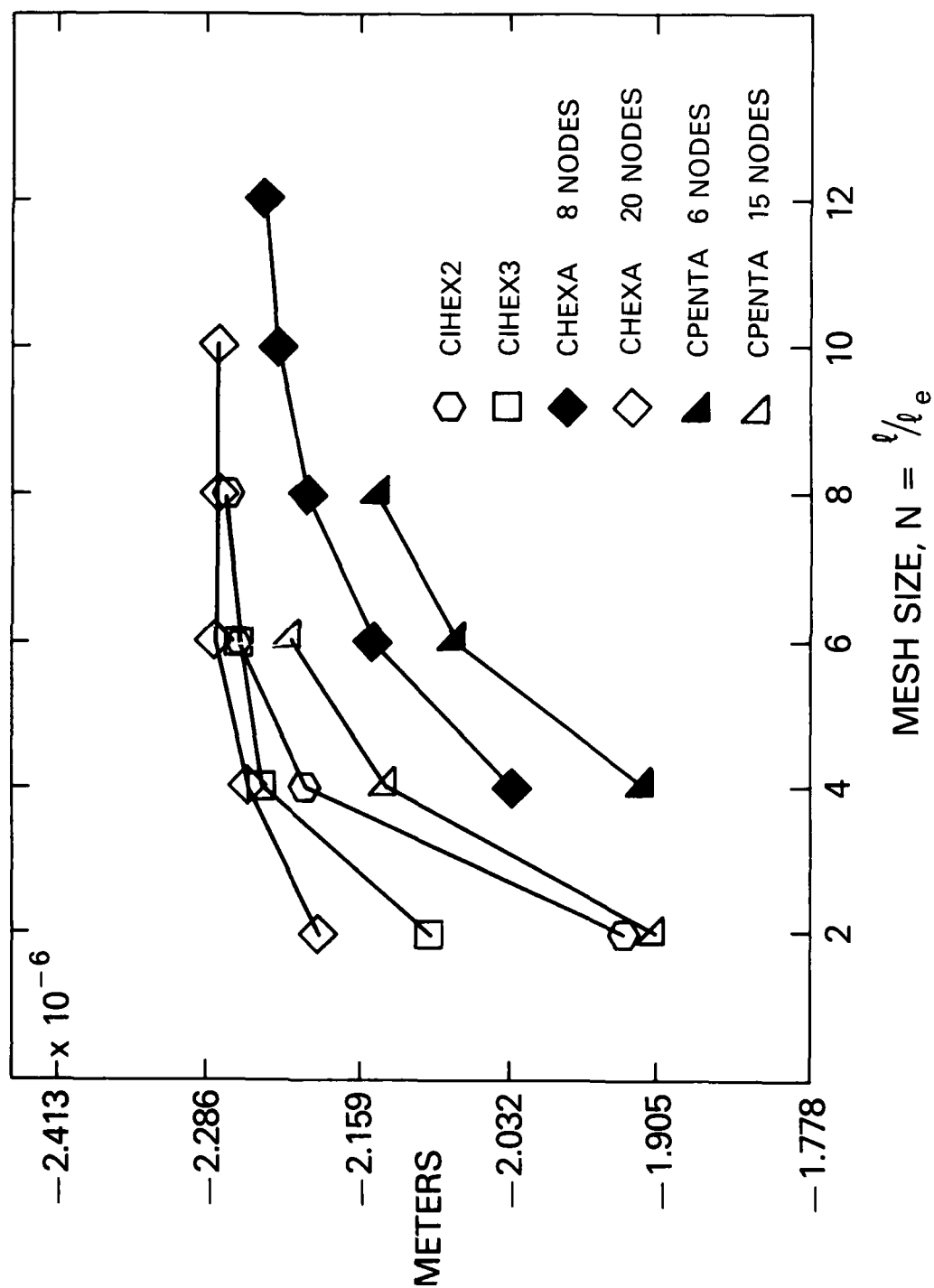
METERS

$\times 10^{-6}$

45

FIG. 9

RELATIVE DISPLACEMENT (A-B)

THIN SLAB—GRAVITY LOADING

(MESH SIZE STUDY)

COSMIC/NASTRAN® ON THE CRAY COMPUTER SYSTEMS

W. K. Brown and P. R. Pamidi
RPK Corporation

SUMMARY

RPK Corporation has converted COSMIC/NASTRAN to the CRAY computer systems. The CRAY version is currently available and provides users with access to all of the machine-independent source code of COSMIC/NASTRAN. Future releases of COSMIC/NASTRAN will be made available on the CRAY by RPK soon after they are released by COSMIC.

INTRODUCTION

RPK Corporation has converted COSMIC/NASTRAN to the CRAY computers that operate under the CRAY operating system (COS). RPK believes that NASTRAN users with CRAY computers desire to have COSMIC/NASTRAN available to them. With RPK's CRAY version, users have access to all of the features in the current release of COSMIC/NASTRAN. These features include not only the analysis capabilities offered by NASTRAN, but also the availability of the machine-independent source code, thereby giving users the freedom and ability for incorporating in-house modifications and enhancements to NASTRAN. It is RPK's commitment to make available and maintain future releases of COSMIC/NASTRAN on the CRAY. RPK will ensure that the CRAY version will always have all of the capabilities available on the latest COSMIC-maintained versions of NASTRAN.

ADVANTAGES OF A CRAY COMPUTER

The CRAY computer is established as one of the fastest computers in the world. The CRAY computer employs a pipeline architecture with scalar and vector processing capabilities (Reference 1). It is capable of a peak computational speed of at least 100 million floating point operations per second and has a central-memory bandwidth of one word per 12.5 nanoseconds, or 80 million words per second. The CRAY computer is highly compact and, because of this, signals can be carried from point to point in it at the velocity attainable with ordinary copper wire: about three-tenths the speed of light. The CRAY also has a very fast scalar speed. This scalar speed is a very dominant factor for programs that are not optimized for vectorization or for programs that do not lend themselves for significant vector optimization.

47

Figure 1 shows a generalized block diagram of the architecture of a vector computer similar to the CRAY computer. In this diagram, the instruction registers are read and processed by the pipelined instruction processor and the scalar registers are used by the pipelined scalar arithmetic and logic unit. The vector processor performs all vector processes. On the CRAY computer, there are five groups of registers: 8 address registers, 64 intermediate address registers, 8 scalar registers, 64 intermediate scalar registers and 8 vector registers containing 64 words each. In addition, the CRAY has 4 sets of 16-word buffers used for storing instructions.

Figure 2 shows the vector processor of a CRAY computer. It includes seven special-purpose pipelined units for executing specific functions. Three are shared with the CRAY's scalar processor. Several of the units can work concurrently on different vector operations. Vector data stream from the eight vector registers, through the functional units and back to registers. The steering module switches operands from the registers to the functional units and back again to the registers. While some registers are serving as sources or destinations of vector operations, others can be transferring data to or from central memory. Because of the register-to-register streaming of vectors, pipelines are short and start-up overhead is small.

One consequence of the register-to-register streaming of vectors is that the curve of efficiency (megaflops or millions of floating point operations per second versus vector length) shows peaks at vector lengths that are multiples of 64. This is shown in Figure 3. The peaks at vector lengths of 64 and 128 are there because there are 64 words in each set of vector registers and the CRAY operates most efficiently when all of these words are used. The curve drops off after 64 because of the time it takes to reload the registers with the next data to be processed (Reference 2).

DESIGN OF THE CRAY VERSION

The design of the CRAY version of COSMIC/NASTRAN is similar to that of the DEC VAX version. There are fifteen programs that correspond to the fifteen standard NASTRAN links. None of these programs contains an overlay structure. The fifteen programs dynamically chain themselves through the use of conditional job control language (JCL) (Reference 3). The I/O is designed to automatically allow for logical file extensions to additional physical files if space is exhausted on any given external file. This will ensure that no jobs are lost due to space limitations on one file.

RPK has designed the CRAY version to allow for easy maintenance and growth. There is no need for a special linkage editor nor for any other special software utilities other than those provided by COS. Users can update and modify the CRAY version using such standard CRAY-supplied utilities as BUILD (Reference 3) and UPDATE (Reference 4). The design also readily lends itself to the use of the Fortran Flow Trace capability (Reference 5). This capability is of immense help in accurately evaluating the performance of the code and in determining the areas of the code where improvements can be made using optimization techniques that will obtain the most benefits.

OPTIMIZATION OF THE CRAY VERSION

Several important areas of code in RPK's CRAY version have been optimized by using the vectorization techniques available on the CRAY. These include the decomposition, forward/backward substitution and multiply/add routines, certain eigenvalue extraction routines and others. The reduction in CPU times resulting from optimization in these areas of code has ranged from a minimum of about 50% to as high as 99%. RPK is committed to optimizing the entire spectrum of capabilities in COSMIC/NASTRAN. However, RPK regards this work as an continuing activity and expects to optimize the bulk of NASTRAN code in the near future.

CONCLUDING REMARKS

In developing the CRAY version of COSMIC/NASTRAN, RPK hopes to satisfy the needs of CRAY users who desire to use COSMIC/NASTRAN on the CRAY and may desire to have access to the machine-independent source code. RPK is fully committed to maintaining the CRAY version in such a manner as to be fully compatible and equal in capability with the latest COSMIC-maintained versions of NASTRAN.
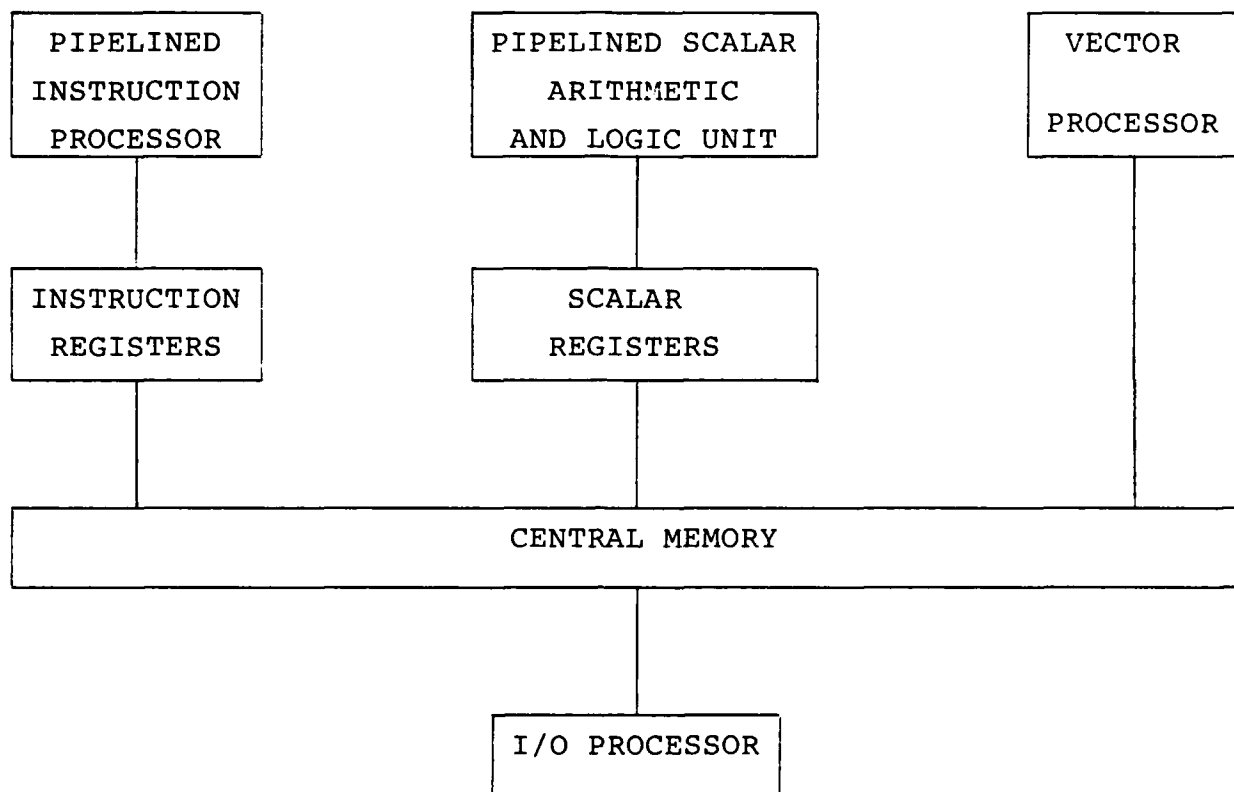
Figure 1. Generalized block diagram of a vector computer

SEVEN SPECIAL-PURPOSE
PIPELINED FUNCTIONAL
UNITS

SHARED WITH SCALAR
PROCESSOR

RECIPROCAL
APPROXIMATION

FLOATING-POINT ×

FLOATING-POINT +

POPULATION
COUNT

SHIFT

LOGICAL UNIT

FIXED +

STEERING MODULE

EIGHT VECTOR
REGISTERS
(64 WORDS EACH)

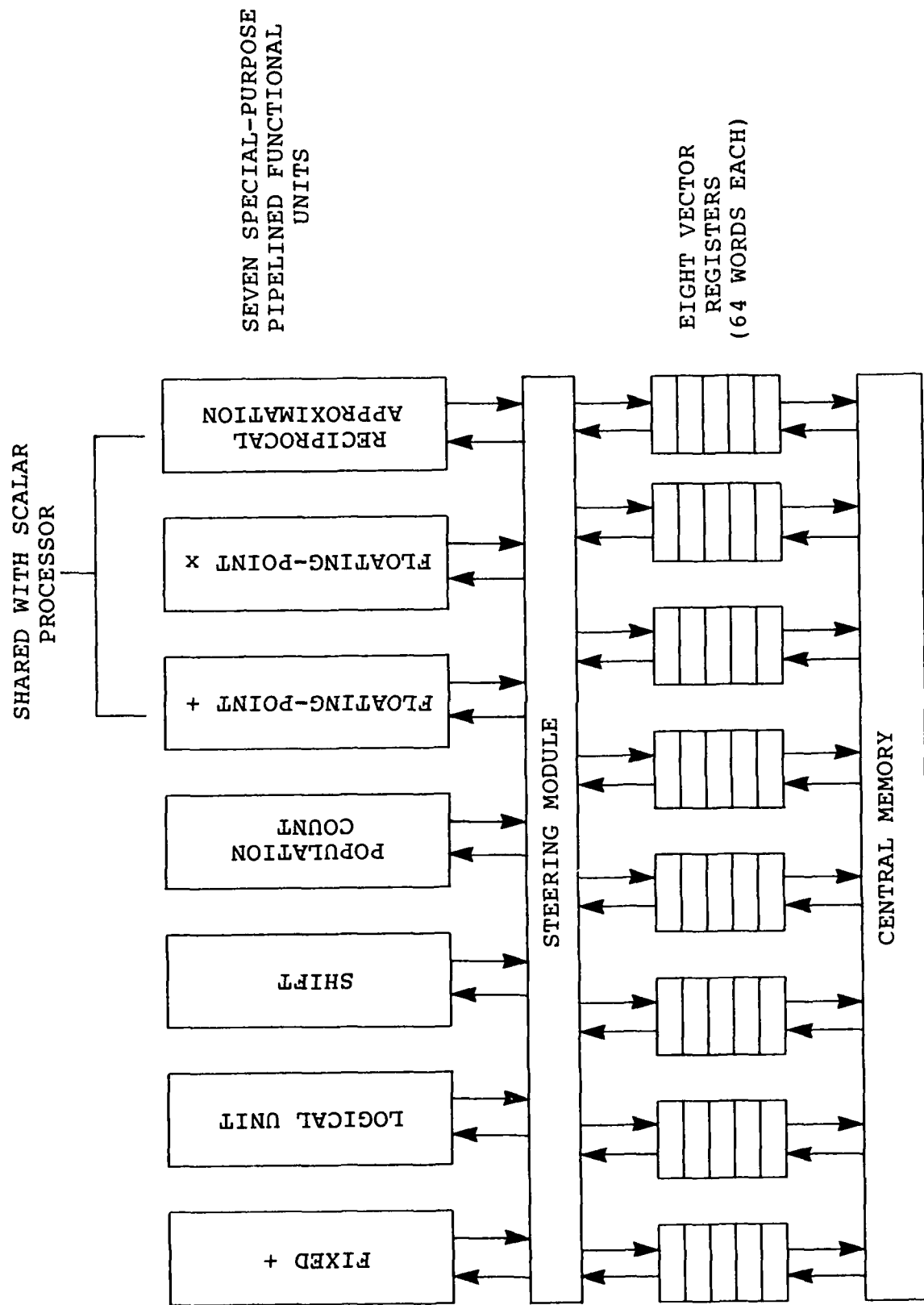CENTRAL MEMORY

Figure 2. Vector processor of a CRAY computer
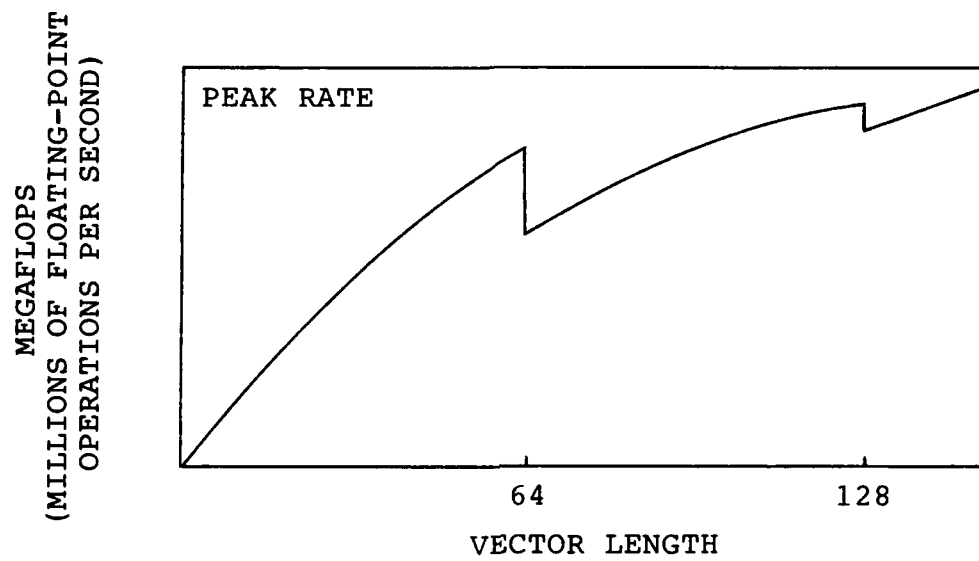
Figure 3. Vector processing on the CRAY

REFERENCES

1. Kozdrowicki, E. W., and Theis, D. J., "Second Generation of Vector Supercomputers", _Computer_, November 1980, pp. 71-83.

2. Levine, R. D., "Supercomputers," _Scientific American_, January 1982, pp. 118-135.

3. _Cray-OS Version 1 Reference Manual_, CRAY-1 Computer Systems, Cray Research, Inc., Publication No. SR-0011.

4. _UPDATE Reference Manual_, CRAY-1 Computer Systems, Cray Research, Inc., Publication No. SR-0013.

5. _Fortran (CFT) Reference Manual_, CRAY-1 Computer Systems, Cray Research, Inc., Publication No. SR-0009.

COMPUTER AIDED MODELING AND POST PROCESSING

WITH NASTRAN ANALYSIS

Robert R. Boroughs
Gates Learjet Corporation

SUMMARY

Computer aided engineering systems have become invaluable tools in performing NASTRAN finite element analysis at Gates Learjet. These techniques have been implemented in both the pre-processing and post-processing phases of the NASTRAN analysis. The finite element model development, or pre-processing phase, has been automated with a computer aided modeling program called Supertab, and the review and interpretation of the results of the NASTRAN analysis, or post-processing phase, has been automated with a computer aided plotting program called Output Display. An intermediate program, Nasplot, which was developed in-house, has also helped to cut down on the model checkout time and reduce errors in the model. An interface has been established between the finite element computer aided engineering (CAE) system and the Learjet computer aided design (CAD) system whereby data can be transferred back and forth between the two. These systems have significantly improved productivity and the ability to perform NASTRAN analysis in response to product development requests.

INTRODUCTION

When finite element analysis programs first began to be widely used in the late 1960's and early 1970's, there were generally many limitation on the size of the problem that could be run on many computers available in those days. Even some of the early virtual memory computers could be easily overwhelmed by the size of many finite element problems. Consequently, the effort required to obtain a single satisfactory run frequently involved a good deal of skill and persistence, and often times the process of obtaining a completed analysis became a real struggle. Thus, when the finite element solution was finally obtained, there normally was a good deal of satisfaction in terms of having an internal loads and stress distribution definition which was not available previously with this amount of accuracy and detail. However, as the years went by, larger and faster computers became available, and the turn-around time for finite element jobs decreased significantly. These new machines with expanded memories and the associated peripheral devices such as the disk drives had improved to the point where a large portion of the analyst's time was no longer spent solving system problems and trying to schedule enough computer resources to obtain a satisfactory run. As the improvements in computer hardware precipitated faster turn-around for finite element jobs, the demand for finite element analysis expanded to a wider range of projects and proposed structural configurations. Information was requested not only about the structural characteristics of a particular installation, but also about the trade-offs between various alternatives and modifications. This demand for more information put a stronger emphasis on compressing the input/output phases of finite element analysis. The input data for the finite element analysis needed to be prepared faster, and the results from the analysis then needed to be interpreted quickly to obtain a description of the configuration's structural characteristics. If the initial analysis generated questions that needed answers from

additional computer runs, then the process needed to be repeated quickly and efficiently to obtain the necessary data. As a result of these types of demands, an investigation was initiated at Learjet to find the tools and/or methods that would permit a more efficient generation and management of the finite element data base and allow the structures analyst to respond to requests faster.

BACKGROUND

One of the first alternatives explored to improve the productivity of the finite element input/output process at Learjet was a system of batch programs to generate NASTRAN bulk data and a max./min. search routine to identify highly stressed areas in the structure from the NASTRAN output. Automated data input batch programs were written to generate NASTRAN grid point, connectivity and property cards. These programs were used to create a large amount of data for many models over a period of about four or five years, but there were obvious areas for productivity improvements even in these routines. However, the development of interactive computer graphics hardware and software during the 1970's was a technology that appeared to offer many more significant advantages for further improvements in finite element input/output productivity than enhancement of existing batch programs. Consequently, Learjet began to emphasize interactive techniques for data base management as opposed to batch job techniques. The initial thrust into computer graphics began in 1975 with the development of an in-house program for NASTRAN model checkout. In 1977 consideration was given to expanding this routine to a complete computer aided modeling program, but at that time the resources and manpower were not available within the company to proceed with a project of this size. A search outside the company was then initiated that same year for an interactive graphics package for finite element modeling and post processing.

SYSTEM EVALUATION AND SELECTION

Two different approaches were evaluated as possible solutions to improving productivity in the input and output phases of NASTRAN analysis using interactive computer graphics. The first alternative was to access a computer aided modeling and post processing program on a service bureau computer using a telephone line connected to a graphics terminal at Learjet's engineering facility. The second alternative was to license or lease the software, and install this program on an in-house computer. Discussions were held with many service bureaus, software vendors and hardware manufacturers over a two year period. The main objective of this investigation was to find the right combination of hardware and software that would meet Learjet's analytical requirements and provide a significantly improved level of productivity. Some of the guidelines used in this selection process were as follows:

-Interface with NASTRAN
-Three dimensional geometry
-Mesh a cubic or higher order surface
-Control over node and element numbering
-Label integer size of at least 10,000,000
-Operation on a variety of computers
-Operation on a variety of terminals
-Maintenance and enhancement support
-Transmission and display rate of at least 9600 baud

55

Each graphics program and supporting hardware system evaluated usually had one or more unique characteristic. Some of these features were beneficial to improved productivity and flexibility while others were restrictive and limited the application of that particular system. After evaluating several computer aided systems, one major fact became obvious about all of these packages, and that fact was the relative infancy of this technology. The potential of computer graphics was immense compared to the capabilities that were reviewed during the evaluation period. Consequently, for a short period of time the best approach appeared to be to wait for these computer aided systems to mature. However, the initial results of the evaluation also indicated that the productivity advantages were available with many of the existing systems at that time, and many of these systems had a dedicated maintenance and enhancement staff that was incorporating corrections and improvements to the code regularly. Another important consideration was that a delay at this time in adopting this technology may have more severe consequences in the future when there may be more difficult problems to overcome. So the search continued for an interactive computer aided modeling and post processing system.

Another important fact evolved from this investigation, and this fact was that productivity appeared to be generally influenced by three major factors. These factors were the computer's capability in terms of size and speed, the magnification of human effort through the unique features in the software, and the speed at which a picture could be displayed on the graphics terminal screen. There may be some subdivisions of these categories, but these items were considered to be the main factors that most influenced computer graphic's productivity by Learjet. Since the modeling and post processing were to be basically interactive functions, a computer system was needed that could best provide quick responses to interactive commands. This meant that the computer could not be loaded with users and/or batch jobs to the point where response times became unacceptable. The interactive method of central processor unit (CPU) utilization was evolving, and this concept was very much incompatible with the existing philosophy of loading the CPU with as many time share jobs as possible to lower the unit costs. Some hardware manufacturers offered a solution to this problem by providing small low cost computers which could be located in the individual work areas. The interactive work was performed on the small work station, and then, if these data needed to be run on a large batch processor, the job could be transferred to a large machine for the analysis work. This type of system generally provided a very fast terminal display rate which some of the other systems could not always match. If several of these work stations were connected to the large computer and possibly even to one another, this system was referred to as distributed computing.

One arrangement which was found to have a very difficult time achieving high transmission rates was operation with a terminal connected to a computer located many miles from the user site. Sometimes these computers were extremely fast and had a great deal of memory and disk space, but the top speed over long distance telephone lines using modems generally restricted response times at the terminal. Eventually, technological improvements in modems and long distance communications may overcome this problem, but with the existing systems higher productivity has been restricted by the speed of data transmission. Consequently, Learjet concentrated on evaluating systems that could be installed on in-house computers and could achieve transmission and display rates of at least 9600 baud. This rate was established after working with other interactive systems and discovering that speeds lower than this value many times resulted in the user waiting unneces-

sarily for the system to return to a ready state.

Learjet was also seeking a program that could work easily with geometry defined by cubic or higher order equations. Many of the surfaces in aircraft structures have been defined by aerodynamic computer programs, wind tunnel testing or a combination of the two. Surface contours frequently are generated using spline fitting routines which define a higher order curve or equation using a series of points. A computer aided modeling program needed to have a great deal of flexibility in meshing complex surfaces and offer a large amount of user control over the grid point and element generation. Large amounts of data needed to be handled by the system without becoming unnecessarily awkward or being limited by system size restrictions.

Discussions along these lines were initiated with Structural Dynamics Research Corporation (SDRC) in the fall of 1978 in regard to the Supertab computer aided modeling program. This program seemed to fill many of Learjet's requirements, and an in-house evaluation of this program was negotiated in the first quarter of 1979 with a ninety day evaluation to be conducted in the second quarter of that year. The software was installed on a Digital Equipment Corporation (DEC) PDP 11/70 during the evaluation period basically due to the availability and easy access to this machine. A small storage tube graphics terminal was attached to the computer using a 9600 baud transmission line.

Many different problems were exercised with this system to determine the capabilities and limitations of the Supertab program. All of the trial cases tested on the system yielded results which generally met Learjet's requirements and expectations for a computer aided modeling program. Shortly after the completion of this ninety day in-house evaluation, Supertab was selected as the computer aided modeling program to be used by Learjet for NASTRAN finite element model generation, and negotiations were initiated with SDRC for the acquisition of this software.

HARDWARE ACQUISITION

One of the reasons that Supertab was selected for Learjet's computer aided modeling tasks was due to the support provided for several different computers and a wide range of terminal configurations. Since Learjet's analytical needs could be expected to change in future years, the company wanted a system that had the product support that would contend with these changes. Also hardware manufacturers frequently bring out new products with enhanced capability that make older equipment obsolete, and software maintenance was necessary to keep pace with the evolution of these new systems.

Although the in-house evaluation of Supertab was performed on a 16 bit PDP 11/70 mini computer, a larger 32 bit computer was planned for the permanent installation site. The 32 bit machine was decided upon over the 16 bit machine due to the limitation of the single precision integer size, or in other words, the gird point label and element label size on the small computer. An in-house IBM 370-158 was originally designated to be the host computer for this software, but this designation was changed when a VAX 11/780 was chosen as the system to replace the PDP 11/70.

During the ninety day evaluation of Supertab, limitations of the small storage type terminal became obvious. The most notable of these restrictions were the

small screen size and lack of hard copy and digitizing capability. If the full potential of this new system were to be realized, a terminal was needed with a larger screen and enhanced graphics capability. This terminal also needed to have a large bus for adding desired options to the system, such as, a hard copy unit and digitizer tablet. Consequently, a review of terminals available on the open market was conducted to determine what units would satisfy the company's requirements. During this review period which was basically most of 1979, there were no satisfactory refresh graphics terminals available, and effort was concentrated on finding a storage type cathode ray tube (CRT) terminal that would perform the desired functions and access various devices. Consequently, the selection process narrowed down to Tektronix equipment such as the 4014 and a new terminal called the MEG 121. The MEG 121 was very similar to the 4014, but many features that were optional on the 4014 were standard on the MEG 121. Also, the MEG 121 could be upgraded to a distributed system with the addition of a mini computer. Thus, the Tektronix MEG 121 was selected as the terminal device for access to Supertab, and the unit was installed in the first quarter of 1980. The lead time for the VAX 11/780 installation was somewhat longer than that for the MEG 121, and the installation of this machine was not scheduled until the second quarter of 1981.

SOFTWARE ACQUISITION AND DEVELOPMENT

Since there was a time frame of over a year between the installation of the MEG 121 graphics terminal and the VAX 11/780 computer, other alternatives were considered as temporary solutions to utilizing Supertab until the new computer installation could be completed and the engineering department was moved into a larger building. The most viable alternative appeared to be installation of Supertab on the PDP 11/70 mini computer until the VAX became available. This option would limit the size of model that could be generated on that system, and consequently restrict the projects which could benefit from this software, but the training and familiarization process could be completed and work could begin on some limited projects.

Arrangements were made for the installation and on-site training, and Supertab was installed on Learjet's PDP 11/70 mini computer. On-site training was accomplished using class room lectures supported by demonstrations on the MEG 121 terminal. Familiarization with Supertab then continued for the next several weeks on an individual basis, and shortly thereafter work started on the first project using Supertab for the computer aided modeling of a structure to be analyzed with NASTRAN.

The VAX 11/780 was installed on schedule and was operational within a few weeks. The engineering department moved into the larger building that same month, and the Supertab data base was transferred from the PDP 11/70 to the VAX 11/780. The move and data base conversion occurred in the period of just a few days, and within a week finite element modeling had resumed on the VAX 11/780 with only minor problems having to be overcome.

Shortly after the completion of the Supertab evaluation on the Learjet PDP 11/70 mini computer, SDRC announced a new computer aided post processing program for finite element analysis called Output Display. This program would use the results from a finite element analysis, such as displacements and stresses, and plot these data using the finite element model as the basis for the display. Displacements were added to nodal coordinates of the finite element model to

provide a deflected shape for a static analysis or a mode shape for a vibration or dynamic analysis. Stresses were plotted in contour form on the surface of a group of membrane or plate elements to provide a stress contour distribution on any desired structural surface. These stress contour plots could be created for both static analysis as well as dynamic analysis.

Since NASTRAN runs were being made more frequently and many models were becoming larger with more voluminous outputs, Learjet was very much interested in an efficient method for reviewing the results of a NASTRAN analysis and effectively managing the resulting data base. Output Display appeared to provide a solution to this problem. This program was directly compatible with Supertab and was integrated into the same program menu structure. Routines in the Supertab and Output Display program structures were modularized so that the user could actually transfer from one program to the other without leaving the main command stream.

The data interface between a finite element program and Output Display was accomplished through a conversion routine called the Data Loader. This program took finite element results that had been written to a disk file and converted these data to a universal file which was suitable for input to the Output Display program. Since there were several finite element programs supported by SDRC on a wide range of computers, SDRC was involved in writing a Data Loader program for each machine that was supported by a given finite element package. Some finite element programs had completed Data Loader routines available, but the Data Loader routine for Cosmic NASTRAN had not yet been written, and the status of this project was in a state of flux. After discussing this situation with SDRC, an agreement was reached where Learjet was designated as a development site for the Cosmic NASTRAN Data Loader project. SDRC provided Learjet with a copy of the Output Display program and a copy of the Data Loader source code for a similar finite element routine. Learjet agreed to acquire the Output Display program if a satisfactory Data Loader Interface could be developed between Cosmic NASTRAN and Output Display, and the Output Display program met Learjet's graphics requirements.

Development of a Data Loader for Cosmic NASTRAN began on a time available basis. There were quite a few major projects in work at that time and only a limited amount of manpower available. The Data Loader for Cosmic NASTRAN was to be developed by extensively modifying the template type Data Loader routine furnished by SDRC. A portion of this work was done in conjunction with the Bendix Corporation which was also working on the development of interfaces between SDRC programs and Cosmic NASTRAN. All the modifications and checkout was completed within a few months. The Output Display program performed up to expectations, and this module was then added to the computer aided engineering system with Supertab. A more detail discussion of the activities involved in this project has been described in the next section of this paper.

IMPLEMENTATION

Once the modeling has been completed, Supertab offered a great deal of flexibility in the way a finite element model can be transformed from the Supertab data base to the NASTRAN or finite element data base. The analyst can output the model using a table format, or the transformation can be accomplished with the Data Formatter module which permits output using a Fortran format. This user oriented approach allows the operator to establish mnemonics, field locations, field sizes, labels, integer values, real values or floating point values for the finite element data. Other features include grid point sequencing on the

connectivity card, batch job control card input, executive and case control card input, loads data input, property card and material card input and constraint card image generation. This routine is adaptable to the point where almost any finite element deck format could be generated using this approach. Output from Supertab through the Data Formatter module is defined by a command file which specifies the grid point connectivity card image format as well as other data that can be copied into the finite element file. If all the parameters and data have been defined by the Data Formatter for the NASTRAN executive control deck, case control deck, and bulk data deck, this file as output from the Data Formatter could be submitted directly for a NASTRAN batch job execution.

At Learjet a NASTRAN file generated by the Data Formatter module has generally not been submitted to the batch computer immediately after the transformation from Supertab. Since there is a possibility for error in the user written command file, a thorough check has normally been performed before going further with the new NASTRAN file. A major portion of this cross check has been accomplished using the NASPLOT graphics program which has been developed by Learjet over the years to support NASTRAN analysis. NASPLOT does not have as many of the sophisticated modules that Supertab utilizes, but this program can provide a very good check on grid point locations and element connectivity by plotting the NASTRAN bulk data deck. This program has currently been made operational on the VAX 11/780 computer and has been able to handle bulk data decks of Learjet's largest models without any major problems.

NASPLOT has a full NASTRAN library of elements and can also handle multiple, stacked local coordinate systems. NASTRAN files can be plotted interactively on the Tektronix MEG 121 terminal and hard copy plots can be obtained by using a screen image plotter (see Figure 1) or by spooling the plot files to a Versatec plotter. This program utilizes the refresh buffer on the MEG 121 for menu selection much as does Supertab. The master menu and sub menus can be scanned and parameters selected without erasing or having to repaint the screen. Large NASTRAN files can be plotted easily by identifying groups with a limited number of elements, and these groups can then be constrained to produce even smaller groups so local areas can be viewed more clearly (see Figure 2). If too many elements were eliminated in the constrained group, other elements can be added to the group to expand the viewing range. This type of approach allows the user to view a very complex model without having detail areas obscured by large numbers of adjacent grid points and elements. Also, the analyst does not have to divide the model into smaller substructures to fit the plot routine size restrictions and then be required to reassemble the model, if changes have been made in the substructure. If the changes are not complex or extensive, the modifications can be made directly in the NASTRAN bulk data deck using the VAX edit routine, and verification of the changes can be accomplished with the NASPLOT routine. The NASPLOT program does not have the extensive computer aided model generation capabilities of Supertab, but this package has served as a valuable checkout tool for NASTRAN bulk data decks before a file has been submitted for batch computing.

Another progam developed at Learjet to provide an interface between existing NASTRAN bulk data decks and Supertab was a program called NASUPER. This routine was written basically to convert an existing NASTRAN bulk data deck to a Supertab universal file. Input to NASUPER consisted of a NASTRAN bulk data deck, and the output from NASUPER was a Supertab universal file which included coordinate system data, grid point data, and element connectivity data. The universal file generated by NASUPER could then be loaded into a Supertab permanent data base

60

where extensive modifications or additions could be incorporated in the model. Upon completing the changes to the existing model with the aid of Supertab, these data could then be transformed to a NASTRAN file again using the Data Formatter routine or the table output module. If there was a significant amount of the model unchanged from the original configuration, this portion of the model remaining in the Supertab data base could be recovered from the original bulk data deck with all the associated property cards, material cards, forces and constraints. This can be accomplished through another module in the NASUPER system where the modified NASTRAN model output from Supertab was compared to the original bulk data deck. Those original members remaining after the Supertab modification were sorted into the new file which contains all the data cards for a NASTRAN analysis with the exception of the property and material cards for any newly added or modified structural members.

When Learjet acquired the Supertab package, the Output Display program which plots finite element displacements and stresses had only been available for a short time, and a Data Loader interface had not yet been developed for Cosmic NASTRAN. As indicated in the previous section of this paper an agreement was reached on the development of a Data Loader where SDRC would provide Learjet with a Data Loader package for a similar finite element code and Learjet would modify and enhance the program so that Output Display would accept Cosmic NASTRAN data.

The first task in this project was to generate the model displacement and stress data using the OUTPUT2 unit in NASTRAN. A set of DMAP alter cards were inserted into the executive control deck of a NASTRAN test deck, but after several attempts there were no data coming through this port for any of the runs. A telephone call was made to Cosmic describing this problem. The support personnel at Cosmic indicated that some updates had not been implemented in the OUTPUT2 module, and this caused the unit not to pass data. Cosmic promptly indicated the necessary corrections to the OUTPUT2 module and offered to provide any additional assistance necessary. These changes were made in the Learjet source code, and the modified routine was compiled and linked into the NASTRAN execuatable code on Learjet's IBM 3033. The test NASTRAN model was resubmitted with the same DMAP alter cards (see Figure 3), and data began to flow from the OUTPUT2 port. This problem occurred in NASTRAN level 17.7 and the later releases now have corrected this problem.

Initial data extracted from the OUTPUT2 module in NASTRAN was from a solution 1.0 statics analysis. The prototype Data Loader was modified and enhanced using these data as an initial checkout tool, and then data from a dynamics analysis solution 3.0 was used to facilitate a vibration analysis checkout. The prototype Data Loader had an element library which recognized some basic finite element members, but this library had to be modified and expanded to accept elements from Cosmic NASTRAN. This conversion was the second task of the Data Loader project. The conversion was accomplished by adding the new elements to the element table and also adding a subroutine for each new element to write the NASTRAN data to a universal file. The third task in this project was to modify the Data Loader to read and identify data from the OUTPUT2 file, and this part of the development took the most time. Source code in the Data Loader had to be modified and/or have lines added to read the NASTRAN data in the proper format, identify the type of data, and convert these data properly for input into Output Display.

Since the DMAP alters had already specified the sequence in which the data was to be output from NASTRAN, this arrangement of data in the OUTPUT2 file

helped to organize the direction of the modification of the Data Loader into related modules and subroutines within the main program. The first series of modules converted were related to the grid point and element definition in the base model. The second series of subroutines modified were related to displacements, and the third series of modules were related to the stress data. Once these corrections and enhancements had been incorporated, the checkout of test problems proceded with very little difficulty. Eventually larger problems were tested using the Output Display program, and the dimensions on the data loader had to be increased, but no other changes than these have been incorporated, since completion of the original modification and enhancement effort. Once the checkout was completed for static analysis problems, a dynamics analysis was performed on a test model using the FEER (see Ref. 1) method in NASTRAN. Data from NASTRAN was run through the Data Loader without any problems, and mode shapes and stress contours for each mode were plotted quickly with Output Display. Since the completion of the Data Loader modification, this program has been used successfully with the updated and enhanced releases of both NASTRAN and Output Display without any problems.

CAD SYSTEM INTERFACE

Geometry definition for a NASTRAN model prior to the acquisition of Supertab was accomplished generally by manually measuring loft drawings. These data were then either key punched on to NASTRAN grid cards, or a small Fortran computer program was written to generate intermediate points between two cross sections using linear interpolation. With Supertab, input of geometry data has been very flexible and could be accomplished using one of several methods. Data could be input directly from the keyboard into the Supertab data base, or several key geometry points could be entered and other points could be generated by interpolating between the established points. If there were areas of uniformity or symmetry in the structure, grid points could be generated using copy or reflection techniques. Supertab also has the capability to accept data from a small or large digitizer tablet. Learjet installed a large digitizer tablet with the MEG 121 terminal, and data from existing drawings has been entered into the Supertab data base for some of the preliminary and conceptual NASTRAN models.

About the same time that the Supertab CAE system was installed for finite element analysis at Learjet, a computer aided design (CAD) system was also being acquired in Learjet's design department. This CAD system was the Unigraphics software package which operates on a Digital PDP 11/70 mini computer. Unigraphics was developed by McDonnell Douglas Automation Company, a division of McDonnell Douglas Corporation, commonly called McAuto. The number of trained users on this system and the number of drawings in the data base has grown significantly in recent years. The drawings in this sytem have generally been more accurate and required fewer manhours to produce than previous drawings. The CAD data base has grown to the extent that several NASTRAN finite element models have been generated by transferring CAD geometry to the Supertab system. Access to this type of information has further compressed the time required to develop finite element models, and in some situations has permitted the generation of a NASTRAN model that would have been impractical or very time consuming using manual techniques.

Development of a Supertab/Unigraphics interface has evolved over a period of months and years, since these systems first began operation. Many discussions have been held with the Unigraphic's users as to the best methods of transferring

data between these two units, and meetings have been continuing in an attempt to improve existing techniques. The method of data transfer currently in use at this time involves a Unigraphics support program called GRIP. The GRIP system allows Unigraphic's users to write small routines or command files which transform the CAD data into any format desired by the user. These data have then been transferred to the VAX 11/780 where the files can be copied into a Supertab data base. Since the file format can be defined in the GRIP routine, geometry data has normally been written as NASTRAN grid points and local coordinate systems have been defined in CORD2C, CORD2R, or CORD2S (Ref. 1) formats. The use of this type of format saves a significant amount of time in the model generation using Supertab. This approach allows the user to skip the geometry definition routine which basically creates points, lines, arcs, curves, and surfaces.

Other methods have been investigated in transferring data between Unigraphics and Supertab, and in the future one of these alternatives may replace the current method. One technique presently under consideration is the IGES, or Initial Graphics Exchange System, format devised by the National Bureau of Standards. Supertab has the capability to extract geometric data from an IGES file and use these data for finite element model development. However, the details of generating these types of data on the Unigraphics system still have to be worked out. Another alternative being considered for speeding up the transfer of data between the two systems has been to connect the PDP 11/70 and VAX 11/780 computers using the DECNET computer network system developed by Digital Equipment Corporation.

PROJECT APPLICATIONS

Since Supertab and Output Display were installed at Learjet, many projects have benefitted from the usage of these packages. One of the first projects to use Supertab for finite element model development was a composite spoiler project. This spoiler was fabricated from graphite epoxy, fiberglass, and nomex honeycomb with three aluminum hinges located along the spoiler leading edge. These hinges attached the spoiler to the rear spar of the Learjet wing, and the center hinge also served as the actuator point for raising and lowering the spoiler (see Figure 4). Although at first glance the mesh may appear uniform along the span, the grid point definitions actually conform to the location of several layered doublers at the three fitting locations as well as to the geometry of these aluminum fittings. Layout of this mesh was defined before ever sitting down at the terminal to begin work, and then when modeling did begin using Supertab, the grid point and element generation went quickly with very few areas that required correction.

The grid points and element connectivity were transformed from the Supertab format to NASTRAN bulk data format using the Data Formatter module in Supertab. This transformation consisted of writing a command file which defined the NASTRAN format. Section properties, material properties, loads and constraints were added to this file, and then a NASTRAN analysis was performed by submitting the file as a batch job on Learjet's IBM 3033. After the Output Display module was made accessable by the development of the Cosmic NASTRAN Data Loader routine, a second NASTRAN analysis was performed with the appropriate DMAP alter commands in the executive control deck (see Figure 3) for extracting data from the OUTPUT2 unit in NASTRAN. These data were processed through the Data Loader into a universal file format and input to the Output Display program. An example of a static deformation plot and stress contour plot from this analysis can be seen in Figures 5 and 6, respectively.

Another application of Supertab and Output Display to NASTRAN analysis was the modification of a conventional Learjet tip tank (see Figure 7) to a special missions tip tank configuration. The major difference between the special mission tip tank and the conventional tip tank was the addition of a radar unit in the nose of the new tip tank. This structural change basically involved making the diameter of the forward portion of the tip tank larger and installing a fuel tight bulkhead aft of the new radar unit.

A NASTRAN model of the conventional tip tank was already in existence at the beginning of this project, and one of the major tasks for the finite element analysis was to modify this tip tank to the special mission configuration. The bulk data deck for the conventional tip tank was converted to a Supertab universal file format by processing the data through the NASUPER routine. Once these data were in the Supertab data base, conversion to the new configuration took only a few hours (see Figure 8). The modified tip tank was output from Supertab and incorporated in the NASTRAN wing model replacing the conventional tip tank, and new loads were added to the file to reflect the changed configuration. A NASTRAN analysis was performed on this updated model, and the deflection and stress data were output through the OUTPUT2 unit and tranformed by the Data Loader for review with Output Display. Plots of the stress contour data can be seen in Figure 9.

A third application of Supertab to NASTRAN finite element model development was the generation of a composite outboard main landing gear door model. This structure was fabricated using laminated graphite epoxy on the inner and outer surfaces with a nomex honeycomb core. The geometry of this installation was quite complex, since the contours had to reflect the curvature of the wing, the fairing of the door around the tire, and the fairing around the actuator support point on the landing gear trunion. Loft data specifying the contour of the inner and outer surfaces were defined using the Unigraphics computer aided design system. These data were then transferred to the Supertab data base utilizing the GRIP routine discussed earlier.

Layout of the gear door model was defined before any work began at the graphics terminal. Consequently, when the Supertab modeling did commence, the time required to complete the finite element definition was less than a week. Data in the Supertab data base were then transformed to a NASTRAN bulk data deck format using the Data Formatter module. Section properties, material properties, loads and constraints were added to the file along with an appropriate set of batch run JCL. A statics solution 1.0 NASTRAN analysis was performed on these data, and the results were plotted using the Output Display module. The deflection and stress contour plots can be seen in Figures 10 and 11. A vibration analysis was also performed on the door model using NASTRAN solution 3.0 with the FEER method of eigenvalue extraction. A plot of one of these mode shapes has been shown in Figure 12.

CONCLUDING REMARKS

Computer aided modeling and post processing has significantly improved the ability to perform NASTRAN finite element analysis at Learjet. These techniques have reduced the time required to prepare NASTRAN models and review and interpret the data from a NASTRAN analysis. This improvement in productivity has permitted a faster response to product development questions and has allowed a wider range of configurations to be investigated during preliminary design exercises. Conse-

quently, the structural characteristics of a given configuration can be identified in more detail sooner than was ever possible using manual methods.

REFERENCES

1. The NASTRAN User's Manual (Level 17.5), NASA SP-222(05), Washington, DC, December 1978.

MODEL 55 WING, FUSELAGE AND VERTICAL TAIL STRUCTURE   3-8-82
NASBUILD: 11-OCT-83   18:00:47   NASPLOT: 15-DEC-83   00:28:34
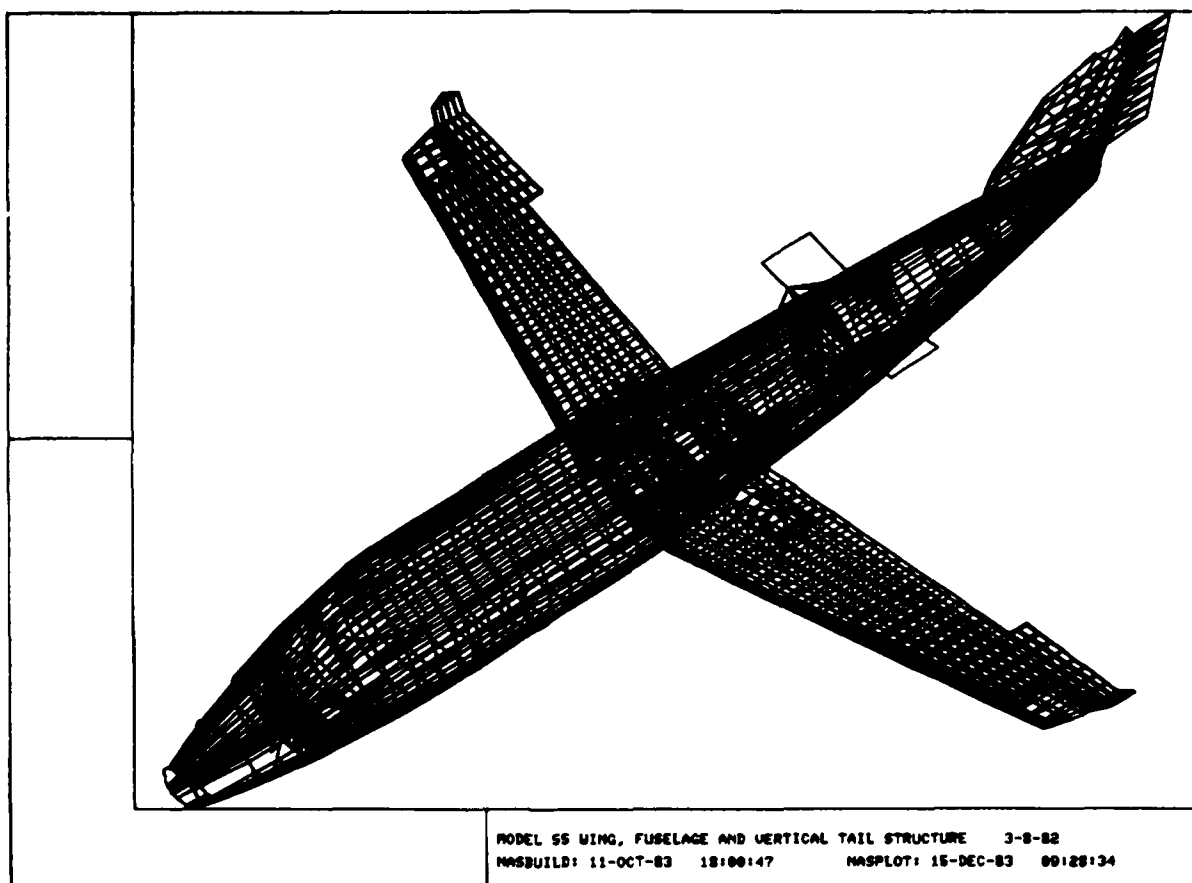
FIGURE 1 - NASPLOT SCREEN IMAGE

MODEL 55 WING, FUSELAGE AND VERTICAL TAIL STRUCTURE   3-8-82
ALPHA = 45.0 DEG.   BETA = 180.0 DEG.   GAMMA = -135.0 DEG.
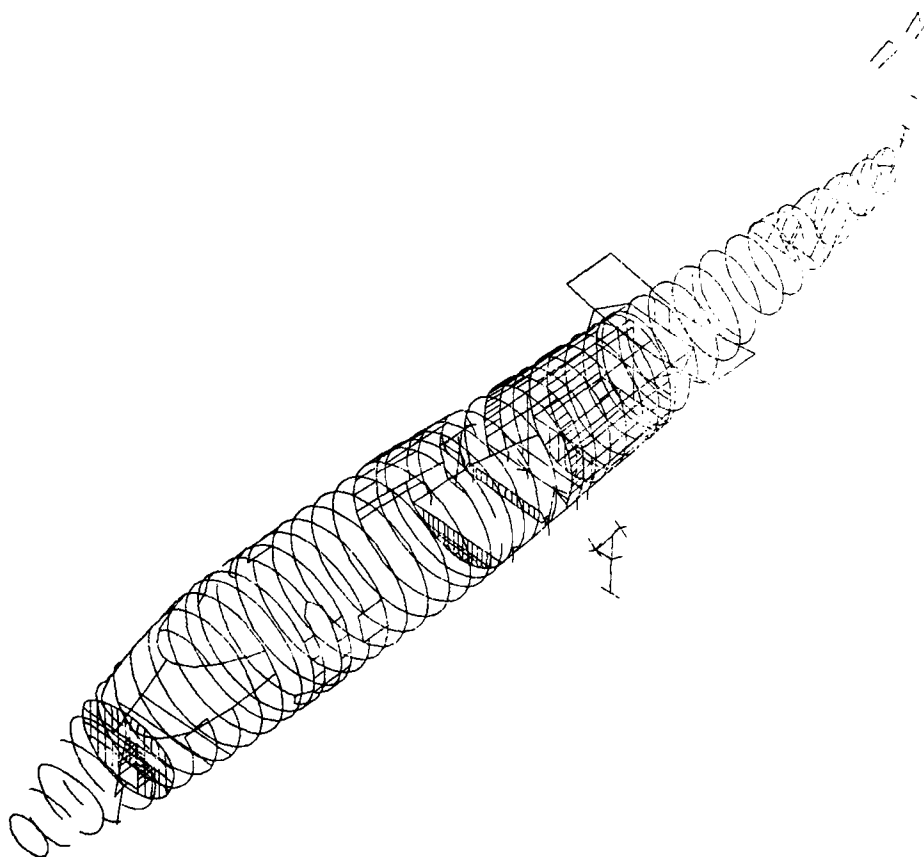NASBUILD: 11-OCT-83 18:00:47   NASPLOT: 16-JAN-84   10.59.41

FIGURE 2 - NASPLOT CONSTRAINED ELEMENT GROUP

```
ID NASTRAN USER
APP DISP
SOL 1,3
DIAG 14
ALTER 106
OUTPUT2   CSTM,GPL,GPDT,GEOM2, //0 $
OUTPUT2   OUGV1,OES1,,, //0 $
OUTPUT2   ,,,, //-9// $
ENDALTER
TIME 180
CEND
```

FIGURE 3 - NASTRAN DMAP ALTER CARDS

COMPOSITE SPOILER ANALYSIS   8-12-83
ALPHA = 60.0   DEG.   BETA = -20.0 DEG.   GAMMA = 60.0   DEG.
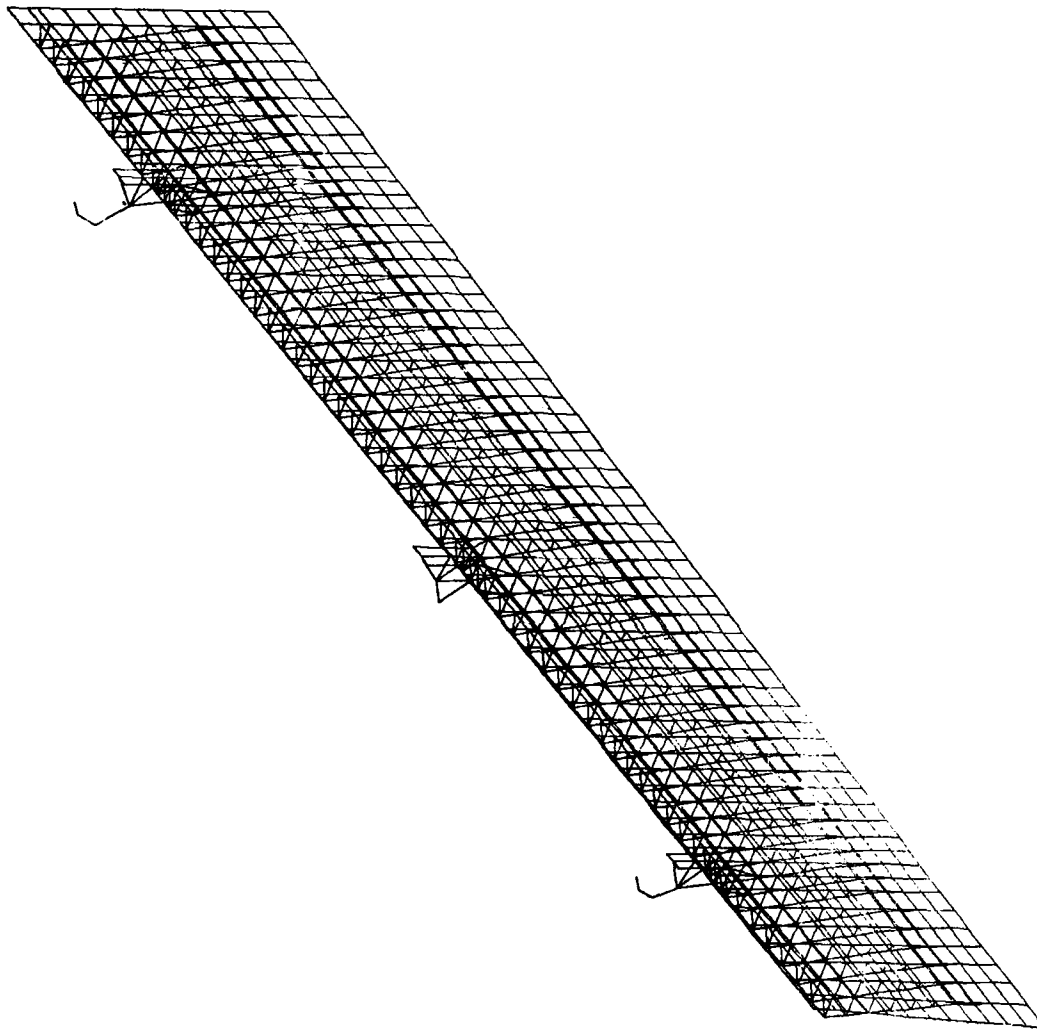NASBUILD: 17-DEC-83   17:46:04   NASPLOT: 23-DEC-83   14:10:15

FIGURE 4 -   COMPOSITE SPOILER NASTRAN MODEL

FIGURE 5 - COMPOSITE SPOILER STATIC DEFORMED SHAPE

SDRC/OUTPUT DISPLAY 3.11   15-SEP-82 15:18:29
COMPOSITE SPOILER REDESIGN (133(ULT DWN LOAD) 1-23-82
MAXIMUM PRINCIPAL STRESS TOP SURFACE
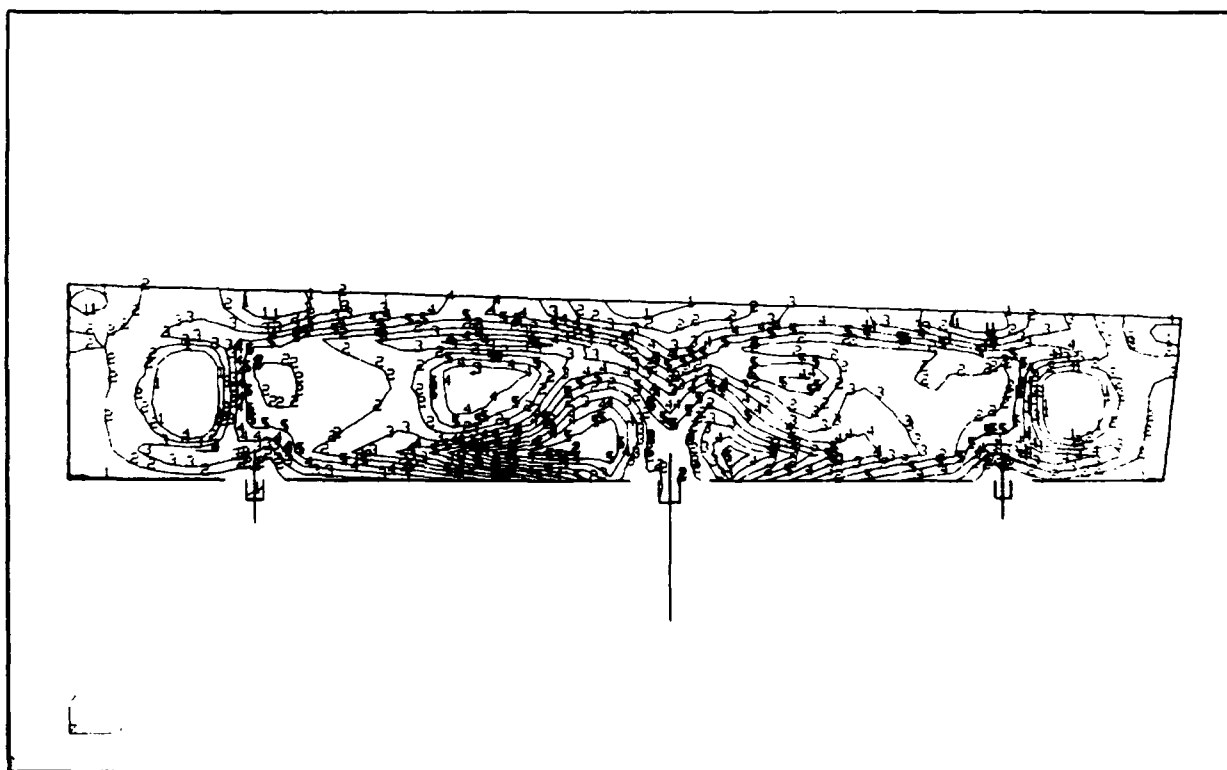
FIGURE 6 - COMPOSITE SPOILER STRESS CONTOURS

71
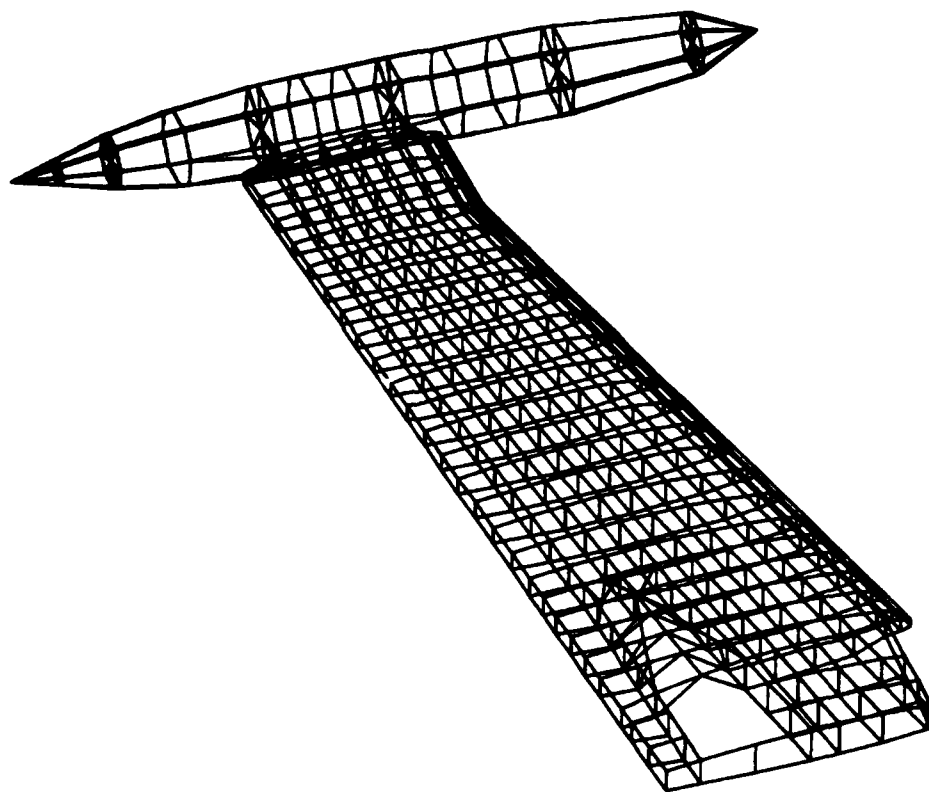
MODEL 35/36 WING STRUCTURE 10-25-78
NASBUILD: 9-JAN-84 10:58:54   NASPLOT: 25-JAN-84 09:26:12

FIGURE 7 - M35/36 WING NASTRAN MODEL WITH CONVENTIONAL TIP TANK
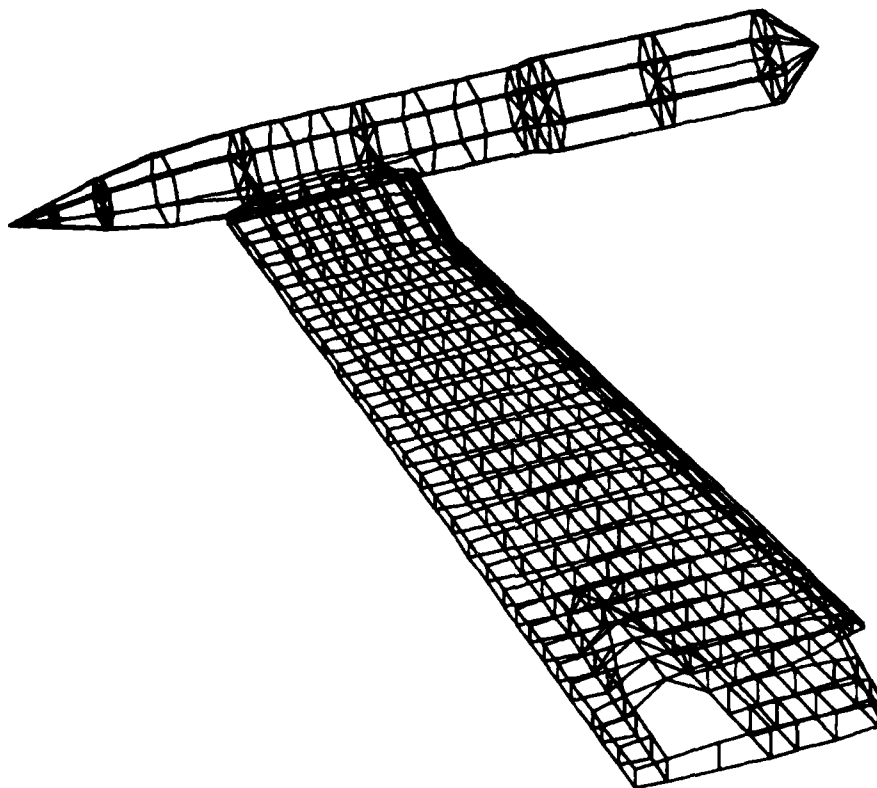
FIGURE 8 - M35/36 WING NASTRAN MODEL WITH SPECIAL MISSION TIP TANK
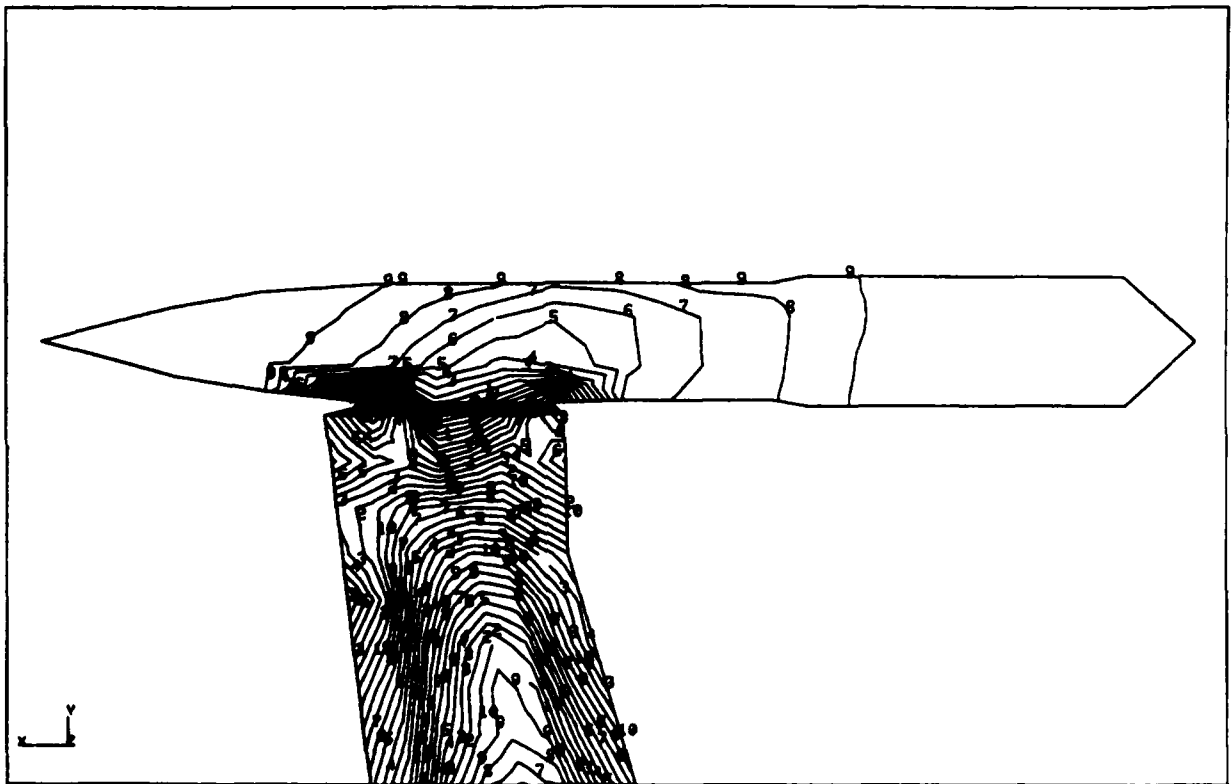
FIGURE 9 - STRESS CONTOURS FOR SPECIAL MISSION WING CONFIGURATION
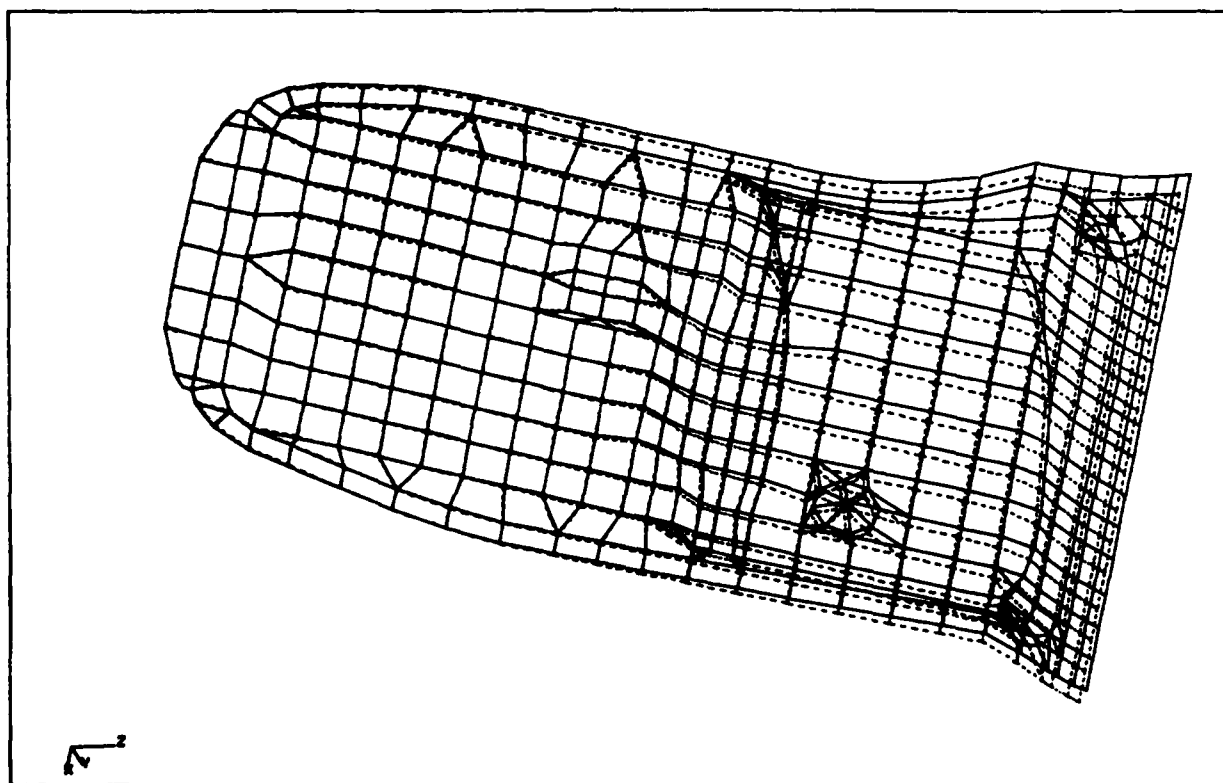
FIGURE 10 - COMPOSITE GEAR DOOR STATIC DEFORMED SHAPE
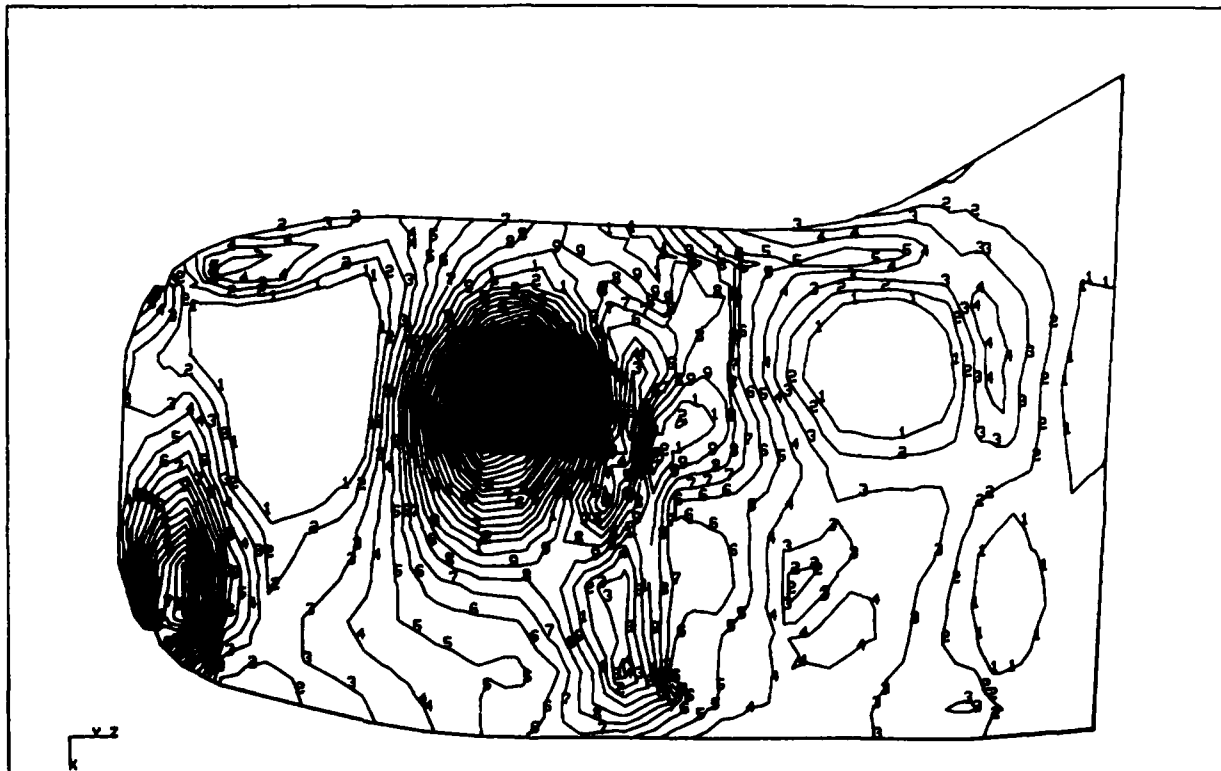
FIGURE 11 - COMPOSITE GEAR DOOR STRESS CONTOURS
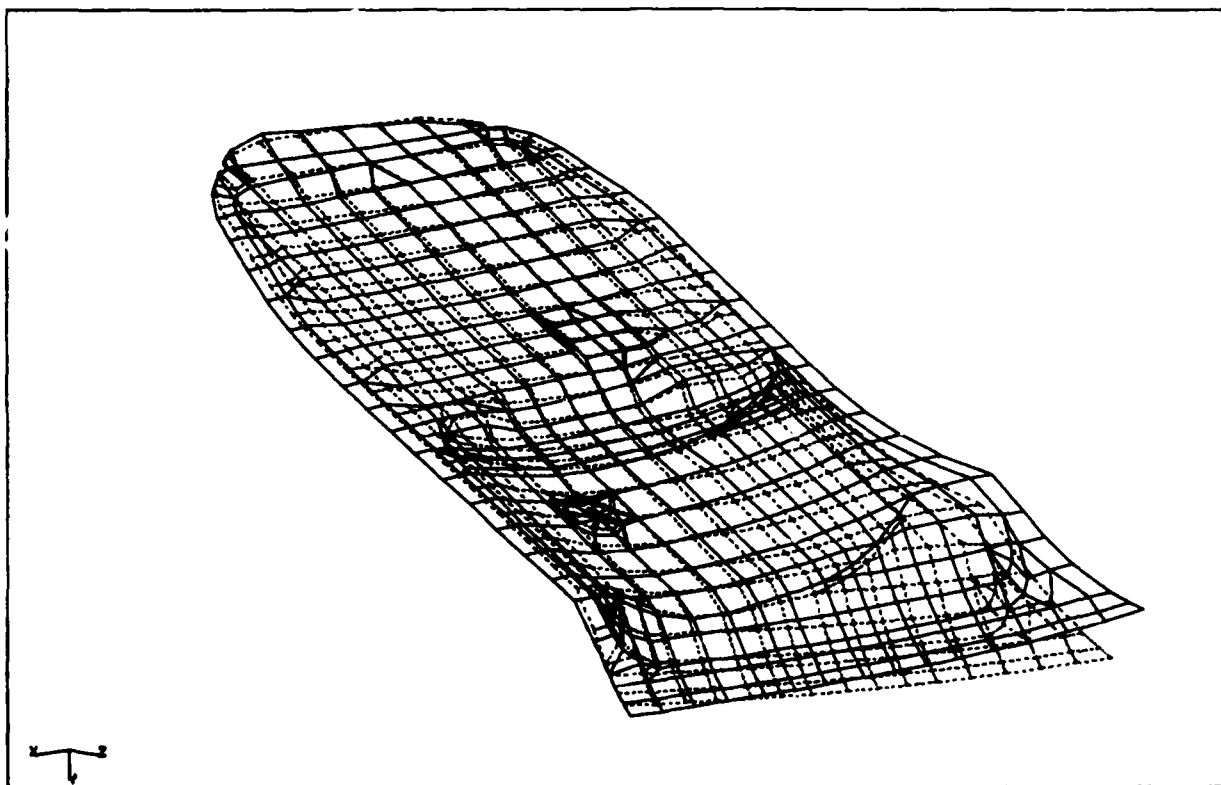
FIGURE 12 - COMPOSITE GEAR DOOR MODE SHAPE

DESIGN SPECTRUM ANALYSIS IN NASTRAN

Thomas G. Butler
BUTLER ANALYSES, Towson, Md.

INTRODUCTION

The utility of Design Spectrum Analysis is to give a mode by mode characterization of the behavior of a design under a given loading. The theory of design spectrum is discussed after operations are explained. User instructions are taken up here in three parts: Transient Preface, Maximum Envelope Spectrum, and RMS Average Spectrum followed by a Summary Table. A single DMAP ALTER packet will provide for all parts of the design spectrum operations.

The starting point for getting a modal break-down of the response to acceleration loading is the Modal Transient rigid format. After eigenvalue extraction, modal vectors need to be isolated in the full set of physical coordinates (P-sized as opposed to the D-sized vectors in RF 12). After integration for transient response the results are scanned over the solution time interval for the peak values and for the times that they occur. A module called SCAN was written to do this job, that organizes these maxima into a diagonal output matrix. The maximum amplifier in each mode is applied to the eigenvector of each mode which then reveals the maximum displacements, stresses, forces and boundary reactions that the structure will experience for a load history, mode by mode. The standard NASTRAN output processors have been modified for this task. It is required that modes be normalized to mass. As such these modes can be averaged by root mean squares giving results which are entirely properties of the structure. The point to be made here is that if modes were normalized to the deflection of a point, the relationship from one mode to another would be artificially distorted by an arbitrary external influence. Conversely, the setting of modal mass to unity is in effect saying that the mass of the system remains constant and the participation of mass in each mode sums to the same value as other modes.

Rms averages are available for displacements in translation and rotation in any one of the six at a time. Taking rms averages of stresses depends on defining the type of stress in each element. The means of defining stresses is available in existing NASTRAN code in the XYPLOT module. Paths for routing the user request to this module and having it interpreted by the RMS module were established via the "frames" section of the XYPLOT command while case control is called on to prescribe a set containing all elements. Consequently, only one type of stress per element is permissible in taking rms averages; however, every element can be represented by a type of stress as different or as like its neighbor as the analyst chooses. Rms averages taken of mass normalized modes are independent of the load and are properties only of the structure. To get an rms representation of the response to loading, it becomes a simple task of multiplying the rms average by the matrix of maximum responses or by the matrix of response time histories. Control of the amount of output information is set up in partnership between switching parameters and case control. The effect is to allocate specific duties to each subcase

and to limit the number of subcases to three. Subcase 1 regulates the modal transient solution in the usual way plus it contains the specifications for output sets of displacements, stresses, forces, and constraints from the modal maxima. Subcase 2 has the sole duty of calling for ELSTRESS in all elements. Subcase 3 is reserved for setting up the modes for which rms responses are wanted.

The bulk of control is vested in 19 parametes which the use turns on or off in the PARAM section of bulk data. One of the factors rthat detemined the design of algorithms was the desire to avoid the creation of any new bulk data cards. Using parameters helped the implementation of this policy, because PARAM is a standard bulk data card that is open-ended as far as the name and value are concerned so the IFP module treats PARAM cards with new seismic names in a routine fashion.

Transient Preface

A modal transient is started as in Modal Seismic Transient Analysis. A reference point is set up with PARAM GRDPNT; however no scaffold point is necessary because there will be no attempt to recover absolute response in design spectrum. Component directions of accelerations are indicated by assigning the appropriate set ID's of DAREA cards on PARAM NRTID# entries. Acceleration histories are put on TABLED1 cards either manually or with the use of the preprocessor TBLGEN. The user must set up the dynamic loading with the usual TLOAD and DLOAD cards. All base points must be gathered into an SPC set. Options ARFIN, QRFIN, AND URFIN are excluded from use in design spectrum analysis. Integration and output time increments need to be set up with a TSTEP card. The normalization on the EIGR card must be set to MASS.

Design Spectrum parameters have no defaults, so the user is obliged to indicate all of his intentions by evaluating every parameter. See the summary table at the end of this section for a review of these parameters. Positive values of parameters enable an option while negative values disable options.

Maximum Envelope Spectrum

After an eigenvalue analysis the modes are normalized to mass. The transient response is determined from a Modal Seismic Transient or a regular modal transient analysis and its solution is examined for the maximum displacement in every mode and each mode is rescaled according to its maximum time response. This gives the maximum deformation that a mode will see from a given load over a forcing interval. With a mode deformed to its maximum extent, it can be examined for the magnitudes of boundary forces, element stresses, and element forces that develop in it. This part of the analysis gives a spatial set of properties mode by mode each under every maximum deformation.

The user controls what behavior is to be computed and what data is to be listed by a combination of case control requests and by using parameters as control switches. There are three subcases with quite distinct functions.

After the module SCAN determines the maximum amplifications for each mode and assembles them in the data block UHMAX, it can be used in various ways; e.g.

>
> UHMAX can be output by setting PARAM AMX = +1. IF AMX = -1, SCAN composes UHMAX but does not print it.
>
> The times at which modal maxima appear are in vector TMAX. Both its compilation and output are controlled by parameter TMX. When TMX = +1 TMAX is compiled and printed. If TMX = -1, they are suppressed.
>
> UHMAX is used to amplify modal vectors to their maximum values giving a matrix called PHIPMAX. PHIPMAX is sent to the output processor where the recovery of three other quantities depend on it. The first subcase is used to organize requests for displacements, single point contstraint forces, element forces and element stresses to be recovered from PHIPMAX. This first subcase is complete in that it contains a full complement of activity: loads, constraints, and outputs.

Maximum mode shapes PHIPMAX are computed and output without
>
> option, but the set of points to be reported are controlled by the DISP specification in the first subcase.
>
> The boundary forces due to maximum modal deformation are computed and output by setting parameter QMX = +1, but the set of points to be reported is controlled by SPCF in the first subcase.
>
> Forces in finite elements due to maximum modal deformation are computed and output only by setting up an ELFORCE request in the first subcase.
>
> Stresses in finite elements due to maximum modal deformation are computed and output only by setting up an ELSTRESS request in the first subcase.

RMS Average Spectrum

An alternative way of looking at a design is to have a single number characterize its behavior. This is obtained by computing root mean square averages (rms) for each mode when normalized to mass before any load is applied. These can be characterized as properties of the design without regard to load, because only ingredients of the structure are used to assemble these properties by normalizing to mass instead of normalizing to maximum deformation or normalizing to the deformation of a particular point. Then these rms properties can be linked to the loading through the amplifier matrix in either of two forms: maximum envelope or time history. Returning to the properties, there are several different quantities that can be averaged. This solution route will apply rms averages to modal displacements and modal stresses. Even this statement is not definitive, because displacements are of about 14 types; i.e., averages in each of 3 translational deformations, averages in each of 3 rotational deformations, averages of 3 resultant vectors of translations taken 2 at a time, averages of 3 resultant vectors of rotations taken two at a time, averages of the resultant vector of translations taken 3 at a time, and averages of the resultant vector of rotations taken 3 at a time. The options could be legion if every grid point were allowed to have different selections of the 14 types and then combined into a single average. The options given to the user in the solution, as here developed, are just 6. Every element will

have the same deformation option as all others and that choice will be limited to one of the 3 translations or one of the 3 rotations.

Options for stress averages are more varied than displacements. Every element is allowed to have a different type of stress to be called into the rms average; or all elements of the same class are allowed to have the same type of stress called into the rms average. For making the selection of stresses in elements, this seismic solution uses a feature which already exists in the XYPLOT module. This is invoked by setting up a second subcase and an X-Y plot packet. The second subcase is not complete; its only purpose is to define an ELSTRESS request that must embrace all elements without using the word ALL. The function of the X-Y plot packet is to utilize the "frames" section of the plot command statement to specify a type of stress to be recovered for every element. The specification permits one or any number of frames to be used but only the "whole" frame form of the specification can be interpreted. The minimum content of this plot packet, if paper plot is called for, is

```
OUTPUT(XYPLOT)
TCURVE=--------   (8 characters or less.  The mask of eight places to the
                   right of = sign is read)
XYPAPLOT STRESS RESPONSE (ID of 2nd subcase) /el #(stress code), ......
CLEAR
```

The 3 lines for TCURVE, XYPAPLOT, and CLEAR must be contiguous. If PAPLOT is used, no plotter card is needed in the packet, nor is an entry of FILES = PLT2 needed on the NASTRAN card, nor is any JCL reference to a plotter needed. The RMS module interprets this plot data and will recognize a short-hand way of setting up the frames specification. If the user wants a block of elements to have a common stress code, the lowest numbered element can represent the block until the next element number starts the next block. For example if there were four types of elements in an analysis, and if the user wanted the same type of stress to be averaged for elements of a given type, then only four items would have to appear in the frames section—the lowest element id number of the first type with its stress code, the lowest element id number of the second type with its stress code, the lowest element id number of the third type with its stress code, and the lowest element id number of the fourth type with its stress code. For even greater convenience there is one predefined set which calls for the maximum stress in every element—no matter what its type. For the MAXSTRES option, the plot packet need not be defined. All that is required is to set parameter TAUR to MAXSTRES. The value TAUR = MAXSTRES is reserved for requesting the predefined set: processing of XYCDB will be bypassed. A TCURVE = MAXSTRES plot request can never be processed by module RMS.

The user is in control of whether the RMS module computes displacement averages or stress averages or both by the values given to parameters. Explanaion of the control parameters follows.

RMS modal displacements are computed and output if param $1 \leq PHIR \leq 6$.
When PHIR = 1, u1 displacements are averaged.
When PHIR = 2, u2 displacements are averaged.
When PHIR = 3, u3 displacements are averaged.
When PHIR = 4, u4 rotations are averaged.
When PHIR = 5, u5 rotations are averaged.
When PHIR = 6, u6 rotations are averaged.
When PHIR $\leq$ 0, no rms averages of modal deformations are computed.

81

Whenever PHIR > 0 the block of rms averages of mass normalized modes
PHIZRMS can be output and/or passed on for further processing.
When parameter PHIZR is set = +1, the matrix PHIZRMS is output.

Two parameters control RMS stress. When TAUSR is >0, rms stress
averages will be computed for elements using the types of
stresses specified by sets which are called by parameter TAUR.
When TAUR is given the name of an XYPLOT TCURVE stress set title,
    stresses due to the modal deformations in the mass normalized
    configuration are computed for each element according to the
    specifications set down by the user in the frames section of
    the XYPLOT command. If TAUSR <0, no rms stresses are computed.
    NOTE!! It is necessary that the user set up an ELSTRESS request
    in the 2nd subcase calling for output of stresses in all elements;
    the RMS module demands that it look at all elements for compu-
    ting rms stress averages. The entry in field 3 of PARAM TAUR
    is the mask of the 8 characters of TCURVE after the = sign,
    which implies that blanks are counted as characters.
When TAUSRMS is computed, it can be output and/or passed on for
    further processing. If parameter TAUSR is set = +1, the matrix
    TAUSRMS is output.

If the rms effect of load on displacements or stresses is wanted,
there are two options: either amplify a matrix of rms averages by the matrix of
maximum responses or by the matrix of response histories.

If the maximum rms averaged response amplitudes in each mode are
wanted, they can be activated by setting parameter URX = +1. This causes the
data blocks UHMAX and PHIZRMS to be multiplied to give the matrix UZRMSM, the
rms averages of maximum modal amplitudes.

If the maximum rms averaged stress responses in each mode are wanted
for a given load, the user sets parameter TAUX = +1. This causes the matrices
UHMAX and TAUSRMS to be multiplied together to give the matrix TAURMSM which is
sent to output.

If time histories of rms displacements or rms stresses are wanted, a
third subcase must be set up. If the third subcase is included, it must be
preceded by two earlier subcases. The 3rd subcase is not complete. Its sole
purpose is to prescribe outputs of SDISP, or SVELOCITY, or SACCELERATION
requests of mode numbers for which rms histories are wanted. Such calls to
mode sets are used for either rms displacements or rms stresses or both. If
only maximum amplifications of rms averages are wanted, the 3rd subcase is not
needed.

If it is desired to have a time history of the rms average deflections
in each mode, the user sets parameter URT = +1. This causes data blocks
PHIZRMS and UHVT to be multiplied to give matrix UZRMST. If a time history of
rms averaged stress responses in each mode are wanted for a given load, the
user sets parameter TAUT = +1. This causes the matrices TAUSRMS and UHVT to be
multiplied together to give the matrix TAURMST which is sent to output. If
plots of UZRMST or TAURMST are wanted, the necessary entries are made in the
XYPLOT packet. The plot command statement is distinct from that used for
specifying element stress types and it must refer to the 3rd subcase for
control of what modes are to be plotted.

Summary Table of Control Options for DESIGN SPECTRUM

Quantity to be Computed	Matrix Name	Control		Module Where	
		Compute Param/S-C	Output Param/S-C	Computed	Output
Max Modal Amplitudes	UHMAX	Automatic	AMX	SCAN	MDLOFP
Time of Max Modal Amp	TMAX	TMX	TMX	SCAN	MDLOFP
Mode Shapes in Max Amplification	PHIPMAX	Automatic	1st S-C	MPYAD	OFPS
SPC Forces in Max Amplification	QPHMAX	QMX	1st S-C	MPYAD	OFPS
El Stresses in Max Amplification	IESMAX	1st S-C	1st S-C	SDR2	OFPS
Element Forces in Max Amplification	IEFMAX	1st S-C	1st S-C	SDR2	OFPS
RMS Avg of Mass Norm- alized Mode Shapes	PHIZRMS	PHIR	PHIZR	RMS	MDLOFP
RMS Avg of Max Defl Response to Load	UZRMSM	URX	URX	MPYAD	MDLOFP
RMS Avg Time History Defl Resp to Load	UZRMST	URT	URT/ 3rd S-C	MPYAD	OFPS
Stress Types for each Element	Parameter TAUR	FRAMES section of XYPLOT		XYPLOT	XYCDB
RMS Avg of Mass Norm- alized El Stresses	TAUSRMS	TAUR/ 2nd S-C	TAUSR	RMS	MDLOFP
RMS Avg of Max Stress Response to Load	TAURMSM	TAUX	TAUX	MPYAD	MDLOFP
RMS Avg Time History Stress Resp to Load	TAURMST	TAUT	TAUT/ 3rd S-C	MPYAD	OFPS

THEORY

Maximum Envelope Spectrum

The transient response by the modal method rests on the principle of summing the contributions of individual modes to the total response.

$$u(x,t) = \sum_{1=1} [\emptyset_i(x)]\{\xi_i(t)\} \qquad (1)$$

where $\emptyset_i(x)$ is the shape that a structure takes while oscillating at a

natural frequency i; and $\xi_i(t)$ is the factor by which the ith mode shape

is amplified at time 't' to represent the participation of the ith mode in the response to some loading. The total response of the structure at all locations in the structure and at all times is the summation of responses from individual modes for an infinity of modes. When fewer than infinite modes are employed, the summation gives an approximation to the true response. Many design situations are addressed in terms of maximum demands. The rationale taken is that; if a structure can meet the maximum demands, it can survive all lesser demands. This general principle has been extended to dynamic response by viewing the maximum demands, mode by mode. After finding the maximum value for $\xi_i(t)$ over

all times, this $\xi_i(max)$ is used to amplify the mode shape $\emptyset_i(x)$ in the

ith mode. Each mode is studied in its maximum amplification for its shape envelope, its stress distributions, its boundary constraint forces, and for the distribution of elastic forces. This has been implemented for NASTRAN in the seismic analysis packet for the mode shapes $\emptyset_i(x)$ and frequencies ωi and the response history $\xi_i(t)$.

A module called SCAN was written to search through all modal accelerations $\ddot{\xi}_i$, modal velocities $\dot{\xi}_i$, and modal displacements ξ_i and to catalog the maximum of modal displacement, only, in each mode and organize these findings of maximum displacement amplitude in a diagonal matrix of $\xi_i(max)$ named UHMAX. The times of occurrence of the maxima are also catalogued in a vector named TMAX.

Each mode is amplified to its maximum and collected into a matrix named PHIPMAX

$$[\emptyset_i] [\backslash\xi_i(max)\backslash] = [\emptyset_i(max)] \qquad (2)$$

The matrix of boundary constraint forces in each mode $Q_i(x)$ is also

amplified to its maximum in each mode and collected into a matrix named QPMAX.

$$[Q_i(x)] [\backslash\xi_i(max)\backslash] = [Q_i(max)] \qquad (3).$$

84

The data block PHIPMAX, representing maximum modal amplification, is delivered to the stress data recovery module to be processed for element stress and force distributions in every mode in its maximum configuration. The user can control how much of this maximum response data is printed out by indicating those elements and grid points for which he wants information by grouping their ID's into sets in Case Control. Output is handled similar to the way that Eigenvalue Analysis Rigid Format treats it.

RMS Spectrum

Another way of measuring design requirements is to characterize structural response in terms of its root mean square (RMS) property. RMS is so general a term that it could mean many different things to many different people. Consequently, it is necessary to be specific as to what property is being described in terms of its RMS value. This discussion will branch into two topics: mode shapes and stresses.

A mode shape is described in terms of its 3 translational and its 3 rotational displacements. An rms average of all six displacements is not meaningful, because rotations and displacements are measured in two different dimensions, lengths and radians. An rms average of translations only or an rms average of rotations only is more meaningful than a mixture. When triggered by a parameter, indicating which one of the six displacements is to be used, the RMS module partitions that one component of the mode shapes at every point 'p' in the structure where the mode is defined. Let 'z' stand for any of the 3 translations or rotations and let $\emptyset_i(z)$ be the partition of the zth displacements in

the ith mode at the N grid points, then this rms computation is carried out:

$$\emptyset_i^{rms}(z) = \left[\frac{1}{N} \sum_{p=1}^{N} [\emptyset_i(z)]_p^2 \right]^{1/2} \qquad (4)$$

$\emptyset_i^{rms}(z)$ is interpreted as the rms value of z displacements in the ith

mode. The RMS module carries out these average computations for all "i" modes and organizes the results in a diagonal matrix.

$$[\backslash \emptyset_i^{rms}(z) \backslash]$$

Only the mode shapes are involved in this computation, but the values computed depend upon the method of normalizing mode shapes. If modes are normalized to mass a truly consistent method of interpreting, the rms values is achieved. An rms value of a mass normalized mode is a property of the structure and can have meaning to a structural designer. Having rms properties of modes, one can use these to make

interpretations of responses. Amplifying the rms averaged modes by the

85

matrix of time varying amplitudes $[\xi_i(t)]$ can be called the rms time varying response of a loading in the chosen z component.

$$[u^{rms}(z,t)] = [\backslash\emptyset_i^{rms}(z)\backslash][\xi_i(t)] \tag{5}$$

$u^{rms}(z,t)$ is interpreted as the rms weighted time response of a structure to a load in component z.

Amplifying the rms averaged modes by the envelope of maximum responses gives a kind of rms of peaks in the chosen component.

$$[\backslash u^{rms}(zmax)\backslash] = [\backslash\emptyset_i^{rms}(z)\backslash][\backslash\xi_i(max)\backslash] \tag{6}$$

The advantage of this rms of peaks is that one number per mode characterizes the response of the system.

Stress at a point is described in terms of a tensor, but the dimension of every stress is the same; i.e., force per unit area. In some part of a structure, one type of stress such as bending may dominate while in another part the dominant type of stress may be shear and in yet another part axial stress may be dominant and so on. The RMS module will allow the user to be specific about which type of stress he wants to designate for each individual element throughout the whole structure to characterize the average stress behavior. Only one type of stress at only one location in any one element may be chosen; e.g., there are 21 stress options for the CIHEX1 element but only one of these 21 may be selected for an element. Call the stress reading in the ith mode $S_i(s)$.

Lower case 's' is the set number of the prescribed stress types at each element over a total of 'n' elements, and let i represent the ith mode. Call the stress reading in the mass normalized ith mode $S_i(s)$, composed

of the stress types in set 's' involving the 'n' elements that were used to model the structure. The rms computation that is carried out for the ith mode is:

$$\zeta_i^{rms}(s) = \left[\frac{1}{n}\sum_{e=1}^{n}[S_i(s)]_e^2\right]^{1/2} \tag{7}$$

The RMS module carries out these average computations for all 'i' modes and organizes the results in a diagonal matrix.

$$[\backslash\zeta_i^{rms}(s)\backslash].$$

Only mode shapes in their normalized deformation were involved in this caculation, so these averages can be considered to be properties of the structure for the 's' combination of stresses. As was done with the rms

displacements, one can characterize the response of the structure under transient load in terms of these rms stress properties.

$$[\zeta^{rms}(s,t)] = [\diagdown \zeta_i^{rms}(s)\diagup] [\mathcal{E}_i(t)]. \qquad (8)$$

Equation (8) represents the rms response time history of stresses in a structure for stress types according to set 's' under a given load.

Once again, a single number to characterize the design mode by mode is possible by amplifying the rms averaged stresses in modes by the envelope of maximum responses. It gives the rms of peak stresses in the chosen stress set 's' for a structure under a given load.

$$[\diagdown \zeta^{rms}(smax)\diagup] = [\diagdown \zeta_i^{rms}(s)\diagup] [\diagdown \mathcal{E}_i(max)\diagup]$$

The Design Spectrum Rigid Format limits the user to one choice of 'z' for rms mode shape calculations and to one choice of 's' for rms stress calculations in any one run.

SOLNDS

$************   SEIRES   ***********
$
$
$*********   THESE ARE DMAP ALTERS FOR SEIRES   ***********
$*********   PERTAINING TO RIGID FORMAT   DMAP   ***********
$*********   SERIES APR 82   ***********
$
$ DESIGN SPECTRUM
$
$PARAMETER DEFINITIONS:
$
$NRTID1,2,3 = SET ID'S TO BE ASSIGNED TO DAREA CARDS REPRESENTING THE
$ SPATIAL ARRANGEMENT OF TRANSLATIONAL ACCELERATION IN THE THREE
$ COORD DIRECTIONS.
$NRTID4,5,6 = SET ID'S TO BE ASSIGNED TO DAREA CARDS REPRESENTING THE
$ SPATIAL ARRANGEMENT OF ROTATIONAL ACCELERATION IN THE THREE
$ COORD DIRECTIONS.
$AMX = CONTROL PARAMETER FOR THE OUTPUT OF THE UHMAX MATRIX.
$TMX = CONTROL PARAMETER FOR THE COMPUTATION AND OUTPUT MATRIX TMAX.
$OUTPUT CONTROL MATRIX PHIPMAX IS BY CASECC IN S/C 1 UNDER DISP=().
$QMX = CONTROL PARAMETER FOR THE COMPUTATION OF THE QPHMAX MATRIX. OUT-
$ PUT CONTROL OF MATRIX QPHMAX IS BY CASECC IN S/C 1 UNDER SPCF=().
$THE COMPUTATION AND OUTPUT OF THE ESMAX MATRIX IS UNDER THE CONTROL
$ OF ELSTRESS IN SUBCASE 1 OF CASE CONTROL
$THE COMPUTATION AND OUTPUT OF THE EFMAX MATRIX IS UNDER THE CONTROL OF
$ ELFORCE IN SUBCASE 1 OF CASE CONTROL
$PHIR = PARAMETER FOR THE COMPONENT SELECTION OF THE PHIZRMS MATRIX.
$URT = CONTROL PARAMETER FOR THE COMPUTATION OF MATRIX UZRMST. OUTPUT IS
$SELECTED BY SVEC OR SDISP OR SVELO OR SACCEL IN S/C 3 OF CASECC.
$URX = CONTROL PARAMETER FOR THE COMPUTATION AND OUTPUT OF MATRIX UZRMSM.
$TAUR = CONTROL PARAM FOR THE STRESS SET SELECTION OF THE TAUSRMS MATRIX.
$TAUT = CONTROL PARAMETER FOR THE COMPUTATION OF THE TAURMST MATRIX. OUT-
$PUT IS SELECTED BY SVEC OR SDISP OR SVELO OR SACCEL IN S/C 3 OF CASECC.
$TAUX = CONTROL PARAM FOR THE COMPUTATION AND OUTPUT OF MATRIX TAURMSM.
$PHIZR = CONTROL PARAMETER FOR THE OUTPUT OF THE PHIZRMS MATRIX.
$TAUSR = CONTROL PARAMETER FOR THE OUTPUT OF TAUSRMS
$
$$***
$ *
$ THE USER MUST USE MASS NORMALIZATION ON THE EIGR CARD   *
$ THE USER MUST USE SUBCASE 1 FOR DLOAD AND MAX MODAL RESPONSE   *
$ THE USER MUST USE SUBCASE 2 FOR MODAL RMS STRESS CALCULATIONS   *
$ XYPLOT FOR SELECTION OF STRESS COMPONENTS FOR RMS *
$ THE USER MUST USE SUBCASE 3 FOR LOAD AMPLIFYING OF RMS AVERAGES   *
$ *
$***
$
$$SECTION A
$
ALTER 49 $ JUST BEFORE MCE
PARAM   //*NOT*/SEISLD/SINGLE $
COND   SYMX,SEISLD $
JUMP   FINIS $
LABEL   SYMX $

88

```
$$  CALL IN RBTM AT THIS POINT.
$
RBTM        BGPDT,CSTM,EQEXIN,MGG,USET/HAICH,MSEIS,  ,HL6/C,Y,GRDPNT/-1/
            *MODAL* $
$
$$GET THE MASS AND STIFFNESS MATRICES READY FOR LOAD AND BASE FORCE
$$RECOVERY.
$$
VEC         USET/GXVEC/*G*/*COMP*/*SB* $ X=SB,COMP,G
VEC         USET/GYVEC/*G*/*COMP*/*R* $ 1'S ON R
ADD         GXVEC,GYVEC/GCVEC/ $ 1'S ON SB & R
$----------INERTIA MATRICES----------------------------------**
PARTN       MSEIS, ,GCVEC/MSIZC,MSIZRB,,/5/O $
ADD         MSIZC, /MMSIZC/(-1.0,0.0) $
MERGE       MMSIZC,MSIZRB,,,,GCVEC/MSIZ/5/O $
$
NRTS        MSIZ,DYNAMICS,EQEXIN/NRTSEIS/C,Y, DEPOP/C,Y,NRTID1/
            C,Y,NRTID2/C,Y,NRTID3/C,Y,NRTID4/C,Y,NRTID5/C,Y,NRTID6 $
EQUIV       NRTSEIS,DYNAMICS/SEISLD $
$$  THE 'DYNAMICS' DATA BLOCK NOW HAS DAREA CARDS IN IT FOR THE INER-
$$  TIA LOAD AND IS READY TO BE PASSED TO DPD FOR SETTING UP THE LOAD
$$  ON THE RELATIVE X COORDS.  IT CONTAINS DAREA NOT JUST FOR THE BASE
$$  MOTION BUT FOR DIRECTLY APPLIED LOAD AS WELL.  RF12 CAN NOW PROCEED
$$  WITH CONDENSATION FROM X-SIZE TO A-SIZE AND DEVELOP MODAL VECTORS
$$  FOR SOL'N IN TRD.
$ $ $                        S    C    A    N                   $ $ $
ALTER 102,126 $ AFTER TRD
$$$  KEEP SDR1 # 127
ALTER 128,144 $ ELIMINATE THRU REPT.
$$$$     USE S/C 1 FOR TRANSIENT LOAD AND FOR SCAN OUTPUT OF MAXIMA
SCAN        UHVT,TOL/UHMAX,TMAX/C,Y,TMX $
MPYAD       PHIPH,UHMAX, /PHIPMAX/O/+1 $ PHIPH COMES FROM SDR1.
$$$$     PHIPMAX ISSUBSEQUENTLY EMPLOYED FURTHER.
COND        BOUND,QMX $
MPYAD       QPH,UHMAX, /QPHMAX/O/+1 $
LABEL       BOUND $
SDR2        CASEXX,CSTM,MPT,DIT,EQDYN,SILD,,,BGPDP,LAMA,QPHMAX,PHIPMAX,
            EST,, / ,IQPHMAX,IPHIPMX,IESMAX,IEFMAX, /
            *MMREIG*/S,N,NOSORT2 $
OFPS        IQPHMAX,IPHIPMX,IESMAX,IEFMAX,,// $
$ $ $                        R    M    S                         $ $ $
$$$$     RMS AVERAGES ARE TAKEN OF DISPLACEMENTS AND STRESSES WITH RE-
$$$$     SPECT TO EIGENVECTORS THAT ARE NORMALIZED TO MASS.  THE USER
$$$$     ASSIGNS THE COMPONENTOF MODAL DISPLACEMENT THAT HE WANTS TO SEE
$$$$     AVERAGED AND INDICATES THIS ON PARAMETER "PHIR".  EVERY ELEMENT
$$$$     IN THE MODEL IS INCLUDED IN AN RMS STRESS AVERAGE.  ONLY ONE TYPE
$$$$     OF STRESS CAN BE USED PER ELEMENT.  THE USER INDICATES WHICH TYPE
$$$$     OF STRESS IS TO BE AVERAGED BY MAKING HIS SELECTION IN THE "FRAMES"
$$$$     SECTION OF AN XYPLOT COMMAND FOR S/C 2, WITH AN ASSOCIATED NAME
$$$$     GIVEN ON "TCURVE".  THE "TCURVE" NAME IS PUBLISHED IN PARAM "TAUR".
```

```
PARAM        //*LE*/V,N,GOP/C,Y,PHIR/C,N,O $
PARAM        //*AND*/V,N,GOTAMP/C,Y,TAUX/C,Y,TAUT $
PARAM        //*AND*/V,N,GOTRMS/V,N,GOTAMP/C,Y,TAUSR $ GOTRMS IS INPUT
$$TO RMS IF GOTRMS IS > 0,RMS CALCULATES TAUSRMS,OR ELSE ONLY PHIZRMS.
PARAM        //*ADD*/V,N,RMS/V,N,GOP/V,N,GOTRMS $IF NEITHER PHIZRMS NOR
$$TAURMS IS WANTED, THIS IS EQUIVALENT TO SETTING PHIR,TAUX,TAUT &
$$TAUSR ALL NEGATIVE. A JUMP IS TAKEN AROUND RMS AND ENDS PROCESSSING.
CASE         CASECC, /CASERR/C N,TRAN/V,N,REPEATT/V,N,NOLOOP $
COND         NORMS,RMS $
COND         NOTAU,GOTRMS $
SDR2         CASERR,CSTM,MPT,DIT,EQDYN,SILD,,,BGPDP,LAMA,QPH,PHIPH,EST,
             XYCDB,/,,,IES1,,/*MMREIG*/S,N,NOSORT2 $
LABEL        NOTAU   $
RMS          PHIPH,EQDYN,IES1,XYCDB,MHH/PHIZRMS,TAUSRMS/C,Y,PHIR/
             V,N,GOTRMS/C,Y,TAUR $
$ $ $              A    M    P    L    I    F    Y              $ $ $
$$$$$  $$$$$  $$$$$  $$$$$  $$$$$
$$  TWO DIFFERENT OPTIONS ARE EXERCISED HERE FOR AMPLIFYING THE RMS
$$  AVG MODAL PROPERTIES WITH EFFECTS OF LOAD: EITHER WITH UHMAX FOR
$$   THE RMS MAX IN EACH MODE; OR WITH UHVT FOR THE RMS HISTORIES IN
$   EA MODE IF THE USER CHOOSES THE RMS MAX INSTEAD OF A TIME HISTORY
$   OF RMS, DMAP TAKES OVER TO MULTIPY UHMAX DIAG INTO EITHER OR BOTH
$   OF THESE TO OBTAIN OUTPUT  DIAG MATRICES [DOFRMSM] AND/OR [TAURMSM].
COND         UX,URX $  MAX RMS DISPLACEMENTS IN EA MODE
MPYAD        PHIZRMS,UHMAX, /UZRMSM/0/+1 $
LABEL        UX $
COND         TX,TAUX $   MAX RMS STRESS IN EA MODE
MPYAD        TAUSRMS,UHMAX, /TAURMSM/0/+1 $
LABEL        TX $
PARAM        //*AND*/V,N,RAMPL/C,Y,URT/C,Y,TAUT $
PARAM        //*ADD*/V,N,REPEATT/C,N,1/C,N,2 $
CASE         CASECC, /CASEUU/C,N,TRAN/V,N,REPEATT/V,N,NOLOOP $
COND         NORMS,RAMPL $
$$$$     IF THERE ARE SOME TIME DEPENDENT PARAMETERS TURNED ON, THEN
$$$$     THE COMBINATION OF MODES FOR WHICH OUTPUT IS SELECTED IS CON-
$$$$     TROLLED IN S/C 3 OF CASE CONTROL USING SOLUTION SET COMMANDS.
COND         UT,URT $  RMS DISPLACEMENT HISTORY IN EACH MODE
MPYAD        PHIZRMS,UHVT, /UZRMST/0/+1 $DIAG PHIZRMS INTO TRIPLET FORMAT
VDR          CASEUU,EQDYN,USETD,UZRMST,TOL,XYCDB,/OUZRMST1,/*TRANRESP*/
             *MODAL*/C,N,0/S,N,NOH/S,N,NOP/S,N,FMODE $
SDR3,        ,,OUZRMST1,,,/,,OUZRMST2,,, $ SDISP OR SVELO OR SACCEL IN
$$  %%  $$  S/C 3 CONTROLS THE OUTPUT.
OFPS         OUZRMST2,,,,,//S,N,CARDNO/S,N,OFPOPT1=-1/C,Y,PHIR/C,Y,TAUSR $
XYTRAN       XYCDB,OUZRMST2,,,,/XYPLRMSZ/*TRAN*/C,N,HSET/V,N,PFILE/
             S,N,CARDNO $
XYPLOT       XYPLRMSZ// $ XYPLOT COMMAND SHOULD SPECIFY S/C 3
LABEL        UT $
COND         TT,TAUT $ RMS STRESS HISTORY IN EACH MODE
MPYAD        TAUSRMS,UHVT,/TAURMST/0/+1 $DIAGONAL TAUSRMS INTO TRIPLET
$$$$$$     FORMAT
VDR          CASEUU,EQDYN,USETD,TAURMST,TOL,XYCDB,/TAURMST1,/*TRANSRESP*/
             *MODAL*/C,N,0/S,N,NOH/S,N,NOP/S,N,FMODE $
```

```
SDR3,         ,,,TAURMST1,,  /  ,,,TAURMST2,,  $ SDISP OR SVELO OR SACCEL
$$   %%   $$   IN S/C 3 CONTROLS THE OUTPUT.
OFPS          TAURMST2,,,,,//CARDNO/S,N,OFPOPT=-1/C,Y,PHIR/C,Y,TAUSR $
XYTRAN        XYCDB,TAURMST2,,,,/XYPLTAUR/*TRAN*/C,N,HSET/V,N,PFILE/
              S,N,CARDNO $
XYPLOT        XYPLTAUR// $ XYPLOT COMMAND SHOULD SPECIFY S/C 3
LABEL         TT $
LABEL         NORMS $
MDLOFP        LAMA,UHMAX,TMAX,PHIZRMS,UZRMSM,TAUSRMS,TAURMSM//
              C,Y,AMX/C,Y,TMX/C,Y,PHIZR/C,Y,URX/C,Y,TAUSR/C,Y,TAUX/
              C,Y,PHIR/C,Y,TAUR $
JUMP     FINIS $
ENDALTER
```

SEISMIC ANALYSIS CAPABILITY IN NASTRAN

Thomas G. Butler
BUTLER ANALYSES, Towson, Md.

Robert F. Strang
COMPUTER SCIENCES CORP., Silver Spring, Md.

INTRODUCTION

Seismic analysis is a technique which pertains to loading described in terms of boundary accelerations. Earthquake shocks to buildings is the type of excitation which usually comes to mind when one hears the word seismic, but this technique also applies to a broad class of acceleration excitations which are applied at the base of a structure such as vibration shaker testing or shocks to machinery foundations. Four different solution paths are available in NASTRAN for seismic analysis. They are: Direct Seismic Frequency Response, Direct Seismic Transient Response, Modal Seismic Frequency Response, and Modal Seismic Transient Response. This capability, at present, is invoked not as separate rigid formats, but as pre-packaged ALTER packets to existing Rigid Formats 8, 9, 11, and 12. These ALTER packets are included with the delivery of the NASTRAN program and are stored on the computer as a library of callable utilities. The user calls one of these utilities and merges it into the Executive Control Section of the data deck to perform any one of the four solutions. There are a number of options available in each solution. These options are invoked by setting parameter values in the bulk data. Each of these solutions operates sufficiently differently that instructions will be discussed individually in the following paragraphs after a general introduction. The only new bulk data cards needed to perform seismic solutions are simple parameters which will be explained in the context of each solution path. The theoretical basis for these solutions is taken up in the Theory Section. Associated with each seismic ALTER packet are a number of new functional modules. Their operations are described in the solution topics.

OPERATION OF SEISMIC SOLUTIONS

Taking Newton's law as it stands Force = Mass x Acceleration, the loading in all cases is organized by putting the spatial distribution of mass on DAREA cards and by putting the description of time-varying or frequency-varying accelerations on TABLED1 cards so that the assembler cards TLOAD or RLOAD will direct the combining of the mass with the acceleration to create force inputs at the indicated massive grid points. This is the heart of the whole seismic scheme. The user can be spared the drudgery of preparing these inputs by employing processors that are supplied to do the job automatically for him. A stand-alone program called TBLGEN will take a file of seismic accelerations and will prepare a file of TABLED1 card images that can be merged into the bulk data section of the data deck. New module RBTM and succeeding ALTER statements prepare a matrix of inertia coefficients, using the rigid body transformation matrix as a transfer function between points having inertias

92

coupled to a base point and that base point for the direct method and acts as a transfer function between the base reference and all superstructure points for the modal method. The module, called NRTS, automatically converts the matrix from RBTM into a data block of DAREA card images of masses. The assignment of masses to DAREA coefficients are made according to the coordinate direction in which they are to be accelerated. NRTS is guided by the user as to which direction to accelerate the inertias through the use of parameters NRTID"i". There are 6 parameters NRTID"i" $1 \leq i \leq 6$. $1 \leq i \leq 3$ represent the three translational directions of the basic coordinate system. $4 \leq i \leq 6$ represent the three rotational directions of the basic coordinate system. NRTS will generate a DAREA set for each parameter NRTID"i" that is included in a run. There must be at least one NRTID"i" in a run. NRTS can accomodate from one to six coordinate accelerations in a run. The user assigns set ID's on the NRTID"i" cards which NRTS transfers to the corresponding DAREA sets that it generates. These DAREA sets are never processed by the Input File Processor (IFP) module. NRTS formats the DAREA data according to the way it is usually output from IFP and incorporates these into the DYNAMICS data block in the form required later by module DPD. These automatically generated DAREA cards do not become part of the bulk data; however, the user is given the opportunity to confirm the DAREA data that was prepared by reading the listing that is automatically included in the output upon the execution of NRTS. The TLOAD and RLOAD cards are prepared by the user in the usual way by assembling ID's of DAREA, DPHASE, DELAY, and TABLEDi for the dynamic loading cases. The difference is that the set ID in field 3 refers to the DAREA set generated by NRTS instead of one contained in bulk data. The TABLED1 cards prepared by TBLGEN do become part of the bulk data so the ID in field 6 does refer to a set of accelerations that is contained in bulk data.

Beside load preparation another feature of seismic operation that is common to all solutions is the selection of options. Options are parameter controlled. They operate slightly differently in each rigid format. The three parameters URFIN, QRFIN, and ARFIN operate according to the sign of the value entered on PARAM bulk data cards. Negative values enable the operation and positive values disable their operation. URFIN controls the option to refine outputs (displacements, velocities, and accelerations) due to contributions from omitted d.o.f.'s. URFIN provides for recovery of displacements at loaded points of the structure which the analyst shunted to the omit set. The chance for loaded points being put into the omit set is much more likely in solutions by the modal method (where every massive point is loaded) than it is in solutions by the direct method. The recommendation is that if condensation is used, to always enable URFIN for modal solutions and do not do so in the direct solution unless important inertias are condensed and loaded. QRFIN controls the option to recover base forces due to the complete complement of stiffness coupling, damping coupling, mass coupling and base inertias. QRFIN augments the reporting of loads on base points, as is currently done in dynamic rigid formats, from just inertia loads to both inertia loads and reaction loads due to coupling. If QRFIN is not enabled, the Case Control request for OLOAD would limit the output on base points to only forces and moments derived from direct inertias. QRFIN does not affect the reporting of loads on points outside the base set. ARFIN controls the option to recover displacements in absolute coordinates.

Solutions differ from each other (1) in the way that loading is applied, (2) in the coordinate system that is used, (3) in the way that coupling is represented, and (4) in the way that data is recovered. Consequently, the descriptions of seismic modifications, from this point on, will be addressed on the basis of the way that the differential equation is solved—direct or modal.

INDIVIDUAL SEISMIC SOLUTIONS

Direct solutions (RF 8 & 9) are performed in absolute coordinates as free bodies. Modal solutions (RF 11 & 12) are performed in relative coordinates on fully clampled rigid bases.

DIRECT SEISMIC (FREQUENCY OR TRANSIENT) RESPONSE.

The features of Direct Seismic Frequency Response and Direct Seismic Transient Response are sufficiently common that they will be discussed in a combined topic.

Loading — Loading consists of the acceleration of inertias on base points and on inertias that are coupled to base points. All degrees of freedom (d.o.f.'s) of base points being accelerated belong in the R-set. This is implemented by entering their ID's on SUPORT cards. The loading is almost completely general in that every boundary point, which is subject to acceleration, can be loaded with an individual acceleration history with individual time delays and individual phase delays. The proviso that keeps this loading from being completely general is that any point that is supplied with inertia solely via DMIG cards cannot engage in acceleration loading. All boundary accelerated points are classified as base points, but they need not physically be located at the base of a structure. Acceleration loading need not take place over a rigid surface; base points may be elastically linked. CAUTION!! since the K & B matrices are singular in the R dof's, it is imperative that all dof's in the mass matrix be non-singular, i.e. 2nd moment terms must appear for rotational dof's.

Structural Matrices — The mass and stiffness matrices are not incorporated into the system of seismic equilibrium equations in the form that they leave the EMG & EMA modules. These matrices must be partitioned in order to honor equilibrium conditions. This is done automatically within the pre-packaged ALTER packet. When all the manipulation has transpired, the structural matrices enter the solution phase as unsymmetrical. Part of the mass matrix is moved to the right hand side to form the load. The base partitions of stiffness, mass and damping are used for base force recovery. The DMIG (direct input matrices) are partitioned according to the same pattern as the automatic matrices are. It is anticipated that DMIG masses will eventually be made part of the loading process, so the matrices that enter the solution phase are so partitioned in order to be consistent with the loading function. DMIG matrices do participate in the base force recovery process, so the DMIG matrices are almost completely general.
CAUTION: The direct seismic solutions are particularly sensitive to singularities in the R-set of mass matrices. In particular, extra effort must be made beyond the usual mass matrix genration to ensure that rotational degrees of freedom in the R-set be supplied with 2nd moments of inertia. Accuracy of load transmittal in this method is also sensitive to the modeling of elastic and damping coupling between base and superstructure.

Damping -- Every type of damping which NASTRAN makes available to solutions by the direct method are similarly available to seismic direct solutions. Every type of damping coupling, if present, can contribute to the recovery of base forces.

Boundaries -- The problem is solved as a free body so there are no boundary constraints. No SPC's are allowed except those entered on GRID cards. There is a physical reason for this. Solution takes place in absolute coordinates, and single point constraints in absolute coordinates means that there is a mechanism located in the absolute frame to which points can be tied which will hold them invariably to zero during the period of application of seismic load. Physically this implies that the mechanism must be anchored outside the seismic zone. To meet such a severe requirement the constraining mechanism would be something like an infinitely rigid sky-hook or a monstrous clamp implanted beyond the fault zone. In the case of a shaker it could be satisfied by a large structure surrounding the shaker. No conceivable reason exists for any such arrangements; therefore this is the logic for disallowing SPC's in solutions by the direct method.

Data Recovery -- All displacements are recovered in absolute coordinates, so the ARFIN option for recovery in absolute coordinates would be redundant. Only options URFIN and QRFIN pertain to solutions by the direct method. Except in special cases, the only option recommended to always consider for direct solutions is QRFIN. Using QRFIN in the direct method is the only way to recover base reactions, because the more usual route of SPC force requests does not apply to the base, since the base points are assigned to R-set. Reporting of seismic base forces is controlled in Case Control by the OLOAD statement.

Because element stress and force recovery involves differencing operations on displacements, and because solution by the direct method takes place in absolute coordinates, it is necessary to intervene to prevent errors that arise from taking small differences between large numbers. Total motion of superstructure points, away from the base, consists of a rigid body component due to actions of the base plus elastic deformations of the superstructure with respect to a reference in the base. The recovery of stresses could be improved by removing the rigid body component before doing the differencing; but obtaining the rigid body component poses a difficulty. In the direct method all points in the non-rigid base are excited, so that that which is called rigid body depends on the chosen reference. The way out of this dilemma is to relax concern for determining true rigid body motion. What is important is not that stress recovery should be represented in true relative coordinates, but that stress recovery should be accomplished in a system of numbers of reduced magnitude compared to the absolute deformations. How the reduction to a lesser magnitude is accomplished is not important, except that it should be done uniformly, so that relative sizes are preserved. Therefore, the reference base point for computing rigid body motion can be chosen arbitrarily, because all absolute displacemnts will be reduced in magnitude by removing the rigid body component as defined according to a single point. The analyst then is in control of which point is to be used as a reference. He designates one of the base points assigned to the R-set by entering its GP ID number on the parameter GRDPNT card.

95

MODAL SEISMIC (FREQUENCY AND TRANSIENT) RESPONSE

The features of Modal Seismic Frequency Response and Modal Seismic Transient Response are sufficiently common that they will be discussed in a combined topic.

Loading -- Loading consists of the acceleration of all inertias of the super-structure while the base is held fixed. This solution, then, determines the behavior of the structure relative to the base. A reference point in the base is required for constructing the rigid body transfer function from the base to superstructure points. How the reference is selected depends on whether the analyst wishes to recover absolute responses. If no absolute responses are wanted, any point in the base can be used, but preferably one in the center. The reference point is flagged by putting it on a PARAM GRDPNT card.

If absolute responses are to be recovered, a scaffold is used. A pair of points, connected by a bar, but disjoint from the structure under analysis, is to be used as a reference system for setting up the load. One point is co-located with a selected base point and is free of any constraints. This is the reference point. The other point is located below the base and is fully constrained. The free point is endowed with unity mass in all 6 dof's, but the bar is massless. (A CONM2 card can be used for this unity mass). Elastic properties of the bar are assigned so that this reed-like reference system has natural frequencies higher than any frequency of interest in the primary structure. The free point is flagged as the reference point by putting it on a PARAM GRDPNT card.

This is the extent of special preparations for load outside of the requirements as described in the paragraph entitled OPERATION OF SEISMIC SOLUTIONS.

Structural Matrices -- The structural matrices are left in the form that they are automatically generated so that they retain their symmetric character during the solution phase. Solution can proceed with maximum efficiency in the symmetric domain. Partitions are made on the matrices, however, to prepare them for recovery of base forces. The DMAP ALTER automatically prepares the partitioning vectors, does the partitioning, and the reassembly of matrices without further intervention by the analyst.

Damping -- In the ordinary modal solutions, only frequency dependent equivalent modal damping is provided for. No scalar dampers or structural damping is taken up in the symmetric path. If other damping is required, it can be supplied by direct input matrices (DMIG). This causes the solution to depart from the symmetric to the more time consuming non-sysmmetric route. If damping contributions to base forces are needed in the solution, then the only type of damping for which provision has been made is direct input matrices -- called B2PP.

Boundaries -- All base points for modal seismic solutions are assigned to the B-set by entering their ID's on SPC (Single Point Constraint) cards. All six dof's must be included in the base constraint set. No other SPC sets should be activated besides this base set. Having just one set enables the scheme to

distinguish the base points in the data recovery process.

Data Recovery -- Displacements are nominally recovered in relative coordinates. Stresses can be recovered directly from these relative responses without having to make further special provisions. If the user wants to recover displacements in absolute coordinates, special provisions are necessary. The rigid body component of displacement must be added to the relative displacements. Since the base is clamped, a base point does not report the acceleration which was applied there. The scaffold, described in the Loading section above does have a free point which does report the acceleration. Since unity mass was prescribed for the free point, the value of force is equal to the value of acceleration, so the report of acceleration in the form of NASTRAN internal data blocks is obtained from the load vector on the free reference point. Once the scaffold reed is installed, no further preparation by the analyst is needed except to include the PARAM ARFIN with a negative value. The only component of seismic transient response that can be recovered in absolute coordinates via the modal route is acceleration, but for seismic modal frequency response, absolute accelerations, velocities, and displacements can be recovered.

Condensations are logical to use with large structures. In the case of seismic solutions by the modal method where the load is distributed over all the superstructure, condensation could cause a considerable amount of inertia to be gathered into the omit-set. Normally the recovery of contributions to displacement response from the omit-set in dynamic rigid formats is limited to the GOD coefficient matrix without regard to the so-called Koo contribution. It is normally left to the user to be judicious in avoiding the condensation of sizeable inertias. Even a judicious regard by the user is not sufficient when a large accumulation of small inertias is involved as in seismic modal analyses. As a consequence, provision has been made to recover the Koo contribution of the omit-set to displacement response. The user invokes this capability by assigning a negative value to the URFIN parameter.

Recovery of base forces is governed by parameter QRFIN. Setting its value to negative automatically invokes the DMAP ALTER for including contributions to the base force from direct inertias, coupled inertias, coupled elasticity, and coupled DMIG damping. No contribution to base forces from frequency dependent modal damping can be recovered.

THEORY

The general dynamics equation for the seismic problem will be written in subscripted form to relate it to the way that NASTRAN would handle it. The subscript P designates the full set of Physical coordinates. It contains all geometric and scalar grid points in the G-set plus the Extra points used to represent transfer functions of attached features such as hydraulic systems.

$$[[MPP]p^2 + [BPP]p + [KPP]]\{UP\} = \{PP\} \tag{1}$$

Let lower case p designate the operator d/dt for differentiation with respect to time. The M matrix represents the mass; the B matrix represents the damping; the K matrix represents the elasticity; and the P matrix represents the load. Since NASTRAN links the E-set only after

it has fully processed the G-set, the E coordinates will be partitioned off and the discussion of the method will start where NASTRAN starts it with the G-set.

$$\left[\begin{bmatrix}MGG & MGE \\ \hline MEG & MEE\end{bmatrix}p^2 + \begin{bmatrix}BGG & BGE \\ \hline BEG & BEE\end{bmatrix}p + \begin{bmatrix}KGG & KGE \\ \hline KEG & KEE\end{bmatrix}\right]\left\{\begin{matrix}UG \\ \hline UE\end{matrix}\right\} = \left\{\begin{matrix}PG \\ \hline PE\end{matrix}\right\} \qquad (2)$$

Ignore the GE coupling for now and isolate the equation in the G-set.

$$[[MGG]p^2 + [BGG]p + [KGG]]\{UG\} = \{PG\} \qquad (3)$$

Seismic load originates in the ground and therefore will produce loading in the base of the structure. If the loading were fully defined in terms of distributed forces, there would be no necessity of engaging in this present task, because NASTRAN is fully capable of analyzing structures under known time dependent forces. Since it is displacement histories that define a seismic disturbance in terms of acceleration or velocity or translations, this task is directed towards the development of an automatic method of determining the response to a seismic disturbance without requiring that the disturbance be converted to a set of forces before proceeding with the solution.

Implementation of seismic response has been carried out for four different types of solutions within NASTRAN. Two solutions use the direct method of integrating the differential equations and two solutions use the modal method of integration. In both types the set of two solutions involve excitation in the time domain for one and excitation in the frequency domain in the other. Specifically, these four solutions are:

DIRECT FREQUENCY RESPONSE — R.F. 8
DIRECT TRANSIENT RESPONSE — R.F. 9
MODAL   FREQUENCY RESPONSE — R.F.11
MODAL   TRANSIENT RESPONSE — R.F.12

The biggest difference in the theory amongst these four solutions lies between the direct approach and the modal approach. The direct solution takes place as a free body in absolute coordinates while the modal solution takes place as a structure clamped at the base and solved in terms of relative coordinates. The direct method will be taken up first.

DIRECT THEORY

That set of points which is assigned to the base where the disturbance acts is designated as the R-set. Partition the G-set into the base points and its complement say Y = R comp G.

$$\left[\begin{bmatrix}MYY & MYR \\ \hline MRY & MRR\end{bmatrix}p^2 + \begin{bmatrix}BYY & BYR \\ \hline BRY & BRR\end{bmatrix}p + \begin{bmatrix}KYY & KYR \\ \hline KRY & KRR\end{bmatrix}\right]\left\{\begin{matrix}UY \\ \hline UR\end{matrix}\right\} = \left\{\begin{matrix}PY \\ \hline PR\end{matrix}\right\} \qquad (4)$$

$\{p^2UR\}$ is the known acceleration on the base. The known forces

resulting from individual base masses are $[MYR]\{p^2UR\}$ and $[MRR]\{p^2UR\}$.

Isolate the upper partition depicting the behavior of the portion of the structure extending beyond the base.

$$[[MYY:MYR]p^2 + [BYY:BYR]p + [KYY:KYR]] \left\{ \frac{UY}{UR} \right\} = \{PY\} \qquad (5)$$

Transfer known terms to the right hand side (RHS) of the equation.

$$[[MYY:0]p^2 + [BYY:BYR]p + [KYY:KYR]] \left\{ \frac{UY}{UR} \right\} = \{PY - [MYR]\{p^2UR\}\} \qquad (6)$$

Incorporate the remaining known forcing term $[MRR]\{p^2UR\}$ by adding it to both sides of the equation.

$$\left[\begin{bmatrix} MYY & 0 \\ \hline 0 & MRR \end{bmatrix} p^2 + \begin{bmatrix} BYY & BYR \\ \hline 0 & 0 \end{bmatrix} p + \begin{bmatrix} KYY & KYR \\ \hline 0 & 0 \end{bmatrix} \right] \left\{ \frac{UY}{UR} \right\} = \left\{ \frac{PY - [MYR]\ \{p^2UR\}}{[MRR]\ \{p^2UR\}} \right\} \qquad (7)$$

When $\{UG\}$ is solved for, the original $p^2\{UR\}$ should be recovered. PY represents known force loading distinct from the base motion forcing. No such external loading is allowed on the points of the R-set. This is the equation that is presented to NASTRAN at the G-level for solution of the $\{UG\}$ response. Further details of the processing will be taken up later, but now turn to the lower partition which depicts the forces that develop on the base due to the inertias, damping coupling, and elastic coupling after the $\{UG\}$ are found from the solution of the upper partition.

$$[[MRY:MRR]p^2 + [BRY:BRR]p + [KRY:KRR]] \left\{ \frac{UY}{UR} \right\} = \{PR\} \qquad (8)$$

$\{PR\}$ is the vector of unknown forces which are found by summing up the terms on the left hand side. There is a way of allowing $\{PR\}$ to contain both known external forces and unknown base forces that develop. The method would involve a looping through the modules DPD and TRSLG twice in order to isolate the direct load so as to subtract it during the solution of the base force. Such a scheme is not being implemented here.

Implementation can go various routes, i.e. rigid base vs. elastic

base, absolute coordinates vs. relative coordinates, exciting individual base points vs. exciting only a reference point, recover complete base force response vs. echo only input force, include direct matrix input contributions to load vs. only G-set contributions, refine displacement response with Koo portion or not, recover stresses via relative coordinates vs. stresses via absolute coordinates, external generation of loads vs. internal assembly, inertia only loading vs. inertia, damping, and elastic loading.

The primary decision was to opt for internal assembly of loads. The scheme is this. Put the masses from the coupling partition MYR and the base masses MRR in the coefficient positions on the DAREA cards and put the base accelerations on TABLED1 cards. When these DAREA and TABLED1 data are delivered to the DPD module, they are multiplied together to produce the time varying forces on the individual grid points. The module RBTM (Rigid Body Transformation Matrix) was designed to determine the orientation of the inertias at local grid points with respect to the orientation of the acceleration field operating on the base points. Acceleration field orientation is defined in terms of the basic coordinate system, consequently RBTM constructs the transformation between points of the structure in their global system and a nominal point in the basic system. This Gx6 transformation matrix [HAICH] is partitioned to Rx6 matrix [HRX6]. When the base partitions of the mass matrix [MRY] and [MRR] are multiplied into [HRX6], inertia terms coupled to the base points are picked up according to their orientations to form the spatial coefficients on DAREA loading cards.

$$\begin{bmatrix} MYR \\ --- \\ MRR \end{bmatrix} [HRX6] = [MSEIS]$$

The module NRTS was written to take the masses, as organized in MSEIS, to deploy them in DAREA format, and finally to assemble them into the sections reserved for them in the DYNAMICS data block amongst the loads that were assembled earlier into DYNAMICS by the IFP module.

Refer to equation (7) and note that the full matrices for M, B, and K cannot be delivered to the NASTRAN chain of matrix condensation without first removing those partitions which are no longer part of the L.H.S. in the equations of equilibrium. The solution will be essentially that of a free body with loads on base points responding in absolute coordinates. Base points will be allowed to be excited in all 6 dof's. Single point constraints imply that points are to be held fixed with respect to coordinates fixed in space, but this is almost physically impossible to do since the ground on which the structure is mounted is also suffering a seismic disturbance. A mechanical connection would be needed to tie the constrained points to the reference frame to maintain zero absolute displacement. But this frame would need to be outside the seismic zone in order to be free of seismic disturbance. Such a mechanical tie is physically unrealistic. The technique, developed here, for the direct method will allow a flexible base with each of its points

to be independently excited. All contributions to base forces will be recovered by implementating equation (8) completely. No contribution to loading from masses defined with DMIG input has been implemented. Every permitted form of damping in R.F. 9 is operational in this seismic analysis.

The modules of rigid format 9 are allowed to process the matrices, prepared as shown above for the L.H.S., down through the DPD module without intervention. When module GKAD goes into operation, it processes the DMIG matrices and assembles the E-points with the G-set to create the P-set. Here the full set of partitions indicated in equation (2) are restored to the system before condensing the P-set to D-size for solution.

The complete expression for the first step in the recovery of displacements from the condensed dynamic solution is:

$$\{UO\} = [GOD]\{UD\} + \{UOO\}, \text{ where } \{UOO\} = [KOO]^{-1}\{POT\}.$$

Currently in the four dynamics rigid formats the $\{UOO\}$ term is omitted from the data recovery sequence. An option is provided to include the $\{UOO\}$ term under the control of the parameter URFIN. Provision for this option was implemented by modifying the TRLG module to include the POT partition of the load vector PPT in its output complement. The strategy used was to allow the recovery of the uncorrected UPV response to proceed in module SDR1 from D-size back up to P-size, but then provide a correction following this step and add it to the UPV vector after it leaves module SDR1.

Several intermediate steps are necessary to recover this incremental correction to P-size to make it commensurable for adding to UPV. DMAP module SOLVE is called upon to find UOO from POT and KOO. UOO is first inflated to FE size by adding zeroes in the positions of the D-set, and then inflating to NE size.

$$\left\{ \frac{0}{UOO} \right\} \implies \{UOOFE\} \qquad \left\{ \frac{0}{UOOFE} \right\} \implies \{UOONE\}$$

The correction for multi-point contraints is applied next.

$$[GMD]\{UOONE\} = \{UOOM\}$$

The final P-sized correction is obtained by merging the M partition with the NE partition.

$$\left\{ \frac{UOONE}{UOOM} \right\} \implies \{UOOP\}$$

101

UOOP is a vector of time varying translations only. Before the correction can be applied to UPV, it has to be converted to the same format as UPV; i.e., a column of translations followed by a column of velocities followed by a column of accelerations for every output time step. The module KREKU was written to differentiate UOOP twice, and reformat it, then add it to UPV.

Stress recovery becomes critical when a problem deals with large displacements, because the first step is the calculation of strain, which involves finding small differences between large numbers. In order to alleviate this hazard, it was decided to transform the response to relative coordinates before computing strains. To implement this idea, one point of the base is arbitrarily selected as a reference point. The absolute response of this one point is partitioned from the total solution. A rigid body transformation from this reference point gives the rigid body motion of the entire structure due to base forcing of this one point. This is not necessarily the true rigid body motion of the whole structure, because the selection of the single reference point was arbitrary and in the actual case many points could have been independently excited. This is of no consequence, because the purpose is not necessarily to determine the true rigid body motion, but to establish numbers on the order of rigid body motion to subtract uniformly from the absolute motion of every point so as to reduce the resulting quantities when differenced for strain computations. This is a correct procedure for all points except E-points. Because they are not geometric points, there is no such thing as a rigid body transformation of E-points. Therefore, E-points are excluded from the transformation to relative coordinates by partitioning from UPV before applying the transformation. The E-partition is merged back with the relative solution to restore it to P-size to satisfy the needs of the recovery module SDR2. The steps are:

$$\{UPV\} \implies \left\{ \begin{array}{c} UEV \\ \hline UGV \end{array} \right\}$$

$$\{UDVT\} \implies \left\{ \begin{array}{c} 0 \\ \hline UVWJVT \end{array} \right\}$$

$$[HGTOJ]\{UVWJVT\} = \{UGRIGD\}$$

$$\{UGV\} - \{UGRIGD\} = \{RELUGV\}$$

$$\left\{ \begin{array}{c} UEV \\ \hline RELUGV \end{array} \right\} \implies \{RELUPV\}. \quad \{RELUPV\} \text{ goes to SDR2 for stress recovery.}$$

Even though {UR} and p{UR} are known and even though force develops from known damping when multiplied into known velocity and force develops from known elasticity when multiplied into known translations, one cannot declare a known forcing function in this case. Damping and elastic forces arise from differences in motion between pairs of points and the history of only one of the two paired points is known. The history of the other of the two points has to be solved for before damping and elastic boundary forces can be determined. With an elastic base, however, differences in motion between pairs of points can be foretold and consequently damping and elastic boundary forces amongst pairs in the R-set can be gathered on the RHS as boundary forces. The lower partition of equation (7) would be augmented to this degree of adding these forces to both sides of the equation.

$$\left[\begin{bmatrix} MYY & 0 \\ \hline 0 & MRR \end{bmatrix} p^2 + \begin{bmatrix} BYY & BYR \\ \hline 0 & BRR \end{bmatrix} p + \begin{bmatrix} KYY & KYR \\ \hline 0 & KRR \end{bmatrix}\right] \begin{Bmatrix} UY \\ \hline UR \end{Bmatrix} = \begin{Bmatrix} PY - [MYR]p2\{UR\} \\ \hline\hline [MRRp2 + BRRp + KRR]\{UR\} \end{Bmatrix} \quad (7A)$$

Equation (8) would remain for the recovery of base forces. No provision has been made in TBLGEN for preparing velocity and translation tables so an entirely elastic formulation has not been implemented in this task as equation (7A) was not followed; however, the groundwork has been laid for eventual implementation. What we have at this point is an elastic base subject to independent time distribution of accelerations over the base. This work in effect has provided an extension beyond that contracted for in that it goes beyond a purely rigid base for inertia forcing. In a rigid base, all points would move synchronously. That restriction has been lifted for inertia loading so that individual time histories with individual time delays at points can be assembled. This is well beyond the rigid body restriction.

The effect on solution times should be addressed. Notice the character of the coefficient matrices M, B, & K in equation (7). M is symmetric but B and K are unsymmetric. As a result, unsymmetric decomposition will be called for during the integration of this equation. Running times can be as much as 4 times longer than the time for similar problems formulated with symmetric matrices, depending on the extent of the coupling terms.

MODAL THEORY

The set of base points for the modal approach are constrained to zero displacement in all 6 d.o.f.'s and loading takes place as a consequence of the inertia reaction of all points extending beyond the base due to the rigid synchronous motion of the base. If recovery of absolute acceleration is required, a reference point is needed at the base which is not clamped (as all other base points are) so as to supply the input base motion in a NASTRAN data block organized in the same time intervals that the response results are in. This can be obtained by choosing a location that is to be used for reference; then duplicating this point and excluding it from the set of constrained base points. Associate unity inertia with each of the 6 d.o.f.'s for this reference point with a CONM2 bulk data card. Make an elastic connection to a

103

grounded point with a BAR element. This reed is completely disjoint from the primary structure. Put the point of the tip of this reed—that lies in the plane of the base—in the R-set by using the SUPORT bulk data card. Partition equation (3) into these components. First partition with respect to the base points; call these the B-set and call the complement of B-set with respect to G-set the X-set.

$$\left[\begin{bmatrix} MXX & MXB \\ \hline MBX & MBB \end{bmatrix} p^2 + \begin{bmatrix} BXX & BXB \\ \hline BBX & BBB \end{bmatrix} p + \begin{bmatrix} KXX & KXB \\ \hline KBX & KBB \end{bmatrix} \right] \left\{ \begin{matrix} UX \\ \hline UB \end{matrix} \right\} = \left\{ \begin{matrix} PX \\ \hline PB \end{matrix} \right\} \quad (9)$$

Next, partition the R-set from the X-set. Name the set that is the complement of the R-set with respect to the G-set the Y-set. And name the set that is the complement of the R-set with respect to the X-set the C-set.

$$\left[\begin{bmatrix} MCC & MCR & MCB \\ \hline MRC & MRR & MRB \\ \hline MBC & MBR & MBB \end{bmatrix} p^2 + \begin{bmatrix} BCC & BCR & BCB \\ \hline BRC & BRR & BRB \\ \hline BBC & BBR & BBB \end{bmatrix} p + \begin{bmatrix} KCC & KCR & KCB \\ \hline KRC & KRR & KRB \\ \hline KBC & KBR & KBB \end{bmatrix} \right] \left\{ \begin{matrix} UC \\ UR \\ UB \end{matrix} \right\} = \left\{ \begin{matrix} PC \\ PR \\ PB \end{matrix} \right\} \quad (10)$$

Introduce a relative set of coordinates between the reference point in the R-set and other parts of the structure with the capability of expressing total motion as being composed of that due to the motion of the base plus that due to the deformation with respect to the base; i.e., rigid body motion plus relative motion. Make three separate definitions for the three sets C, R, and B. First the C-set.

$$\{UC\} = [HCR]\{UR\} + \{Uv\} \quad (11).$$

In words this equation says: the displacement of points in the C-set extending away from the reference point in the base consists of the rigid body motion of the C-set due to the enforced motion of the reference point [HCR]{UR} plus the deformation of the C-set away from the base reference {Uv}, where [HCR] is the rigid body transformation matrix between the R-set and the C-set. Next the R-set.

$$\{UR\} = [IRR]\{UR\} \quad (12).$$

Base reference motion is equal to itself, where [IRR] is the identity matrix for the R-set. Third the B-set.

$$\{UB\} = [HBR]\{UR\} + \{Ue\} \quad (13).$$

The displacement of points in the B-set, lying entirely in the base, consists of the rigid body motion of the B-set due to the enforced motion of the reference point [HBR]{UR} plus the deformation of the B-set away from the reference point {Ue}, where [HBR] is the rigid body transformation matrix between the R-set and the B-set. Impose the rigid body condition that there is no elastic deformation of the base; i.e., {Ue} = 0, which says that the base position is always known in terms of

the motion of the reference point. Combine these 3 statements into a single matrix.

$$\{UG\} = \begin{Bmatrix} UC \\ \hline UR \\ \hline UB \end{Bmatrix} = \begin{bmatrix} Ivv & HCR & 0 \\ \hline 0 & IRR & 0 \\ \hline 0 & HBR & Iee \end{bmatrix} \begin{Bmatrix} Uv \\ \hline UR \\ \hline Ue \end{Bmatrix} \qquad (14).$$

The product [Iee]{Ue} = 0; set the deformation {Ue} null. Retention of [Iee] preserves the integrity of the coefficient matrices for proper handling internally within NASTRAN. Apply this transformation matrix to the dynamic equation.

$$\left[\begin{bmatrix} MCC & MCR & MCB \\ \hline MRC & MRR & MRB \\ \hline MBC & MBR & MBB \end{bmatrix} p^2 + \begin{bmatrix} BCC & BCR & BCB \\ \hline BRC & BRR & BRB \\ \hline BBC & BBR & BBB \end{bmatrix} p + \begin{bmatrix} KCC & KCR & KCB \\ \hline KRC & KRR & KRB \\ \hline KBC & KBR & KBB \end{bmatrix} \right] \begin{bmatrix} Ivv & HCR & 0 \\ \hline 0 & IRR & 0 \\ \hline 0 & HBR & Iee \end{bmatrix} \begin{Bmatrix} Uv \\ \hline UR \\ Ue \end{Bmatrix} = \begin{Bmatrix} PC \\ PR \\ PB \end{Bmatrix} (15)$$

Expand and recombine:

$$\left[\begin{bmatrix} (MCC{\cdot}Ivv{+}MCR{\cdot}0{+}MCB{\cdot}0) & (MCC{\cdot}HCR{+}MCR{\cdot}IRR{+}MCB{\cdot}HBR) & (MCC{\cdot}0{+}MCR{\cdot}0{+}MCB{\cdot}Iee) \\ (MRC{\cdot}Ivv{+}MRR{\cdot}0{+}MRB{\cdot}0) & (MRC{\cdot}HCR{+}MRR{\cdot}IRR{+}MRB{\cdot}HBR) & (MRC{\cdot}0{+}MRR{\cdot}0{+}MRB{\cdot}Iee) \\ (MBC{\cdot}Ivv{+}MBR{\cdot}0{+}MBB{\cdot}0) & (MBC{\cdot}HCR{+}MBR{\cdot}IRR{+}MBB{\cdot}HBR) & (MBC{\cdot}0{+}MBR{\cdot}0{+}MBB{\cdot}Iee) \end{bmatrix} p^2 + \right.$$

$$\begin{bmatrix} (BCC{\cdot}Ivv{+}BCR{\cdot}0{+}BCB{\cdot}0) & (BCC{\cdot}HCR{+}BCR{\cdot}IRR{+}BCB{\cdot}HBR) & (BCC{\cdot}0{+}BCR{\cdot}0{+}BCB{\cdot}Iee) \\ (BRC{\cdot}Ivv{+}BRR{\cdot}0{+}BRB{\cdot}0) & (BRC{\cdot}HCR{+}BRR{\cdot}IRR{+}BRB{\cdot}HBR) & (BRC{\cdot}0{+}BRR{\cdot}0{+}BRB{\cdot}Iee) \\ (BBC{\cdot}Ivv{+}BBR{\cdot}0{+}BBB{\cdot}0) & (BBC{\cdot}HCR{+}BBR{\cdot}IRR{+}BBB{\cdot}HBR) & (BBC{\cdot}0{+}BBR{\cdot}0{+}BPB{\cdot}Iee) \end{bmatrix} p +$$

$$\left. \begin{bmatrix} (KCC{\cdot}Ivv{+}KCR{\cdot}0{+}KCB.0) & (KCC{\cdot}HCR{+}KCR{\cdot}IRR{+}KCB{\cdot}HBR) & (KCC{\cdot}0{+}KCR{\cdot}0{+}KCB{\cdot}Iee) \\ (KRC{\cdot}Ivv{+}KRR{\cdot}0{+}KRB{\cdot}0) & (KRC{\cdot}HCR{+}KRR{\cdot}IRR{+}KRB{\cdot}HBR) & (KRC{\cdot}0{+}KRR{\cdot}0{+}KRB{\cdot}Iee) \\ (KBC{\cdot}Ivv{+}KBR{\cdot}0{+}KBB{\cdot}0) & (KBC{\cdot}HCR{+}KBR{\cdot}IRR{+}KBB{\cdot}HBR) & (KBC{\cdot}0{+}KBR{\cdot}0{+}KBB{\cdot}Iee) \end{bmatrix} \right] \begin{Bmatrix} Uv \\ UR \\ Ue{=}0 \end{Bmatrix}$$

$$= \begin{Bmatrix} PC \\ PR \\ PB \end{Bmatrix} \quad (16)$$

Observe that [Ijj][MTX] = [MTX]. Delete zero products. Rewrite.

$$\left[\begin{bmatrix} MCC & (MCC{\cdot}HCR + MCR{\cdot}IRR + MCB{\cdot}HBR) & MCB \\ MRC & (MRC{\cdot}HCR + MRR{\cdot}IRR + MRB{\cdot}HBR) & MRB \\ MBC & (MBC{\cdot}HCR + MBR{\cdot}IRR + MBB{\cdot}HBR) & MBB \end{bmatrix} p^2 + \right.$$

$$\begin{bmatrix} BCC & (BCC{\cdot}HCR + BCR{\cdot}IRR + BCB{\cdot}HBR) & BCB \\ BRC & (BRC{\cdot}HCR + BRR{\cdot}IRR + BRB{\cdot}HBR) & BRB \\ BBC & (BBC{\cdot}HCR + BBR{\cdot}IRR + BBB{\cdot}HBR) & BBB \end{bmatrix} p +$$

$$\left. \begin{bmatrix} KCC & (KCC{\cdot}HCR + KCR{\cdot}IRR + KCB{\cdot}HBR) & KCB \\ KRC & (KRC{\cdot}HCR + KRR{\cdot}IRR + KRB{\cdot}HBR) & KRB \\ KBC & (KBC{\cdot}HCR + KBR{\cdot}IRR + KBB{\cdot}HBR) & KBB \end{bmatrix} \right] \begin{Bmatrix} Uv \\ UR \\ Ue{=}0 \end{Bmatrix} = \begin{Bmatrix} PC \\ PR \\ PB \end{Bmatrix} \quad (17)$$

105

Interpret the term [BCC][HCR]p{UR}. Move the operator ahead of the constant matrix and look first at just the product [HCR]{UR}. This says that the position of the coordinates {UC} are precisely known according to the movement of coordinate {UR} by obeying the proscription of matrix [HCR]. This implies that as time goes by (p{UC} - p{UR}) remains invariant. The development of force within a damper depends on change in the relative positions of connecting points. Consequently, the complete term [BCC][HCR]p{UR} says that since BCC sees no change in (p{UC} - p{UR}), no force develops. The reasoning applies to all damping and elastic terms that are post multiplied by [HiR]{UR}. All of these null contributions can be removed from the dynamic equation.

Apply these observations and the dynamic equation becomes

$$
\left[\begin{bmatrix} MCC & (MCC^{\cdot}HCR + MCR^{\cdot}IRR + MCB^{\cdot}HBR) & MCB \\ MRC & (MRC^{\cdot}HCR + MRR^{\cdot}IRR + MRB^{\cdot}HBR) & MRB \\ MBC & (MBC^{\cdot}HCR + MBR^{\cdot}IRR + MBB^{\cdot}HBR) & MBB \end{bmatrix} p^2 + \begin{bmatrix} BCC & BCR & BCB \\ BRC & BRR & BRB \\ BBC & BBR & BBB \end{bmatrix} p \right.
$$

$$
\left. + \begin{bmatrix} KCC & KCR & KCB \\ KRC & KRR & KRB \\ KBC & KBR & KBB \end{bmatrix} \right] \left\{ \begin{matrix} Uv \\ UR \\ Ue=0 \end{matrix} \right\} = \left\{ \begin{matrix} PC \\ PR \\ PB \end{matrix} \right\} \quad (18)
$$

Now interpret the inertia terms. The first term in parentheses

[MCC][HCR]p^2{UR} says that all inertias on the C-coordinates provide a force contribution to the dynamic equilibrium in the C-coordinates proportional to the amount of rigid body acceleration produced in the C-coordinates by enforced motion of the reference point. Skip the next

quantity in parentheses and look at the term [MCB][HBR]p^2{UR}. It says that all inertias on the C-coordinates due to coupling with the B coordinates provide a force contribution to the dynamic equilibrium in the C-coordinates proportional to the amount of rigid body acceleration acting in the B coordinates defined by the enforced motion of the reference point. Note that each part of these two products are known--the inertias, the transformation and the acceleration. These constitute the inertia loading of the structure. These two terms can be transformed to the R.H.S. of the equation as part of the known loading on the C-coordinates.

Before interpreting other inertia terms, reflect on the purpose of the reed scaffold that was synthetically introduced into the problem. The tip of the reed was to respond in exactly the same way that it was excited. The tip was given a mass and only that mass was to be accelerated with the loading specification.

106
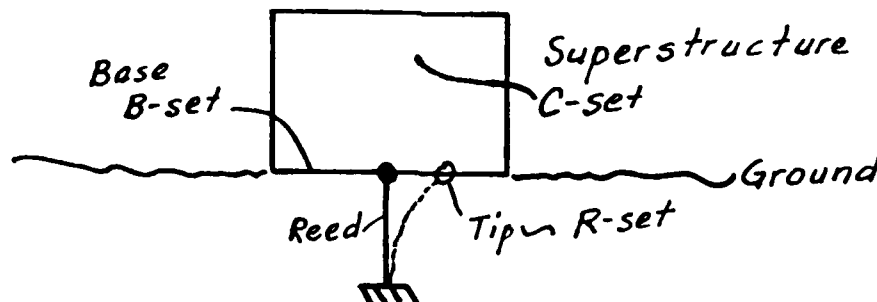
Looking at the diagram, one sees that the tip of the reed is the only thing in the R-set. If the user chooses to put intermediate points on the reed, those points would be grouped with the C-set. If the mass on the tip of the reed were supplied as a CONM2, and if the reed from tip to ground were massless, then the mass matrix for the reed would consist of the partition MRR only and would be devoid of MCR and MBR and so would their transposes; i.e., no mass coupling between the R-set and either the C or B sets. Apply these observations to the dynamic equation. The reed could also be modeled with no damping coupling between the C and R sets, but this is not mandatory. There would be no conceivable utility to have either damping or elastic coupling between the B-set and the R-set, however.

$$
\left[
\begin{bmatrix}
MCC & MCR=0 & MCB \\
MRC=0 & MRR & MRB=0 \\
MBC & (M_{b}C^{\bullet}HCR + MBR=0 + MBB^{\bullet}HBR) & MBB
\end{bmatrix} p^2 +
\begin{bmatrix}
BCC & BCR & BCB \\
BRC & BRR & BRB \\
BBC & BBR & BBB
\end{bmatrix} p +
\right.
$$

$$
\left.
\begin{bmatrix}
KCC & KCR & KCB \\
KRC & KRR & KRB \\
KBC & KBR & KBB
\end{bmatrix}
\right]
\begin{Bmatrix}
Uv \\
UR \\
Ue=0
\end{Bmatrix}
=
\begin{Bmatrix}
PC - [MCC^{\bullet}HCR + 0 + MCB^{\bullet}HBR] p^2 \{UR\} \\
PR \\
PB
\end{Bmatrix}
\quad (19)
$$

There are two things to notice at this point. First, all coefficient matrices are symmetric except the 3-2 term in the mass matrix. Second, the {PR} load on the reed mass is not defined. As to the first, the assymmetry comes about in the recovery of base loading. The unsymmetric [MBC·HCR + MBB·HBR] quantities need not be introduced during the solution phase of the execution. They can be introduced during data recovery. This is not a case of illegal tampering, because when the base constraints are imposed during the solution phase, the B-partition in relative coordinates is dormant (that is fully constrained by an SPC condition). Symmetry in the coefficient matrices can be preserved during the solution phase and all the solution efficiencies associated with symmetric matrices can be enjoyed.

Inflate MSIZB with zeroes in the Y positions to bring it to G-size

[0:MSIZB] ==> [MBRG].

If MBCG and MBRG are added, it will leave the resulting matrix null in the B positions. Since the {Ue} vector of relative displacements in the B-set is zero, it does not matter in equation (27) if the elements in the coefficient matrix to these terms is null.

[MBCG] + [MBRG] = [MFBG].

The technique that NASTRAN uses in the solution by the transient method is to handle the responses in displacements, velocities, and accelerations by combining them into a triplet at every time step. Notice in equation (23) that the accelerations, velocities, and displacements operate independently to recover base response forces. Consequently, the UPV matrix of solution responses will have to be split from their triplet format. The module KREKU

107

was written to do this job. It puts out 3 G-sized time varying components. Now comes an explanation for setting up the auxiliary reed structure. Since all base points were fully constrained to zero, they are not available as a reference for the {UR} vector in equation (11). The mass at the tip of the reed is co-located with one point chosen from the set of base points, and it is accelerated with the specified time history—as the unconstrained mass points in the principal structure are. A unit diagonal mass matrix is assigned to the reed tip in the bulk data with a CONM2 card. When the load on the tip of the reed is formed, it is numerically equal to the seismic acceleration. Thus the R partition of the load vector PRT contains the acceleration converted to a NASTRAN data block.

Partition the load vector on the reference point PRT from the vector of loads on all physical points PPT.

$$\{PPT\} \implies \left\{ \frac{PZT}{PRT} \right\}$$

In order to get the effect of absolute motion in the recovery of base forces, the exciting acceleration needs to be restored to the R-set. Partition ACGVT as it is output from KREKU and retain only the Y-set (ACYVT). Then merge in the base acceleration PRT to restore the acceleration to G-size.

$$\{ACGV\} \overset{GYVEC}{\implies} \left\{ \frac{ACYVT}{} \right\} \qquad ; \qquad \left\{ \frac{ACYVT}{PRT} \right\} \overset{GYVEC}{\implies} \{ACCG\}$$

Form the base forcs from inertias per equation 27 with PRT substituted for UR.

[MFBG][ACCG] = Base Inertia Forces,

and next the elastic component,

[KBG][DIGV] = Base Elastic Forces.

Note, damping defined in terms of grid point partitions are available only through DMIG input. Modal damping B(omega) is not available for base force recovery, because it is not defined in terms of geometric coordinates. The B2PP matrix can be partitioned and can be used for recovery of base forces from

[B2BG][VEGV] = Base Damping Forces.

All 3 forces sum to BASEF and are attached to the PPT vector for output processing. Therefore, to get a listing of base force response, the user inserts a command for OLOAD to include base points.

$$\{UGV\} \implies \left\{ \frac{UYV}{URV} \right\}. \quad \text{UYV is the relative response on the Y-coordinates.}$$

Merge zeroes into UYV in the R-set locations to get a G-sized relative response vector.

$$\left\{ \dfrac{UYV}{0} \right\} ==> \{UGREL\}$$

Now use the rigid body transformation matrix with respect to the reference point HAICH and reconstruct absolute response in accordance with equation (11).

$$\{UABSG\} = [HAICH]\{URV\} + \{UGREL\}.$$

Merge the E-partition back onto the G-set to get a P-sized absolute response vector ready to complete processing in modules SDR2, OFP, and PLOT. This method works only if the reed has a frequency content to match that of the load. Lacking sufficient spectral content in the reed gives values for URV far less than those of the input specification. This puts too much burden on the analyst to model the reed well for each different loading. Consequently, a substitute method has been implemented that is repeatable and dependable and is independent of the skill of the analyst. The method, however, is less general. <u>Only</u> absolute accelerations can be recovered <u>instead of</u> absolute displacements, absolute velocities and absolute accelerations. Tests were successful in producing the tabulations of load at the required solution time intervals. Since unity mass is to be used, these loads are numerically identical to the forcing accelerations and are therefore quite suitable as a set of reference values for recovery of absolute acceleration in the required organization to suit NASTRAN's bookkeeping.

Begin the process of recovering absolute accelerations by inflating the Y partition of response with zeroes in the R-positions back to G-size.

$$\left\{ \dfrac{ACYVT}{0} \right\} \overset{GYVEC}{==>} \{RELACG\}$$

Use rigid body transformation between the reference R-set and all other points in the structure to reconstruct the rigid body accelerations throughout the structure, then add the relative accelerations to this result to obtain the absolute accelerations.

$$[HAICH]\{PRT] + \{RELACG\} = \{ABSACG\}.$$

Inflate ABSACG back to P-size and back to triplet format so as to be able to make the resulting ABSACPT data block acceptable to data recovery modules SDR2 and SDR3 and OFP for final output processing.

The resulting absolute accelerations can be passed to the XYPLOT module for answering plot requests in Case Control. DMAP alters have been incorporated into the seismic packet to accomplish this.

For the first time as a result of implementing this theory there is an acceleration loading capability in the public domain. In the following pages are packets of the DMAP ALTER's that were written to splice this capability into the four dynamic rigid formats.

$ DMAP ALTER PACKET PERTAINING TO R.F. 8 SIESMIC ANALYSIS
$ SOLN8I.TXT
$
$SOLUTION TAKES PLACE IN ABSOLUTE COORDS IN THE FN. RESP. DIRECT RIGID
$
$FORMAT.   ALL COMPONENTS OF BASE POINTS TO BE ACCELERATED ARE ASSIGNED
$
$TO THE R-SET THRU THE USE OF THE SUPORT CARD.
$
$ASSIGN DAREA ID'S ON BULK PARAM NRTID# CARDS AND RLOAD CARDS.   ASSIGN
$
$TABLED1 ID'S TO RLOAD CARDS AND TO TABLED1 CARDS DIRECTLY OR TO TBLGEN
$
$FOR THE FOR THE DISPLACEMENT HISTORIES.   NRTID#'S WILL BE PICKED UP BY
$
$MODULE NRTS FOR INTERNAL GENERATION OF DAREA CARDS GIVING THE DISTRI-
$
$BUTION OF MASS MAGNITUDES.   THESE INTERNALLY GENERATED DAREA CARDS WILL
$
$BE PICKED UP BY THE RLOAD CARD FOR MULTIPLICATION AND ASSEMBLY WITH THE
$
$DISPLACEMENT HISTORIES THAT RLOAD PICKS UP FROM TABLED1 CARDS.
$
$SPC'S (ON OTHER THAN THE GRID CARDS) ARE PHYSICALLY UNREALISTIC, BE-
$
$CAUSE THEY RELATE TO ABSOLUTE COORDINATES WHICH IMPLIES BEING FIXED
$
$OUTSIDE THE SEISMIC ZONE.
$
$TWO OPTIONS ARE AVAILABLE: REFINEMENT OF THE DISPLACEMENT RESPONSE BY
$
$ INCLUDING THE RECOVERY OF THE KOO PORTION OF THE O-SET, AND THE RE-
$
$ COVERY OF BASE FORCES WHICH REACT THE SPECIFIED INPUT TIME HISTORIES.
$
$FOR THE RECOVERY OF STRESSES, ONE OF THE POINTS IN THE R-SET MUST BE
$
$ NAMED ON A PARAM GRDPNT CARD TO BE USED AS A RIGID BODY REFERENCE FOR
$
$ SUBTRACTING THE LARGE BASE MOTION FROM ALL POINTS SO AS TO KEEP ALL
$
$ DIFFERENCING FORSTRESS RECOVERY A MATTER OF MUCH SMALLER NUMBERS.
$
$PARAMETER DEFINITIONS:
$
$NRTID1,2,3= SET ID'S TO BE ASSIGNED TO DAREA CARDS REPRESENTING THE
$ SPATIAL ARRANGEMENT OF INERTIAS ASSOCIATED WITH TRANSLATIONAL
$ ACCELERATIONS IN THE FIRST, SECOND, & THIRD COORD DIRECTIONS.
$NRTID4,5,6= SET ID'S TO BE ASSIGNED TO DAREA CARDS REPRESENTING THE
$ SPATIAL ARRANGEMENT OF INERTIAS ASSOCIATED WITH ROTATIONAL
$ ACCELERATIONS ABOUT THE FIRST, SECOND, & THIRD COORD DIRECTIONS.

```
$URFIN WHEN SET < OR = -1 ENABLES THE OPTION TO REFINE OUTPUT DISPLACE-
$        MENTS WITH CONTRIBUTIONS FROM OMITTED SETS.
$        WHEN SET  > OR = 0 DISABLES THE OPTION TO REFINE OUTPUT DISPLACE-
$        MENTS WITH CONTRIBUTIONS OMITTED SETS.   DEFAULT = + 1.
$QRFIN WHEN SET < OR = -1 ENABLES THE OPTION TO RECOVER BASE FORCES FROM
$    STIFFNESS, DAMPING, & MASS COUPLING AND FROM BASE INERTIAS.
$        WHEN SET  > OR = 0 DISABLES THE OPTION TO RECOVER THIS COMPONENT OF
$        BASE FORCE.   DEFAULT = + 1.
$GRDPNT IS DECLARED AS THE REFERENCE GP ON THE PARAM GRDPNT CARD.
$$***********************************************************************
$                        USER PREPARATIONS                            *
$                                                                     *
$   USER MUST SUPPLY SUPORT CARD FOR ALL EXCITED BASE POINTS          *
$                    PARAM GRDPNT BASE REFERENCE POINT (ONE OF R-SET)  *
$                    PARAM NRTID(1-6) FOR DAREA REGARDING ACCELERATIONS*
$                    RLOAD OF ACCEL FOR ALL BASE POINTS               *
$                    ID's TO TBLGEN FOR TABLES OF ACCEL               *
$   USER MAY OVERIDE PARAM URFIN OPTION FOR KOO REFINEMENT            *
$                    PARAM QRFIN OPTION FOR RECOVERY OF BASE REACTIONS *
$   USER MAY SUPPLY  RLOAD FOR DIRECT LOAD ON ALL PTS XCP R-SET       *
$                    E-POINTS FOR TFL                                 *
$                    DAMPING TYPES VISC, DMIG(B2PP), MAT(G), OR AVG(G) *
$                                                                     *
$***********************************************************************

ALTER   63 $ JUST BEFORE MCE
PARAM       //*NOT*/V,N,SEISLD/V,N,REACT $
COND        SYMX,SEISLD $
JUMP        FINIS  $
LABEL       SYMX  $
$$  CALL IN RBTM AT THIS POINT TO ACT AS A VEHICLE FOR ROUTING LOADS TO
$$  ALL POINTS WHICH ARE COUPLED TO THE BASE THROUGH INERTIA.
$$
RBTM        BGPDT,CSTM,EQEXIN,,USET/HAICH,,H1RY6,/C,Y,GRDPNT/+1/*DIRECT* $
$$
$$  NOTICE GRDPNT IS USED HERE AS A REFERENCE FOR TRANSFORMING FROM
$$  GLOBALTO BASIC COORDINATES AND AS A REFERENCE TO RECOVER STRESSES
$$  IN A QUASIRELATIVE COORDINATE SYSTEM.   IT IS NOT DECLARED OUTRIGHT
$$  AS A TRULY RELATIVE COORDINATE SYSTEM BECAUSE THE SELECTION OF THE
$$  REFERENCE GRID-POINT IS LEFT UP TO THE USER AS AN ARBITRARY CHOICE.
$$  THE STRESSES WILL BE THE SAME REGARDLESS OF THE  POINT CHOSEN AS REF.
$$
VEC         USET/GYVEC/*G*/*COMP*/*R* $ 1'S ON R. Y=R(COMP)G
COPY        GYVEC/GY1VEC $
PARTN       HAICH,,GYVEC/,HRX6,,/5/0 $ FRACTION OFF THE R ROWS OF HAICH.
$$
$$  THE HRR TRANSFORMATION MATRIX WILL BE USED BELOW IN THE DAREA
$$  PREPARATION SECTION
```

```
$$
$$REMOVE THE INERTIA COUPLING TERMS FROM THE LEFT HAND SIDE WHICH ARE
$$BEING USED ON THE RHS.   THE ZR INERTIA COUPLING TERMS MUST NOT BE
$$CONDENSED INTO THE DD SET, SO THE YR INERTIA COUPLING TERMS MUST BE
$$PARTITIONED OUT BEFORE MCE.   WHILE SO DOING THE WHOLE MATTER OF
$$SETTING UP THE EQUATION IN Y-ROWS AND R-ROWS CAN ALL BE DONE AT ONE
$$SITTING.
$***************ELASTICITY*************************************************
PARTN     KGG,GYVEC, /KYY,KRY,KYR,KRR/-1/2/6/2/2/6 $
MERGE     KYY,,KYR, ,GYVEC,GYVEC/TKGG/+1/2/1 $ FOR CONDENSATION
MERGE     KRY,,KRR,,GYVEC, /KRG/5/2/2 $ FOR BASE FORCES
$***************MASS*****************************************************
PARTN     MGG,GYVEC, /MYY,MRY,MYR,MRR/-1/2/6/2/2/6 $
MERGE     MYY,,,MRR,GYVEC, /TMGG/-1/2/6 $ FOR CONDENSATION
MERGE     MRY,,MRR,,GYVEC, /M1RG/5/2/2 $ FOR BASE FORCES
$***************VISCOUS DAMPING******************************************
PARTN     BGG,GYVEC, /BYY,BRY,BYR,BRR/-1/2/6/2/2/6 $
MERGE     BYY,,BYR,,GYVEC,GY1VEC/TBGG/+1/2/1 $ FOR CONDENSATION
MERGE     BRY,,BRR,,GYVEC, /B1RG/5/2/2 $ FOR GASE FORCES
$***************DISTRIBUTED DAMPING**************************************
PARTN     K4GG,GYVEC, /K4YY,K4RY,K4YR,K4RR/-1/2/6/2/2/6 $
MERGE     K4YY,,K4YR,,GYVEC,GY1VEC/TK4GG/+1/2/1 $ FOR CONDENSATION
MERGE     K4RY,,K4RR,,GYVEC, /K4RG/5/2/2 $ FOR BASE FORCES
$***************SUMMARY*************************************************
$***************SUMMARY*************************************************
EQUIV     TKGG,KGG/SEISLD/TMGG,MGG/SEISLD/TBGG,BGG/SEISLD/
          TK4GG,K4GG/SEISLD $ FOR CONDENSATION OF STRUCTURAL MATRICES
$$NOW THAT THE INERTIA MATRIX HAS HAD THE YR COUPLING TERMS REMOVED,
$$CONDENSATION DOWN TO A-SIZE FOR GKAD CAN NOW BEGIN.
$
PARAMR    //*COMPLEX*/ /0.0/1.0/EYE/ / / $
PARAMR    //*COMPLEX*/ /1.0/C,Y,G/STRUD/ / / $
ADD       KRG,K4RG/K3RG/V,N,STRUD/V,N,EYE $ FOR BASE FORCES
$***************PREPARE DAREA VALUES FOR DYNAMICS DATA BLOCK***********
MPYAD     MYR,HRX6, /MYY6/0/-1 $ NEGATIVE PRODUCT
MPYAD     MRR,HRX6, /MRR6/0/+1 $ POSITIVE PRODUCT
MERGE     MYY6,MRR6,,,,GYVEC/MSEIS/5/2/2 $  FOR LOAD
$***************LOAD SUMMARY*****************************************
ALTER  87 $ JUST BEFORE DPD
NRTS      MSEIS,DYNAMICS,EQEXIN/NRTSEIS/DEPOP/C,Y,NRTID1/C,Y,NRTID2/
          C,Y,NRTID3/C,Y,NRTID4/C,Y,NRTID5/C,Y,NRTID6 $
EQUIV     NRTSEIS,DYNAMICS/SEISLD $
$$  DATA BLOCK 'DYNAMICS' NOW HAS ALL DAREA ENTRIES FOR LOADING.
$$
ALTER 100 $ JUST AFTER MTRXIN.  PARTITION THE DMIG MATRICES.
VEC       USETD/PZVEC/*P*/*COMP*/*R* $ 1'S ON R.  Z=R,COMP,P.
COPY      PZVEC/PZ1VEC $
COND      AUTOM,NOM2PP $
PARTN     M2DPP,PZVEC, /M2DZZ,M2DRZ,M2DZR,M2DRR/-1/0/6/2/2/6 $
MERGE     M2DZZ,,,M2DRR,PZVEC, /TM2DPP/-1/0/6 $ FOR CONDENSATION
MERGE     M2DRZ,,M2DRR,,PZVEC, /M2DRP/5/0/2 $ FOR BASE FORCES
EQUIV     TM2DPP,M2DPP/SEISLD $ FOR CONDENSATION
LABEL     AUTOM $
```

```
COND        AUTOB, NOB2PP $
PARTN       B2PP, PZVEC, PZ1VEC/B2ZZ, B2RZ, B2ZR, B2RR/+1/0/0/0/0/0 $
MERGE       B2ZZ,, B2ZR,, PZVEC, PZ1VEC/TB2PP/+1/0/1 $ FOR CONDENSATION
MERGE       B2RZ,, B2RR,, PZVEC, /B2RP/5/0/2 $ FOR BASE FORCES
EQUIV       TB2PP, B2PP/SEISLD $ FOR CONDENSATION
LABEL       AUTOB $
COND        AUTOK, NOK2DPP $
PARTN       K2DPP, PZVEC, PZ1VEC/K2DZZ, K2DRZ, K2DZR, K2DRR/+1/0/0/0/0/0 $
MERGE       K2DZZ,, K2DZR,, PZVEC, PZ1VEC/TK2DPP/+1/0/1 $ FOR CONDENSATION
MERGE       K2DRZ,, K2DRR,, PZVEC, /K2DRP/5/0/2 $ FOR BASE FORCES
EQUIV       TK2DPP, K2DPP/SEISLD $ FOR CONDENSATION
LABEL       AUTOK $
$$$$$$$     GKAD TAKES CARE OF COMBINING THE REVISED MTRXIN DATA WITH
$$$$$$$      THE AUTO-STRUCTURAL MATRICES.
$$  GET MATRICES READY FOR BASE FORCE RECOVERY
ALTER 113
EQUIV       M1RG, M1RP/NOUE/B1RG, B1RP/NOUE/K3RG, K3RP/NOUE $
COND        BASEG, NOUE $
VEC         USETD/PGVEC/*P*/*G*/*E* $ 1'S ON E
$$  INFLATE RG MATRICES TO P-SIZE SO AS TO OPERATE WITH UPVC
MERGE       M1RG,,,, PGVEC, /M1RP/5/2/2 $
MERGE       B1RG,,,, PGVEC, /B1RP/5/0/2 $
MERGE       K3RG,,,, PGVEC, /K3RP/5/4/2 $
PURGE       M1RG, B1RG, K3RG/SEISLD $
LABEL       BASEG  $
EQUIV       M1RP, MRP/NOM2DPP/B1RP, BRP/NOB2PP/K3RP, KRP/NOK2DPP $
COND        BASO, NOM2DPP $
ADD         M1RP, M2DRP/MRP/ $
LABEL       BASO $
COND        BAS1, NOB2PP $
ADD         B1RP, B2RP/BRP/ $
LABEL       BAS1 $
COND        BAS2, NOK2DPP $
ADD         K3RP, K2DRP/KRP/ $
LABEL       BAS2 $
$$##@@!!*******************************************************************
$
ALTER 121, 121 $REPLACE FRRD
$
FRSLG       CASEXX, USETD, DLT, FRL, GMD, GOD, DIT, /PPF, PSF, PDF, POF, FOL, /
            *DIRECT*/FREQY=-1/APP=FREQ/S, N, FRQSET/S, N, NFREQ/
            S, N, NLOAD $
FRRD3       KDD, BDD, MDD, PDF, FRL/UDVF/C, N, DISP/C, N, DIRECT/
            V, N, NONCUP/FRQSET=2/V, N, NFREQ/V, N, NLOAD $
$
ALTER 123, 123 $ USE FOL INSTEAD OF PPF FOR A FREQUENCY TEMPLATE.
VDR         CASEXX, EQDYN, USETD, UDVF, FOL, XYCDB, /OUDVC1, /*FREQRESP*/
            *DIRECT*/S, N, SORT2/S, N, NOD/S, N, NOP/0 $ $
$ COMPUTE KOO REFINEMENT TO RESPONSE AND RECOVER BASE FORCES BEFORE
$ PROCESSING OUTPUT.
ALTER 139, 139 $
$$  DEFAULT VALUES OF PARAMETERS ARE SET HERE.   $
PARAM       //*NOP*/V, Y, QRFIN = + 1 $
PARAM       //*NOP*/V, Y, URFIN = + 1 $
```

```
PARAM      //*NOT*/XISTOMIT/OMIT $
PARAM      //*AND*/UORFIN/XISTOMIT/C,Y,URFIN $
COND       UMPRUV,UORFIN $
JUMP       UNRFIN $
LABEL      UMPRUV $
SOLVE      KOO,POF/RUOOF/0/+1/2/0 $
$RUOOF IS A VECTOR OF RELATIVE DISPLACEMENTS.  NO CONVERSION TO
$ ABSOLUTE COORDINATES IS NECESARY BECAUSE NASTRAN HAS ALREADY
$PROCESSED ONE CORRECTION FOR THE O-SET IN ABSOLUTE COORDINATES.
$INFLATE RUOOF TO P-SIZE TO BE COMMENSURATE WITH UPVC.
VEC        USETD/FEDVEC/*FE*/*D*/*O* $ 1'S ON O
MERGE,      ,RUOOF,,,,FEDVEC/UOOFFE/5/4/2 $
EQUIV      UOOFFE,UOOFNE/SINGLE $IT IS NOT ADVISABLE TO HAVE BOUNDARY
$ SPC'S IN THESE PROBLEMS.
COND       POSN1,SINGLE $
VEC        USETD/NEFEVEC/*NE*/*FE*/*S* $ 1'S ON S
MERGE      UOOFFE,,,,,NEFEVEC/UOOFNE/5/4/2 $
LABEL      POSN1 $
EQUIV      UOOFNE,UOOFP/MPCF1 $
COND       POSN2,MPCF1 $
MPYAD      GMD,UOOFNE,/UOOFM/0/+1 $
VEC        USETD/PNEVEC/*P*/*NE*/*M* $ 1'S ON M
MERGE      UOOFNE,UOOFM,,,,PNEVEC/UOOFP/5/4/2 $
LABEL      POSN2 $
ADD        UPVC,UOOFP/UMPRUVF/ $
EQUIV      UMPRUVF,UPVC/URFIN $
LABEL      UNRFIN $
$
$IF THE USER WANTS TO RECOVER BASE RESPONSE FORCES HE SETS QRFIN
$ = -1, HOWEVER IF HE SETS QRFIN=+1, ANY CASECC REQUEST FOR OLOAD
$ WILL CONTAIN ONLY THE EXCITATION INERTIA FORCES AND NOT THE TOTAL
$ SET OF BASE REACTIONS.
COND       OLOD,QRFIN $
JUMP       REGLR $
LABEL      OLOD $
$ THE RECOVERY OF BASE FORCES IS UNDER THE CONTROL OF CASECC OLOAD
$ REQUESTS.  A CALL TO KREKU AT THIS POINT WILL PROVIDE THE DIAGONAL
$ MATRIX [I*OMEGA] WHICH WILL BE USED TO DIFFERENTIATE RESPONSE
$ DISPLACEMENTS INTO VELOCITIES AND ACCELERATIONS BY MULTIPLYING IT
$ INTO UDVF BY IN SUCCEDDING OPERATIONS.
$
$ ARRANGE THE STRUCTURAL MATRICES FOR RECOVERY OF BASE RESPONSE
$ FORCES.  OF THE DAMPING AND ELASTIC MATRICES, ONLY THE COUPLED
$ PARTITION IS NON-ZERO.
$ WITH REGARD TO OTHER PARTITIONS OF BGG AND KGG, BECAUSE
$ [BRR]*[BASEACC] & [KRR]*[BASEACC] ACT ON RIGID MOTIONS WHICH
$ LEAVES ZERO DIFFERENTIAL AMONGST THE R SET, SO THE PRODUCTS ARE
$ NULL.  THIS IS NOT THE CASE FOR INERTIA BECAUSE THEY ACT ON
$ [ISOLATED] GP MOTION AS OPPOSED TO [DIFFERENTIAL] GP MOTION
$
PARTN      PPF, ,PZVEC/PSIZF, , , /5/4/2 $
```

```
KREKU,     ,FOL,,/ ,IW,,,/V,N,OMIT/C,Y,QRFIN/*FREQRESP*/*DIRECT* $
MPYAD      UPVC,IW, /VEPVC/0/+1 $
SMPYAD     MRP,VEPVC,IW,,,/NRTCPLF/3/+1 $
PARAM      //*OR*/V,N,NO12B/NOBGG/NOB2PP $
COND       BAS3,NO12B $
MPYAD      BRP,VEPVC,NRTCPLF/TWOCPLF/0/+1/+1 $
EQUIV      TWOCPLF,NRTCPLF/SEISLD $
LABEL      BAS3 $
MPYAD      KRP,UPVC,NRTCPLF/BASPF/0/1/1 $
MERGE      PSIZF,BASPF,,,,PZVEC/PPFULL/5/4/2 $
EQUIV      PPFULL,PPF/QRFIN $
LABEL      REGLR $
$ NOW THE LOAD VECTOR PPF IS READY TO RESPOND TO CASECC OLOAD REQUESTS
$       FOR BASE FORCE RESPONSE HISTORY.
$***************DATA RECOVERY***************************************
$ RECOVER DISPLACEMENTS AND FORCES (BUT NOT ELEMENT RESPONSES) WITH
$ ABSOLUTE MOTION.
$ USE FOL INSTEAD OF PPF FOR A FREQUENCY TEMPLATE IN SDR2.
$
SDR2       CASEXX,CSTM,MPT,DIT,EQDYN,SILD,,,BGPDP,FOL,QPC,UPVC,EST,
           XYCDB,PPF/OPPC1,OQPC1,OUPVC1,,,PUPVC1/*FREQRESP*/
           S,N,NOSORT2 $
$
$ REMOVE RIGID BODY MOTION TO RECOVER STRESSES IN RELATIVE MOTION
$ WITHOUT THE E-SET.
$
$
$ PARTITION UDVF WRT GRDPNT TO FIND REFERENCE MOTION OF GRDPNT ONLY.
SETPT      EQDYN,USETD/DJVEC/*D*/C,Y,GRDPNT $
PARTN      UDVF,,DJVEC/,UJVF,,/5/4//2 $
EQUIV      UPVC,UGVC/NOUE  $
COND       GSIZ,NOUE $
PARTN      UPVC,,PGVEC/UGVC,UEVC,,/5/4/2/2 $
LABEL      GSIZ $
PARTN      UGVC,,GYVEC/UYVC,,,/5/4/2 $
MPYAD      H1RY6,UJVF,UYVC/UYFREL/0/-1/+1 $
$ INFLATE UYFREL TO G-SIZE WITH ZEROES ON THE R-SET
MERGE      UYFREL,,,,,GYVEC/UGFREL/5/4/2 $
$ PUT THE NON-GEOMETRIC E-SET BACK TO ELEVATE THE RESPONSE TO P-SIZE.
EQUIV      UGFREL,UPVCREL/NOUE $
COND       GOUT,NOUE $
MERGE      UGFREL,UEVC,,,,PGVEC/UPVCREL/5/4/2 $RECOVER EL FORCE & STRESS
LABEL      GOUT  $
SDR2       CASEXX,CSTM,MPT,DIT,EQDYN,SILD,,,BGPDP,FOL,,UPVCREL,EST,
           XYCDB,/,,,OESC1,OEFC1,/*FREQRESP*/S,N,NOSORT2 $
ENDALTER
```

*THIS IS THE END OF THE ALTER PACKET FOR SEISMIC ANALYSIS FOR R.F. 8

$ DMAP ALTER PACKET PERTAINING TO R.F. 9 SIESMIC ANALYSIS
$ SOLN9I.TXT
$
$SOLUTION TAKES PLACE IN ABSOLUTE COORDS IN THE TRANSIENT DIRECT RIGID
$
$FORMAT. ALL COMPONENTS OF BASE POINTS TO BE ACCELERATED ARE ASSIGNED
$
$TO THE R-SET THRU THE USE OF THE SUPORT CARD.
$
$ASSIGN DAREA ID'S ON BULK PARAM NRTID# CARDS AND RLOAD CARDS. ASSIGN
$
$TABLED1 ID'S TO TLOAD CARDS AND TO TABLED1 CARDS DIRECTLY OR TO TBLGEN
$
$FOR THE FOR THE DISPLACEMENT HISTORIES. NRTID#'S WILL BE PICKED UP BY
$
$MODULE NRTS FOR INTERNAL GENERATION OF DAREA CARDS GIVING THE DISTRIBU-
$
$TION OF MASS MAGNITUDES. THESE INTERNALLY GENERATED DAREA CARDS WILL
$
$BE PICKED UP BY THE TLOAD CARD FOR MULTIPLICATION AND ASSEMBLY WITH THE
$
$DISPLACEMENT HISTORIES THAT RLOAD PICKS UP FROM TABLED1 CARDS.
$
$SPC'S (ON OTHER THAN THE GRID CARDS) ARE PHYSICALLY UNREALISTIC, BECAUSE
$
$ THEY RELATE TO ABSOLUTE COORDINATES WHICH IMPLIES BEING FIXED OUTSIDE
$
$ THE SEISMIC ZONE.
$
$TWO OPTIONS ARE AVAILABLE: REFINEMENT OF THE DISPLACEMENT RESPONSE BY
$
$ INCLUDING THE RECOVERY OF THE KOO PORTION OF THE O-SET, AND THE RE-
$
$ COVERY OF BASE FORCES WHICH REACT THE SPECIFIED INPUT TIME HISTORIES.
$
$FOR THE RECOVERY OF STRESSES, ONE OF THE POINTS IN THE R-SET MUST BE
$
$ NAMED ON A PARAM GRDPNT CARD TO BE USED AS A RIGID BODY REFERENCE FOR
$
$ SUBTRACTING THE LARGE BASE MOTION FROM ALL POINTS SO AS TO KEEP ALL
$
$ DIFFERENCING FOR STRESS RECOVERY A MATTER OF MUCH SMALLER NUMBERS.
$
$PARAMETER DEFINITIONS:
$
$NRTID1,2,3= SET ID'S TO BE ASSIGNED TO DAREA CARDS REPRESENTING THE
$ SPATIAL ARRANGEMENT OF INERTIAS ASSOCIATED WITH TRANSLATIONAL
$ ACCELERATIONS IN THE FIRST, SECOND, & THIRD COORD DIRECTIONS.
$NRTID4,5,6= SET ID'S TO BE ASSIGNED TO DAREA CARDS REPRESENTING THE
$ SPATIAL ARRANGEMENT OF INERTIAS ASSOCIATED WITH ROTATIONAL
$ ACCELERATIONS ABOUT THE FIRST, SECOND, & THIRD COORD DIRECTIONS.

```
$URFIN WHEN SET < OR = -1 ENABLES THE OPTION TO REFINE OUTPUT DISPLACE-
$         MENTS WITH CONTRIBUTIONS FROM OMITTED SETS.
$       WHEN SET  > OR = 0 DISABLES THE OPTION TO REFINE OUTPUT DISPLACE-
$         MENTS WITH CONTRIBUTIONS FROM OMITTED SETS.   DEFAULT = + 1.
$QRFIN WHEN SET < OR = -1 ENABLES THE OPTION TO RECOVER BASE FORCES FROM
$         STIFFNESS, DAMPING, & MASS COUPLING AND FROM BASE INERTIAS.
$       WHEN SET  > OR = 0 DISABLES THE OPTION TO RECOVER THIS COMPONENT
$         OF BASE FORCE.   DEFAULT = + 1.
$GRDPNT IS DECLARED THE PRIMARY REFERENCE ON THE PARAM GRDPNT CARD.
$$*****************************************************************************
$                       USER PREPARATIONS                                   *
$                                                                           *
$   USER MUST SUPPLY SUPORT CARD FOR ALL EXCITED BASE POINTS                *
$                    PARAM GRDPNT BASE REFERENCE POINT (ONE OF R-SET)        *
$                    PARAM NRTID(1-6) FOR DAREA REGARDING ACCELERATIONS*
$                    TLOAD OF ACCEL FOR ALL BASE POINTS                      *
$                    ID's TO TBLGEN FOR TABLES OF ACCEL                      *
$   USER MAY OVERIDE PARAM URFIN OPTION FOR KOO REFINEMENT                   *
$                    PARAM QRFIN OPTION FOR RECOVERY OF BASE REACTIONS *
$   USER MAY SUPPLY  TLOAD FOR DIRECT LOAD ON ALL PTS XCP R-SET              *
$                    E-POINTS FOR TFL.                                       *
$                    DAMPING TYPES VISC, DMIG(B2PP), MAT(G), OR AVG(G) *
$                                                                           *
$*****************************************************************************

ALTER    63 $ JUST BEFORE COND JUMP AROUND MCE
PARAM       //*NOT*/V,N,SEISLD/V,N,REACT $
COND        SYMX,SEISLD $
JUMP        FINIS  $
LABEL       SYMX  $
$$ CALL IN RBTM AT THIS POINT TO ACT AS A VEHICLE FOR ROUTING LOADS TO
$$ ALL POINTS WHICH ARE COUPLED TO THE BASE THROUGH INERTIA.
$$
RBTM        BGPDT,CSTM,EQEXIN,,USET/HAICH,,H1RY6,/C,Y,GRDPNT/+1/*DIRECT* $
$$
VEC         USET/GYVEC/*G*/*COMP*/*R* $ 1'S ON R.  Y=R(COMP)G
COPY        GYVEC/GY1VEC $
PARTN       HAICH,,GYVEC/,HRX6,,/5/0 $ FRACTION OFF THE R ROWS OF HAICH.
$$
$$ THE HRX6 TRANSFORMATION MATRIX WILL BE USED BELOW IN THE DAREA
$$ PREPARATION SECTION
$$
$$REMOVE THE INERTIA COUPLING TERMS FROM THE LEFT HAND SIDE WHICH ARE
$$BEING USED ON THE RHS.   THE ZR INERTIA COUPLING TERMS MUST NOT BE
$$CONDENSED INTO THE DD SET, SO THE YR INERTIA COUPLING TERMS MUST BE
$$PARTITIONED OUT BEFORE MCE.   WHILE SO DOING THE WHOLE MATTER OF
$$SETTING UP THE EQUATION IN Y-ROWS AND R-ROWS CAN ALL BE DONE AT ONE
$$SITTING.
$***************ELASTICITY****************************************************
PARTN       KGG,GYVEC, /KYY,KRY,KYR,KRR/-1/2/6/2/2/6 $
MERGE       KYY,,KYR, ,GYVEC,GY1VEC/TKGG/+1/2/1 $ FOR CONDENSATION
MERGE       KRY,,KRR,,GYVEC,/K1RG/5/2/2 $ FOR BASE FORCES
```

117

```
$**************MASS**********************************************************
PARTN      MGG,GYVEC, /MYY,MRY,MYR,MRR/-1/2/6/2/2/6 $
MERGE      MYY,,,MRR,GYVEC, /TMGG/-1/2/6 $ FOR CONDENSATION
MERGE      MRY,,MRR,,GYVEC, /M1RG/5/2/2 $ FOR BASE FORCES
$**************VISCOUS DAMPING***********************************************
PARTN      BGG,GYVEC, /BYY,BRY,BYR,BRR/-1/2/6/2/2/6 $
MERGE      BYY,,BYR,,GYVEC,GY1VEC /TBGG/+1/2/1 $ FOR CONDENSATION
$**************DISTRIBUTED DAMPING*******************************************
PARTN      K4GG,GYVEC, /K4YY,K4RY,K4YR,K4RR/-1/2/6/2/2/6 $
MERGE      K4YY,,K4YR,,GYVEC,GY1VEC/TK4GG/+1/2/1 $ FOR CONDENSATION
$**************SUMMARY*******************************************************
PARAMR     //*DIV*/V,N,HHH/1.0/C,Y,W4//// $
PARAMR     //*COMPLEX*//HHH/0.0/JJJ/// $
PARAMR     //*DIV*/V,N,YYY/C,Y,G/C,Y,W3//// $
PARAMR     //*COMPLEX*//YYY/0.0/ZZZ/// $
EQUIV      TKGG,KGG/SEISLD/TMGG,MGG/SEISLD/TBGG,BGG/SEISLD/
           TK4GG,K4GG/SEISLD $ FOR CONDENSATION OF STRUCTURAL MATRICES
$$NOW THAT THE INERTIA MATRIX HAS HAD THE YR COUPLING TERMS REMOVED,
$$CONDENSATION DOWN TO A-SIZE FOR GKAD CAN NOW BEGIN.
$
ADD5       BRY,KRY,K4RY,,/TBRY/(1.0,0.0)/V,N,ZZZ/V,N,JJJ  $FOR BASE FORCE
ADD5       BRR,KRR,K4RR,,/TBRR/(1.0,0.0)/V,N,ZZZ/V,N,JJJ $FOR BASE FORCE
MERGE      TBRY,,TBRR,,GYVEC, /B1RG/5/0/2$ FOR BASE FORCE
$**************PREPARE DAREA VALUES FOR DYNAMICS DATA BLOCK***********
MPYAD      MYR,HRX6, /MYYR/0/-1 $ NEGATIVE PRODUCT
MPYAD      MRR,HRX6, /MRRR/0/+1 $ POSITIVE PRODUCT
MERGE      MYYR,MRRR,,,,GYVEC/MSEIS/5/2/2 $  FOR LOAD
$**************LOAD SUMMARY**************************************************
ALTER   87 $ JUST BEFORE DPD
NRTS       MSEIS,DYNAMICS,EQEXIN/NRTSEIS/DEPOP/C,Y,NRTID1/C,Y,NRTID2/
           C,Y,NRTID3/C,Y,NRTID4/C,Y,NRTID5/C,Y,NRTID6 $
EQUIV      NRTSEIS,DYNAMICS/SEISLD $
$$  DATA BLOCK 'DYNAMICS' NOW HAS ALL DAREA ENTRIES FOR LOADING.
$$
ALTER 98 $ JUST AFTER MTRXIN.   PARTITION THE DMIG MATRICES.
VEC        USETD/PZVEC/*P*/*COMP*/*R* $ 1'S ON R.   Z=R(COMP)P
COPY       PZVEC/PZ1VEC $
COND       AUTOM,NOM2DPP $
PARTN      M2DPP,PZVEC, /M2DZZ,M2DRZ,M2DZR,M2DRR/-1/2/6/2/2/6 $
MERGE      M2DZZ,,,M2DRR,PZVEC, /TM2DPP/-1/2/6 $ FOR CONDENSATION
MERGE      M2DRZ,,M2DRR,,PZVEC, /M2DRP/5/2/2 $ FOR BASE FORCES
EQUIV      TM2DPP,M2DPP/SEISLD $
LABEL      AUTOM $
COND       AUTOB,NOB2PP $
PARTN      B2PP,PZVEC, /B2ZZ,B2RZ,B2ZR,B2RR/-1/0/6/2/2/6 $
MERGE      B2ZZ,,B2ZR,,PZVEC,PZ1VEC/TB2PP/+1/0/1 $ FOR CONDENSATION
MERGE      B2RZ,,B2RR,,PZVEC, /B2RP/5/0/2 $ FOR BASE FORCES
EQUIV      TB2PP,B2PP/SEISLD $
LABEL      AUTOB $
COND       AUTOK,NOK2DPP $
PARTN      K2DPP,PZVEC, /K2DZZ,K2DRZ,K2DZR,K2DRR/-1/2/6/2/2/6 $
MERGE      K2DZZ,,K2DZR,,PZVEC,PZ1VEC/TK2DPP/+1/2/1 $ FOR CONDENSATION
MERGE      K2DRZ,,K2DRR,,PZVEC, /K2DRP/5/2/2 $ FOR BASE FORCES
EQUIV      TK2DPP,K2DPP/SEISLD $
LABEL      AUTOK $
```

```
$$$$$$$   GKAD TAKES CARE OF COMBINING THE REVISED MTRXIN DATA WITH
$$$$$$$   THE AUTO-STRUCTURAL MATRICES.
$ COMPUTE KOO REFINEMENT TO RESPONSE AND RECOVER BASE FORCES BEFORE
$ PROCESSING OUTPUT.
ALTER 123,123  $   REPLACE TRLG WITH TRSLG TO GET LOAD PARTITIONS
$
TRSLG       CASEXX,USETD,DLT,SLT,BGPDT,SIL,CSTM,TRL,DIT,GMD,GOD,,EST,
            MGG/PPT,PST,POT,PDT,PD,,TOL/S,N,NOSET/NCOL $
$
$ THE RESPONSE OF THE STRUCTURE INCLUDING THE BASE IS SOLVED AS A
$ FREE BODY.
$$   DEFAULT VALUES OF PARAMETERS ARE SET HERE.  $
PARAM       //*NOP*/V,Y,GRFIN=+1 $
PARAM       //*NOP*/V,Y,URFIN=+1 $
PARAM       //*NOT*/XISTOMIT/OMIT $
PARAM       //*AND*/UORFIN/V,N,XISTOMIT/C,Y,URFIN $
COND        UMPRUV,UORFIN $
JUMP        NOCHNG $
LABEL       UMPRUV $
SOLVE       KOO,POT/RUOO/0/+1/2/0 $
$$$$
$$$$   RUOO IS A TIME VARYING COMPONENT OF RELATIVE DISPLACEMENT (ONLY
$$$$   DISP--WITHOUT ACCELERATION OR VELOCITY) DUE TO THE EFFECTS OF
$$$$   OMITTED DOF'S.   IT NEEDS TO BE CONVERTED TO THE STANDARD TRIPLET
$$$$   FORM OF TRANSIENT DIRECT ANALYSIS.   NASTRAN TAKES CARE OF THE
$$$$   OTHER PARTITIONS AT THE P-LEVEL.   IN PREPARING IT FOR ADDING AT
$$$$   THE P-LEVEL, IT HAS TO BE INFLATED WITH ZEROES TO P-SIZE AND
$$$$   UNDERGO MULTIPLICATION BY RECOVERY COEFFICIENTS AS IT EXPANDS.
$$$$    INFLATE RUOO UP TO NE-SIZE IN TWO STEPS, 1ST TO FE-SIZE AND
$$$$    THEN UP TO NE-SIZE.
VEC         USETD/FEDVEC/*FE*/*D*/*O* $ ONE'S ON THE O'S $
MERGE,      ,RUOO,,,,FEDVEC/RUOOFE/5/2/2 $
VEC         USETD/NEFEVEC/*NE*/*FE*/*S* $ ONE'S ON THE S'S.
MERGE       RUOOFE,,,,,NEFEVEC/RUOONE/5/2/2 $
MPYAD       GMD,RUOONE,/RUOOM/0/+1/0 $
VEC         USETD/PNEVEC/*P*/*NE*/*M* $   1'S ON M
MERGE       RUOONE,RUOOM,,,,PNEVEC/RUOOP/5/2/2 $ TYPE=REAL SINGLE PREC
LABEL       NOCHNG $$
ALTER       139,139 $ REPLACE SDR2
EQUIV       PZVEC,PYVEC/NOUE $
COND        P2G,NOUE $
VEC         USETD/PGVEC/*P*/*G*/*E* $ 1'S ON E
ADD         PGVEC,PZVEC/PYVEC/ $ 1'S ON E AND R.
LABEL       P2G $
PARAM       //*OR*/V,N,SOMFIN/C,Y,URFIN/C,Y,GRFIN $
COND        TOKRK,SOMFIN $
JUMP        REGLR $$
LABEL       TOKRK $
KREKU       RUOOP,TOL,USETD,UPV/UMPRUV,,ACPVT,VEPVT,DIPVT/
            V,N,OMIT/C,Y,GRFIN/*TRANSRESP*/*DIRECT* $
EQUIV       UMPRUV,UPV/URFIN $
```

```
$$$$    IF THE USER WANTS TO RECOVER BASE FORCES HE SETS QRFIN=-1.   IF HE
$$$$    SETS QRFIN=+1, ANY CASECC REQUEST FOR OLOAD WILL CONTAIN ONLY THE
$$$$    EXCITATION INERTIA FORCES AND NOT THE TOTAL SET OF BASE REACTIONS.
COND        BASEF,QRFIN $
JUMP        REGLR $
LABEL       BASEF $
EQUIV       M1RG,M1RP/NOUE/B1RG,B1RP/NOUE/K1RG,K1RP/NOUE $
COND        JUSG,NOUE $
MERGE       M1RG,,,,PGVEC,/M1RP/5/2/2 $ FOR BASE FORCE
MERGE       B1RG,,,,PGVEC,/B1RP/5/0/2 $ FOR BASE FORCE
MERGE       K1RG,,,,PGVEC,/K1RP/5/2/2 $ FOR BASE FORCE
LABEL       JUSG $
EQUIV       M1RP,MRP/NOM2DPP/B1RP,BRP/NOB2PP/K1RP,KRP/NOK2DPP $
COND        BASEO,NOM2DPP $
ADD         M1RP,M2DRP/MRP/ $
LABEL       BASEO $
COND        BASE1,NOB2PP $
ADD         B1RP,B2RP/BRP/ $
LABEL       BASE1 $
COND        BASE2,NOK2DPP $
ADD         K1RP,K2DRP/KRP/ $
LABEL       BASE2 $
PARTN       PPT, ,PZVEC/PSIZT,,,/5/2/2 $REPLACE THE R-SET WITH BASE FORCES
MPYAD       MRP,ACPVT, /NRTCPL/0/+1/ $ BASE INERTIA FORCES
PARAM       //*ADD*/V,N,DMP2/V,N,NOBGG/V,N,NOK4GG $
PARAMR      //*FLOAT*/RDMP2/ / / / / /DMP2 $
PARAMR      //*MPY*/V,N,DMP3/V,N,RDMP2/C,Y,G $
PARAMR      //*LT*/ /0.0/V,N,DMP3/ / / /V,N,NODMP $
COND        BASO,NODMP $
MPYAD       BRP,VEPVT,NRTCPL/TWOCPL/0/+1/+1/0 $ BASE FORCES OF
$$$$    COUPLED DAMPING ADDED TO BASE INERTIA FORCES.
EQUIV       TWOCPL,NRTCPL/QRFIN $
LABEL       BASO $
MPYAD       KRP,DIPVT,NRTCPL/BASP/0/+1/+1/0 $ BASE FORCES OF COUPLED
$$$$    ELASTICITY ADDED TO OTHERS TO GET TOTAL BASE FORCE.
MATPRN      BASP,,,,// $
MERGE       PSIZT,BASP,,,,PZVEC/PRESPNS/5/0 $
EQUIV       PRESPNS,PPT/QRFIN $ THE BASE RESPONSE FORCES ARE NOW
$$$$     IMBEDDEDIN THE DATA BLOCK PPT IN THE R-PARTITION SO THAT
$$$$     OFP WILL RECOVER THEM WHEN REQUESTED BY OLOAD.
LABEL       REGLR $
$ DELETE OESC1 AND OEFC1 FROM 1ST EXECUTION OF SDR2 AND USE ABSOLUTE
$ MOTION ON WHICH TO BASE THE RECOVERY OF DISPLACEMENTS AND GP FORCES.
SDR2        CASEXX,CSTM,MPT,DIT,EQDYN,SILD,,,BGPDP,TOL,GP,UPV,EST,
            XYCDB,PPT/OPP1,OGP1,OUPV1,,,PUGV/*TRANSRESP* $
EQUIV       UPV,UGV/NOUE $
COND        NORELP,NOUE $
$$$$    RECOVERY OF STRESSES WILL BE BASED ON RELATIVE DISPLACEMENTS
$$$$    AND CAN OPERATE WITH REFINED DISPLACEMENTS OR NOT AS CONTROLLED
$$$$    BY THE USER IN THE QUALITY OF THE UPV VECTOR THAT IS SUPPLIED.
$$$$    FIRST CONVERT UPV TO RELATIVE COORDINATES.
PARTN       UPV,,PGVEC/UGV,UEV,,/5/0/2/2
LABEL       NORELP $$
```

```
SETPT      EQDYN,USETD/DJVEC/*D*/C,Y,GRDPNT $
PARTN      UDVT,,DJVEC/ ,UVWJVT,,/5/0/0/2 $ UVWJVT IS THE RESPONSE
$$$$     TRIPLET OF ACC:VEL:DISP OF THE BASE REFERENCE POINT "GRDPNT"
$$$$     WHICH ACTS TO ESTABLISH QUASI-RELATIVE MOTION.
$
MPYAD      HAICH,UVWJVT,UGV/RELUGV/0/-1/+1 $
EQUIV      RELUGV,RELUPV/NOUE $
COND       RELG,NOUE $
MERGE      RELUGV,UEV,,,,PGVEC/RELUPV/5/0/2 $RESTORE E-PART'N TO P-SIZE.
LABEL      RELG $
$ HAND A P-SIZED TRIPLET OF RELATIVE RESPONSES TO SDR2 TO RECOVER
$ ELEMENT STRESSES AND FORCES THRU DATA BLOCKS OES1 & OEF1.
SDR2       CASEXX,CSTM,MPT,DIT,EQDYN,SILD,,,BGPDP,TOL,,RELUPV,EST,
           XYCDB,/,,,,OES1,OEF1,/*TRANSRESP* $
ENDALTER
$END OF ALTER PACKET FOR SEISMIC SOLUTION BY RIGID FORMAT 9 INTERNAL
```

$********* THIS IS SEISTM FOR RF 11 *****
$********** SOLUTION TAKES PLACE IN RELATIVE COORDS IN THE MODAL *****
$********** FREQUENCY RESPONSE R.F. ALL BASE POINTS ARE PUT INTO AN*****
$********** SPC SET. NO OTHER SPC SETS ARE ALLOWED EXCEPT THOSE *****
$********** CONSTRAINTS ON GRID CARDS. IF ARFIN = +1, ONE OF THE *****
$********** BASE POINTS CAN BE DESIGNATED AS PRIMARY REFERENCE IF A *****
$********** SCAFFOLD POINT IS NOT ALREADY SET UP. IF RECOVERY IN *****
$********** ABSOLUTE COORD IS DESIRED, (I.E. IF ARFIN = -1) THEN *****
$********** ADDITIONAL STEPS ARE NECESSARY. ONE OF THE BASE POINTS *****
$********** SHOULD BE DUPLICATED AND GIVEN A SEPARATE ID AND SHOULD *****
$********** BE ASSIGNED TO THE R-SET ON A SUPORT CARD. IT IS SIMUL-*****
$********** TANEOUSLY ENTERED ON THE PARAM GRDPNT CARD TO INDICATE *****
$********** IT IS THE PRIMARY REFERENCE POINT FOR LOAD GENERATION *****
$********** AND FOR RECOVERY OF ABSOLUTE COORDS. MAKE A HIGH FREQ *****
$********** QUENCY SEPARATE CANTILEVER BY APPLYING A 6X6 UNIT MASS *****
$********** TO THE REFERENCE POINT WITH CONM2 AND CONNECTING IT *****
$********** WITH A BAR TO A GROUNDED POINT. *****
$PARAMETER DEFINITIONS:
$
$NRTID1,2,3= SET ID'S TO BE ASSIGNED TO DAREA CARDS REPRESENTING THE
$ SPATIAL ARRANGEMENT OF TRANSLATIONAL ACCELERATIONS IN THE FIRST,
$ SECOND, & THIRD COORDINATE DIRECTIONS.
$NRTID4,5,6= SET ID'S TO BE ASSIGNED TO DAREA CARDS REPRESENTING THE
$ SPATIAL ARRANGEMENT OF ROTATIONAL ACCELERATIONS ABOUT THE FIRST,
$ SECOND, & THIRD COORDINATE DIRECTIONS.
$URFIN WHEN SET < OR = -1 ENABLES THE OPTION TO REFINE OUTPUT DISPLACE-
$ MENTS WITH CONTRIBUTIONS FROM OMITTED SETS.
$ WHEN SET > OR = 0 DISABLES THE OPTION TO REFINE OUTPUT DISPLACE-
$ MENTS WITH CONTRIBUTIONS FROM OMITTED SETS. DEFAULT = + 1.
$QRFIN WHEN SET < OR = -1 ENABLES THE OPTION TO RECOVER BASE FORCES FROM
$ STIFFNESS, DAMPING, & MASS COUPLING AND FROM BASE INERTIAS.
$ WHEN SET > OR = 0 DISABLES THE OPTION TO RECOVER THIS COMPONENT
$ OF BASE FORCE. DEFAULT = + 1.
$ARFIN WHEN SET < OR = -1 ENABLES THE OPTION TO RECOVER DISPLACEMENTS IN
$ ABSOLUTE COORDINATES.
$ WHEN SET > OR = 0 DISABLES THE OPTION TO RECOVER DISPLACEMENTS
$ IN ABSOLUTE COORDINATES. DEFAULT = + 1.
$B2PARM WHEN SET < OR = -1 ENABLES THE RECOGNITION OF DIRECT INPUT
$ DAMPING TO SUBSTITUTE FOR MODAL DAMPING DURING THE RECOVERY OF
$ BASE FORCES. DEFAULT = + 1.
$$***
$ USER PREPARATIONS *
$ *
$ USER MUST SUPPLY SPC SET FOR ALL BASE POINTS *
$ PARAM GRDPNT BASE REFERENCE POINT IF ARFIN < 0. *
$ OMIT PARAM MODACC OR MAKE IT NEG WHEN URFIN < 0 *
$ RLOAD FOR ALL BASE POINTS *
$ TBLGEN FOR TABLE OF BASE AMPLITUDES VS FREQUENCIES*
$ PARAM NRTID'S FOR DAREA OF ACC LOAD *
$ IF ARFIN = -1, DEFINE GP COINCIDENT W REF PT AND *
$ ASSIGN IT TO R-SET. CONNECT IT WITH A BAR TO A *
$ FULLY CONSTRAINED POINT. PUT UNITY MASS IN EVERY *
$ DOF WITH CONM2. CALL THIS A SCAFFOLD POINT. *

```
$                      MAKE PARAM GRDPNT = SCAFFOLD POINT WHEN ARFIN < 0*
$                      DMIG DAMPING FOR BASE FORCE RECOVERY NAME == B2DMIG*
$   USER MAY OVERIDE PARAM URFIN OPTION FOR KOO REFINEMENT              *
$                      PARAM QRFIN OPTION FOR RECOVERY OF BASE REACTIONS *
$                      PARAM ARFIN OPTION FOR RECOVERY OF ABS RESPONSES  *
$                      PARAM B2PARM FOR DAMPING BASE FORCE.              *
$**********************************************************************************
$
$*********          THIS IS SEISTM FOR RF 11                    *****
$********* IT IS POSSIBLE TO GET IMPROVED DISPLACEMENTS, BASE   *****
$********* FORCES, AND ABSOLUTE DISPLACEMENTS BY OPTION. EXCITATION*****
$********* IS PERMITTED TO STEM FROM  INERTIA EFFECTS.   DAMPING BY *****
$********* G(OMEGA) EFFECT WILL PROVIDE DAMPING IN THE PROBLEM AT  *****
$********* THE LEVEL OF MODAL MATRICES, BUT IS NOT AVAILABLE FOR   *****
$********* RECOVERY OF DAMPING CONTRIBUTIONS TO THE BASE FORCE.    *****
$********* DAMPING CONTRIBUTIONS TO BASE FORCE CAN BE OBTAINED BY  *****
$********* USING DISTRIBUTED STRUCTURAL DAMPING FROM DMIG INPUT OF *****
$********* B2DMIG.   SOLUTION IN THIS R.F.  IS BY RELATIVE COORDS  *****
$********* THEREFORE ANY SPC RELATIONS ARE NOT FIXED IN SPACE BUT  *****
$********* ARE RELATED TO THE UNDEFORMED POSITIONS OF THE COORDS.  *****
$
$SECTION A
$
ALTER 50 $ JUST BEFORE MCE
PARAM       //*NOT*/SEISLD/SINGLE $
COND        SYMX,SEISLD $
JUMP        FINIS  $
LABEL       SYMX $
$$   CALL IN RBTM AT THIS POINT.
$
RBTM        BGPDT,CSTM,EQEXIN,MGG,USET/HAICH,MSEIS,  ,HL6/C,Y,GRDPNT/-1/
            *MODAL* $
$
$$GET THE MASS AND STIFFNESS MATRICES READY FOR LOAD AND BASE FORCE
$$RECOVERY.
$$
VEC         USET/GXVEC/*G*/*COMP*/*SB* $ X=SB,COMP,G
VEC         USET/GYVEC/*G*/*COMP*/*R* $ 1'S ON R
ADD         GXVEC,GYVEC/GCVEC/ $ 1'S ON SB & R
$-----------------------------MATRICES-----------------------------------**
PARTN       MGG,GCVEC,GXVEC/ ,MBC,,/5/2/0/2 $ FOR BASE FORCE
PARTN       MSEIS,,GXVEC/MSIZX,MSIZB,,/5/2/2/2 $ FOR LOAD & BASE FORCE
MERGE       MSIZX,,,,,GXVEC/MSIZG/5/2/2 $
PARTN       MSIZG, ,GCVEC/MSIZC,MSIZRB,,/5/2/2/2 $
ADD         MSIZC, /MMSIZC/(-1.0,0.0) $
MERGE       MMSIZC,MSIZRB,,,,GCVEC/MSIZ/5/2/2 $
$------DAMPING MATRICES NOT AVAILABLE IN GEOMETRIC COORDS**********
$
$--------STIFFNESS MATRICES**************************************
$
PARTN       KGG, ,GXVEC/ ,KBG,,/5/2/0/2 $ FOR BASE FORCE
$
NRTS        MSIZ,DYNAMICS,EQEXIN/NRTSEIS/C,Y, DEPOP/C,Y,NRTID1/
            C,Y,NRTID2/C,Y,NRTID3/C,Y,NRTID4/C,Y,NRTID5/C,Y,NRTID6 $
```

```
EQUIV      NRTSEIS,DYNAMICS/SEISLD $
$$  THE 'DYNAMICS' DATA BLOCK NOW HAS DAREA CARDS IN IT FOR THE IN-
$$  ERTIA LOAD AND IS READY TO BE PASSED TO DPD FOR SETTING UP THE
$$  LOAD ON THE RELATIVE X COORDS.   IT CONTAINS DAREA NOT JUST FOR
$$  THE BASE MOTION BUT FOR DIRECTLY APPLIED LOAD AS WELL.   RF11
$$  CAN NOW PROCEED WITH CONDENSATION FROM X-SIZE TO A-SIZE AND
$$  DEVELOP MODAL VECTORS FOR SOL'N IN FRRD3.
$
ALTER 99,99 $REPLACE FRRD
FRSLG      CASEXX,USETD,DLT,FRL,GMD,GOD,DIT,PHIDH/PPF,PSF,PDF,POF,
           FOL,PHF/*MODAL*/FREQY=-1/APP=FREQ/S,N,FRQSET/S,N,NFREQ/
           S,N,NLOAD $
FRRD3      KHH,BHH,MHH,PHF,FRL/UHVF/*DISP*/*MODAL*/
           V,N,NONCUP/V,N,FRQSET/V,N,NFREQ/V,N,NLOAD $
$
ALTER 101,101 $ USE FOL INSTEAD OF PPF FOR A FREQUENCY TEMPLATE.
VDR        CASEXX,EQDYN,USETD,UHVF,FOL,XYCDB,/OUHVC1,/*FREQRESP*/
           *MODAL*/S,N,SORT2/S,N,NOH/S,N,NOP/FMODE $ $
ALTER  114,114 $ THIS CAUSES OSCAR TO IGNORE A JUMP AROUND SDR1.
ALTER  116,117  $ THIS ELIMINATES ANY IMPROVEMENTS FROM MODACC.
$
$ COMPUTE KOO REFINEMENT TO RESPONSE AND RECOVER BASE FORCES BEFORE
$ PROCESSING OUTPUT.
ALTER 122,122  $
SETPT      EQEXIN,USET/GXREF/*G*/C,Y,GRDPNT $ 1'S ON GRDPNT.  NEEDED
$ LATER IN GRFIN AND ARFIN.
$$ PARAMETER DEFAULTS ARE SET HERE.  $
PARAM      //*NOP*/V,Y,ARFIN = +1 $
PARAM      //*NOP*/V,Y,GRFIN = +1 $
PARAM      //*NOP*/V,Y,URFIN = +1 $
COND       P2G,NOUE $
VEC        USETD/PGVEC/*P*/*G*/*E* $ 1'S ON E
LABEL      P2G $
PARAM      //*NOT*/XISTOMIT/OMIT $
PARAM      //*AND*/UORFIN/XISTOMIT/C,Y,URFIN $
PARAM      //*NOT*/NOARFIN/C,Y,ARFIN $
COND       UMPRUV,UORFIN $
JUMP       UNRFIN $
LABEL      UMPRUV $
SOLVE      KOO,POF/RUOOF/+1/+1/2/0 $
$RUOOF IS A VECTOR OF RELATIVE DISPLACEMENTS.  NO CONVERSION TO
$ ABSOLUTE COORDINATES IS NECESARY BECAUSE NASTRAN HAS ALREADY
$PROCESSED ONE CORRECTION FOR THE O-SET IN ABSOLUTE COORDINATES.
$INFLATE RUOOF TO P-SIZE TO BE COMMENSURATE WITH UPVC.
VEC        USETD/FEDVEC/*FE*/*D*/*O* $ 1'S ON O
MERGE,     ,RUOOF,,,,FEDVEC/UOOFFE/5/0 $
EQUIV      UOOFFE,UOOFNE/SINGLE $
$ THESE PROBLEMS.
COND       POSN1,SINGLE $
VEC        USETD/NEFEVEC/*NE*/*FE*/*S* $ 1'S ON S
MERGE      UOOFFE,,,,,NEFEVEC/UOOFNE/5/0 $
LABEL      POSN1 $
EQUIV      UOOFNE,UOOFP/MPCF1 $
COND       POSN2,MPCF1 $
```

```
MPYAD       GMD,UOOFNE,/UOOFM/0/+1 $
VEC         USETD/PNEVEC/*P*/*NE*/*M* $ 1'S ON M
MERGE       UOOFNE,UOOFM,,,,PNEVEC/UOOFP/5/0 $
LABEL       POSN2 $
ADD         UPVC,UOOFP/UMPRUVF/ $
EQUIV       UMPRUVF,UPVC/URFIN $
LABEL       UNRFIN $
$
$IF THE USER WANTS TO RECOVER BASE RESPONSE FORCES HE SETS QRFIN
$ = -1, HOWEVER IF HE SETS QRFIN=+1, ANY CASECC REQUEST FOR OLOAD
$ WILL CONTAIN ONLY THE EXCITATION INERTIA FORCES AND NOT THE TOTAL
$ SET OF BASE REACTIONS.
COND        SPCFALL,QRFIN $
JUMP        REGLR $
LABEL       SPCFALL $
EQUIV       PPF,PGF/NOUE $
COND        GSIZ,NOUE $
PARTN       PPF,,PGVEC/PGF,PEF,,/5/0 $
LABEL       GSIZ $
PARTN       PGF,,GXVEC/PXF,,,/+1 $
$ THE RECOVERY OF BASE FORCES IS UNDER THE CONTROL OF CASECC OLOAD
$ REQUESTS.
$ DIAGONAL MATRIX   I*OMEGA COMING FROM MODULE KREKU WILL
$ BE USED TO DIFFERENTIATE RESPONSE DISPLACEMENTS INTO VELOCITIES AND
$ ACCELERATIONS BY MULTIPLYING UDVF BY I*OMEGA.
$
KREKU,      ,FOL,, / ,IW,,,/V,N,OMIT/C,Y,QRFIN/*FREQRESP*/*MODAL* $
$
$ ARRANGE THE STRUCTURAL MATRICES FOR RECOVERY OF BASE RESPONSE
$ FORCES.   ONLY COUPLED DAMPING AND COUPLED ELASTIC TERMS ARE NON ZERO
$ BECAUSE [BRR]*[BASEACC] & [KRR]*[BASEACC] ACT ON RIGID MOTIONS WHICH
$ LEAVES ZERO DIFFERENTIAL AMONGST THE R SET, SO THE PRODUCTS ARE NULL.
$ THIS IS NOT THE CASE FOR INERTIA BECAUSE THEY ACT ON {ISOLATED} GP
$ MOTION AS OPPOSED TO {DIFFERENTIAL} GP MOTION
$
COPY        IW/IFREQ/-1 $ CLONE OF COMPLEX IW
MPYAD       IW,IFREQ, /WSQR/0/-1/0/0 $(-)IW*IW =\(+W**2,0.0)\
DIAGONAL    WSQR/INVASQR/*SQUARE*/-1.0 $INVERSES OF REAL POS. DIAGONALS
ADD         INVASQR/INVWSQR/(-1.0,0.0) $INVERSES OF REAL NEG. DIAGONALS
EQUIV       UPVC,UGVC/NOUE $
COND        BASO,NOUE $
PARTN       UPVC,,PGVEC/UGVC,UEVC,,/+1/3/2/2 $
LABEL       BASO $
PARTN       UGVC,,GYVEC/UYVC,,,/5/3/2 $ SPLIT OFF THE REF DISP & KEEP COMP
VEC         USETD/PZVEC/*P*/*COMP*/*R* $ 1'S ON R'S.
PARTN       PPF,,PZVEC/,PRF,,/5/4/0/2 $ ISOLATE THE EXCITING ACCELERATION
MPYAD       PRF,INVWSQR,-/URVC/0/+1 $
MERGE       UYVC,URVC,,,,GYVEC/UGBAS/5/0/2 $ RECONSTRUCT UG FOR BASE FORCES
MERGE       MBC,,,,QCVEC,/MBCQ/5/2/2 $
MERGE,      ,,MSIZB, ,GXREF,/MBRQ/5/0/2 $
ADD         MBCG,MBRQ/MFBQ/ $
MPYAD       UGBAS,IW,/VEQVC/0/+1 $
SMPYAD      MFBQ,VEQVC,IW,,,/MCPLQF/3/+1 $
```

```
PARAM       //*MPY*/V,N,NOB2/C,N,-1/V,Y,B2PARM = +1 $
$$   THIS SETS THE DEFAULT VALUE OF NOB2 TO NEGATIVE ONE.   IF THE USER
$$   WANTS TO PUT IN DIRECT MATRIX DAMPING AS A GRID POINT EQUIVALENT
$$   SURROGATE FOR MODAL DAMPING, HE OVERRIDES THE DEFAULT BY ENTERING
$$   A BULK PARAM CARD FOR B2PARM SET TO -1 AND HE THEN ENTERS BULK DMIG
$$   CARDS FOR THE DAMPING VALUES USING A MATRIX NAME OF B2DMIG OF ORDER
$$   EQUAL TO P-SIZE.
PARAM       //*AND*/V,N,NODMP/V,N,NOB2/V,N,NOB2PP $
COND        BAS1,NODMP $
$$   IF BOTH B2PP AND B2DMIG ARE ABSENT, JUMP AROUND THE COMPUTATION OF
$$   DAMPING CONTRIBUTION TO BASE FORCES.
COND        BASB,NOB2 $
MTRXIN,     ,MATPOOL,EQDYN,,/B2DMIG,,/LUSETD/V,N,NOB2 $
EQUIV       B2PP,B2DMIG/NOB2PP $
COND        BASB,NOB2PP $
$$   IF B2DMIG IS ABSENT, JUMP AROUND INPUT OF THIS MATRIX, OTHERWISE
$$   INPUT THE MATRIX.   RETAIN THE NAME OF B2DMIG IF B2PP IS PRESENT,
$$   OTHERWISE EQUIVALENCE B2PP TO IT.
ADD         B2PP,B2DMIG/B2BOTH/ $
EQUIV       B2BOTH,B2PP/SEISLD $
LABEL       BASB $
$$   IF B2PP IS ABSENT, JUMP AROUND THE COMBINING OF B2DMIG WITH B2PP.
$$   AT THIS POINT, THE RESULT OF ANY OF THE OPTIONS IS NAMED B2PP.
$$   PROCEED WITH THE PROCESSING OF THE DAMPING FORCE CONTRIBUTION TO
$$   THE BASE FORCE RECOVERY.
PARTN       B2PP, PGVEC,/B2GG,,,/-1/0/6 $
PARTN       B2GG, ,GXVEC/ ,B2BG, ,/5/0/0/2 $
MPYAD       B2BG,VEGVC,MCPLGF/BCPLGF/0/+1/+1 $
EQUIV       BCPLGF,MCPFLGF/SEISLD $
LABEL       BAS1 $
MPYAD       KBG,UGVC,MCPLGF/BASEGF/0/+1/+1 $
MERGE       PXF,BASEGF,,,,GXVEC/PXBF/5/4/2 $
EQUIV       PXBF,PPBF/NOUE $
COND        JUSG,NOUE $
MERGE       PXBF,PEF,,,,PGVEC/PPBF/5/4/2 $
LABEL       JUSG $
EQUIV       PPBF,PPF/SEISLD $
LABEL       REGLR $
$$   PPF IS NOW COMPLETE AND IS READY TO BE PASSED TO SDR2 FOR RECOVERY
$$   OF BASE FORCES AS REQUESTED BY THE USER WITH OLOAD IN CASECC.
$ NOW THE LOAD VECTOR PPF IS READY TO RESPOND TO CASECC OLOAD REQUESTS
$        FOR BASE FORCE RESPONSE HISTORY.
$****************DATA RECOVERY*********************************************
$ USE FOL INSTEAD OF PPF FOR A FREQUENCY TEMPLATE.
SDR2        CASEXX,CSTM,MPT,DIT,EQDYN,SILD,,,BGPDP,FOL,QPC,UPVC,EST,
            XYCDB,PPF/OPPC1,OQPC1,OUPVC1,OESC1,OEFC1,PUGV/*FREQ*/
            S,N,NOSORT2 $
$$   ALL OUTPUT RECOVERED UP TO THIS POINT HAS BEEN BASED ON RELATIVE
$$   COORDS.   IF DISP, VELO, AND ACCEL ARE NEEDED IN ABSOLUTE COORDS,
$$   SET PARAM ARFIN = -1. THE SCAFFOLD POINT IN THE R SET IS EXCITED
$$   TO SPECIFIED VALUES AND IT WILL BE USED FOR THE TRANSFORMATION TO
$$   ABSOLUTE COORDS.
```

```
COND       NOABS,NOARFIN $
MERGE      UYVC,,,,,GYVEC/UGCREL/5/3/2 $INFLATE THE RELATIVE COMPLIMENT
$$ TO G-SIZE.
MERGE,     ,,HAICH,,GXREF,/HAIG/5/1/2 $ INFLATES HAICH FROM GX6 TO GXG.
PARTN      HAIG,GYVEC,/,,HAIR,/5/1/0/0/2 $ EXTRACTS GXR PART'N OF HAICH.
MPYAD      HAIR,PRF ,UGCREL/UGCABS/0/+1/+1 $ TRANSFORMS TO ABS BY ADDING
$$   THE RIGID BODY MOTION TO THE RELATIVE MOTION.  G-SIZE.
EQUIV      UGCABS,UPCABS/NOUE $
COND       GABS,NOUE $
MERGE      UGCABS,UEVC,,,,PGVEC/UPCABS/5/3/2 $E-SET AREN'T IN ABS COORDS.
$$ PUT BACK E-SET TO SATISFY SDR AND OFP.
LABEL      GABS $
SDR2       CASEXX,CSTM,,,EQDYN,SILD,,,,FOL,,UPCABS,,XYCDB,/
           ,,OUPCABS1,,,/*FREQRESP*/S,N,NOUABS2 $
COND       ABSOUT1,NOUABS2 $
SDR3,      ,,OUPCABS1,,,/,,OUPCABS2,,, $
OFPS       OUPCABS2,,,,,//CARDNO $
XYTRAN     XYCDB,,,OUPCABS2,,/XYCPLABS/*TRAN*/*PSET*/S,N,PFILE $
XYPLOT     XYCPLABS// $
JUMP       NOABS $
LABEL      ABSOUT1
OFPS       OUPCABS1,,,,,//CARDNO $
JUMP       LBL18 $
LABEL      NOABS $
ENDALTER
$THIS IS THE END OF THE MODIFICATION TO R.F.11.
```

```
$*********       THESE ARE DMAP ALTERS FOR SEIRES      ***********
$*********       PERTAINING TO RIGID FORMAT   DMAP      ***********
$*********             SERIES  APR  82                  ***********
$                    SOLN12I. TXT
$
$*********              THIS IS SEISTM FOR RF 12            *****
$********* SOLUTION TAKES PLACE IN RELATIVE COORDS IN THE MODAL   *****
$********* TRANSIENT RESPONSE R. F.   ALL BASE POINTS ARE PUT INTO AN*****
$********* SPC SET.   NO OTHER SPC SETS ARE ALLOWED EXCEPT THOSE  *****
$********* CONSTRAINTS ON GRID CARDS.   IF ARFIN = +1, ONE OF THE *****
$********* BASE POINTS CAN BE DESIGNATED AS PRIMARY REFERENCE IF A *****
$********* SCAFFOLD POINT IS NOT ALREADY SET UP.   IF RECOVERY IN  *****
$********* ABSOLUTE COORD IS DESIRED, (I. E.  IF ARFIN = -1) THEN  *****
$********* ADDITIONAL STEPS ARE NECESSARY.   ONE OF THE BASE POINTS *****
$********* SHOULD BE DUPLICATED AND GIVEN A SEPARATE ID AND SHOULD *****
$********* BE ASSIGNED TO THE R-SET ON A SUPORT CARD.   IT IS SIMUL-*****
$********* TANEOUSLY ENTERED ON THE PARAM GRDPNT CARD TO INDICATE  *****
$********* IT IS THE PRIMARY REFERENCE POINT FOR LOAD GENERATION   *****
$********* AND FOR RECOVERY OF ABSOLUTE COORDS.   MAKE A HIGH FREQ -*****
$********* QUENCY SEPARATE CANTILEVER BY APPLYING A 6X6 UNIT MASS  *****
$********* TO THE REFERENCE POINT WITH CONM2 AND CONNECTING IT     *****
$********* WITH A BAR TO A GROUNDED POINT.                         *****
$********* IT IS POSSIBLE TO GET IMPROVED DISPLACEMENTS, BASE      *****
$********* FORCES, AND ABSOLUTE DISPLACEMENTS BY OPTION. EXCITATION*****
$********* IS PERMITTED TO STEM FROM  INERTIA EFFECTS.   DAMPING BY *****
$********* G(OMEGA) EFFECT WILL PROVIDE DAMPING IN THE PROBLEM AT   *****
$********* THE LEVEL OF MODAL MATRICES, BUT IS NOT AVAILABLE FOR    *****
$********* RECOVERY OF DAMPING CONTRIBUTIONS TO THE BASE FORCE.    *****
$********* DAMPING CONTRIBUTIONS TO BASE FORCE CAN BE OBTAINED BY  *****
$********* USING DISTRIBUTED STRUCTURAL DAMPING FROM DMIG INPUT OF *****
$********* B2DMIG.   SOLUTION IN THIS R. F. IS BY RELATIVE COORDS, *****
$********* THEREFORE ANY SPC RELATIONS ARE NOT FIXED IN SPACE BUT  *****
$********* ARE RELATED TO THE UNDEFORMED POSITIONS OF THE COORDS.  *****
$
$PARAMETER DEFINITIONS:
$
$NRTID1,2,3= SET ID'S TO BE ASSIGNED TO DAREA CARDS REPRESENTING THE
$         SPATIAL ARRANGEMENT OF TRANSLATIONAL ACCELERATIONS IN THE FIRST,
$         SECOND, & THIRD COORDINATE DIRECTIONS.
$NRTID4,5,6= SET ID'S TO BE ASSIGNED TO DAREA CARDS REPRESENTING THE
$         SPATIAL ARRANGEMENT OF ROTATIONAL ACCELERATIONS ABOUT THE FIRST,
$         SECOND, & THIRD COORDINATE DIRECTIONS.
$URFIN WHEN SET < OR = -1 ENABLES THE OPTION TO REFINE OUTPUT DISPLACE-
$         MENTS WITH CONTRIBUTIONS FROM OMITTED SETS.
$      WHEN SET  > OR = O DISABLES THE OPTION TO REFINE OUTPUT DISPLACE-
$         MENTS WITH CONTRIBUTIONS FROM OMITTED SETS.   DEFAULT = + 1.
$QRFIN WHEN SET < OR = -1 ENABLES THE OPTION TO RECOVER BASE FORCES FROM
$         STIFFNESS, DAMPING, AND MASS COUPLING AND FROM BASE INERTIAS.
$      WHEN SET  > OR = O DISABLES THE OPTION TO RECOVER THIS COMPONENT
$         OF BASE FORCE.   DEFAULT = + 1.
$ARFIN WHEN SET < OR = -1 ENABLES THE OPTION TO RECOVER ACCELERATIONS IN
$         ABSOLUTE COORDINATES.
$      WHEN SET  > OR = O DISABLES THE OPTION TO RECOVER ACCELERATIONS
$         IN ABSOLUTE COORDINATES.   DEFAULT = + 1.
```

```
$B2PARM WHEN SET < OR = -1 ENABLES THE RECOGNITION OF DIRECT INPUT
$         DAMPING TO SUBSTITUTE FOR MODAL DAMPING DURING THE RECOVERY OF
$         BASE FORCE.  DEFAULT = + 1.
$$****************************************************************.***********
$                        USER PREPARATIONS                                 *
$                                                                          *
$   USER MUST SUPPLY SPC SET FOR ALL BASE POINTS                           *
$                      PARAM GRDPNT BASE REFERENCE POINT IF ARFIN < 0      *
$                      OMIT PARAM MODACC OR MAKE IT NEG WHEN URFIN < 0     *
$                      TLOAD FOR ALL BASE POINTS                          *
$                      TBLGEN FOR TABLE OF BASE TIME HISTORIES            *
$                      PARAM NRTID'S FOR DAREA OF ACC LOAD                *
$                      IF ARFIN = -1, DEFINE GP COINCIDENT W REF PT AND   *
$                       ASSIGN IT TO R-SET. CONNECT IT WITH A BAR TO A    *
$                       FULLY CONSTRAINED POINT. PUT UNITY MASS IN EVERY  *
$                       DOF WITH CONM2. CALL THIS A SCAFFOLD POINT.       *
$                       SET RHO = 0.0 ON MAT1 SO AS TO BE A MASSLESS REED *
$                      DMIG DAMPING FOR BASE FORCE RECOVERY NAME IS B2DMIG*
$   USER MAY OVERIDE PARAM URFIN OPTION FOR KOO REFINEMENT                *
$                      PARAM GRFIN OPTION FOR RECOVERY OF BASE REACTIONS  *
$                      PARAM ARFIN OPTION:   RECOVERY OF ABS ACCELERATIONS*
$                      PARAM B2PARM FOR DAMPING BASE FORCE                *
$***************************************************************************
$
ALTER 49   $ JUST BEFORE MCE
PARAM      //*NOT*/SEISLD/SINGLE $
COND       SYMX,SEISLD $
JUMP       FINIS  $
LABEL      SYMX $
$$  CALL IN RBTM AT THIS POINT.
$
RBTM       BGPDT,CSTM,EQEXIN,MGG,USET/HAICH,MSEIS,,HL6/C,Y,GRDPNT/-1/
           *MODAL* $
$
$$GET THE MASS AND STIFFNESS MATRICES READY FOR LOAD AND BASE FORCE
$$RECOVERY.
$$
VEC        USET/GXVEC/*G*/*COMP*/*SB* $ X=SB,COMP,G
VEC        USET/GYVEC/*G*/*COMP*/*R* $ 1'S ON R
ADD        GXVEC,GYVEC/GCVEC/ $ 1'S ON SB & R
$----------INERTIA MATRICES------------------------------------------------**
PARTN      MGG,GCVEC,GXVEC/ ,MBC,,/5/2/0/2 $ FOR BASE FORCE
PARTN      MSEIS,,GXVEC/MSIZX,MSIZB,,/5/2/2/2 $ FOR LOAD & BASE FORCE
MERGE      MSIZX,,,,,GXVEC/MSIZG/5/2/2 $
PARTN      MSIZG, ,GCVEC/MSIZC,MSIZRB,,/5/2/2/2 $
ADD        MSIZC, /MMSIZC/(-1.0,0.0) $
MERGE      MMSIZC,MSIZRB,,,,GCVEC/MSIZ/5/2/2 $
$
$--------DAMPING MATRICES NOT AVAILABLE IN GEOMETRIC COORDS************
$
$--------STIFFNESS MATRICES*********************************************
$
PARTN      KGG, ,GXVEC/ ,KBG,,/5/2/0/2 $ FOR BASE FORCE
```

```
NRTS        MSIZ,DYNAMICS,EQEXIN/NRTSEIS/C,Y, DEPOP/C,Y,NRTID1/
            C,Y,NRTID2/C,Y,NRTID3/C,Y,NRTID4/C,Y,NRTID5/C,Y,NRTID6 $
EQUIV       NRTSEIS,DYNAMICS/SEISLD $
$$ THE 'DYNAMICS' DATA BLOCK NOW HAS DAREA CARDS IN IT FOR THE INERTIA
$$ LOAD AND IS READY TO BE PASSED TO DPD FOR SETTING UP THE LOAD ON
$$ THE RELATIVE X COORDS.   IT CONTAINS DAREA NOT JUST FOR THE BASE
$$ MOTION BUT FOR DIRECTLY APPLIED LOAD AS WELL.  RF12 CAN NOW PROCEED
$$ WITH CONDENSATION FROM X-SIZE TO A-SIZE AND DEVELOP MODAL VECTORS
$$ FOR SOLUTION IN THE TRD MODULE. MODULE TRSLG SUPPLIES THE LOAD
$$ VECTOR IN AN O-SIZED PARTITION TO ENTER LATER INTO DECOMP WITH KOO
$$ TO OBTAIN RELATIVE DISPLACEMENT CONTRIBUTIONS FROM OMITTED DOF'S.
$$ PREPARES INCREMENT OF DISPLACEMENT RECOVERY DUE TO OMITTED DOF'S.
$
ALTER 99,99 $   REPLACE TRLG WITH TRSLG.
TRSLG       CASECC,USETD,DLT,SLT,BGPDT,SIL,CSTM,TRL,
            DIT,GMD,GOD,PHIDH,EST,MGG/PPT,PST,POT,PDT,PD,
            PH,TOL/S,N,NOSET/NCOL $
ALTER 113,113 $
$
$$ THIS CAUSES OSCAR TO IGNORE A JUMP AROUND SDR1
$
ALTER       121  $   JUST AFTER SDR1
SETPT       EQEXIN,USET/GXREF/*G*/C,Y,GRDPNT $ 1'S ON GRDPNT.   NEEDED FOR
$  BOTH QRFIN AND URFIN.
$$  PARAMETER DEFAULTS ARE SET HERE.  $$
PARAM       //*NOP*/V,Y,ARFIN=+1 $
PARAM       //*NOP*/V,Y,QRFIN=+1 $
PARAM       //*NOP*/V,Y,URFIN=+1 $
COND        P2G,NOUE $
VEC         USETD/PGVEC/*P*/*G*/*E* $
LABEL       P2G $
VEC         USETD/PZVEC/*P*/*COMP*/*R* $ ONE'S ON R'S.  Z=R,COMP,P.
VEC         USETD/GNVEC/*G*/*N*/*M* $
VEC         USETD/NFVEC/*N*/*F*/*S* $
VEC         USETD/FAVEC/*F*/*A*/*O* $
PARAM       //*NOT*/XISTOMIT/V,N,OMIT $
PARAM       //*AND*/RFINBIZ/C,Y,URFIN/V,N,XISTOMIT $
PARAM       //*OR*/V,N,COLPTN/C,Y,QRFIN/C,Y,ARFIN $
COND        UMPRUV,RFINBIZ $
JUMP        AFTKOO $
LABEL       UMPRUV $
SOLVE       KOO,POT/RELUOO/+1/+1/2/2 $
$$  INFLATE RELUOO FROM O-SIZE TO N-SIZE.
MERGE,      ,RELUOO,,,,FAVEC/RUOOT/+5/2/2 $
MERGE       RUOOT,,,,,NFVEC/ROON/+5/2/2 $
$$ NOW MULTIPLY ROON BY GM TO GET THE M PARTITION OF THE UOO CORRECTION
MPYAD       GM,ROON,/ROOM/0/+1 $
$$ PUT THE M AND N PARTN'S BACK TOGETHER INTO A G-SIZED MATRIX.
MERGE       ROON,ROOM,,,,GNVEC/ROOG/5/2/2 $ ROOG IS SINGLE PREC FOR KREKU
LABEL       AFTKOO $
```

```
$$$$    ROOG IS A TIME VARYING COMPONENT OF RELATIVE DISPLACEMENT (ONLY
$$$$    DISP--WITHOUT ACCELERATION OR VELOCITY) DUE TO THE EFFECTS OF
$$$$    OMITTED DOF'S.   IT NEEDS TO BE CONVERTED TO THE STANDARD TRIPLET
$$$$    FORM OFTRANSIENT DIRECT ANALYSIS.   KREKU MAKES THE CONVERSION AND
$$$$    OUTPUTS  THE DISPLACEMENTS AUGMENTED WITH KOO REFINEMENTS.
PARAM       //*OR*/V,N,QU/C,Y,QRFIN/C,Y,URFIN $
PARAM       //*OR*/V,N,AQU/V,N,QU/C,Y,ARFIN $
COND        TOKRK,AQU $
JUMP        REGLR $
LABEL       TOKRK $
$$  BREAK THE SOL'N VEC UPV INTO INDIVIDUAL ACCEL, VELO AND DISP VECTORS
$$  TO GET READY TO RECOVER BASE FORCES DUE TO INERTIA COUPLING, DAMPING
$$  COUPLING, AND ELASTIC COUPLING.
KREKU       ROOG,TOL,USETD,UPV/UMPRUV,,ACGVT,VEGVT,DIGVT/
            V,N,OMIT/V,N,COLPTN/*TRANSRESP*/*MODAL* $
EQUIV       PPT,PGT/NOUE $
COND        POZ1,NOUE $
PARTN       PPT, ,PGVEC/PGT,PET,,/5/2/2/2 $
LABEL       POZ1 $
PARTN       PGT,,GXVEC/PXT,,,/5/2/2 $
PARTN       PGT,,GYVEC/ ,PRT,,/5/2/0/2 $PRT IS THE REF FOR SPECIFIED ACCEL.
PURGE       PPT,PGT/COLPTN $
PARTN       ACGVT,,GYVEC/ACYVT,,,/5/2/0/2 $
MERGE       ACYVT,PRT,,,,GYVEC/ACCG/5/0/2 $
COND        GA,OMIT $
EQUIV       UMPRUV,UPV/URFIN $
LABEL       GA $
COND        QORA,COLPTN $
JUMP        REGLR $
LABEL       QORA $
COND        SPCFALL,QRFIN  $
JUMP        REGLR  $
LABEL       SPCFALL  $
MERGE       MBC,,,,GCVEC,/MBCG/5/2/2 $
MERGE,      ,,MSIZB, ,GXREF,/MBRG/5/2/2 $
ADD         MBCG,MBRG/MFBG/ $
MPYAD       MFBG,ACCG,/MCPLG/0/+1 $
PARAM       //*MPY*/V,N,NOB2/C,N,-1/V,Y,B2PARM = +1 $
$$  THIS SETS THE DEFAULT VALUE OF NOB2 TO NEGATIVE ONE.   IF THE USER
$$  WANTS TO PUT IN DIRECT MATRIX DAMPING AS A GRID POINT EQUIVALENT
$$  SURROGATE FOR MODAL DAMPING, HE OVERRIDES THE DEFAULT BY ENTERING
$$  A BULK PARAM CARD FOR B2PARM SET TO -1 AND HE THEN ENTERS BULK
$$  DMIGCARDS FOR THE DAMPING VALUES USING A MATRIX NAME OF B2DMIG OF
$$  ORDER EQUAL TO P-SIZE.
PARAM       //*AND*/V,N,NODMP/V,N,NOB2/V,N,NOB2PP $
COND        BAS1,NODMP $
$$  IF BOTH B2PP AND B2DMIG ARE ABSENT, JUMP AROUND THE COMPUTATION
$$  OF DAMPING CONTRIBUTION TO BASE FORCES.
COND        BASB,NOB2 $
MTRXIN,     ,MATPOOL,EQDYN,,/B2DMIG,,/LUSETD/V,N,NOB2 $
EQUIV       B2PP,B2DMIG/NOB2PP $
```

```
COND       BASB,NOB2PP $
$$  IF B2DMIG IS ABSENT, JUMP AROUND INPUT OF THIS MATRIX, OTHERWISE
$$  INPUT THE MATRIX.  RETAIN THE NAME OF B2DMIG IF B2PP IS PRESENT,
$$  OTHERWISE EQUIVALENCE B2PP TO IT.
ADD        B2PP,B2DMIG/B2BOTH/ $
EQUIV      B2BOTH,B2PP/SEISLD $
LABEL      BASB $
$$  IF B2PP IS ABSENT, JUMP AROUND THE COMBINING OF B2DMIG WITH B2PP.
$$  AT THIS POINT, THE RESULT OF ANY OF THE OPTIONS IS NAMED B2PP.
$$  PROCEED WITH THE PROCESSING OF THE DAMPING FORCE CONTRIBUTION TO
$$  THE BASE FORCE RECOVERY.
PARTN      B2PP, PGVEC,/B2GG,,,/-1/0 $
PARTN      B2GG, ,GXVEC/ ,B2BG, ,/5/0 $
MPYAD      B2BG,VEGVT,MCPLG/BCPLG/0/+1/+1 $
EQUIV      BCPLG,MCPLG/SEISLD $
LABEL      BAS1 $
MPYAD      KBG,DIGVT,MCPLG/BASEG/0/+1/+1 $
MERGE      PXT,BASEG,,,,GXVEC/PXBT/5/2/2 $
MERGE      PXBT,PET,,,,PGVEC/PPBT/5/2/2 $
EQUIV      PPBT,PPT/SEISLD $
LABEL      REGLR $
$$  PPT IS NOW COMPLETE AND IS READY TO BE PASSED TO SDR2 FOR RECO-
$$  VERY OF BASE FORCES AS REQUESTED BY THE USER WITH OLOAD IN CASECC.
$
ALTER  135 $ JUST AFTER OFP FOLLOWING SDR3.
$$  ALL OUTPUT RECOVERED UP TO THIS POINT HAS BEEN BASED ON RELATIVE
$$  COORDS.  IF DISP, VELO, AND ACCEL ARE NEEDED IN ABSOLUTE COORDS,
$$  SET PARAM ARFIN = -1. THE SCAFFOLD POINT IN THE R SET IS EXCITED
$$  TO SPECIFIED VALUES AND IT WILL BE USED FOR THE TRANSFORMATION TO
$$  ABSOLUTE COORDS.
COND       ABSA,ARFIN $
JUMP       FINIS $
LABEL      ABSA $
MERGE      ACYVT,,,,,,GYVEC/RELACG/5/1/2 $ RELATIVE ACCELERATION G-SIZE
MERGE,     ,,HAICH,,,GXREF,/HAIG/5/1/2 $ INFLATES HAICH FROM GX6 TO GXG.
PARTN      HAIG,GYVEC,/,,HAIR,/5/1/0/0/2 $EXTRACTS GXR PARTN FROM HAICH.
MPYAD      HAIR,PRT,RELACG/ABSACG/0/+1/+1 $ABSOLUTE ACCELERATION G-SIZE
ACDR       ABSACG,USETD/ABSACGT/C,Y,ARFIN $ABS ACC. TRIPLET FORMAT P-SIZE
EQUIV      ABSACGT,ABSACPT/NOUE $
COND       GZZ,NOUE $
MERGE      ABSACGT,,,,,PGVEC/AGSACPT/5/1/2 $
LABEL      GZZ $
SDR2       CASEXX,CSTM,,,EQDYN,SILD,,,,TOL,,ABSACPT,,XYCDB,/
           ,,OACABSP1,,,/*TRANSRESP* $
SDR3,      ,,OACABSP1,,,/,,OACABSP2,,, $
OFPS       OACABSP2,,,,,//CARDNO $
```

```
$$   ALL PLOTS UP TO THIS POINT HAVE BEEN BASED ON RELATIVE COORDS.
$$   IF PLOTS OF ACCEL IN ABS COORDS ARE NEEDED SET ARFIN=-1
$
ALTER   141 $ AFTER XYPLOT
COND        ABSPLT,ARFIN $
JUMP        FINIS  $
LABEL       ABSPLT $
XYTRAN      XYCDB,,,OACABSP2,,/XYPLABS/*TRAN*/*PSET*/S,N,PFILE $
XYPLOT      XYPLABS// $
ENDALTER
$THIS IS THE END OF THE INTERNAL MODIFICATION TO R.F.12.
```

TRANSIENT RESPONSE DYNAMIC MODULE MODIFICATIONS TO INCLUDE
STATIC AND KINETIC FRICTION EFFECTS

J. E. Misel*, S. B. Nenno*, and D. Takahashi*
Shuttle Integration and Satellite Systems Division
Rockwell International

SUMMARY

A methodology that supports forced transient response dynamic solutions when both static and kinetic friction effects are included in a structural system model is described herein. Modifications that support this type of nonlinear transient response solution are summarized for the transient response dynamics (TRD) NASTRAN module. An overview of specific modifications for the NASTRAN processing subroutines, INITL, TRD1C, and TRD1D, are described with further details regarding inspection of nonlinear input definitions to define the type of nonlinear solution required, along with additional initialization requirements and specific calculation subroutines to successfully solve the transient response problem.

The extension of the basic NASTRAN nonlinear methodology is presented through several stages of development to the point where constraint equations and residual flexibility effects are introduced into the finite difference Newmark-Beta recurrsion formulas. Particular emphasis is placed on cost effective solutions for large finite element models such as the Space Shuttle with friction degrees of freedom between the orbiter and payloads mounted in the cargo bay. An alteration to the dynamic finite difference equations of motion is discussed, which allows one to include friction effects at reasonable cost for large structural systems such as the Space Shuttle. Also presented is an hypothesis that suggests that a correlation exists between flexibility loss data at the friction degrees of freedom and solution accuracy when truncated modal coordinates are employed in the equations of motion for a structural system. A friction demonsration problem is included to show how residual flexibilities dramatically improve the solution accuracy of the forced dynamic response when truncated modal coordinates are implemented for the structural response problem. The residual flexibility correction effects may be applied to other nonlinear transient response problems not considered in this paper. The numerical results of the idealized and highly simplified structural transient response problem also demonstrates the completeness of the approach by providing the capability to obtain nonlinear response solutions when either physical or modal coordinates are used.

Finally, data are presented to indicate the possible impact of transient friction loads to the payload designer for the Space Shuttle. Transient response solution data are also included, which compare solutions without friction forces and those with friction forces for payloads mounted in the Space Shuttle cargo bay. These data indicate that payload components can be sensitive to friction induced loads.

INTRODUCTION

The Space Shuttle has been designed to carry a large class of payloads to low earth orbit (LEO). The standard structural load path between the orbiter and the payload is a set of trunnions. A longeron trunnion is illustrated in figure 1. This system of attaching payloads offers much flexibility in the types, sizes, locations in the orbiter cargo bay, and mixes of payloads that can be integrated into the Space Shuttle.

The trunnion restraint system allows relative motion between the orbiter and the payload in the axial direction of the trunnion, as shown in figure 1. Relative motion can also be accommodated in the orbiter longitudinal direction. The relative motions are necessary to preclude large thermally induced loads between the orbiter and the payload during on-orbit mission operations and reentry; however, transient relative motion will be experienced during dynamic events, and the resulting transient friction loads acting on the trunnion may be a factor for the payload system structural design.

As a result of these inherent design features, the effects of trunnion friction on Space Shuttle payload transient loads have become a concern to various payload organizations. Friction behavior at the interface between payloads and the orbiter or within the payload system imposes nonlinear responses on the payload that are not generally included in payload

---

*Member of the Technical Staff

linear load analysis. These nonlinearities associated with friction forces can significantly affect dynamic responses, which, in turn, will impact certain payload design parameters. Nonlinear friction characteristics such as these have been investigated for satellites cantilevered to the inertial upper stage (IUS).

Various methodologies have been developed recently to perform loads analyses with interface friction forces included for Shuttle payloads. These methodologies have resulted in differing payload responses, that are apparently caused by different approximations. Because of the importance to the payload structural design, it is imperative that the nonlinear friction methodology accurately reflect all aspects of the friction phenomenon. Thus, this new analysis procedure that has been developed, and as described here, addresses both types of friction effects: kinetic (or sliding friction), and static friction (or stiction), which exhibits a nonuniform friction coefficient as forces change.

As friction surfaces lock and unlock, the system modal characteristics also change. Modal data are considered for two primary reasons. First, the large size of the orbiter and payload finite element structural models prohibit the use of direct solutions without the sophistication of modal coordinate transformations. Secondly, modal data are generally employed in analyzing large finite element structural models for linear transient loads analyses. For a system with N friction surfaces, 2^N different sets of modal data are possible. The 2^N possible sets of modes are accounted for in the approach described later by including N constraint equations in the system equations of motion. The constraining equations are imposed on the system equations of motion according to program solution logic that enforces stiction or sliding friction as required throughout the transient response solution. As a result, the accuracy of the relative displacement terms associated with the interface compatibility constraint relations must be enhanced by the use of residual flexibilities. The nonlinear capabilities of NASTRAN have been expanded to include both kinetic and static friction conditions in Space Shuttle payload transient loads analysis.

NASTRAN NONLINEAR METHODOLOGY

The equations representing the dynamic behavior of a structure may be written in matrix form as

$$[M]\{\ddot{u}\} + [B]\{\dot{u}\} + [K]\{u\} = \{F\} \tag{1}$$

Reduction of solution costs are usually accomplished through transformation to a set of uncoupled modal coordinates followed by truncation of higher frequency modes. This approximation is generally sufficient to represent a system whose response is primarily confined to the lower frequency regions. After substitution of the normal coordinate transformation, the equations of motion in modal coordinates are

$$\lceil I \rfloor \{\ddot{q}\} + 2\lceil \zeta \omega \rfloor \{\dot{q}\} + \lceil \omega^2 \rfloor \{q\} = [\Phi]^T\{F\} = \{\bar{P}\} \tag{2}$$

Equation (2) was obtained from the relation

$$\{u\} = [\Phi]\{q\} \tag{3}$$

The inclusion of nonlinear effects into a linear structural system can be accomplished by employing NASTRAN's standard nonlinear capability. This involves treating nonlinearities as a combination of calculated nonlinear loads, which are added to the external load vector, and a set of auxiliary equations used in the calculation of these nonlinear loads that is appended to the linear equations of motion. The auxiliary equations are defined using the NASTRAN extra point and DMIG features. The resulting system of equations is

$$\begin{bmatrix} I & 0 & 0 \\ A & 0 & 0 \\ 0 & 0 & 0 \end{bmatrix} \begin{Bmatrix} \ddot{q} \\ \ddot{e} \\ \ddot{N} \end{Bmatrix} + \begin{bmatrix} 2\zeta\omega & 0 & 0 \\ C & 0 & 0 \\ 0 & 0 & 0 \end{bmatrix} \begin{Bmatrix} \dot{q} \\ \dot{e} \\ \dot{N} \end{Bmatrix} + \begin{bmatrix} \omega^2 & 0 & F \\ D & I & E \\ 0 & 0 & I \end{bmatrix} \begin{Bmatrix} q \\ e \\ N \end{Bmatrix} = \begin{Bmatrix} \bar{P} \\ 0 \\ \bar{N} \end{Bmatrix} \tag{4}$$

In the above equation, e represents a response vector of velocities, relative displacements, and normal forces that are used in calculating N, the nonlinear forces. These equations may be formulated and solved in any desired system of coordinates by applying the appropriate transformations.

The presence of auxiliary equations in equation (4) results in a coupled system that must be solved using a numerical integration procedure. The method used in NASTRAN is a modified Newmark-Beta scheme. This finite difference algorithm is noniterative and inherently stable. A brief development of the finite difference equations used in the TRD module will be given here. A more rigorous treatment can be found in the NASTRAN theoretical manual (ref. 1). To aid in developing the finite difference equations, equation (4) may be written in symbolic form as

$$[\overline{M}]\{\ddot{\overline{u}}\} + [\overline{B}]\{\dot{\overline{u}}\} + [\overline{K}]\{\overline{u}\} = \{\overline{Q}\} = \{\overline{P}\} + \{\overline{N}\} \tag{5}$$

where $\overline{P}$ represents the linear external forces and $\overline{N}$ represents the nonlinear forces. The finite difference equations used in the integration scheme are as follows

$$\dot{\overline{u}} = 1/2\Delta t(\overline{u}_{n+1} - \overline{u}_{n-1}) \tag{6}$$

$$\ddot{\overline{u}} = 1/\Delta t^2(\overline{u}_{n+1} - 2\overline{u}_n + \overline{u}_{n-1}) \tag{7}$$

$$\overline{u} = 1/3(\overline{u}_{n+1} + \overline{u}_n + \overline{u}_{n-1}) \tag{8}$$

$$\overline{P} = 1/3(\overline{P}_{n+1} + \overline{P}_n + \overline{P}_{n-1}) \tag{9}$$

$$\overline{N} = 1/3(\overline{N}_n + \overline{N}_{n-1} + \overline{N}_{n-2}) \tag{10}$$

Substitution of equations (6) through (10) into equation (5) results in the recursion relation

$$(1/\Delta t^2\overline{M} + 1/2\Delta t\overline{B} + 1/3\overline{K})\overline{u}_{n+1} = 1/3(\overline{P}_{n+1} + \overline{P}_n + \overline{P}_{n-1})$$
$$+ 1/3(\overline{N}_n + \overline{N}_{n-1} + \overline{N}_{n-2}) + (2/\Delta t^2\overline{M} - 1/3\overline{K})\overline{u}_n +$$
$$(-1/\Delta t^2\overline{M} + 1/2\Delta t\overline{B} - 1/3\overline{K})\overline{u}_{n-1} \tag{11}$$

The unknown displacements $\overline{u}_{n+1}$ can then be solved for in terms of previously determined quantities. This equation may be written as

$$\vec{\overline{K}}\overline{u}_{n+1} = \vec{\overline{P}}_{n+1} \tag{12}$$

where

$$\vec{\overline{K}} = 1/\Delta t^2\overline{M} + 1/2\Delta t\overline{B} + 1/3\overline{K} \tag{13}$$

and $\vec{\overline{P}}_{n+1}$ is the entire right-hand side of equation (11).

Here, $\vec{\overline{K}}$ is constant for constant Δt. By applying this scheme, forces and displacements are assumed to be essentially invariant over the integration step. In order for this assumption to hold, it is imperative that Δt be sufficiently small.

NONLINEAR METHODOLOGY WITH FRICTION FORCES

The inclusion of friction nonlinearities into an analysis presents a problem that cannot be solved using the standard NASTRAN nonlinear methodology just described. This occurs because friction is actually a combination of two complementary phenomena. There is kinetic friction, which is treated as a finite force that opposes the relative motion of two contacting surfaces and static friction.

Kinetic friction is straightforward in nature and may be simulated by using the equation

$$f_k = \mu_k \cdot N \cdot \text{sign}(\Delta\dot{u}_{rel}) \tag{14}$$

In equation (14), f_k is the kinetic friction force, μ is the kinetic coefficient of friction, N is the normal force between the two friction surfaces, and $\Delta\dot{u}_{rel}$ is the relative velocity of the friction surfaces. Kinetic friction is a nonlinearity that is similar in nature to the discrete damper and may thus be analyzed with standard NASTRAN solution procedures.

However, the inclusion of static friction or stiction poses a problem. Static friction exists when the relative velocity of two surfaces tends to zero. Physically, the friction surfaces lock and provide a continuous load path. In effect, the equations of motion experience additional constraint relationships. In order to model this occurrence, a new methodology has been developed and implemented in NASTRAN.

Static friction is modeled by adding a set of constraint equations enforcing a constant relative displacement over the period of integration to equation (11). A set of friction degrees of freedom (DOF) u_I may be defined, with u_D being its complementary set of friction DOF, and u_F being all remaining DOF. Equation (12) may be expanded, using e points, to include the constraint equations between u_I and u_D. The friction model equation then becomes

$$
\begin{bmatrix}
\bar{K}_{FF} & \bar{K}_{FI} & \bar{K}_{FD} & 0 \\
\bar{K}_{IF} & \hat{K}_{II} & \bar{K}_{ID} & \ ^{-}I \\
\bar{K}_{DF} & \bar{K}_{DI} & \bar{K}_{DD} & \ ^{-}I \\
0 & \ ^{-}I & \ ^{-}I & 0
\end{bmatrix}
\begin{Bmatrix}
\bar{u}_F \\
\bar{u}_I \\
\bar{u}_D \\
f_s
\end{Bmatrix}_{n+1}
=
\begin{Bmatrix}
\bar{P}_F \\
\bar{P}_I \\
\bar{P}_D \\
q_r
\end{Bmatrix}_{n+1}
\tag{15}
$$

where f_s is the stiction force required to enforce a constant relative displacement q_r. These equations serve to enforce stiction between $\bar{u}_I$ and $\bar{u}_D$. Equation (15) can further be expressed as the following three equations:

$$
\left[
\begin{array}{c:c}
\bar{K}_{FF} & \bar{K}_{FI} + \bar{K}_{FD} \\
\hdashline
\bar{K}_{IF} + \bar{K}_{DF} & \bar{K}_{II} + \bar{K}_{DI} + \bar{K}_{ID} + \bar{K}_{DD}
\end{array}
\right]
\begin{Bmatrix}
\bar{u}_F \\
\bar{u}_I
\end{Bmatrix}_{n+1}
=
\tag{15a}
$$

$$
\begin{Bmatrix}
\bar{P}_F + \bar{K}_{FD}q_r \\
\bar{P}_I + \bar{P}_D + (\bar{K}_{DD} + \bar{K}_{ID})q_r
\end{Bmatrix}_{n+1}
$$

$$
\{\bar{u}_D\}_{n+1} = \{\bar{u}\}_{n+1} - \{q_r\}_{n+1}
\tag{15b}
$$

$$
\{f_s\}_{n+1} = \{\bar{P}_I\}_{n+1} - [\bar{K}_{IF}]\{\bar{u}_F\}_{n+1} - [\bar{K}_{II}]\{\bar{u}_I\}_{n+1} - [\bar{K}_{ID}]\{\bar{u}_D\}_{n+1}
\tag{15c}
$$

The solution of equations (15a) and (15b) yield the displacements u_I and u_D. The static friction force f_s can then be determined from equation (15c). Note that f_s does not appear in equations (15a) or (15b); therefore, it is considered to be an internal load. For the state when all friction surfaces are free to slide (kinetic friction only), the constraint equations in equation (15) are modified and read as

$$
\begin{bmatrix}
\bar{K}_{FF} & \bar{K}_{FI} & \bar{K}_{FD} & 0 \\
\bar{K}_{IF} & \bar{K}_{II} & \bar{K}_{ID} & \ ^{-}I \\
\bar{K}_{DF} & \bar{K}_{DI} & \bar{K}_{DD} & \ ^{-}I \\
0 & 0 & 0 & \ ^{-}I
\end{bmatrix}_{n+1}
\begin{Bmatrix}
\bar{u}_F \\
\bar{u}_I \\
\bar{u}_D \\
f_s
\end{Bmatrix}_{n+1}
=
\begin{Bmatrix}
\bar{P}_F \\
\bar{P}_I \\
\bar{P}_D \\
f_k
\end{Bmatrix}_{n+1}
\tag{16}
$$

As stated earlier, kinetic and static friction are complementary events and thus equations (15) and (16) may be used to represent any combination of sliding and nonsliding surfaces. In the analysis procedure, f_k is calculated at every time step and compared against f_s, which is computed only during periods of near-zero relative motion. The kinetic and static friction forces are then compared and the appropriate constraint equations are applied. This set of constraint equations

135

defines the friction state of the structure. For a structure having N friction surfaces, there are 2^N possible friction states. Finally, the actual friction force at any instant of time is chosen to be either the kinetic or static friction force.

This presentation indicates that the friction solution is dependent on a set of calculated displacements. As a result, the displacement field representing the set of friction surfaces should be as accurate as possible. When a system is represented in terms of truncated modal coordinates, equation (2), a problem could arise if modes describing the motion of the friction surfaces have been truncated. This truncation would effectively constrain the system, yielding an incorrect displacement field and, consequently, an erroneous friction solution. In order to avoid or minimize this inaccuracy, a correction known as residual flexibility (ref. 2) may be applied to the friction DOF. This is basically an attempt to approximate the contribution of truncated higher order modes to the system response. The application of this procedure necessitates modifications to equation (2) as follows:

$$
\begin{bmatrix} K_Q + \phi_b^T G_{\rho bb}^{-1} \phi_b & -\phi_b^T G_{\rho bb}^{-1} \\ -G_{\rho bb}^{-1} \phi_b & G_{\rho bb}^{-1} \end{bmatrix} \begin{Bmatrix} q \\ \bar{u}_b \end{Bmatrix} + \begin{bmatrix} M_Q & 0 \\ 0 & 0 \end{bmatrix} \begin{Bmatrix} \ddot{q} \\ \ddot{\bar{u}}_b \end{Bmatrix} = [\Phi_\rho]^T \begin{Bmatrix} F \\ 0 \end{Bmatrix}
\tag{17}
$$

where

$$
\Phi_\rho = \begin{bmatrix} \phi_i - \bar{G}_{\rho ib} G_{\rho bb}^{-1} \phi_b & \bar{G}_{\rho ib} G_{\rho bb}^{-1} \\ 0 & I \end{bmatrix}
\tag{18}
$$

is the corrected system transformation matrix. The terms $G_{\rho bb}$ and $\bar{G}_{\rho ib}$ are as defined as follows

$$
\bar{G}_\rho = \begin{bmatrix} G_{\rho ii} & G_{\rho ib} \\ G_{\rho bi} & G_{\rho bb} \end{bmatrix}
\tag{19a}
$$

$$
\bar{G}_{\rho ib} = \begin{bmatrix} G_{\rho ib} \\ G_{\rho bb} \end{bmatrix}
\tag{19b}
$$

where $\bar{G}_\rho$ is the full residual flexibility matrix. In these equations, the subscript b refers to friction related DOF, while i refers to all other DOF. The matrix K_Q represents the original generalized stiffness matrix (ω^2), while M_Q is the generalized mass matrix (identity). Note that the damping terms have not been included for the sake of brevity. Substitution of equations (17) and (18) into equation (3) yields the nonlinear system equations that are now densely populated.

Applying this integration scheme to these equations is very costly because the required matrix decompositions and multiplications are functions of matrix density. This situation may be remedied by recalling that such a system can be uncoupled through a matrix transformation. The required transformation matrix can be obtained by solving the eigenproblem associated with equation (17) and retaining all modes; however, this approach, is feasible only if the system mass matrix is positive definite. The mass matrix in equation (17) contains null terms at friction surface DOF and is thus nonpositive definite. This problem can be avoided by applying a residual mass correction to the friction surface DOF. The residual mass correction, which is entirely analogous to the residual flexibility correction, results in the equation

$$
\begin{bmatrix} K_Q + \phi_b^T G_{\rho bb}^{-1} \phi_b & -\phi_b^T G_{\rho bb}^{-1} \\ -G_{\rho bb}^{-1} \phi_b & G_{\rho bb}^{-1} \end{bmatrix} \begin{Bmatrix} q \\ \bar{u}_b \end{Bmatrix} + \begin{bmatrix} M_Q + \phi_b^T M_{\rho bb} \phi_b & -\phi_b^T M_{\rho bb} \\ -M_{\rho bb} \phi_b & M_{\rho bb} \end{bmatrix} \begin{Bmatrix} \ddot{q} \\ \ddot{\bar{u}}_b \end{Bmatrix} = [\Phi_\rho]^T \begin{Bmatrix} F \\ 0 \end{Bmatrix}
\tag{20}
$$

in which $M_{\rho bb}$ is the partition of the residual mass matrix related to friction DOF. The eigensolution of equation (17) should yield a set of modes consisting of the original modes appended by a set of residual modes corresponding to the friction DOF. The generalized mass and stiffness matrices associated with this new set of modes is completely diagonal and may be used, with the appropriate transformation matrices, in equation (2). The final result is a system of nonlinear equations that is relatively sparse.

If the residual mass matrix is unavailable, the mass matrix in equation (14) can still be made positive definite by substituting a diagonal matrix containing terms of relatively small magnitude (S) for M. Equation (17) can then be rewritten as

$$
\begin{bmatrix} K_Q + \phi_b^T G_{\rho bb}^{-1} \phi_b & -\phi_b G_{\rho bb}^{-1} \\ -G_{\rho bb}^{-1} \phi_b & G_{\rho bb}^{-1} \end{bmatrix} \left\{ \begin{array}{c} q \\ \bar{u}_b \end{array} \right\} \begin{bmatrix} M_Q & 0 \\ 0 & S \end{bmatrix} \left\{ \begin{array}{c} \ddot{q} \\ \ddot{u}_b \end{array} \right\} = [\Phi_\rho]^T \left\{ \begin{array}{c} F \\ 0 \end{array} \right\}
\tag{21}
$$

The eigensolution of equation (21) should yield results that are almost identical to those obtained using residual mass if S is properly chosen.

Once the corrected equations of motion have been generated, they may be used in equations (15) and (16) such that q is a subset of $\bar{u}_F$. $\bar{u}_b$ in equation (20) includes the friction DOF $\bar{u}_I$ and $\bar{u}_D$. The resulting system equations now provide a much more accurate representation of the friction surfaces. Since there are 2^N possible friction states, there must be 2^N corresponding sets of modal data. These are defined by the constraint equations as a function of the transient solution. In this way, variations in modal content may be effected by merely changing the constraint equations.

TRANSIENT RESPONSE DYNAMICS MODULE MODIFICATIONS

The capability to solve the nonlinear equations of motion with friction forces in NASTRAN required extensive modification to the TRD module. A general approach and an overview of the logic that was adapted is illustrated in figure 2. The logic path on the left of this figure represents the original TRD module with one additional test for a friction solution approach. The logic path to the right represents the requirements when friction forces are evaluated. The nonlinear force output data appears in both logic paths with one significant variation. Output for the nonlinear forces with friction effects occurs after the integration step because the static friction force is a term included with the displacement data.

Two essential ingredients are necessary to evaluate the nonlinear solution when friction is introduced. It is first necessary to monitor the friction forces (f_s and f_k). Secondly, it is required to adjust the coefficients of the constraint equations during the transient solution. For any friction state, the finite difference equation with all nonlinear dependent terms is of the form expressed in equation (12). Because of friction solution requirements, the stiffness operator coefficients, which is $\bar{K}$ in equation (12), will change whenever the friction state changes.

In typical orbiter payload transient loads analyses, $\bar{K}$ will be of order 400 to 800 and any number of friction state changes will occur. A friction state change requires a change in the coefficient matrix, $\bar{K}$; therefore, a solution of equation (12) would require the inverse of $\bar{K}$ whenever the friction state changes. A solution approach without further study was defined as not feasible because of economic considerations for matrix coefficients of order 400 to 800.

Computational expense is reduced significantly by noting the following: the changes in $\bar{K}$ are local in the matrix array, and equation (12) has the form of a statics problem. Thus, the finite difference formulation lends itself to the method of static condensation (ref. 3). Equation (12) is partitioned as follows:

$$
\begin{bmatrix} \bar{K}_{ii} & \bar{K}_{if} \\ \bar{K}_{fi} & \bar{K}_{ff} \end{bmatrix} \left\{ \begin{array}{c} \bar{u}_i \\ \bar{u}_f \end{array} \right\}_{n+1} = \left\{ \begin{array}{c} \bar{P}_i \\ \bar{P}_f \end{array} \right\}_{n+1}
\tag{22}
$$

In equation (22), $\bar{u}_f$ is the DOF set needed to define the friction state and $\bar{u}_i$ is the set of all remaining DOF. Two sets of simultaneous equations are represented by equation (22).

If u_i is eliminated and the time step subscript is dropped for simplicity, the following expressions are obtained.

$$
[\overline{K}_{ff}] = [\bar{K}_{ff}] - [\bar{K}_{fi}][\bar{K}_{ii}]^{-1}[\bar{K}_{if}]
\tag{23}
$$

$$
\{\overline{P}_f\} = \{\bar{P}_f\} - [K_{fi}][\bar{K}_{ii}]^{-1}\{\bar{P}_i\}
\tag{24}
$$

$$
[\overline{K}_{ff}]\{\bar{u}_f\} = \{\overline{P}_f\}
\tag{25}
$$

The solution for the friction dependent functions, $\bar{u}_f$, is now tractable for any friction state. Essentially, the approach requires an iterative solution of a much smaller set of equations in which the coefficients are adjusted to satisfy

$$\{f_s\} \leq \{f_k\} \tag{26}$$

Equation (26) is a set of constraint variables for an acceptable solution to equation (25). The minimum friction force is selected as the optimum at each friction surface for all trial solutions. Solutions of linear equations with constraint variables similar to those represented by equations (25) and (26) are discussed in ref. 4.

Since an iterative solution procedure is used on a set of variables to obtain particular solutions for equation (25), a criteria is required for changing friction states. All friction force variables that have a relative velocity near zero are first assumed to be in a static friction state. The coefficients of equation (26) as well as the appropriate $\overline{P}_f$ term are adjusted accordingly. A trial solution is obtained. When multiple friction surfaces do not satisfy equation (26), the friction surface reflecting a static friction force, f_s, which is greater than the kinetic friction force, f_k, by the largest percentage is changed to a sliding state and the kinetic friction force is used in the solution of equation (25). Because the relative velocity is by definition zero during stiction dwells, the sign of the kinetic friction force is also assumed to have the same sign as the static friction force for transition from a stuck state to a sliding state. Thus, equation (26) is satisfied by obtaining a particular solution derived from a constant relative displacement criteria, as illustrated in equations (15) and (25). If equation (26) cannot be satisfied, the solution form represented by equation (16) is chosen and the kinetic friction state is assumed. The solution for the $\bar{u}_i$ set is obtained from the following:

$$\{\bar{u}_i\} = [\bar{K}_{ii}]^{-1}\{\bar{P}_i\} - [\bar{K}_{ii}]^{-1}[\bar{K}_{if}]\{\bar{u}_f\} \tag{27}$$

Table I defines all subroutine functional characteristics in relation to each modified or new subroutine implemented for solving the transient response with static and kinetic friction forces. It begins wtih the DMAP module, TRDNL, which is an expanded version of the original TRD module. All subroutines and subroutine entry points to perform discrete functions are identified in a logical path from initialization through the computational sequence and on to the specific friction solution iterative subroutine, DUDEQZ. In addition, all subroutines are identified as either modified NASTRAN fortran code or newly developed fortran code. Data are also provided that indicate the degree of difficulty incurred in developing or implementing the specific subroutine even though this may have a personal bias.

An additional feature that was implemented required special and unique provisions in subroutine TRD1D. Specific scaler values on NOLIN bulk data were used for two special purposes not defined by NASTRAN. The use of specific scaler values also allows all necessary input data modifications to remain local to the TRD module as opposed to also modifying the input processing region of NASTRAN and passing specific data to the TRD module. The first special purpose scaler value was defined to generate a vector sum of two variables, such as the root-sum-square of two forces. This provided the capability to evaluate a normal force as a function of two independent variables, which is required to define the kinetic friction force in equation (14). A second function embedded in subroutine TRD1D defines sets of variables for each of the friction surfaces. By combining the definitions of each of the friction surface sets, it is possible to define a system partition vector. These data provide the appropriate definitions for initialization of the finite difference coefficient matrices as well as partitioning data, coefficient matrix manipulations, and solution procedures to solve the system of equations in a partitioned form, which is indicated by equation (22). The partitioning data are also used to monitor the friction solution states in subroutine DUDEQZ.

Thus, NASTRAN's capability is expanded to modify the finite difference form of the equations of motion by using constraint equations. The constraints are further modified by a solution logic choice between static friction or kinetic friction during the finite difference integration process. In addition, static condensation of the finite difference coefficient matrix is implemented to reduce the computational cost of solving for the friction state and the resultant friction forces.

FRICTION DEMONSTRATION PROBLEM

The primary intent of this demonstration problem is to illustrate the effects of modal truncation on dynamic response data when friction forces are included. A secondary intent is to examine friction methodologies that can be effectively implemented for payload loads analyses.

138

For simplicity, a one-dimensional problem was developed consisting of masses connected by springs, as shown in figure 3. Also included in figure 3 are the physical properties required to generate the structural model. Basically, it consists of 23 DOF interconnected by linear springs and includes three friction surfaces.

Four approaches to solve this transient response problem with friction were studied. The four solution approaches, which are also summarized in table II are:

1. Solve the problem in the physical coordinate system.

2. Solve the problem using a truncated mode set; (two sets of results are presented later): one set using 12 of the possible 23 modes and another set using 18 of the possible 23 modes.

3. Solve the problem using the same truncated modes as solution approach 2 (12 mode set), but include residual flexibility corrections for the friction surfaces.

4. Solve the problem using the same truncated modes as solution approach 2 (12 mode set), but include both residual mass and flexibility corrections for the friction surfaces.

These transient response solutions will be referred to as solution approaches 1 through 4 in the following discussions. Solution approach 1 is considered as a reference solution to which solution approaches 2 through 4 are compared to understand the effects of modal truncation on the transient response solution when friction forces are also included. The methodology used in solution approaches 3 and 4 is identical to that which Rockwell has employed for payload loads analyses.

Figures 4 through 8 are selected response terms for the four different approaches to solving the transient response problem and figure 9 is the time history plot of the applied forcing function at block 7 in figure 3. It is appropriate to note that all response data not shown demonstrates results similar to those depicted by these selected response terms. Also, the first approach (i.e., no modal truncation) was solved using all 23 system modes and the transient response solution was essentially identical to that obtained using physical coordinates. The natural frequencies for this friction demonstration problem are included in table III.

There is a serious degradation when solution approach 2 (i.e., a modal transformation that approximates the system with 12 and 18 of the possible 23 modes of vibration) is compared to any of the other three solution approaches. It is a preferred method for linear transient response solutions and is particularly useful for large finite element models, but figures 4 through 8 indicate distortions in the response data. The friction force time histories, which are shown in figure 6, indicate a potential degradation to the stiffness characteristics of the system because of a more rapid change of the friction force when the modally truncated solution is compared to the solution that uses physical coordinates. These observations tend to indicate a difficulty with the friction surfaces alone. They also suggest that something was deleted from the system synthesis by solely transforming to generalized coordinates, as was done in solution approach 2.

Residual flexibility data for the friction DOF provides a measure of the flexibility loss when a truncated modal transformation is used. Conversely, it indicates the degree of stiffening brought about by the truncated modal transformation. For this demonstration problem, these data are presented in table IV and provide a qualitative measure of the flexibility loss at the friction surfaces when the 12 modes that were used in solution approach 2 are compared to the total flexibility of the structural system (i.e., 23 modes). Except for block 27, the flexibility loss data suggests a severe truncation approximation has taken place for all friction surfaces. The flexibility data also suggest that difficulties may be encountered in arriving at a realistic solution when a compatibility assessment for the friction surfaces during a transient response solution is required.

When physical displacement data are approximated by truncated system modes times the generalized displacements, the relative displacement terms used to evaluate the friction force data are likely to be distorted. Since relative displacements for the friction surfaces are equal to the difference of two physical displacement terms, the transient response data are likely to be distorted when the two physical displacements are approximated to different levels of accuracy. This situation is indicated by a comparison of the truncated flexibility percentage data for blocks 17 and 27 in table IV. The approximation to different levels of accuracy may be a contributing factor to the relative displacement

139

distortions for the friction surfaces, such as indicated in Figure 4, when there are extended dwells at a constant relative displacement.

Therefore, it is hypothesized that the friction forces, when derived as a function of relative displacement terms that are obtained from a structural system that is too stiff, will be distorted when compared to a factual solution, such as solution approach 1 Illogical consequences in a transient response analysis with friction could be significant, as evidenced by the results using truncated modes only and the related time history response data comparisons. Thus, when related to a friction surface, the relative displacements should not retain a significant local stiffness approximation for transient response solutions with friction forces included if a significant flexibility loss is noted for the friction DOF. As presented in table III, the flexibility loss ratio data are variables required to recognize when such a situation exists.

The previous discussions suggest that the modal transformation approximation implemented in solution approach 2 be enhanced before the transient solution with friction is attempted. Because a compatibility assessment is required to evaluate the stiction friction force during periods of zero or near-zero relative velocity, it is also suggested that the transient response will likely be distorted unless the friction DOF are corrected to reflect valid local system stiffnesses. Solution approaches 3 and 4 are formulated to alleviate the difficulty of acquiring a quality compatibility assessment for the friction surfaces. The modal transformation from physical to generalized coordinates is accomplished first. Afterwards, an enhancement to the relative displacements for the friction surfaces is performed by a residual flexibility correction for solution approach 3 (see equation (21)), and by both a residual flexibility and mass correction for solution approach 4 (see equation (20)).

Evidence that the system stiffness characteristics are enhanced by implementing solution approaches 3 and 4 may be observed by inspecting any of the time history plots. Of particular significance are the variations in the friction force time histories (see figure 6). It is noted that these time history data for solution approaches 3 and 4 are nearly identical to the more exact representation when physical coordinates are employed (solution approach 1). Since the variation in the relative displacements and the friction forces has virtually vanished, the conclusion is that a valid compatibility descrip tion is now maintained at the friction DOF.

It is appropriate to specifically note the response characteristics of accelerations and element force time history data because they provide an indication of the solution impact on payload acceleration transformation matrix (ATM) and load transformation matrix (LTM) response recovery data. The acceleration item recoveries for mass item 35, shown in figure 7, has significant amplitude deviations as well as slight phase shifts when solution approach 2 is compared to solution approaches 1, 3, and 4. Solution approaches 3 and 4 may have amplitude deviations when compared to the reference solution, but they are difficult to measure by eye. Any apparent amplitude distortions of solution approaches 3 and 4 would appear to be minor when the larger approximation introduced by the truncated modal solution, solution approach 2, is compared to the reference solution. The selected element force time histories exhibit similar distortions, as indicated in figure 8 for solution approach 2, and are improved in solution approaches 3 and 4 when compared to solution approach 1. These data comparisons indicate that ATM and LTM response recovery data for payloads could be altered if one did not adjust the modally truncated system stiffness characteristics to acquire a valid compatibility assessment at the friction surfaces. It is not implied that the percentage differences would be identical or even close to what is indicated by these data but rather that a truncated modal transformation would alter the transient response solution by employing a degenerative compatibility description for the friction surfaces.

From the results of this demonstration problem, it is observed that solution approach 2, which relies only on a set of modally truncated gener .zed coordinates, significantly distorts the dynamic behavior of the transient response solution with friction forces. Evidence that a system flexibility degradation is present is deduced by inspecting the residual flexibility data for the friction DOF. Both the residual flexibility and the residual mass adjustments tend to alleviate the response distortions by enhancing the structural system stiffness characteristics so that a quality compatibility assessment for the friction surfaces can be maintained during the transient solution. All time history plots indicate that both solution approaches 3 and 4 tend to converge to the results obtained from solution approach 1, the reference solution.

APPLICATION TO LARGE FINITE ELEMENT PROBLEMS

The methodology presented here has been implemented in several Space Shuttle payload transient loads analyses. These problems are generally large, typically on the order of 1,200 physical DOF. In order to reduce solution costs to a more reasonable level, the transient loads analysis is usually solved in truncated modal coordinates. The cutoff frequency

140

may range from 35 to 50 Hertz. While this representation may be adequate for a linear analysis, a severe loss in flexibility at the orbiter payload friction interfaces is generally experienced. Table V illustrates the loss in flexibility that occurred in a typical Space Shuttle/IUS coupled modal model. Therefore, residual flexibility corrections are necessary in order to ensure a valid solution, as illustrated in the demonstration problem. Results for an analysis conducted with and without residual flexibility corrections are also presented in figures 10 and 11. The stiffening effect of truncation on the friction interface results in a more rapid static friction force response to a dynamic loading. Figure 10 illustrates this effect. Figure 11 depicts the total friction force (static plus kinetic) time history corresponding to figure 10. A comparison of the data suggests that the dynamic input from the friction forces into the system can be radically altered by modal truncation.

The costs associated with a friction analysis are significant in a large-order problem because of the requirements for a small integration step size and the number of matrix operations involved; however, data from several loads analyses indicate that friction may have a major impact on payload component responses. Tables VI and VII present results for two spacecraft cantilevered from the IUS. The data consists of the maximum accelerations experienced by spacecraft components for an analysis conducted with and without the effects of friction. Table VI contains data for the tracking and data relay satellite (TDRS) 11 spacecraft for a lift-off transient event while table VII contains similar data for the DSCS-III/DSCS-III spacecraft based on overall landing transient maximums. The primary difficulty with these data is to recognize that the percentage variations are as large if not larger than uncertainty factors that are generally employed in linear loads analyses, which presents the payload designer with a dilemma. Thus, it appears as though it may be justified to investigate friction effects in a transient loads analysis.

FRICTION SOLUTION

The friction solution is outlined as follows.

1. The equations of motion are prescribed as outlined in equation (4). Static constraint equations are applied as illustrated in equation (15) with static friction on all trunnions as the initial friction state.

2. The friction DOF in equation (4) are augmented by use of residual flexibilities to correct for modal truncation errors (equation (21)). The initial displacements are calculated such that f_s is zero.

3. Either residual mass or a small fictitious mass is applied to the mass matrix, an eigen analysis is performed, and the equations of motion are transformed to this new modal coordinate system with no truncation. Any numeric round-off error in the rigid body modes is eliminated.

4. The transient solution is executed and the constraint equations are adjusted according to programmed solution logic that chooses between stiction and sliding friction states as required (equations (15) and (16)). The method of static condensation (equations (22) through (25)) is employed to minimize computational cost of the required matrix inversion whenever the friction state changes.

CONCLUSIONS

The methodology presented allows an analyst to include aspects of the friction phenomenon neglected in some other approaches. In particular, use of the total flexibility on the friction DOF is a necessity if the static friction forces and the corresponding payload response are to be accurately represented. Implementation of residual flexibilities with the appropriate constraint equations lead to an accurate representation of the modal content for each particular friction state and appears to be a logical extension of a linear loads analysis that has used truncated modal coordinates. Static condensation on the recurrence equation provides efficient and cost effective adjustment of the equations of motion any time the friction state changes. Also, diagonalizing the equations of motion and retaining the complete set of modes (i.e., original plus residual) leads to a substantial cost savings with no apparent degradation of the analytic results.

The method is generally applicable to a large class of transient response problems. It has direct application to problems involving surface contact and separation. In particular, a similar problem of launch vehicle to launch pad separation might also be investigated with this approach if friction forces are considered to be a dominating influence.

141

Finally, application of residual modes to other transient friction methodologies that have employed truncated modal transforms appears to be feasible. Incorporating residual flexibilities expands the retained modal data by the number of friction DOF. The modified system equations of motion include the total flexibility at the friction interfaces and can be diagonalized a second time. Implementing a residual modes correction will enhance the accuracy of other approaches that presently employ standard truncated modal transforms.

REFERENCES

1. *The NASTRAN Theoretical Manual (Level 17.5)*. NASA SP-221(03), general release (Mar. 1, 1979).

2. Rubin, S. "Improved Component-Mode Representation for Structural Dynamic Analysis," AIAA Journal; Vol 13, Number 8 (Aug. 1975) pp. 995-1006.

3. Bathe, Klaus-Jurgen and Sheryl Gracewski. "On Nonlinear Dynamic Analysis Using Substructuring and Mode Superposition," Computers and Structures, Vol 13 (1981) pp. 699-707.

4. Wagner, H. M. *Principles of Operations Research*. Prentice-Hall, Inc.; Englewood Cliffs, N.J. (1975).

5. Henkel, E. E., J. E. Misel, and D. H. Frederick. "A Methodology to Include Static and Kinetic Friction Effects in Space Shuttle Payload Transient Loads Analysis." Presented at AIAA Shuttle Environment and Operations Meeting, Washington, D.C., (Oct. 3, 1983).

TABLE I. — FUNCTIONS ASSIGNED TO SUBROUTINES FOR THE TRD MODULE WITH FRICTION FORCES

NASTRAN subroutine			Degree of difficulty*	Subroutine function/comment
Name	Modified	New		
TRDNL	X		1	Modified TRD module with additional entry parameters, scratch files, and control logic for new subroutine processing and additional initialization for static condensation.
TRD1C	X		3	Modified NASTRAN computational control subroutine to implement the finite difference algorithm. When friction forces are defined the following capabilities are activated: • Evaluate the finite difference recursion formula by static condensation • Evaluate the friction state and forces • Output nonlinear forces corrected for friction state
TRD1CI	X		1	This is a new entry in subroutine TRD1C, which calls subroutine TRD1D to inspect the NOLIN bulk data inputs for friction defini- tions. If friction inputs are defined, a partition vector is output to a scratch file.
TRD1CN		X	2	This new entry in subroutine TRD1C, which forms the appropriate coefficient matrices for the friction problem, inspects the partition vector, and prepares to solve the finite difference algorithm by parts.
GENPVF		X	1	This subroutine writes a NASTRAN-type partition vector to a specified scratch file.
INITIL	X		2	This subroutine forms the finite difference equation coefficient matrices (equation (11)). If friction is defined, it prepares to parti- tion, $\bar{K}$, in equation (12).
INITLD	X		2	Entry point in subroutine INITL to decompose K_{ii} of equation (22) if friction is defined. It also completes the finite difference coefficient matrix computation when a friction solution is specified.
PARTKC		X	2	Partition the finite difference coefficient matrix, $\bar{K}$, in equation (12) for a static condensation solution, as indicated in equation (22).
FINITL		X	2	This subroutine is required to finish initialization when a friction solution is required and a static condensation solution procedure is in process. It prepares matrix products for solution of equations (23), (24), and (27).
CFBSOR	X		1	NASTRAN forward-backward substitution subroutine for solution of linear equations.
CFBSOF	X		1	Entry in subroutine CFBSOR to alter memory allocation.

NASTRAN subroutine			Degree of difficulty*	Subroutine function/comment
Name	Modified	New		
TRD1D	X		3	This subroutine performs the following functions: • Allocate memory for nonlinear functions • Initialize tabular data tables • Evaluate friction definitions, if any • Evaluate nonlinear functions • Calculate nonlinear force data It was modified extensively to recognize specific scaler values of the NOLIN1 and NOLIN2 bulk data types, alter memory allocation, process a root-sum-square force term of the type required for kinetic friction forces, and monitor friction solution states in regions of near-zero relative velocity.
TRD1DF	X		3	This is a new entry in subroutine TRD1D to update the nonlinear force data when a friction state change is indicated by subroutine DUDEQZ.
STEP	X		3	Subroutine STEP controls the numerical evaluation of the finite difference recursion relation shown in equation (11). It was expanded to support static condensation evaluation requirements.
STEP2A		X	3	Entry in subroutine STEP to evaluate the inverse matrix product in equation (24).
STEP2B		X	3	Entry in subroutine STEP to complete the evaluation of equation (24).
STEP2C		X	3	Entry in subroutine STEP to evaluate the displacement data of equation (27)
MATVEC	X		1	Subroutine MATVEC forms the product $X = X + Ay$, where A is a matrix and y is a vector.
NEVGEC		X	2	Entry in subroutine MATVEC to form the product $X = X - Ay$, where A is a matrix and y is a vector.
DUDEQZ		X	3	This subroutine is the iterative solution control subroutine to evaluate equation (25) with the friction solution constraints presented in equation (26).
NLCMXR		X	2	A subroutine to adjust the constraint relationships for static and kinetic friction force solution requirements. The row terms for a constraint relationship (see equation (15)) are set to zero and the appropriate diagonal is set to unity (see equation (16)).

NASTRAN subroutine			Degree of difficulty*	Subroutine function/comment
Name	Modified	New		
FI2FPN	X		2	This subroutine locates specific terms for the solution of equations (25) and (26). It provides the capability to locate particular friction surface, quantities such as a static friction force term.
GDEC		X	2	This subroutine prepares to solve a set of linear equations of the form AX = B where A is a coefficient array, B is a specified vector, and X is the desired solution. The coefficient array A is triangularized by Gaussian elimination.
GSOL		X	2	This subroutine evaluates the linear system of equations prepared previously by subroutine GDEC.
INCVP		X	1	A subroutine to partition a vector given a NASTRAN-type partition vector. The data are all memory resident.
INCVM		X	1	A subroutine to merge a vector given a NASTRAN-type partition vector. The data are all memory resident.

*1 = Minor
 2 = Moderate
 3 = Extensive

TABLE II. — DESCRIPTION OF SOLUTION APPROACHES

Solution approach	Solution approach description
1	• A solution approach that retains the displacements, velocities, and accelerations in a physical coordinate system • A finite difference integration procedure is used to generate the time history response data • No damping is used
2	• A solution that employs a modal transformation approximation for the physical displacements, velocities, and accelerations • Only the first 12 of the possible 23 modal vectors are used to approximate the displacements, velocities, and accelerations • No damping is used • A second solution was obtained using 18 of the possible 23 modal vectors
3	• A solution that employs a modal transformation approximation for the physical displacements, velocities, and accelerations • The same 12 modes as selected for solution approach 2 are employed in this solution; however, friction forces were calculated as a function of relative displacement data measured from additional degrees of freedom that have been corrected by residual flexibility functions • No damping is used
4	• This solution approach was identical to solution approach 3 with the addition of residual mass functions to the degrees of freedom retained for the friction force relative displacement data • No damping is used

TABLE III. — FRICTION DEMONSTRATION PROBLEM; NATURAL FREQUENCIES

Mode	Frequency (Hz)
1	1.67
2	2.52
3	4.93
4	5.74
5	7.89
6	8.08
7	10.04
8	10.99
9	12.30
10	12.33
11	13.48
12	14.24
13	70.14
14	70.14
15	70.15
16	70.15
17	70.15
18	70.15
19	70.15
20	70.15
21	70.15
22	70.16
23	221.81

TABLE IV. — FRICTION DEMONSTRATION PROBLEM; PERCENT TRUNCATED FLEXIBILITY

Description*		Percent of total flexibility truncated	
		Upper block*	Lower block*
Blocks	13X	49	N/A
	23X	N/A	49
Blocks	15X	25	N/A
	25X	N/A	25
Blocks	17X	17	N/A
	27X	N/A	2

Modes above 14.24 Hz truncated
*Refer to table III and figure 3.

TABLE V. — IUS-ORBITER FRICTION DEGREES OF FREEDOM; PERCENT TRUNCATED FLEXIBILITY

Description	Percent of total flexibility truncated	
	Orbiter side	IUS side
Forward ASE Y*	43	3
Aft ASE forward Y*	42	16
Coulomb damper Y*	90	6
Coulomb damper Z*	83	2
Aft ASE aft X*	66	79
Aft ASE aft Y*	53	37
Keel Z	51	31

From DSCS/IUS loads analysis, M60W01 orbiter math model, P3B IUS math model, landing condition, modes above 50 Hz truncated (ref. 5)
*Symmetry from right-hand side to left-hand side

TABLE VI. — TDRS-11 COMPONENT ACCELERATIONS COMPARISON OF LIFT-OFF CASE L0942H

Component description	Orbiter direction	Maximum absolute acceleration (g's)		Percent difference
		Frictionless	Friction	
SGL antenna	X	3.062	2.939	−4
	Y	2.754	2.636	−4
	Z	3.131	3.188	2
SGL feed	X	4.877	4.317	−11
	Y	2.276	2.320	2
	Z	5.459	4.861	−11
C-band antenna	X	3.693	3.238	−12
	Y	1.151	1.273	11
	Z	4.015	3.435	−14
Top C-band antenna	X	4.083	3.537	−13
	Y	4.095	3.979	−3
	Z	12.375	9.721	−21
Propellant tank c.g.	X	3.113	3.060	−2
	Y	0.505	0.466	−8
	Z	0.987	1.056	7
+Y solar panel outer hinge	Z	1.277	1.312	3
	Y	3.677	4.795	30
+X solar array antenna	Z	8.461	13.393	58
	Y	12.134	9.596	−21

148

TABLE VII. — DSCS PAYLOAD COMPONENT ACCELERATION COMPARISON FOR LANDING CASES

Component description	Orbiter direction	Maximum absolute acceleration (g's)		Percent difference
		Frictionless	Friction	
Aft spacecraft:				
Center-body multibeam antenna	Z	2.05	2.23	9
Center-body multibeam antenna	Y	2.13	2.43	14
Center-body tank	Y	2.15	2.28	6
Center-body tank	Z	0.51	0.89	75
Center-body dish antenna	Y	3.17	5.98	87
Center-body dish antenna	Z	2.05	3.88	89
Solar array	Y	2.02	2.22	10
Solar array	Z	2.36	2.68	14
Solar array	Z	2.38	5.94	150
Forward spacecraft:				
Center-body multibeam antenna	Z	2.51	2.49	−1
Center-body multibeam antenna	Y	0.75	0.62	−17
Center-body tank	Y	0.84	0.72	−14
Center-body tank	Z	2.71	1.04	−62
Center-body dish antenna	Y	3.58	3.87	8
Center-body dish antenna	Z	2.72	2.74	1
Solar array	Y	0.79	0.86	9
Solar array	Z	3.01	3.69	23
Solar array	Z	3.47	4.02	16
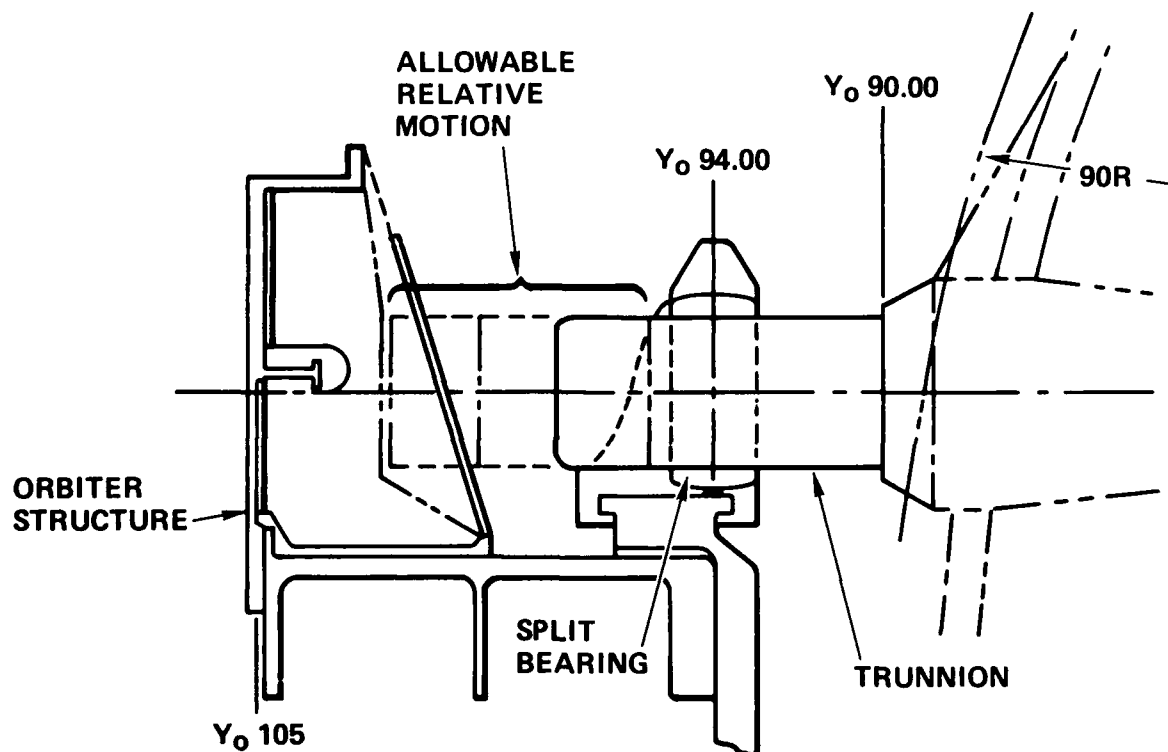
FIGURE 1. — *LONGERON ATTACHMENT MECHANISM AND ASSOCIATED PAYLOAD TRUNNION FOR NONDEPLOYABLE PAYLOAD*
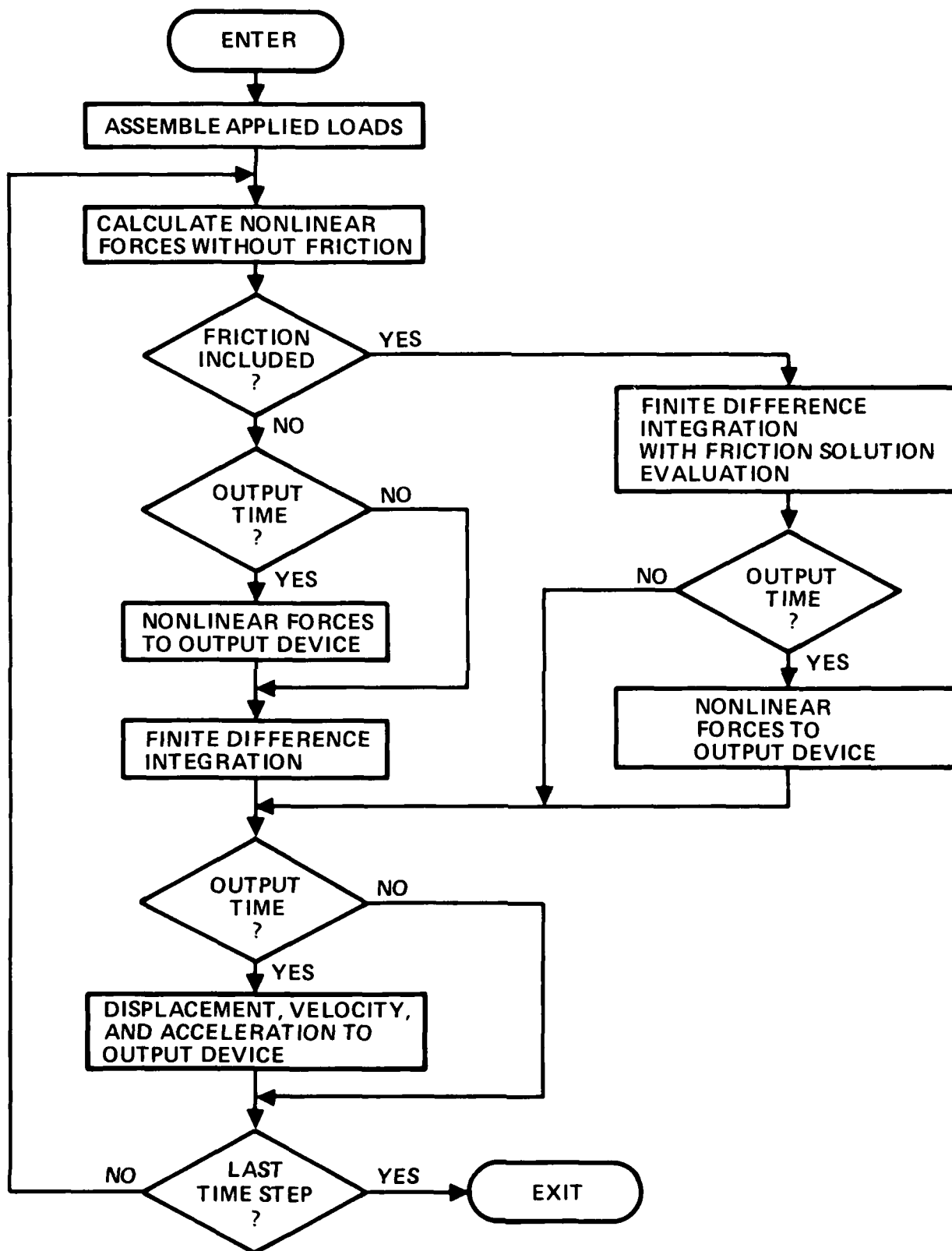
FIGURE 2. — NONLINEAR TRANSIENT RESPONSE WITH FRICTION
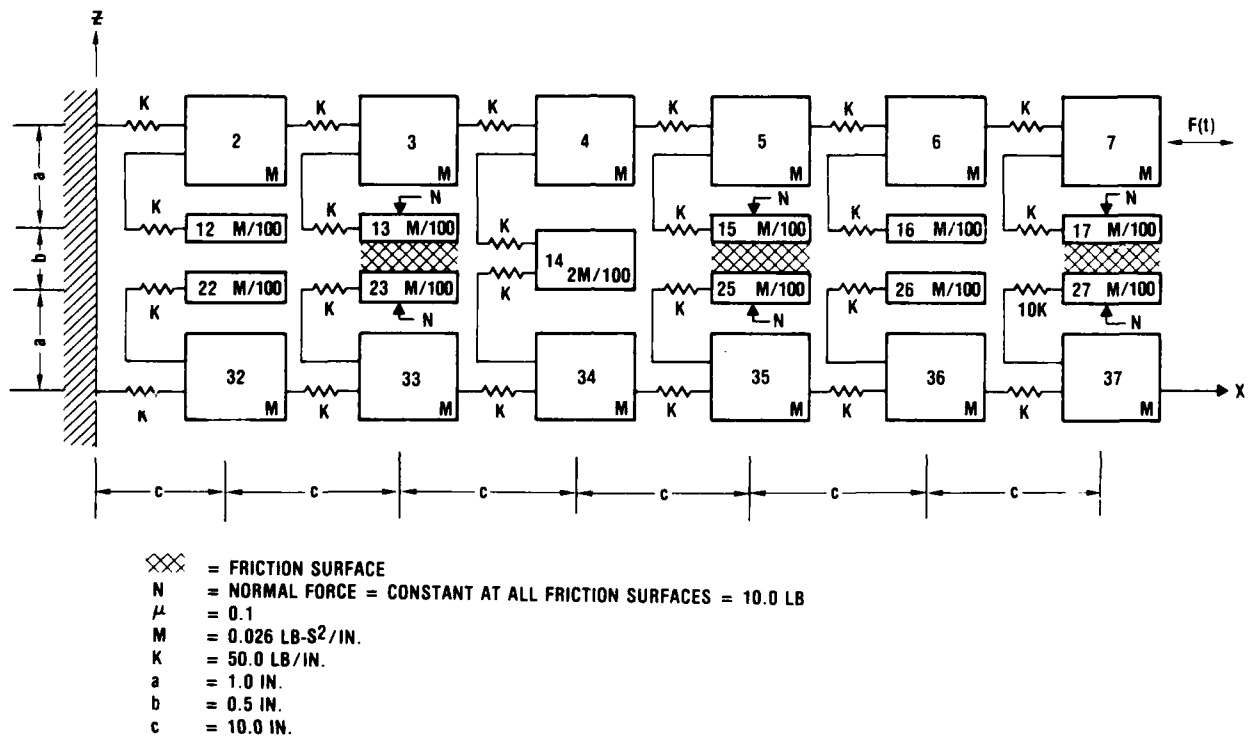
FIGURE 3. — FRICTION DEMONSTRATION PROBLEM
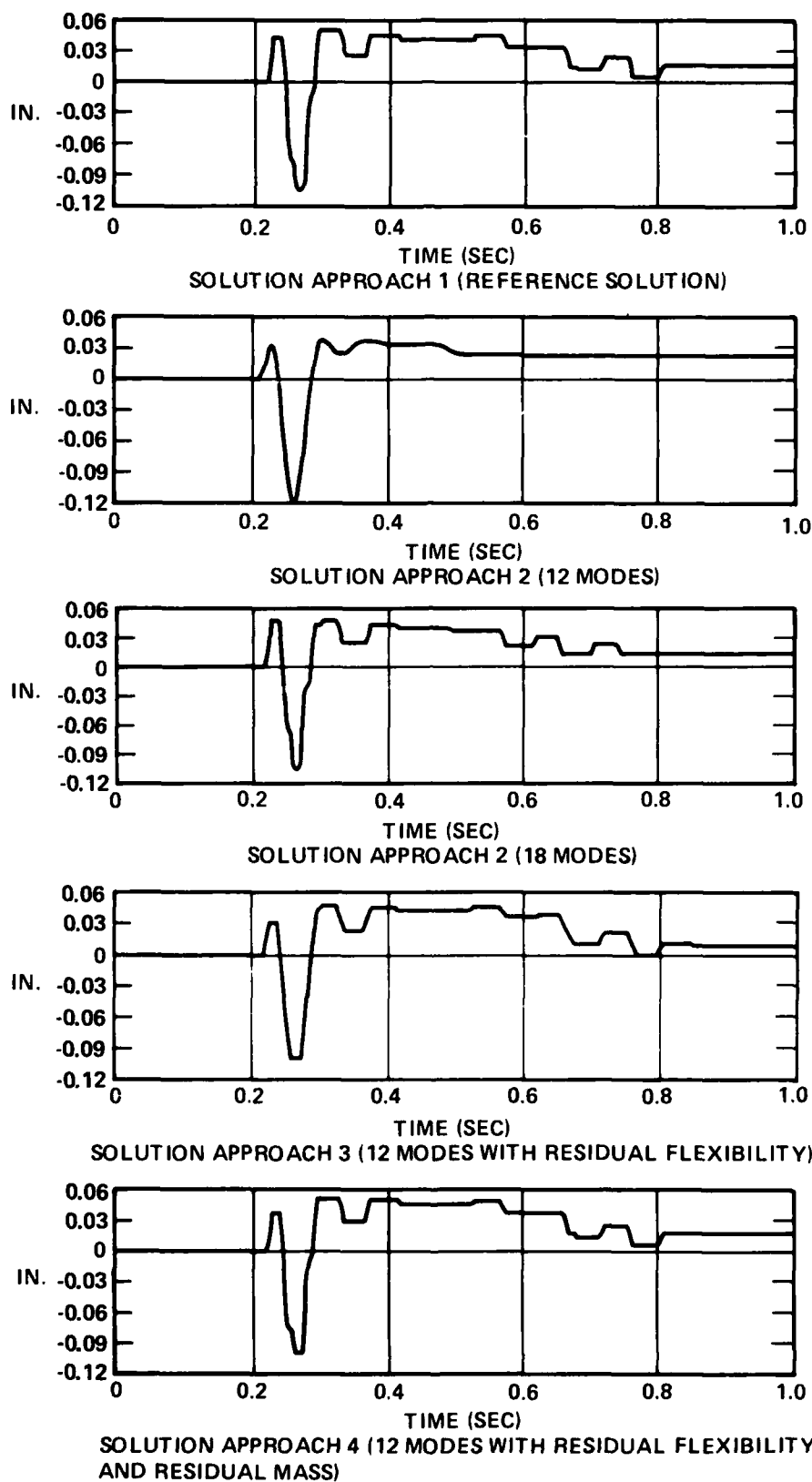
FIGURE 4. — RELATIVE DISPLACEMENT; 17/27

153
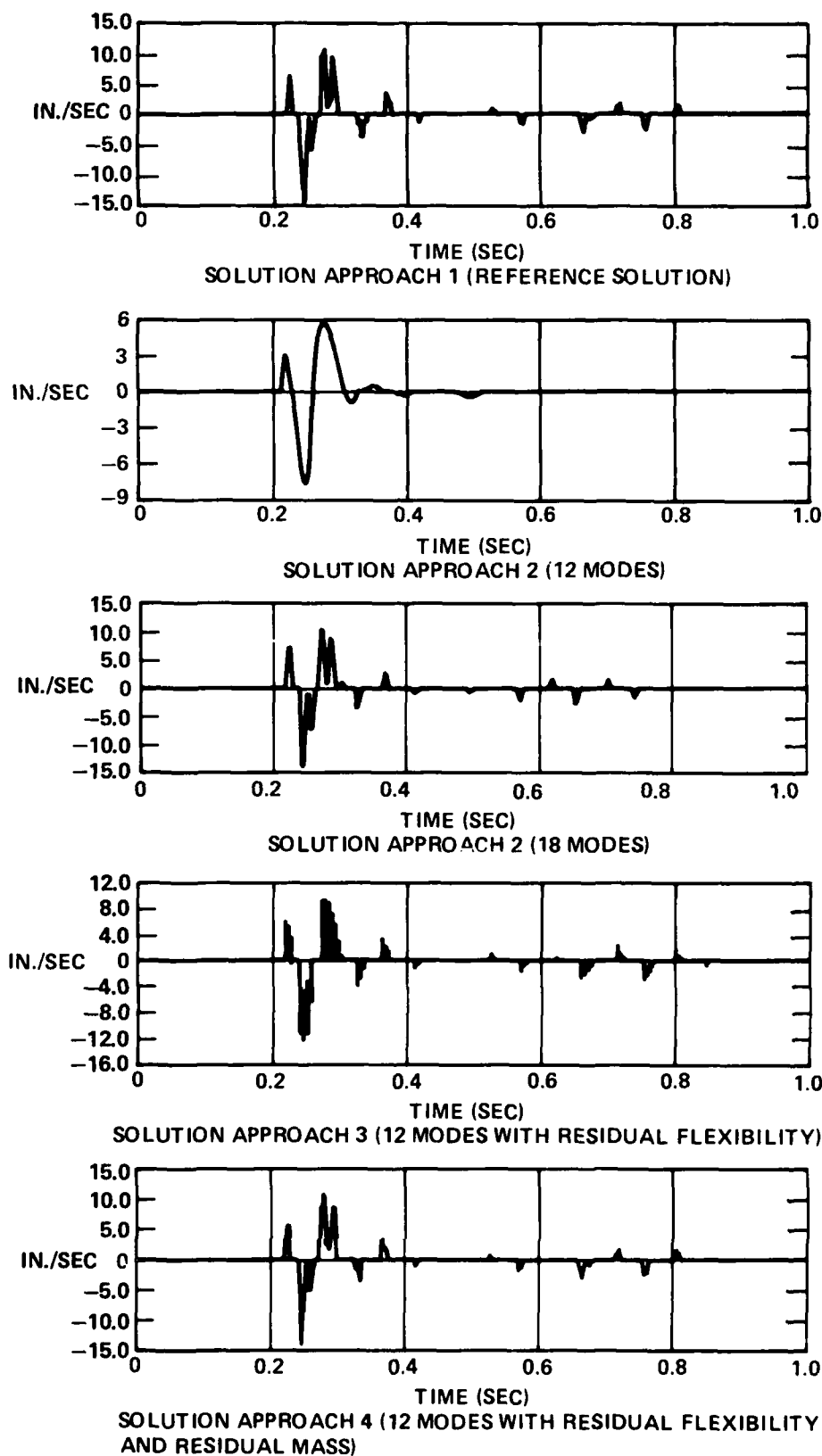
FIGURE 5. — RELATIVE VELOCITY; 17/27
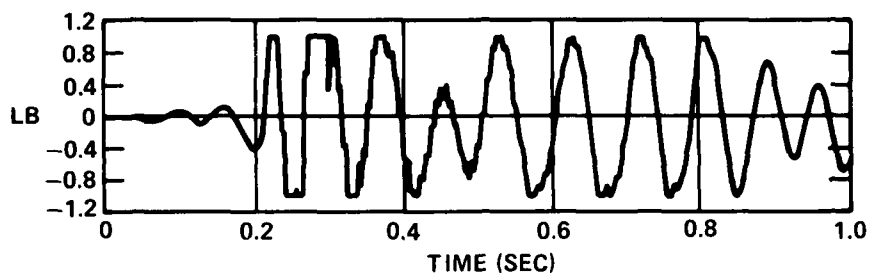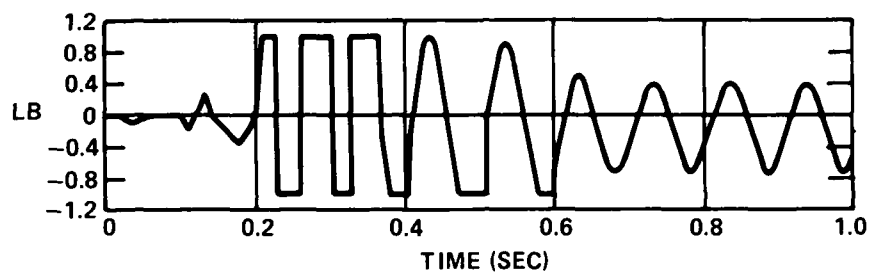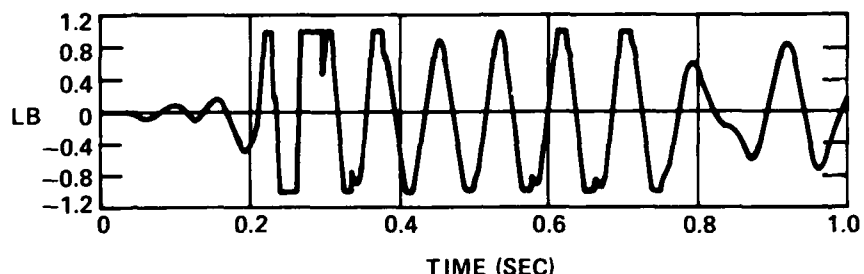
154
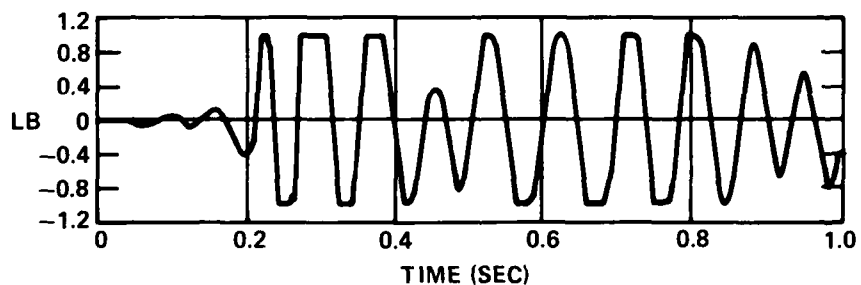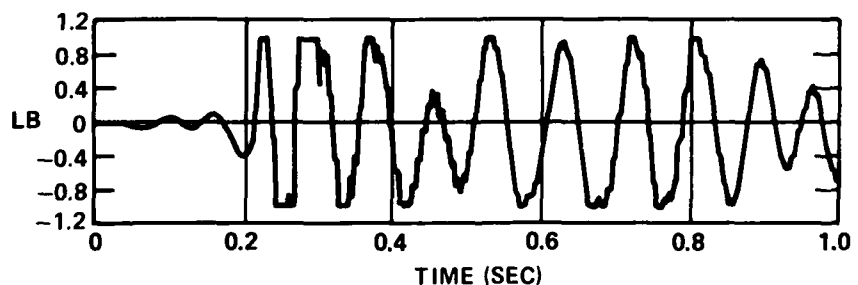
FIGURE 6. — FRICTION FORCE; 17/27

155
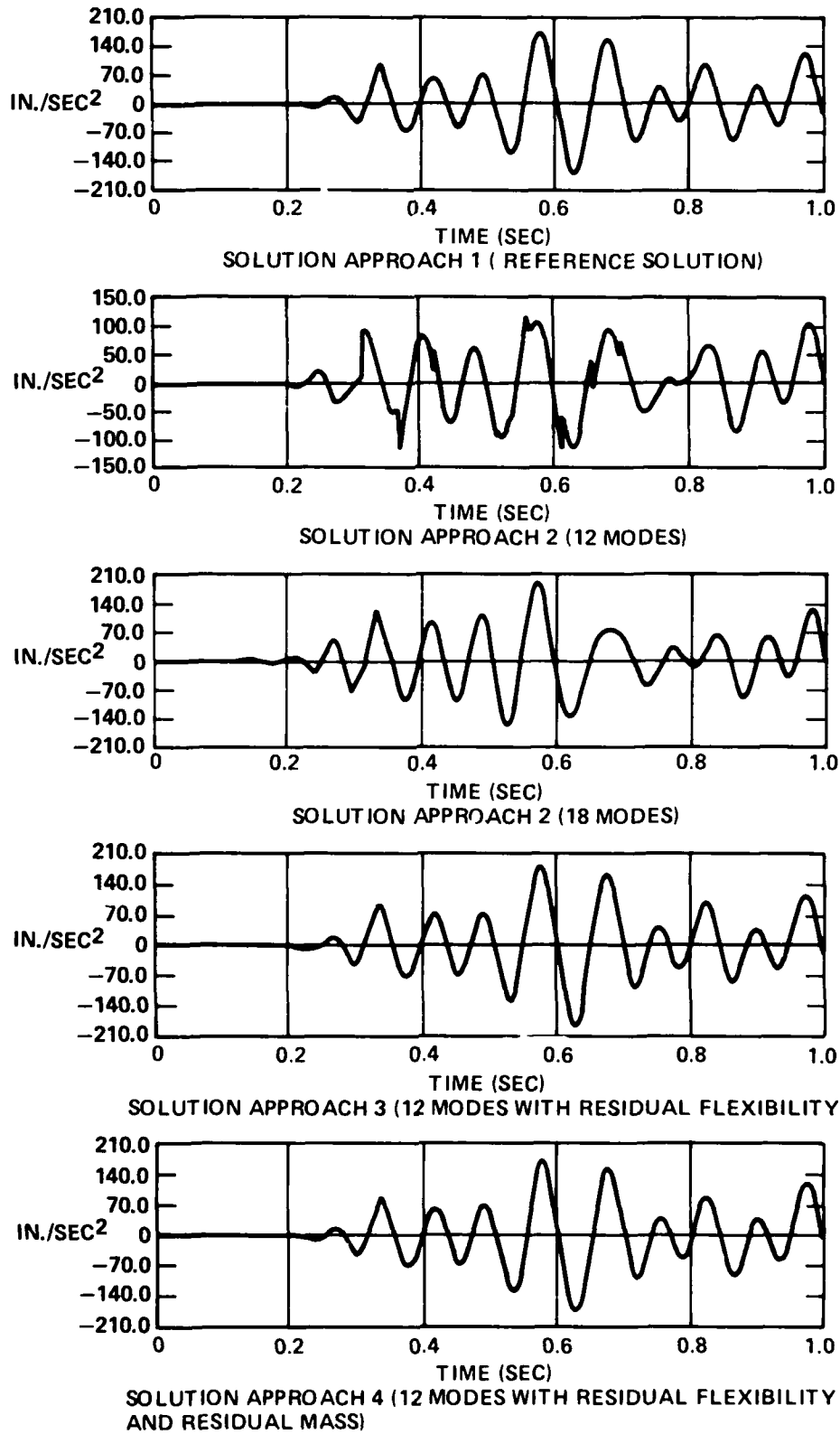
FIGURE 7. — ACCELERATION; 35
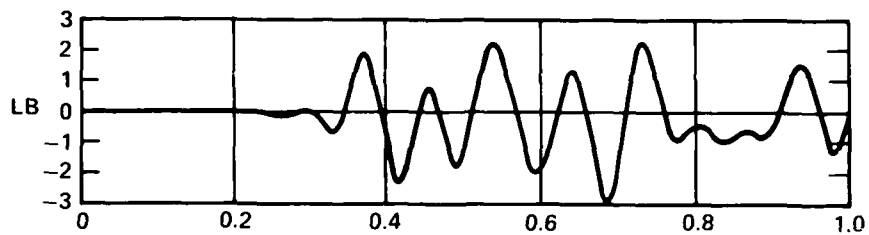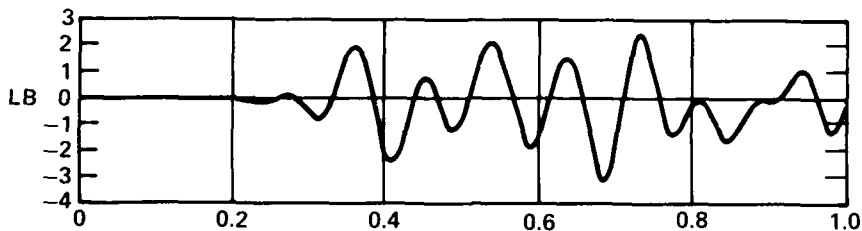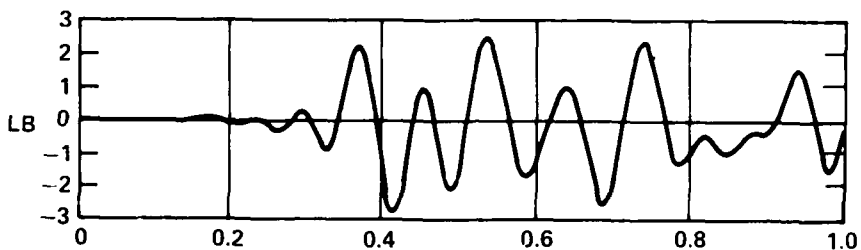
156
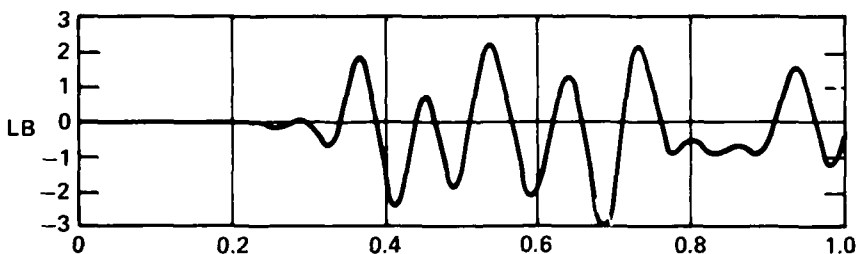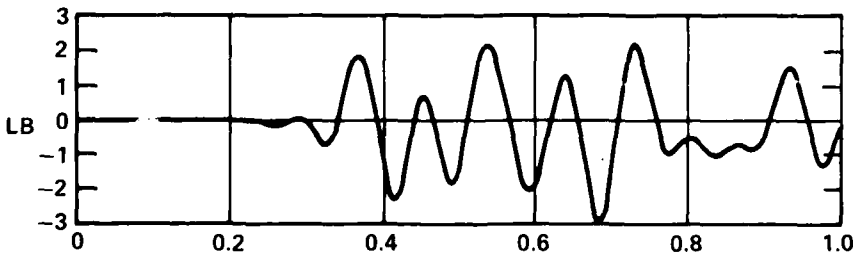
FIGURE 8. — ELEMENT FORCE; 34/35

157
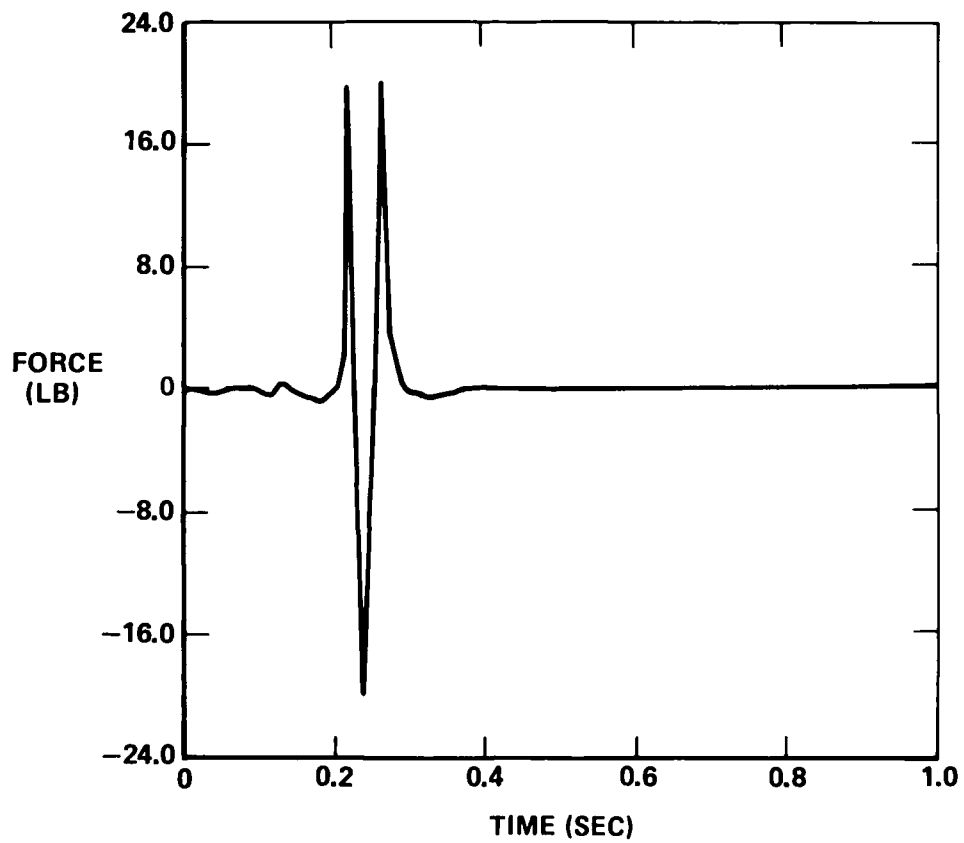
*FIGURE 9. — FRICTION DEMONSTRATION PROBLEM WITH
APPLIED FORCE; 7 DOF*
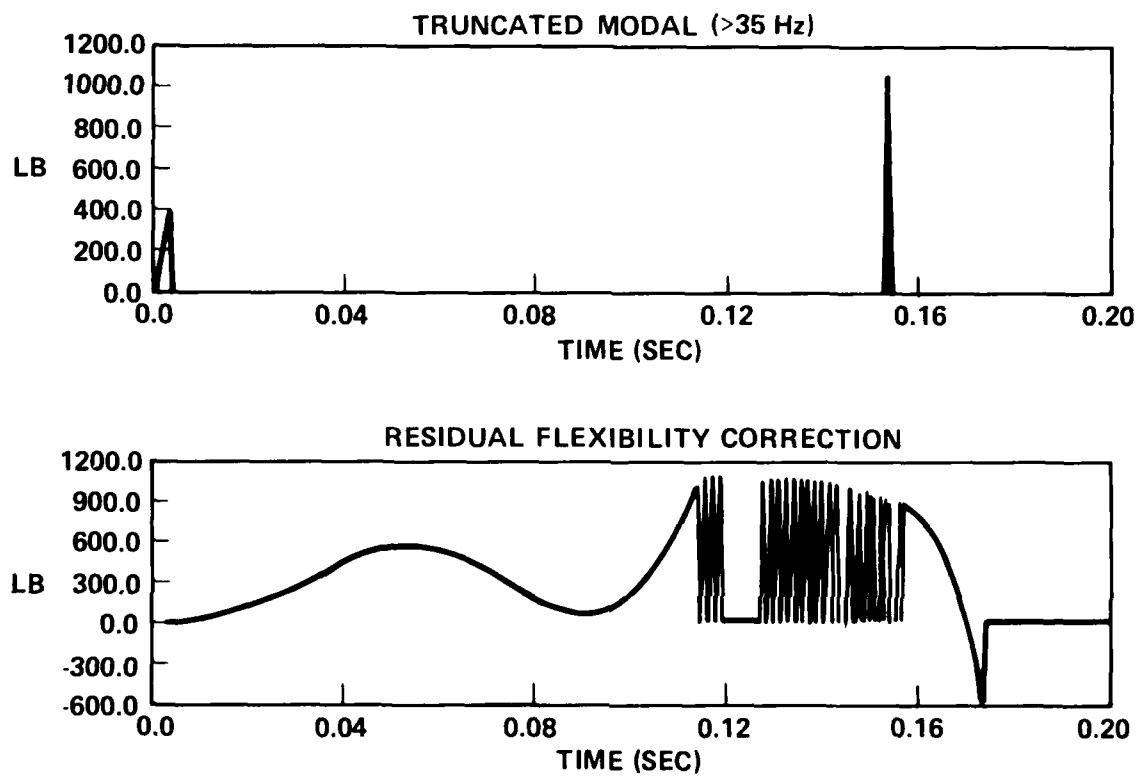
FIGURE 10. — STATIC FRICTION FORCES — RESIDUAL FLEXIBILITY VERSUS
TRUNCATED MODAL
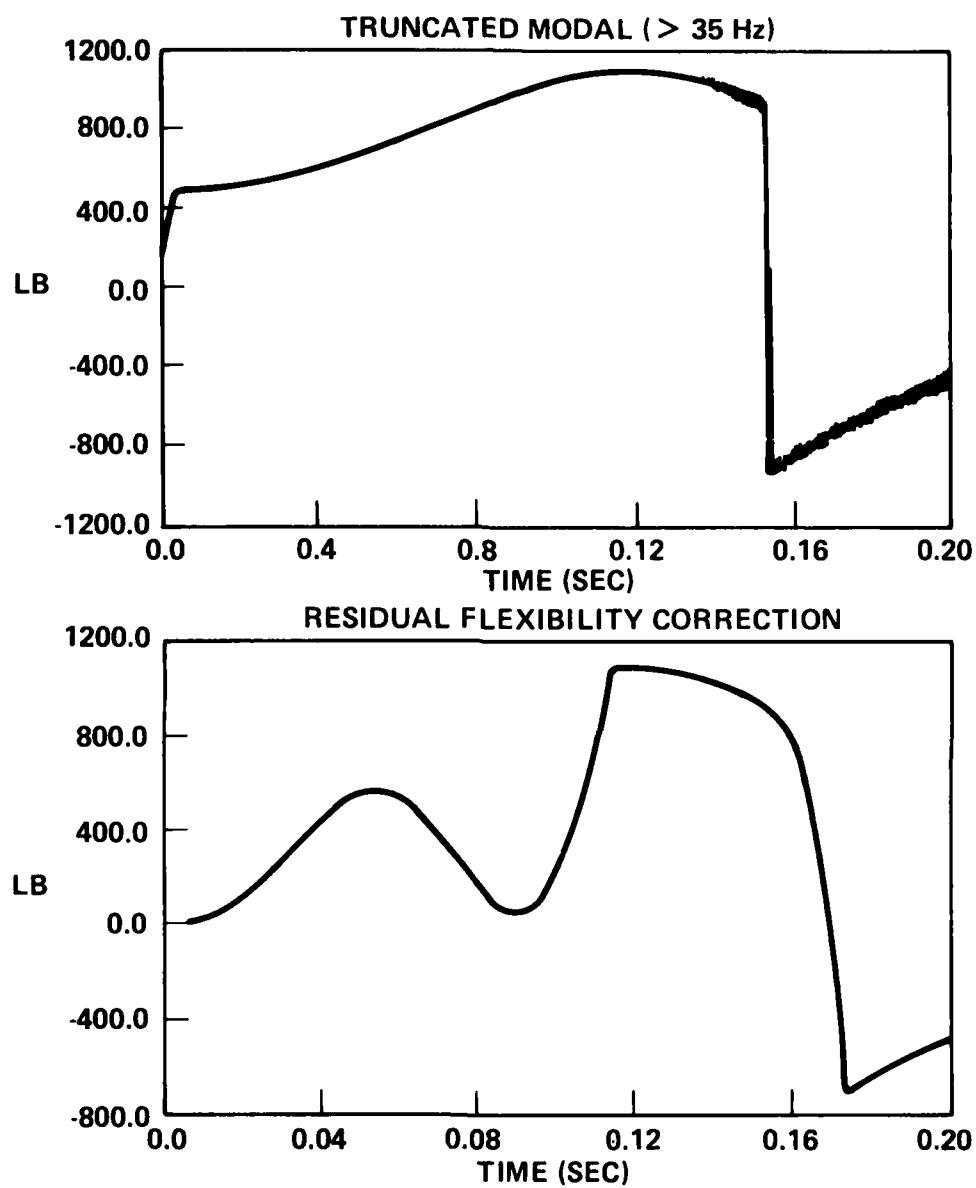
FIGURE 11. — TOTAL FRICTION FORCES — RESIDUAL FLEXIBILITY
VERSUS TRUNCATED MODAL

STRUCTURAL ANALYSIS OF THE SUPPORT SYSTEM FOR
A LARGE COMPRESSOR DRIVEN BY A SYNCHRONOUS ELECTRIC MOTOR

J. Ronald Winter

Tennessee Eastman Company

Summary

For economic reasons, the steam drive for a large compressor was replaced by a large synchronous electric motor. Due to the resulting large increase in mass and because the unit was mounted on a steel frame approximately 18 feet above ground level, it was deemed necessary to determine if a steady state or transient vibration problem existed. There was a definite possibility that a resonant or near resonant condition could be encountered. The ensuing analysis, which led to some structural changes as the analysis proceeded, did not reveal any major steady state vibration problems. However, the analysis did indicate that the system would go through several natural frequencies of the support structure during start-up and shutdown. This led to the development of special start-up and shutdown procedures to minimize the possibility of exciting any of the major structural modes. A coast-down could result in significant support structure and/or equipment damage, especially under certain circumstances. In any event, dynamic field tests verified the major analytical results. The unit has now been operating for over three years without any major vibration problems.

Introduction

Due to the increased cost of generating steam from natural gas or oil, it was necessary to replace the existing steam drive for a large compressor with a large synchronous electric motor. To achieve the desired compressor speed, a gear system (increaser) was also required. The particular synchronous motor was rated at 2,500 hp at 1200 rpm. The motor/exciter, couplings, gear box and compressor weighed about 43,600 lbs (21.8 tons). See Tables A-1 and A-2 in Appendix A for additional data.

The existing steam-driven compressor was mounted on a steel frame/platform about 18 ft above concrete footers. To prevent extended process downtime, it was necessary to have the electric motor and gear drive mounted at the same level. This posed some potential dynamic problems due to the large increase in mass. Start-up, shutdown, coast down and steady state operation had to be investigated to determine if any resonant or near resonant conditions existed between the various operating speeds and the support structure. We basically did not want any major structural natural frequency (mode) near the operating speeds of the system. We would have preferred to have the major structural natural frequencies above the highest operating speed of any component in the system; i.e., the motor, gear drive and compressor.

It is important to realize that this was a rush analysis. In fact the drawings were being revised and the replacement support structure was under fabrication during the final stages of the analysis.

Discussion of the Model

Two basic models were developed. Model A consisted of the support frame, motor, increaser, compressor and the piping. The second model, B, consisted of all of model A except the inlet and outlet piping. These basic models are shown in Figures 1 thru 5 and the Appendix.

Figure 1: Basic Model With Piping (Model A)
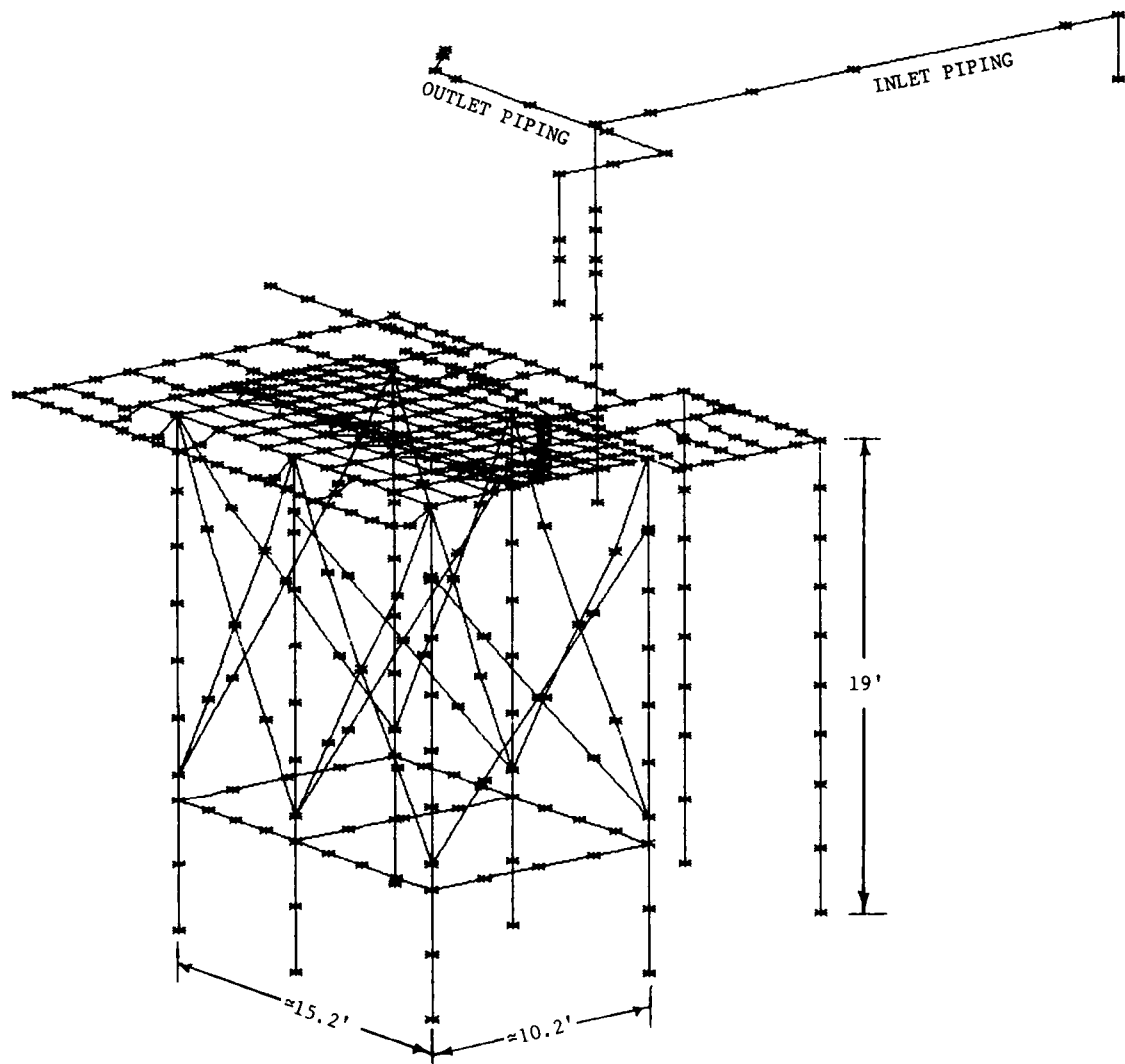
Figure 2:   Basic Model Without Piping (Models B and C)
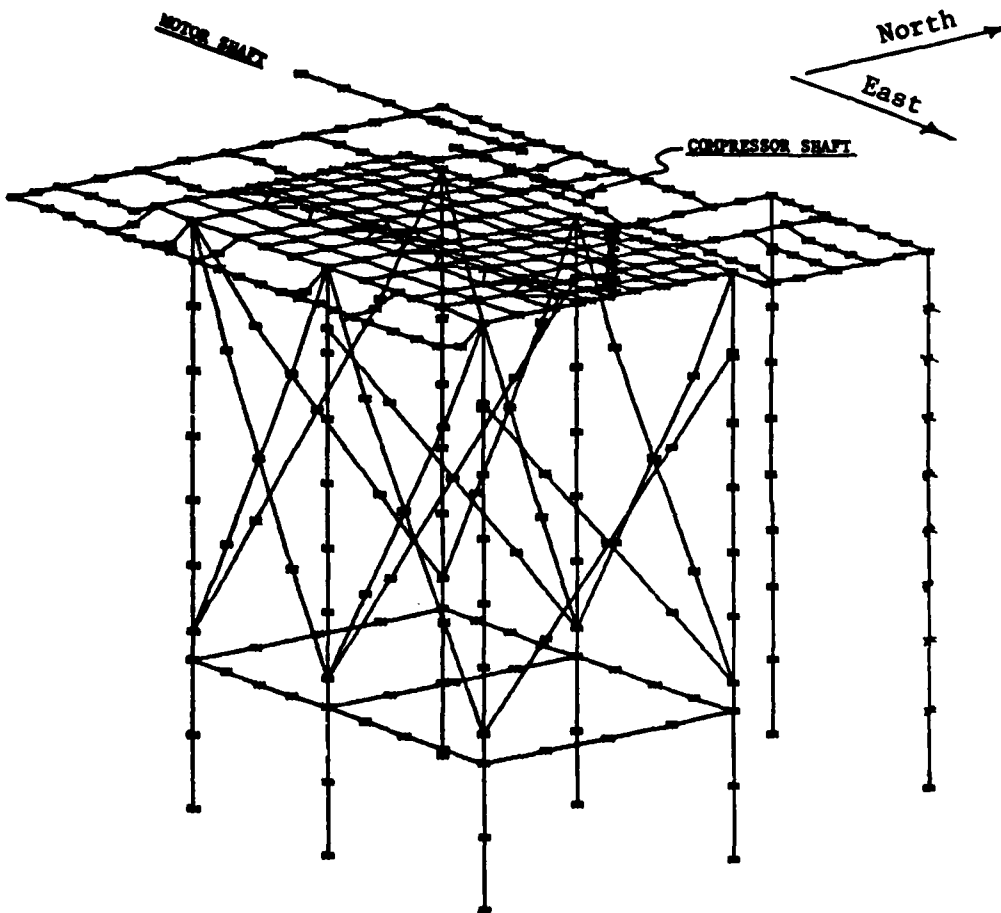
Figure 3:   Concrete Portion of the Support Structure
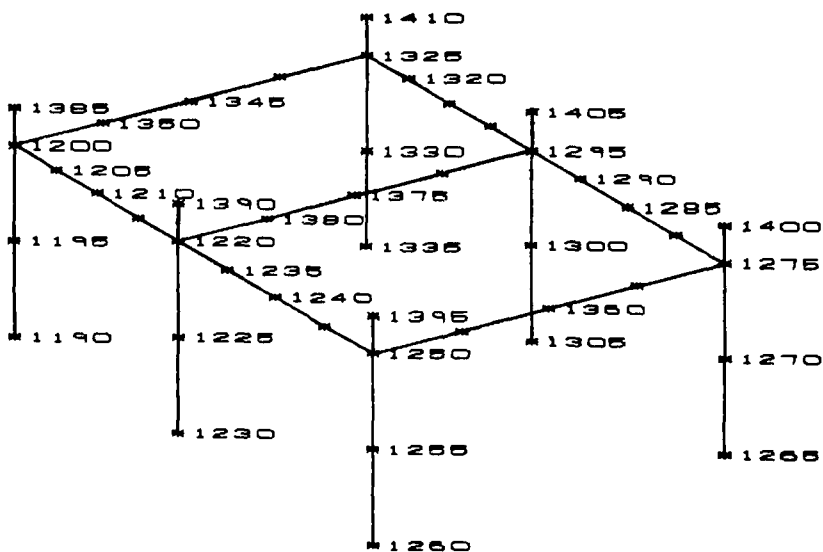
Figure 4: Special View of the Sole Plate, Piping and Shafting
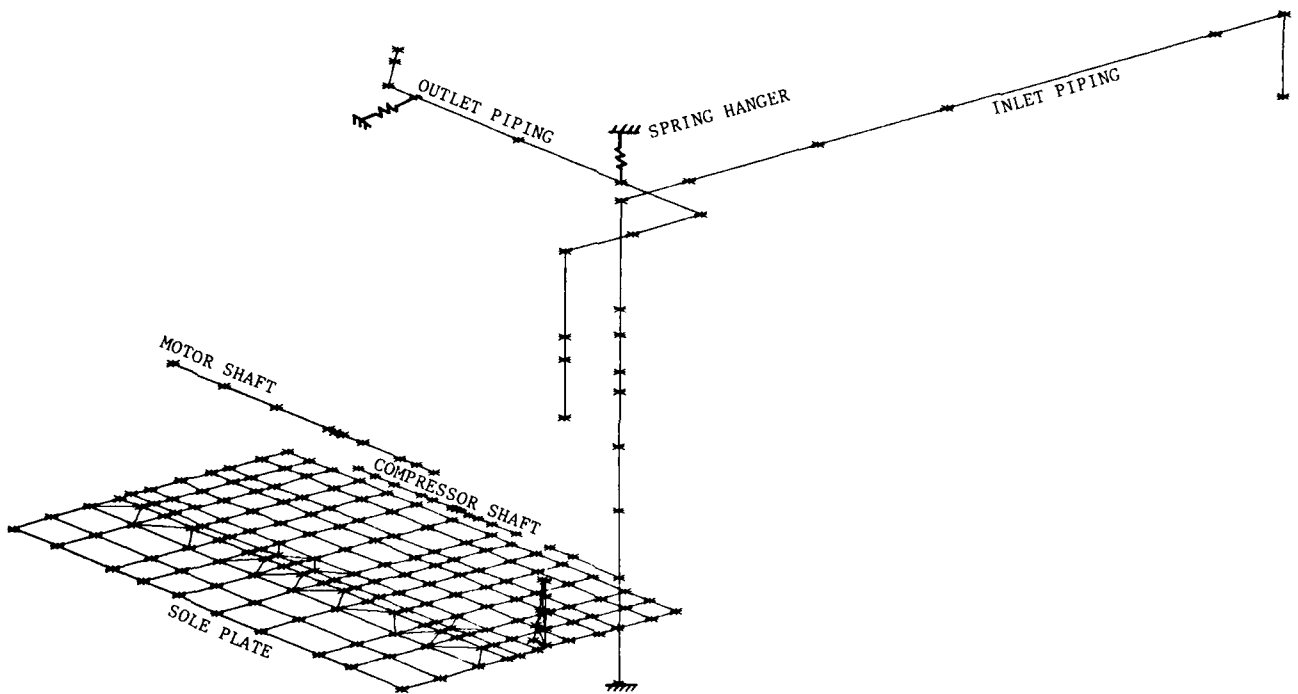
Figure 5: Basic Layout of the Motor, Increaser, Compressor and Shafting

164
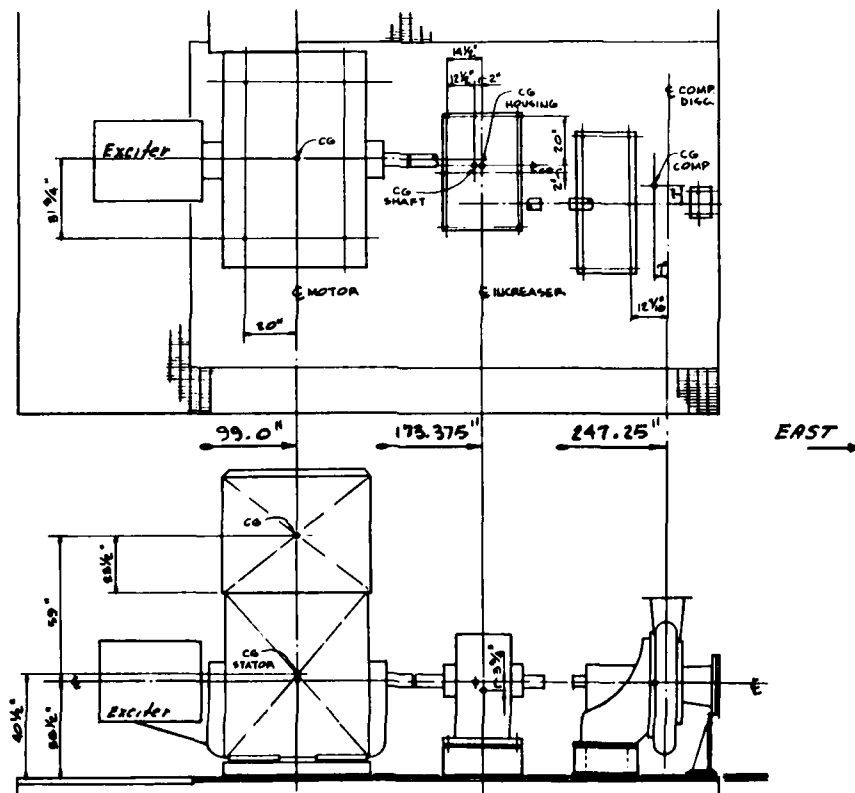
The number of grid points and primary elements used in each model are shown in Table I.

Table I: Grid Point and Element Summary Table

Model ID	CQUAD2/CTRIA2/CBAR	Grid Points
A	865	468
B	838	440

Both models also contained CONM2 elements, CELAS2 elements and a large number of MPC equations.

Static Analysis

The structure was statically analyzed both to determine its adequacy and to uncover any problems with the model. The static analysis consisted of nine subcases as listed below.

Table II: Static Loads Used in Analyses of Models A and B

Load SID	Load Description	Magnitude (lbf)	Applicable Subcase
1	Gravity		1
2	Gravity plus maximum motor torque		2
3	Maximum motor torque	10,500	3
4	Maximum torque on motor and increaser	10,500 18,800	4
5	Maximum torque on motor, increaser and compressor	2,950 10,500 18,800	5
6	Pull out torque on motor and increaser	1,570 2,810	6
7	Maximum motor torque reversed	-10,500	7
8	Maximum torque on motor and increaser reversed	-10,500 -18,800	8
9	Compressor freeze	2,950 18,800	9

Results from the Static Analysis

The static analysis did not reveal any major problems. The worst situation by far involved the deflection of the structure due to gravity (dead weight). Even in this situation the deflections were not excessive. Some typical deflection contour plots of the sole plate are shown in Figures 6 and 7.

Figure 6: Sole Plate Displacement Contour Plot for Gravity Loading (δ_z)

SYMBOL	Z-Displacement
1	-7.818777E-03
2	-7.167690E-03
3	-6.516602E-03
4	-5.865514E-03
5	-5.214427E-03
6	-4.563339E-03
7	-3.912251E-03
8	-3.261166E-03
9	-2.610080E-03
10	-1.959000E-03
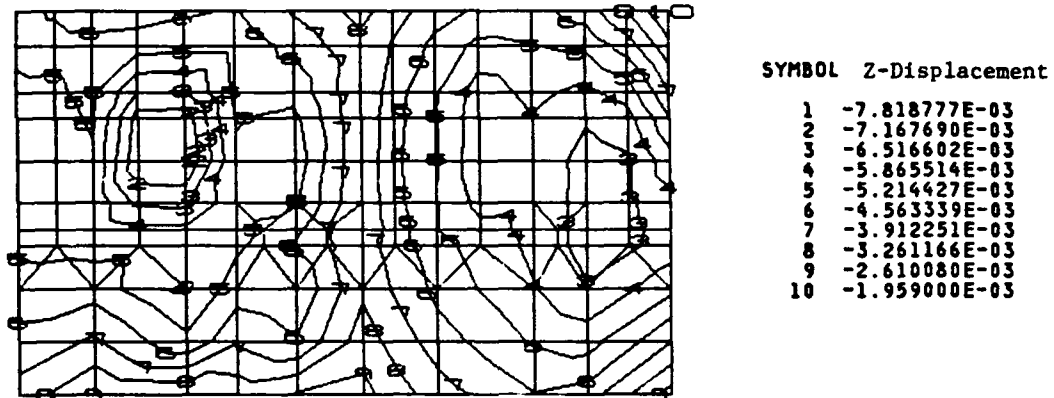
Figure 7: Sole Plate Displacement Contour Plots for Subcase 3 (Maximum Motor Torque)

SYMBOL	Z-Displacement
1	-3.331339E-04
2	-2.645201E-04
3	-1.959065E-04
4	-1.272928E-C4
5	-5.867924E-05
6	9.934360E-06
7	7.854796E-05
8	1.471616E-04
9	2.157752E-04
10	2.843887E-04
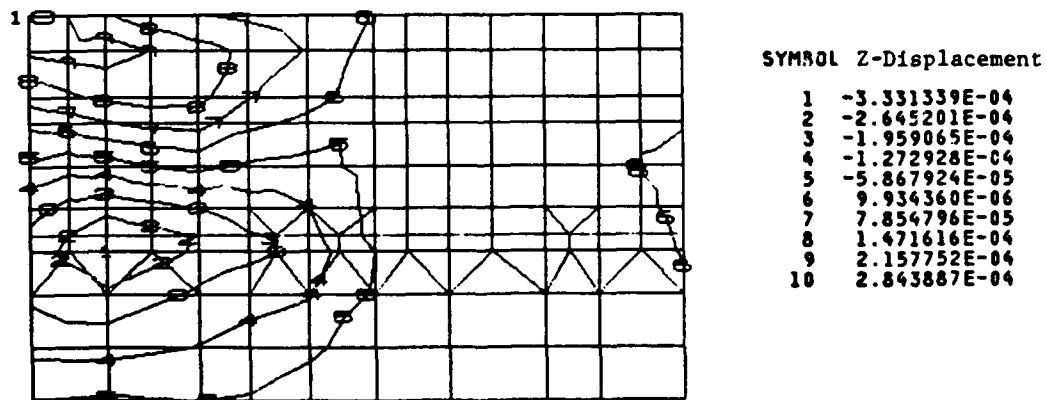
The only item of some concern was the non-symmetrical distribution of the reactions at the footers. Such a non-symmetric load distribution could result in some unusual dynamic responses and mode shapes.

An unexpected situation was encountered in the shafting under the action of only gravity loading. Bending stress levels of 3,434 psi and 2,740 psi were predicted in the compressor shaft. However, these were fictitious stresses since they were a result of differential deflections that would be removed by proper shimming of the motor, increaser, and compressor bases. Thus, for all intents and purposes, the stress levels in the shafts under gravity loading would be zero.
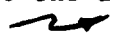
Dynamic Analysis

The dynamic analysis only involved determination of the structural natural frequencies via Rigid Format 3. Again two basic models were used; one with the piping (model A) and one without the piping (model B). A special run of model B was used to investigate the maximum possible effect of the fill dirt around the concrete footer and first level cross beams as shown in Figure 3. This special analysis was designated as Model C.

The applicable forcing frequencies are listed in Table III.

Table III: Major Forcing Frequencies

Source	RPM	CPS(Hz)	Comments
Electric Motor	0-1200	0-20	2500 HP, Synchronous Motor
Gear Output & Compressor	0-5027	0-83.78	4.189:1 gear ratio
Line Frequency	7200	120	
Comp. Speed times Number of vanes	0-50,270	0-837.8	No. of vanes is 10, also called the cut-off frequency

Both the Inverse Power and FEER eigenvalue extraction routines were used. In reviewing the various modes; the modal frequency, the percentage of the structure participating in the mode and the location of the maximum modal displacement were used to evaluate the damage potential involved in exciting a given mode. In the tabular listing of the modal results, the column labeled "Mode Evaluation (Damage Potential)" is indicative of the probability of encountering support structure and/or equipment damage if the particular mode is excited in a resonant or near resonant condition. In the case of the support structure and piping system, damage is indicative of encountering dynamic plus static stress levels exceeding 90% of the yield strength of the material. Equipment damage would be characterized by excessive shaft bending, fatigue cracks developing in the housing of a component, bearing damage and/or the development of rotational interferences due to component deformations. An example of the later situation would involve the compressor blades rubbing the housing. The preceding discussion applies to the data in Tables IV through VIII. In the associated figures, an arrow (⟿) indicates the area where damage would most likely occur if the particular mode was excited.

For model A, 80 eigenvalues were extracted. The modal results are summarized in Table IV. The lowest natural frequency at 7.24 cps involved a piping mode. As shown in Table IV, the next three modes were also piping modes. Surprisingly, there were no major structural modes below 20 cps. In fact, the next 21 modes (20 to 44 cps) only involved minor structural members such as the X-bracing, the grating supports and outlet piping. Thus none of the first 25 modes (7.24 thru 44 cps) were deemed to have a high potential for causing structural and/or equipment damage. Two of the piping modes were relatively close to the motor speed. However, the location of the piping relative to the motor would require excellent transmissibility and a rather large motor imbalance to excite either of these modes. If such excitation did occur, it would be relatively simple to supply damping or otherwise alter the pipe's natural frequency. A typical piping mode is shown in Figure 8.

Figure 8: First Inlet Piping Mode (7.24 cps)
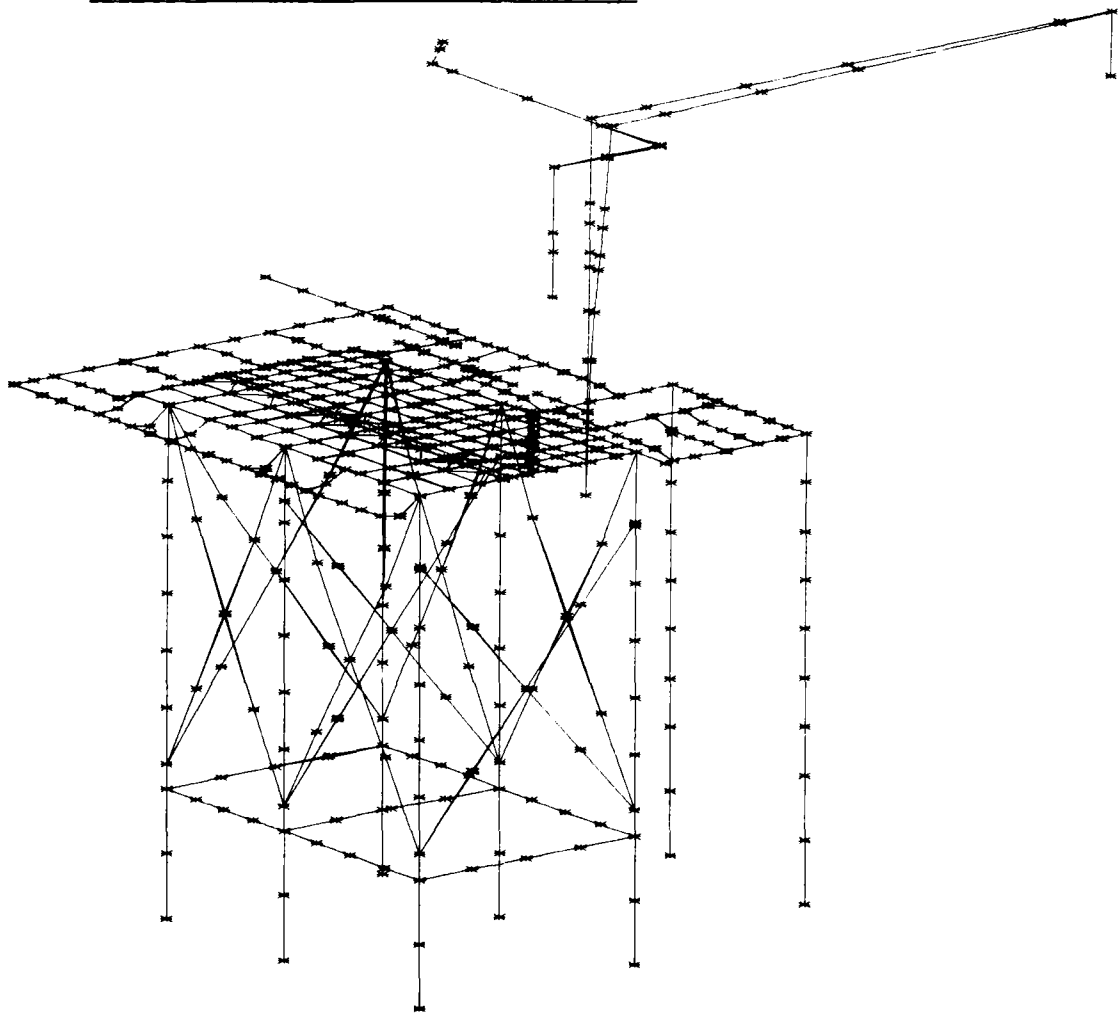
The first mode to be rated as having a high potential to cause structural and/or equipment damage was mode 26 (44.37 cps). A mode having an even greater potential for causing damage is shown in Figure 9 (mode 29). This 47.46 cps mode is so classified because of the large modal displacement being experienced by all of the major support columns. Some sole plate and shaft motion is also present.

168

Figure 9: Mode 29 (47.46 cps): Major Mode
Involving Most of the Structure
Plus the Piping and Includes Some
Shaft Bending (High Damage Potential)
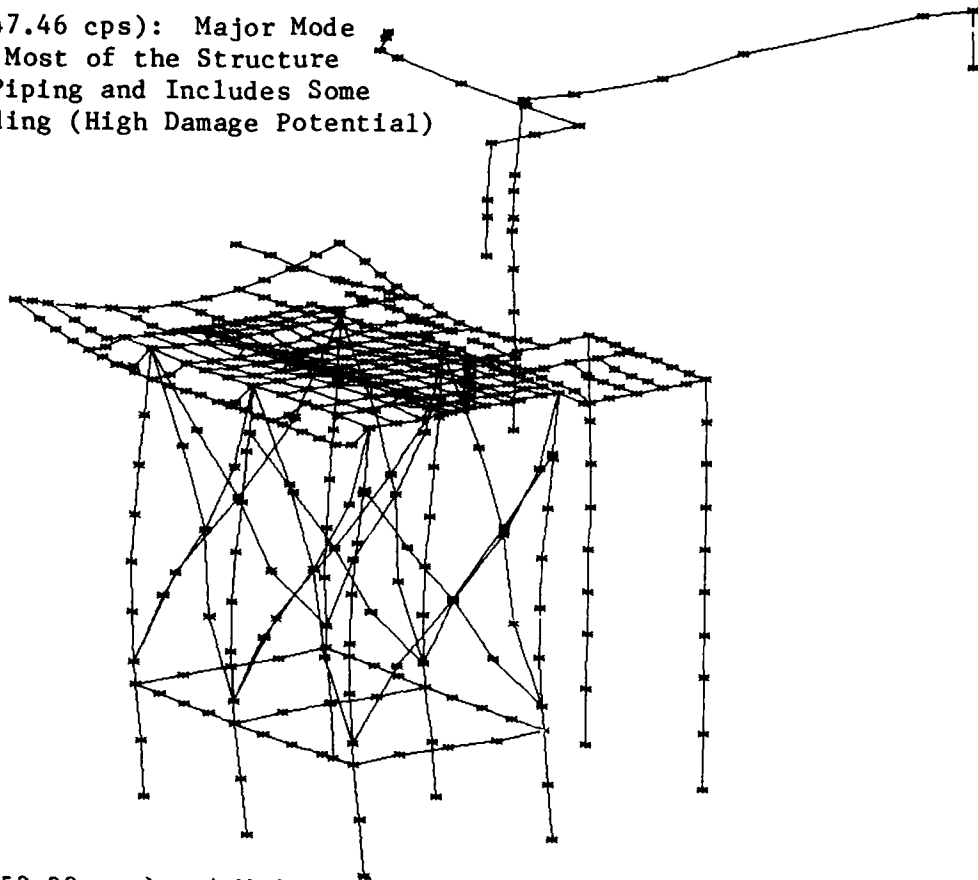
Figure 10: Mode 33 (53.39 cps): A Mode
Involving the Outlet Piping
With Considerable Deflection
of the Sole Plate at the
Compressor (Very High Damage
Potential)
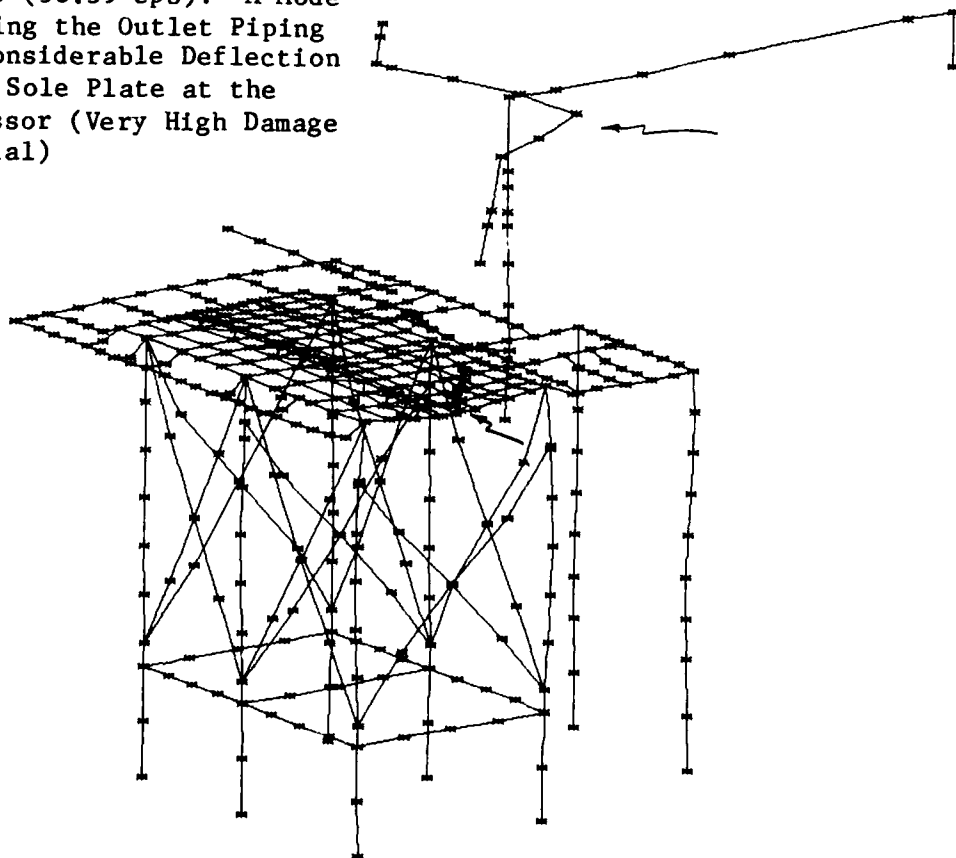
Mode 33 as shown in Figure 10 also has a high potential to cause damage. As shown in the deformed plot, large displacements are being encountered at the compressor which is also causing quite large outlet pipe deflections. This mode also results in severe deflection of the compressor shaft. Needless to say, if this mode was excited in a resonant or near resonant fashion, a compressor failure would be encountered. In addition the outlet pipe line would probably rupture.

As shown in Table IV, the next 23 modes (55.49 cps - 65.11 cps) were all deemed to have a minor damage potential. Mode number 57 with a frequency of 67.66 cps is classified as having a high damage potential. It is a major structural mode involving all major support columns, sole plate motion under the motor and some inlet pipe motion. The plot of this mode is shown in Figure 11. If this mode was excited, major support structure failures would be encountered.

Figure 11: Mode 57 (67.66 cps): A Major Structural Mode Involving All Major Columns, Sole Plate Motion Under the Motor and Some Inlet Pipe Motion (High Damage Potential)
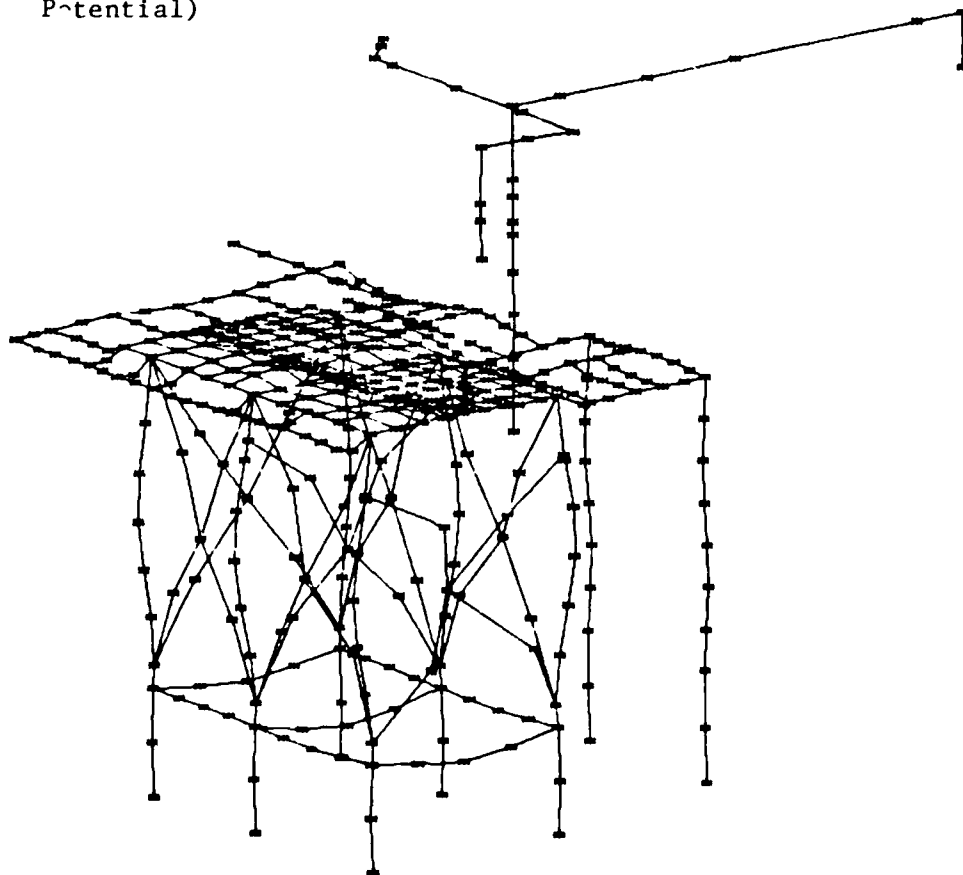

170
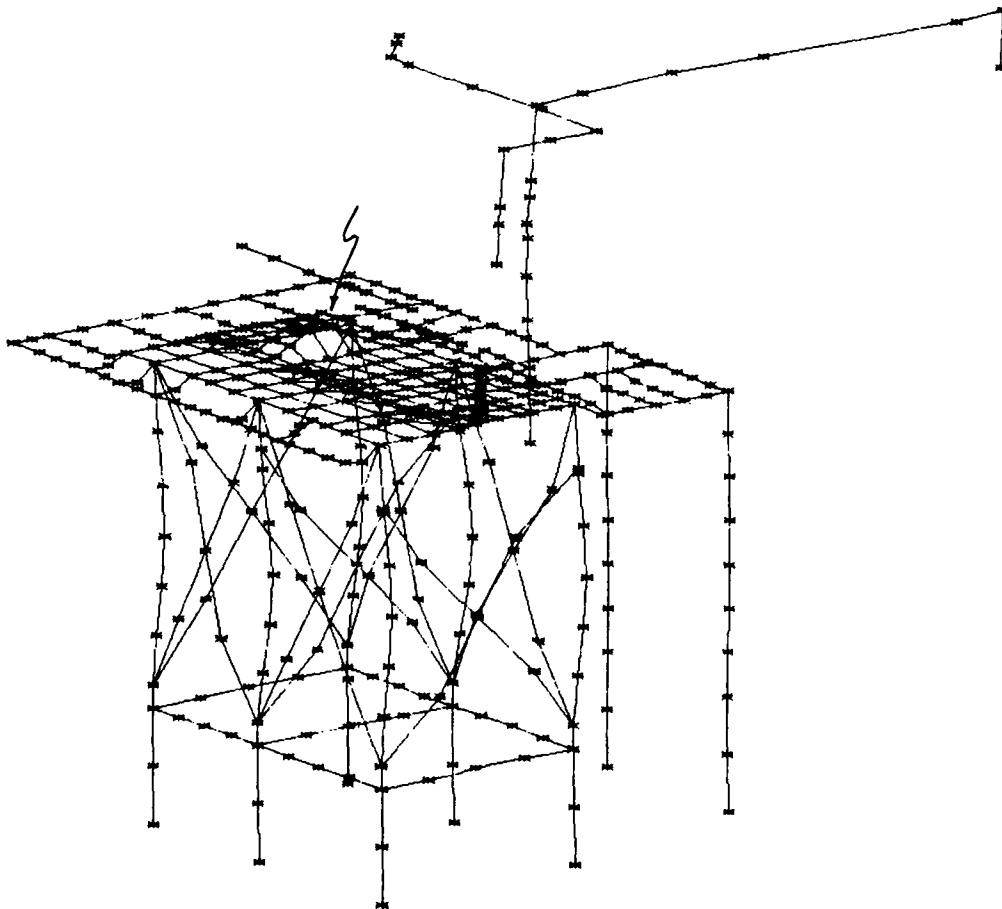
Table IV: Modal Results from Model A Which Includes the Piping (0-90 cps)

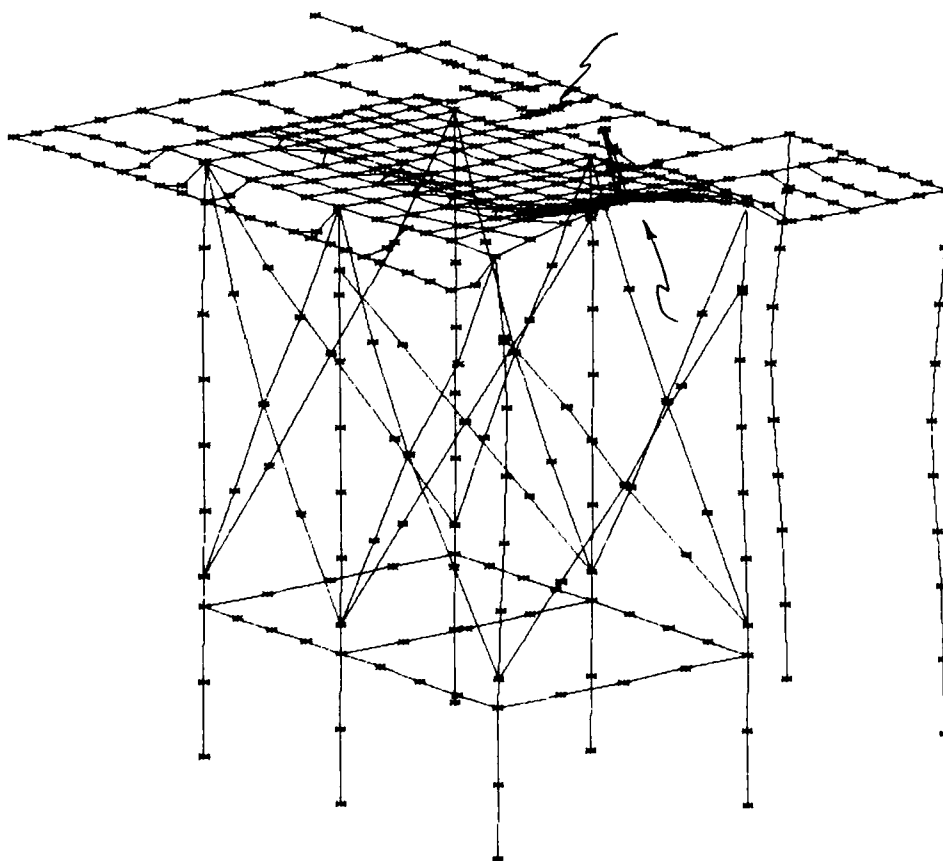| Mode Number	Natural Frequency (cps, Hz)	Description of Mode	Mode Evaluation* (Damage Potential)	Applicable Figure	Nearest Steady State Forcing Frequency
1	7.24	1st major inlet piping mode	Moderate	Figure 8	20.00
2	18.07	1st outlet piping mode	Moderate	-	20.00
3	18.44	2nd inlet piping mode	Moderate	-	20.00
4	19.73		Minor	-	20.00
		Minor support member modes			
25	43.99		Minor	-	20.00
26	44.37	A mode involving most of the support structure and piping	High	-	20.00
27	45.99	South west grating mode	Minor	-	20.00
28	46.45	West grating mode	Minor	-	20.00
29	47.46	Major mode involving most of structure plus piping. Some motor shaft bending.	High	Figure 9	83.78
30	47.86		Minor	-	83.78
		Minor support member modes			
32	51.82		Minor	-	83.78
33	53.39	Mode involving outlet piping with considerable deflection of sole plate at the compressor	Very High	Figure 10	83.78
34	55.49		Minor	-	83.78
		Minor support member modes			
56	65.11		Minor	-	83.78
57	67.66	A structural mode involving all major columns, sole plate motion under the motor and some inlet pipe motion	High	Figure 11	83.78
58	68.00	A mode involving sole plate motion directly under the motor	Moderate	-	83.78
59	68.26		Minor	-	83.78
		Minor support member modes			
76	81.47		Minor	-	83.78
77	82.83	A rather mild mode involving motion of some Columns as well as sole plate motion between the increaser and compressor. Normalized at point on north grating.	Minor +	-	83.78
78	84.07	A rather mild mode with some sole plate motion	Minor +	-	83.78
79	84.99	Minor support member mode	Minor	-	83.78
80	86.83	Minor support member mode	Minor	-	83.78

*Mode Evaluation (Damage Potential) is indicative of the probability of encountering support structure and/or equipment damage if the particular mode is excited in a resonant or near-resonant condition.

As indicated in Table IV, modes 77 and 78 are rather mild but they do involve some major portions of the structure. The peak motions in these cases involve the north grating. If these modes were excited for a long period of time, some problems could be encountered. Since their frequencies, 82.83 and 84.07 cps, are rather close to the operating speed of 83.78 cps such long time excitations are possible. This situation should be monitored during start-ups and shutdowns. If these modes had involved the motions of major structural members as in the case of modes 33 or 57, then a major structural change would have been required.

The next series of modes involve natural frequencies in the range of the line frequency (120 cps). They are also shown in Table V. All the modes below 120 cps were classified as minor. There is a mode just above 120 cps which has a high damage potential. This is mode 2A-12 with a frequency of 120.76 cps. It is shown in Figure 12. This major structural mode involves motion of the lateral concrete beams as well as the rest of the structure. Needless to say, this frequency is too close to the 120 cps forcing frequency. Fortunately, the fill dirt around the concrete beams and the concrete portions of the columns should serve to shift the frequency of this mode upward, out of range, since the lateral concrete beams would not be allowed to deflect as shown in Figure 12. This essentially eliminated this mode.

Modes 2A-14 (124.21 cps) and 2A-20 (128.72 cps) are rated as having moderate and high damage potentials. However, they are sufficiently above the 120 cps range to not be of any great concern.

Figure 12:   Mode 2A-12 (120.76 cps): A Major Structural Mode Involving Columns, Grating and *Portions of the Sole* Plate (High Damage P⌐tential)

Table V: Modal Results from Model A Which Includes the Piping (110 to 130 cps)

Mode Number	Natural Frequency (cps, Hz)	Description of Mode	Mode Evaluation* (Damage Potential)	Applicable Figure	Nearest Steady State Forcing Frequency
2A-1	110.09		Minor		120
---	---	Minor support member modes	---		120
2A-11	120.39		Minor		120
2A-12	120.76	A major structrual mode involving columns, grating and portions of sole plate	High	Figure 12	120
2A-13	122.65	A piping mode	Minor +		120
2A-14	124.21	A structural mode involving most columns and grating	Moderate +		120
2A-15	124.91		Minor		120
---	---	Minor support member modes	---		120
2A-19	127.58		Minor		120
2A-20	128.72	A structural mode involving all major columns and horizontal concrete beams and sole plate motion between compressor and increaser.	High		120

*Mode Evaluation (Damage Potential) is indicative of the probability of encountering support structure and/or equipment damage if the particular mode is excited in a resonant or near-resonant condition.

173

Discussion of Model B Analysis

The B model is identical to the A model except that the piping system was removed. Likewise, the boundary conditions at the bottom of the columns were the same as those of model A. The final results are presented in Table VI.

The modal results are quite similar to those of model A except that no piping modes are present. The first 15 modes are classified as minor. Mode 16 has a very high damage potential. It involves excessive motion of the compressor and the east portion of the sole plate as well as some column motion. As shown in Figure 13, considerable shaft deflection is also present for this 36.89 cps mode. Needless to say, excitation of this mode would lead to a rather dramatic failure.

Figure 13: Mode B-16 (36.89 csp): Major Compressor/East Sole Plate Mode With Major Shaft Deflections and Minor Movement of Some X-braces and Columns (Very High Damage Potential)

Two additional modes with high damage potentials occur at 47.65 and 49.94 cps. They are modes 22 and 23 and are shown in Figures 14 and 15. Mode 22 has the highest damage potential of the two since it involves motion of all major support columns.

Table VI: Modal Results from Model B (0-90 cps)

Mode Number	Natural Frequency (cps, Hz)	Description of Mode	Mode Evaluation* (Damage Potential)	Applicable Figure	Nearest Steady State Forcing Frequency
1	19.62		Minor		20
15	33.88	Minor support member modes	Minor		20
16	36.89	Major compressor/east sole plate mode with major shaft deflections	Very High	Figure 13	20
17	42.37	Minor support member modes	Minor		20
21	46.29		Minor		20
22	47.65	First major structural mode involving motion of complete structure. Sole plate motion at motor with considerable shaft motion from motor to gearbox.	High	Figure 14	20
23	49.94	West and north grating mode with considerable sole plate motion near the motor.	High	Figure 15	83.78
24	52.02	Considerable motor shaft deflection.	Minor		83.78
45	68.52	Minor support member modes	Minor		83.78
46	71.14	2nd major structural mode involving all major columns	High	Figure 16	83.78
47	72.77	Mode of X-brace	Minor		83.78
48	75.01	Major structural mode involving motion of concrete portion of the columns and the X-braces	High	Figure 17	83.78
49	76.12	Mode of electrical panel support columns	Minor +		83.78
50	80.21	X-brace mode	Minor		83.78
51	81.34	A mode involving some columns and X-braces and shaft deflection	Moderate	Figure 18	83.78
52	82.49		Minor		83.78
63	90.05	Minor support member modes	Minor		83.78

*Mode Evaluation (Damage Potential) is indicative of the probability of encountering support structure and/or equipment damage if the particular mode is excited in a resonant or near-resonant condition.

175

Figure 14: Mode B-22
(47.65 cps):
First Major
Structural Mode
Involving Motion
of the Complete
Structure. Sole
Plate Motion at
Motor with Con-
siderable Shaft
Motion from Motor
to Gear Box (High
Damage Potential)
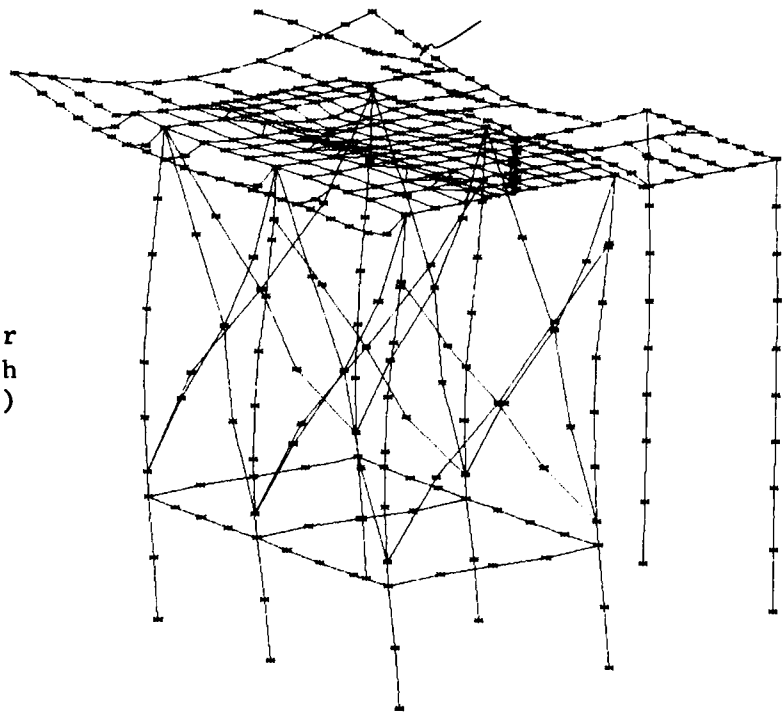
Figure 15: Mode B-23 (49.94 cps): West/North Grating Mode
with Considerable Sole Plate Motion Near the
Motor and Some Motor Shaft Delfection (Moderate
to High Damage Potential)

Shaft Deflection Detail

176
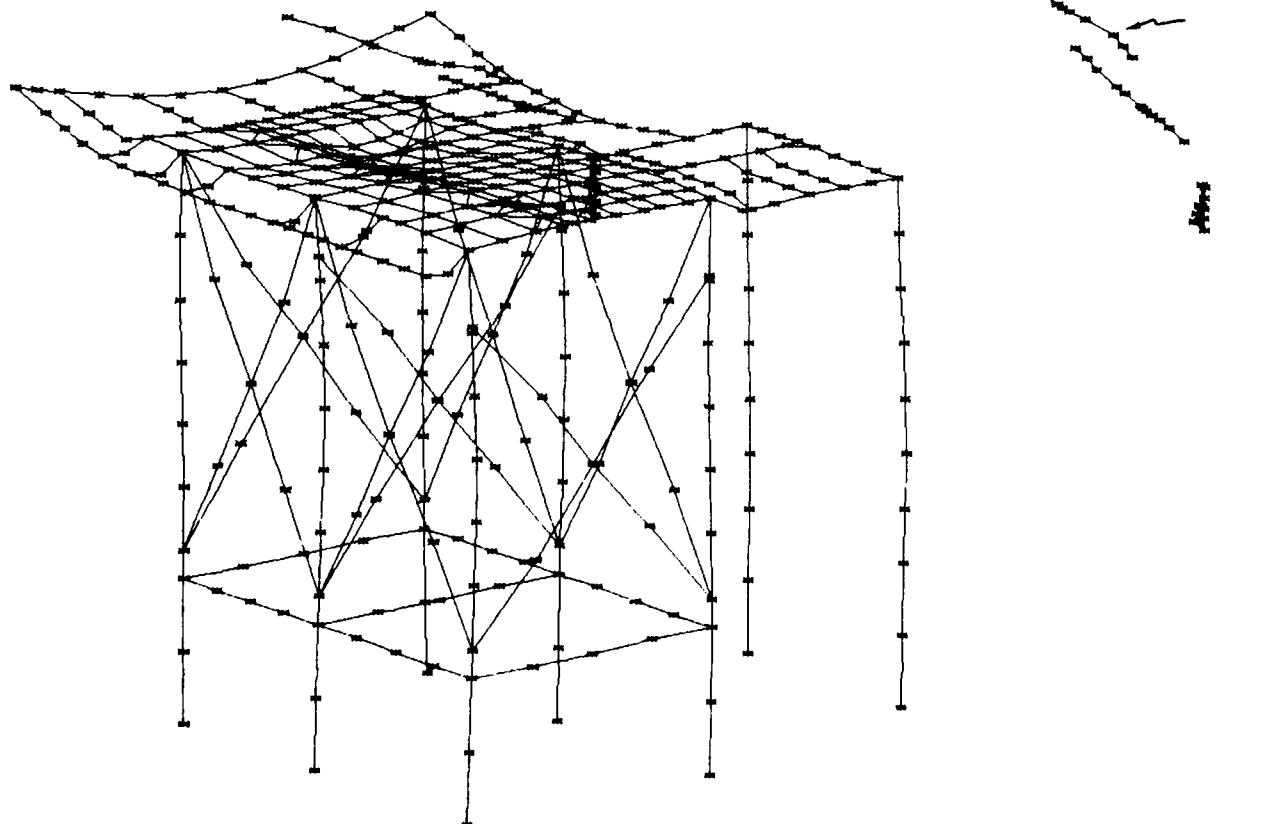
The second major support structure mode is number 46. This 71.14 cps mode involves large displacements of all major support columns. It is also a mode with a high damage potential. See Figure 16.

Figure 16: Mode B-46 (71.14 cps): Second Major Structural Mode Involving All Major Columns (High Damage Potential)
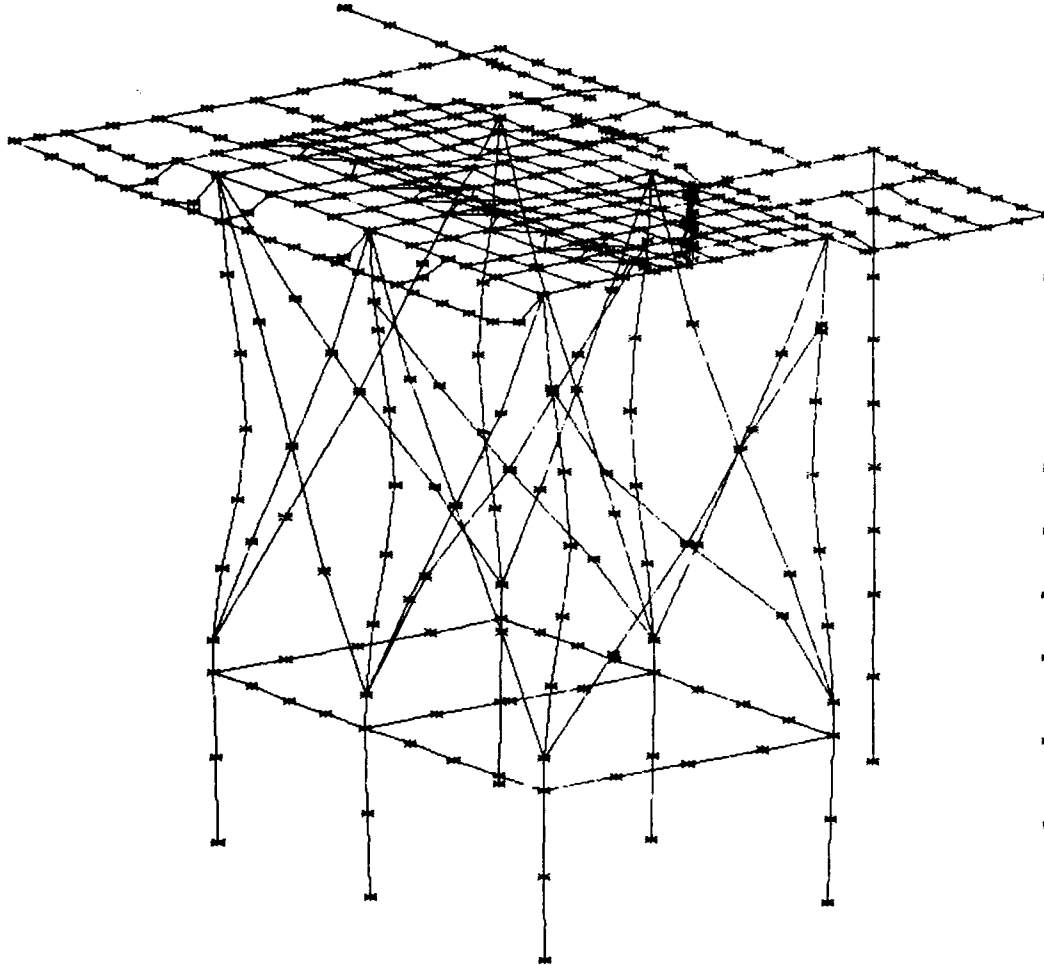
Mode 48 also has a high damage potential. It is the first mode to involve motion of the concrete portion of the structure. The X-brace motion of this 75.01 cps mode as shown in Figure 17 is quite severe. Mode 51 could also have a relatively high damage potential. Shaft deflection associated with mode 51 is shown in Figure 18.

Figure 17: Mode B-48 (75.01): Second Major Structural Mode Involving Motion of the Concrete Portion of All Columns (Quite High Damage Potential)
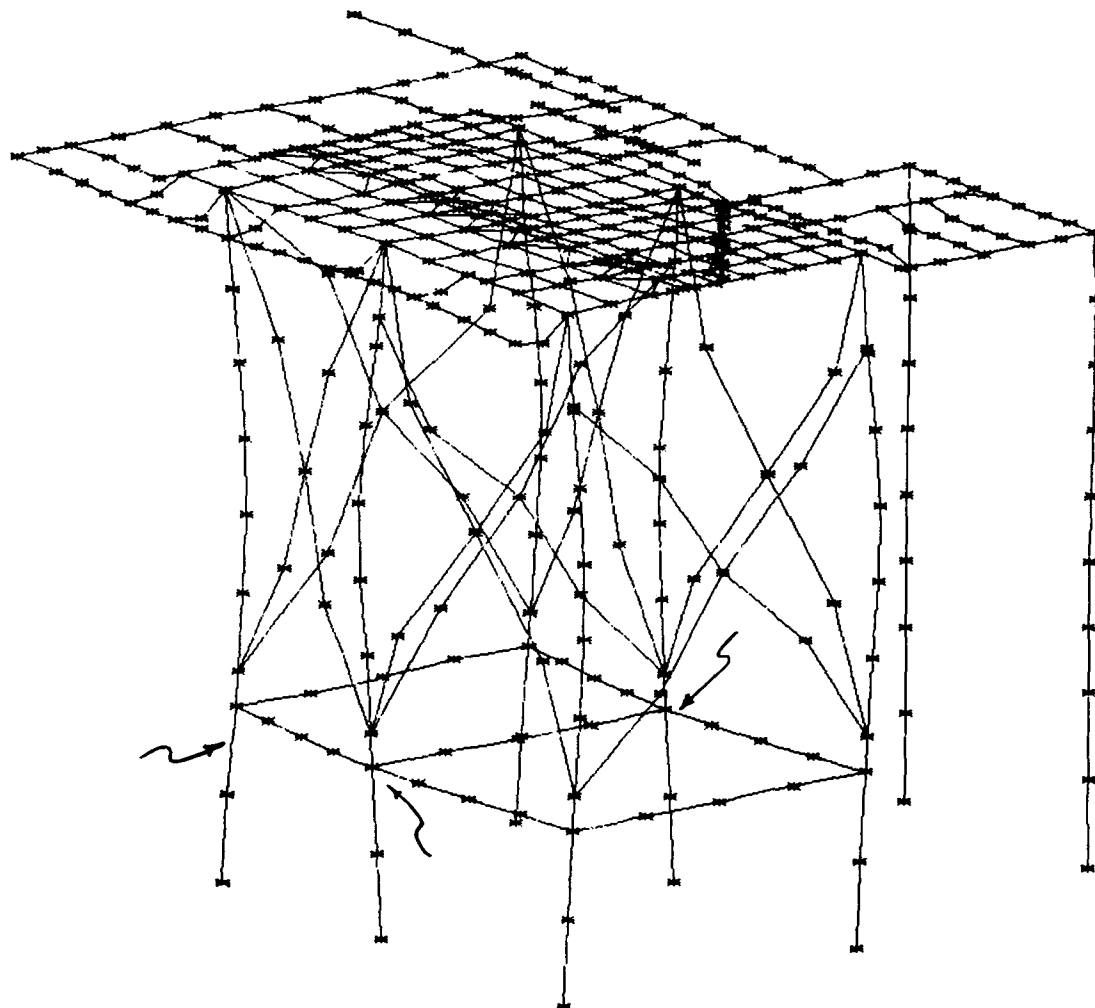
Figure 18: Mode B-51 (81.34 cps): Shaft Deflection Associated With Mode B-51

178
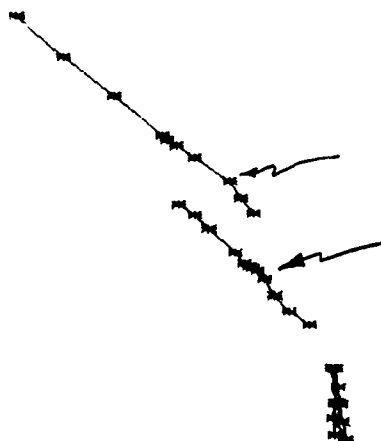
The next group of modes, as shown in Table VII, are in the 120 cps range. Only one mode (number 2-6) in this region has a high damage potential. This 122.2 cps mode is shown in Figure 19. This mode has a high damage potential because it involves motion of nearly the complete structure.

Figure 19: Mode 2-6 (122.2 cps): A Major Structural Mode Involving Nearly All of the Structure (High Damage Potential)
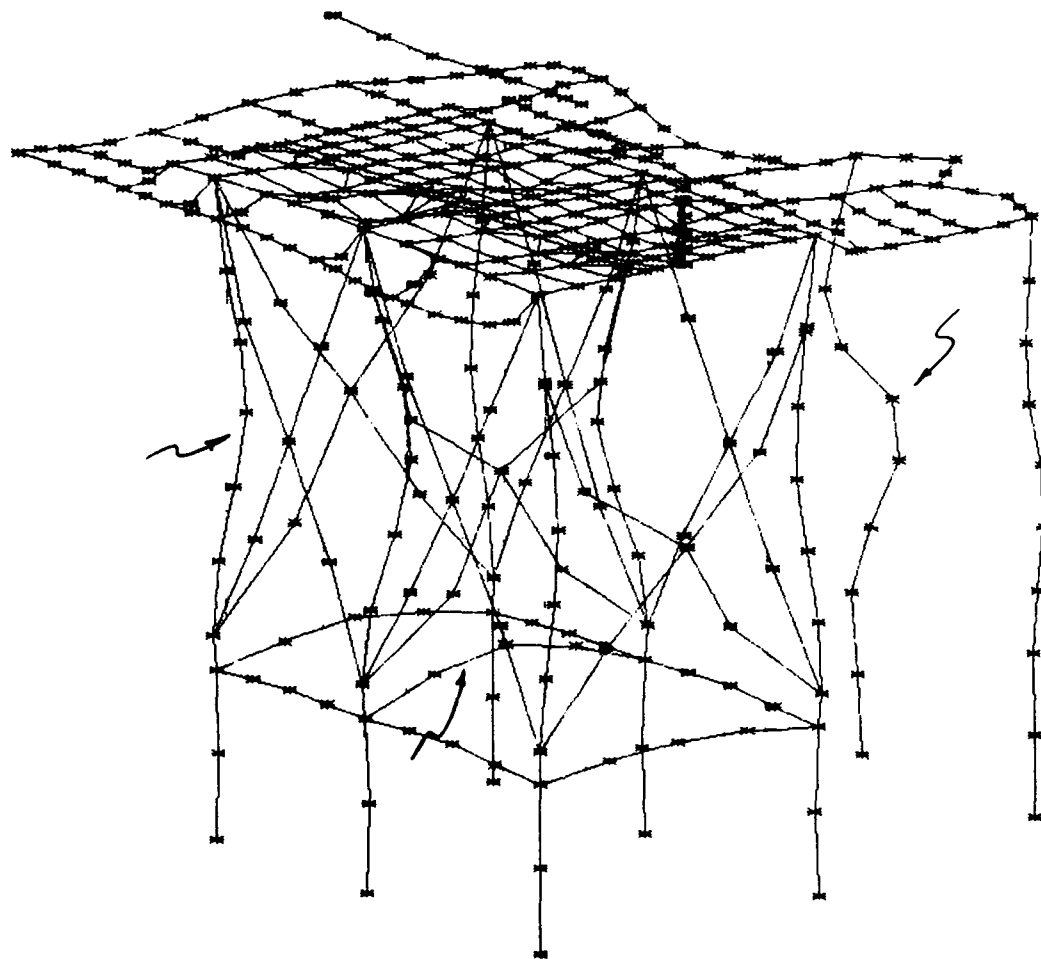
Table VII: Modal Results from Model B in the 114 to 125 cps and 820 to 850 cps Frequency Ranges

Mode Number	Natural Frequency (cps, Hz)	Description of Mode	Mode Evaluation* (Damage Potential)	Applicable Figure	Nearest Steady State Forcing Frequency
2-1	114.8	Minor support member modes	Minor		120
2-5	120.47		Minor		120
2-6	122.20	A major structural mode involving nearly all of the structure	Very High	Figure 19	120
3-1	820.86	Minor support member modes	Minor		837.8
3-3	825.92		Minor		837.8
3-4	831.16	Mode involving most of the structure with quite severe deformation of the increaser shaft	High	Figure 20	837.8
3-5	838.21		Minor to Moderate		837.8
3-10	850.85	Minor support member modes	Minor to Moderate		837.8

Table VIII: Modal Results from Model C (Piping Excluded, Fill Dirt Boundary Conditions)

Mode Number	Natural Frequency (cps, Hz)	Description of Mode	Mode Evaluation* (Damage Potential)	Applicable Figure	Nearest Steady State Forcing Frequency
C-1	19.96	Minor support member modes	Minor		20
C-9	24.51		Minor		20
C-37	64.79	Mode involving motion of all columns as well as electrical panel support structure	Moderate +		83.78
C-38	65.82		Minor		83.78
C-46	72.76	Minor support member modes	Minor		83.78
C-47	80.89	Major structural mode with deformation at compressor, severe shaft bending and sole plate motion between motor and increaser. Also includes column and X-brace motion.	Very High	Figure 21	83.78
2C-5	112.4	Minor support member modes	Minor		120
2C-10	120.5	Mode involving grating, electrical support panel, sole plate, and some columns	Minor		120
2C-11	126.3	Mainly a grating mode with some sole plate motion behind compressor as well as some electrical support panel motion	Moderate		120
2C-12	127.5		Moderate		120

*Mode Evaluation (Damage Potential) is indicative of the probability of encountering support structure and/or equipment damage if the particular mode is excited in a resonant or near-resonant condition.

Another computer run was made to investigate the high frequency region around 837.8 cps. See Table VII. Of the ten modes obtained, five were rated as having moderate to high damage potentials. This is a rather large percentage. The mode with the highest damage potential was number 3-4 which has a frequency of 831.16 cps. It is shown in Figure 20. This mode, along with modes 3-1, 3-7, 3-8, 3-9, and 3-10, show considerable shaft deformation. This indicates that shaft bending modes may be prevalent in this frequency range. A detailed study might be desirable if unusual bearing or seal wear is encountered. Such a study would have to include elastic simulation of the bearings and their supports for the results to be meaningful.

Figure 20:   Mode 3-4 (831.16 cps): A Mode Involving Most of the Structure with Quite Severe Increasor Shaft Deformation (High Damage Potential)
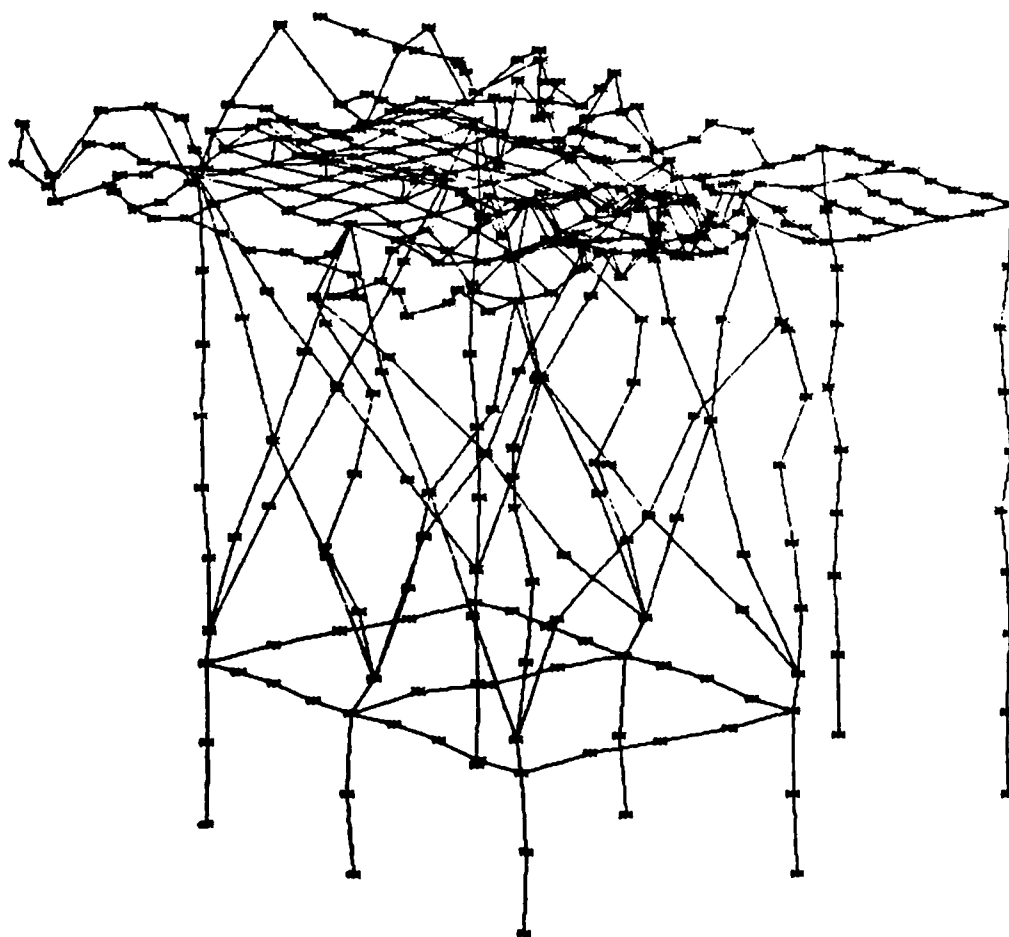
Discussion of Model C Analysis

Model C is identical to model B except that the boundary conditions are different. Various degrees of freedom were constrained to better simulate the effect of the fill dirt. The modal results are presented in Table VIII.

The first computer run covered the 19 to 30 cps range. All modes in this frequency range were classified as minor. They were generally X-brace or grating modes and for the most part were identical to those from the B model in the same frequency range.

The second run was used to investigate the frequency shift of several moderate to high damage potential modes that might be encountered due to the fill dirt. A frequency shift was expected for any modes from models A and B that had involved some motion of the concrete portion of the structure. Most of the modes in this region were again classified minor to moderate. However, two modes, C-37 and C-47, were classified as having "moderate to very high damage potentials." The C-37 mode (64.79 cps) is so classified due to the large response of several of the major support columns. Mode C-47 which is shown in Figure 21 does indeed have a very high damage potential. Excitation of this 80.89 cps mode could lead to a major failure. The deflections in the vincinity of the compressor and the severe shaft deflections are proof of the consequences of exciting this mode.

Figure 21: Mode C-47 (80.89 cps): A Major Structural Mode Involving Deflections at the Compressor, Severe Shaft Bending and Column and X-brace Motion (Very High Damage Potential)
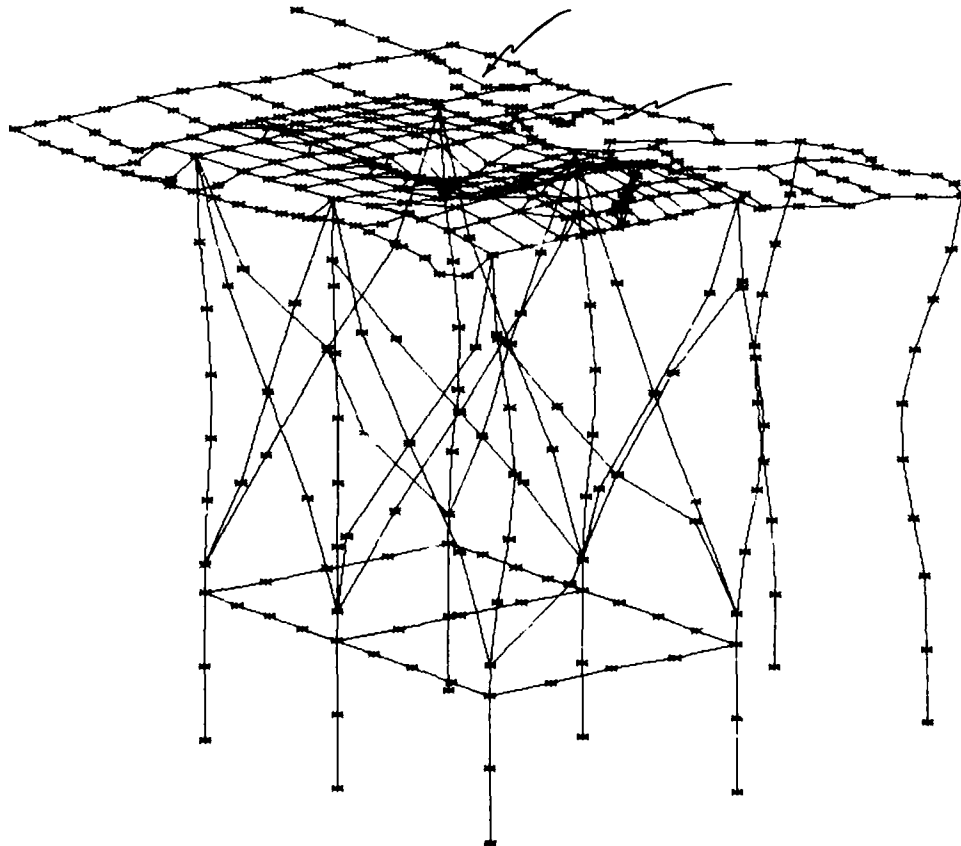
The next run covered the 110 to 132 cps range. As shown in Table VIII, no high damage potential modes were found in this region. Modes 2C-11 and 2C-12 were classified as moderate. Mode 2C-7 is a plate bending mode involving a section of the sole plate between the motor and increaser.

Modal Comparisons

Because various conditions such as including or excluding the piping, changes in support boundary conditions, etc., can result in a sizeable shift in the natural frequency of various modes, and in some cases eliminate certain modes, it was necessary to compare the modes from the different models and assess any potential problems associated with different boundary conditions.

If you exclude the pure piping modes, then from 0 to 35 cps you can generally find a good correspondence between the A-i, B-i, and C-i modes. Some of these modes are not identical but in groups they are collectively similar to each other. The general conclusion that can be reached concerning the 0 to 35 cps region is that including the piping slightly decreased the natural frequency of equivalent modes while the fill dirt boundary conditions of model C-i generally resulted in a slight increase in the natural frequencies. This is not unexpected since most of the modes in this region are minor or do not pertain to a portion of the structure that would be significantly affected by the piping or the boundary conditions at the base.

However, mode B-16, which was classified as having a very high damage potential, is not even present in the A-i modes. From this, one can conclude that any modes in models B-i and C-i that involve compressor motion will either be eliminated or have a substantially different frequency than the corresponding modes of model A due to the piping.

Mode number A-29, which has a very high damage potential, has essentially the same frequency as the corresponding B mode number 22. This is because this mode does not involve appreciable motion in the compressor/pipe region. The same is true for modes 31 and 23 of models A and B respectively.

High damage potential mode A-33 does not appear to have a B counterpart. However, in some ways it is similar to mode 16 of model B. This mode could be the result of adding the piping to B mode 16.

In the 65 to 68 cps range, the fill dirt constraint of model C served to eliminate the high damage potential modes 57 and 46 of models A and B. They may have been shifted above the 90 cps level.

Another moderate to high damage potential mode occurs at 70.33 cps for model A. Removal of the piping resulted in this mode's frequency moving upward about 5 cps. (Mode 48 of model B). Another 5 cps increase in this mode occurred with the fill dirt constraint (Mode C-47). In both of these cases the mode's damage potential increased. In this case inclusion of the piping prevents the development of a mode with a very high damage potential at a frequency very close to the steady state operating speed.

183

No other modes up to the 87 cps level appear to have a very high damage potential. The next region of modal comparison is from 110 to 132 cps. Only one really high damage potential mode exists in this region. It is 2A-12, 2-6, and 2C-11 for models A, B, and C respectively. This mode for model A is far too close to the forcing frequency of 120 cps. Fortunately, the fill dirt constraint would serve to increase the frequency of mode 2A-12 to a value of about 124 cps as indicated by the frequency of mode 2C-11 of model C. This value is reduced from that of mode 2C-11 because the addition of the piping should reduce this frequency by about 2 cps; i.e., from 126.3 to about 124 cps. Removal of the piping in this frequency range tended to produce a 2 cps frequency increase. The other high damage potential mode, 2A-20, is above the forcing frequency of 120 cps and thus should not be a problem.

Discussion of Steady State Operation

The modes of model A are the most representative of the actual structure. But some of these modes need to have their frequency adjusted to account for the fill dirt restraint. In any event, there does not appear to be a serious problem at steady state operation provided the piping is attached. Only in the 120 cps range is their some question about the response. This situation should be monitored during the initial year of operation.

However, if the system was run without the piping attached, the results of models B and C would be applicable. In fact, the results from these models indicate that the system should not be operated without the piping attached. An imbalance in this situation could readily excite several high damage potential modes.

In the region of the cut-off frequency (837.8 cps), there does not appear to be an immediate problem. However, there are several modes involving shaft bending in this region that could result in increased bearing and/or seal wear if they were excited. A more detailed analysis of the shafting would be required to determine if a significant problem exists. If unusual bearing or seal problems are encountered, such a study may be warranted.

Discussion of Transient Response (Start-up, Shutdown, Coast Down)

In this case, some reasonable conclusions relative to the transient response of the support structure can be inferred from the modal results. The first step in such a discussion involves establishing the frequency range of the various forcing functions. They vary from 0 to 20 cps for the motor, 0 to 83.7 cps for the compressor/increaser, 0 to 837.8 cps for the compressor (cut-off frequency) and a 120 cps line frequency. Generally, structural natural frequencies at the upper or lower region of these frequency ranges cause problems. To better understand the situation, consider a typical frequency time curve associated with start-up.

184

Figure 22: Typical Start-Up Curve
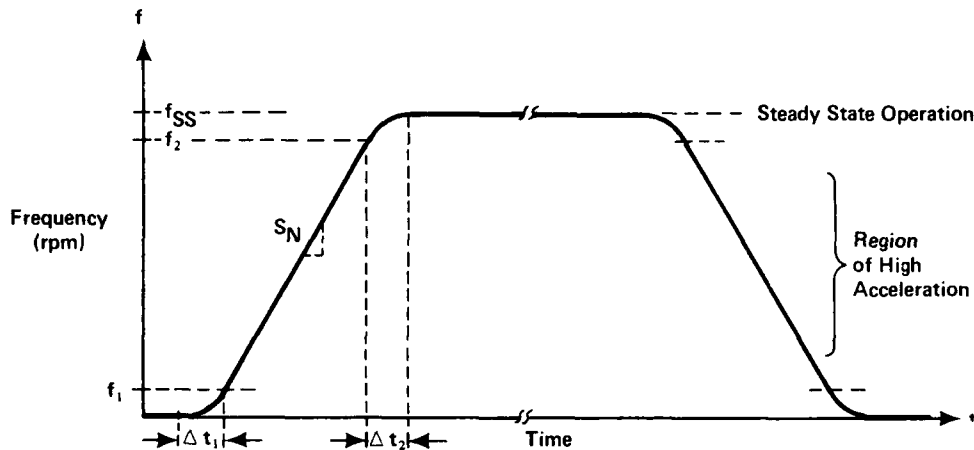
Any natural frequencies that exist below f_1 or in the region from f_2 to f_{SS} can cause serious transient oscillations because the forcing function will stay at or near that structural natural frequency for a relatively long period of time. In the high acceleration region from f_1 to f_2, the forcing frequency is usually going through the natural frequencies fast enough to not produce a noticeable resonant response.

Occasionally you can encounter an easily excitable mode which will tend to track the forcing frequency and thus get a much larger response than anticipated. In this case the natural frequency tends to change with the forcing frequency for a certain range before they become uncoupled. Some classical cases of this have been encountered with large stacks (chimneys) when excited by vortex shedding. In this situation, the two frequencies actually augment each other.

In an effort to minimize the possibility of large transient oscillations during normal start-ups and shutdowns, special start-up and shutdown procedures should be employed to maximize the acceleration and deceleration (rate of change of the rotational frequency) of the system. The major aspects of this procedure would involve:

1. Starting the system with the compressor unloaded until the synchronous speed is attained, then proceed to gradually load the compressor.

2. Shutting down the system with the compressor completely loaded until zero rpm is reached.

The situation that involves the greatest probability of exciting the high damage potential modes involves a coast down. In this situation, the slope of the rpm vs time curve would decrease dramatically. This is shown in Figure 23.

185

Figure 23: Possible Coast Down Curve
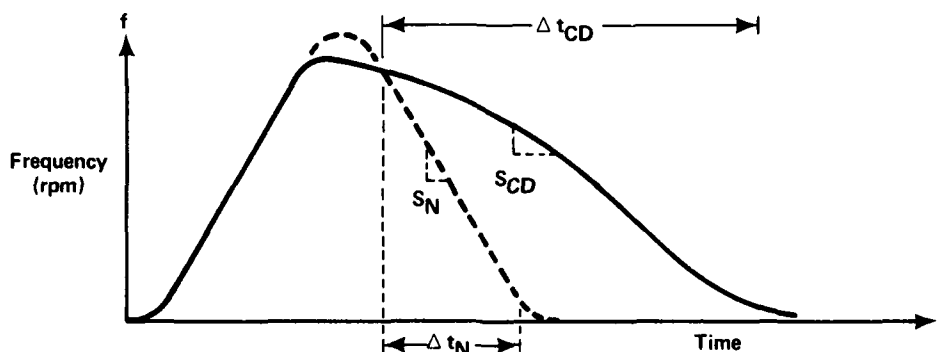
There are two or three conditions that could make a coast down much more serious. One would involve a structural failure which would produce a large imbalance (eccentric load). The other would involve a coast down just before or just as the motor reaches synchronous speed, but before the compressor has been loaded. Of course, a structural failure (eccentric loads) along with this latter situation would have a high probability of damaging the unit and/or support structure. The amount of damage would depend on the magnitude of the eccentric load.

Conclusions

The results of this NASTRAN static and modal analysis indicate:

1. No major static problems.

2. No major resonant condition exists at steady state operation. However, two minor modes (77 and 78) are quite close to the compressor speed of 83.78 cps. The structure should be monitored during several start-ups and shutdowns to determine if these two minor modes are being excited. If it appears these two modes are being excited to some extent, some minor structural changes should be undertaken.

3. Normal start-up and shut-down does not appear to pose a problem provided procedures are employed to minimize both start-up and shutdown times. Only around 837.8 cps does it appear that there could be a vibration problem. To minimize this possibility, every effort should be made to balance the compressor and properly align all shafting.

4. A serious vibration problem could be encountered if a coast down occurs, especially if a compressor or gear train imbalance is also encountered during the coast down. A compressor failure such as losing a section of a vane could cause some rather dramatic oscillations.

5. Test operation of the system without the piping attached has a much greater probability causing structural and/or equipment damage than encountered during normal operation, i.e., with the piping attached.

186

6. The absence of any major structural natural frequencies below 20 cps makes this particular support structure ideal for use of an isolation pad/spring system since such systems transmit low frequencies, usually below 10 cps, but not the higher frequencies in the operating range.

7. Most of the modes were independent of the boundary conditions at the base. In other words, the fill dirt constraint affected only a few of the calculated modes. Only the modes that involved motion of the concrete portion of the columns were affected by the boundary conditions. This is basically due to the very high relative stiffness of the concrete beams and columns. The inclusion of the piping had a much more dramatic effect.

The following conclusions were reached relative to the modeling of such structures:

1. You should include the piping in such analyses; otherwise, the results will not be correct for numerous pertinent modes.

2. The Fast Eigen Value Extraction Routine (FEER) in NASTRAN gave results that were identical to those of the Inverse Power Method. This was somewhat surprising since this method is rated for speed, but is reportedly not quite as accurate as the Inverse Power Method. It extracted the eigenvalues 1.8 times as fast as the Inverse Power Method.

3. The availability of an excellent deformed and overlay plot capability as available in NASTRAN was indispensable in reviewing the mammoth amount of data generated by the program.

Closing Comment

After installation, before and after the piping connections were made, a dynamic test of the structure using strain gages and accelerometers was performed. The results verified the major modes established in the analyses and supported the conclusions. The system has now been operating over three years without any major problems. This includes several normal start-ups and shut-downs using the recommended procedure. During this period a coast down has not occurred.

Table A-1: Weight and CG of Structure

Model ID	Description	Total Weight (lbs)	Center of Gravity		
			X	Y	Z
A	Total Structure Including Piping	139,971	178.7"	106.4"	210.5"
B	Total Structure Excluding Piping	111,700	159.0"	94.5"	170.0"
--	Piping System Only	28,271	------	------	------
--	Support Structure	68,110	161.1"	85.3"	107.0"

Table A-2: Typical Structural Member Sizes

Member Description	Size
Sole Plate	1/2" thick
Main Columns (6, steel)	W10 x 68
Electrical Panel Support Columns (6, steel)	W6 x 15
Reinforced Concrete Footers (6)	22" x 18"
Reinforced Concrete Footer Under Electrical Panel	12" x 12"
Horizontal Reinforced Concrete Beams	24" x 22", 24" x 18"
X-braces (12)	WT4 x 9
Main Sole Plate Support Beams	W16 x 67
Minor Support Beams Under Electrical Panel	C8 x 11.5, W8 x 24
Grating Supports	C10 x 15.3, W8 x 18, W14 x 22
Electrical Panel Support Beams	C8 x 11.5, W8 x 24

Figure A-1:   Shafting and Piping Grid Point Layout
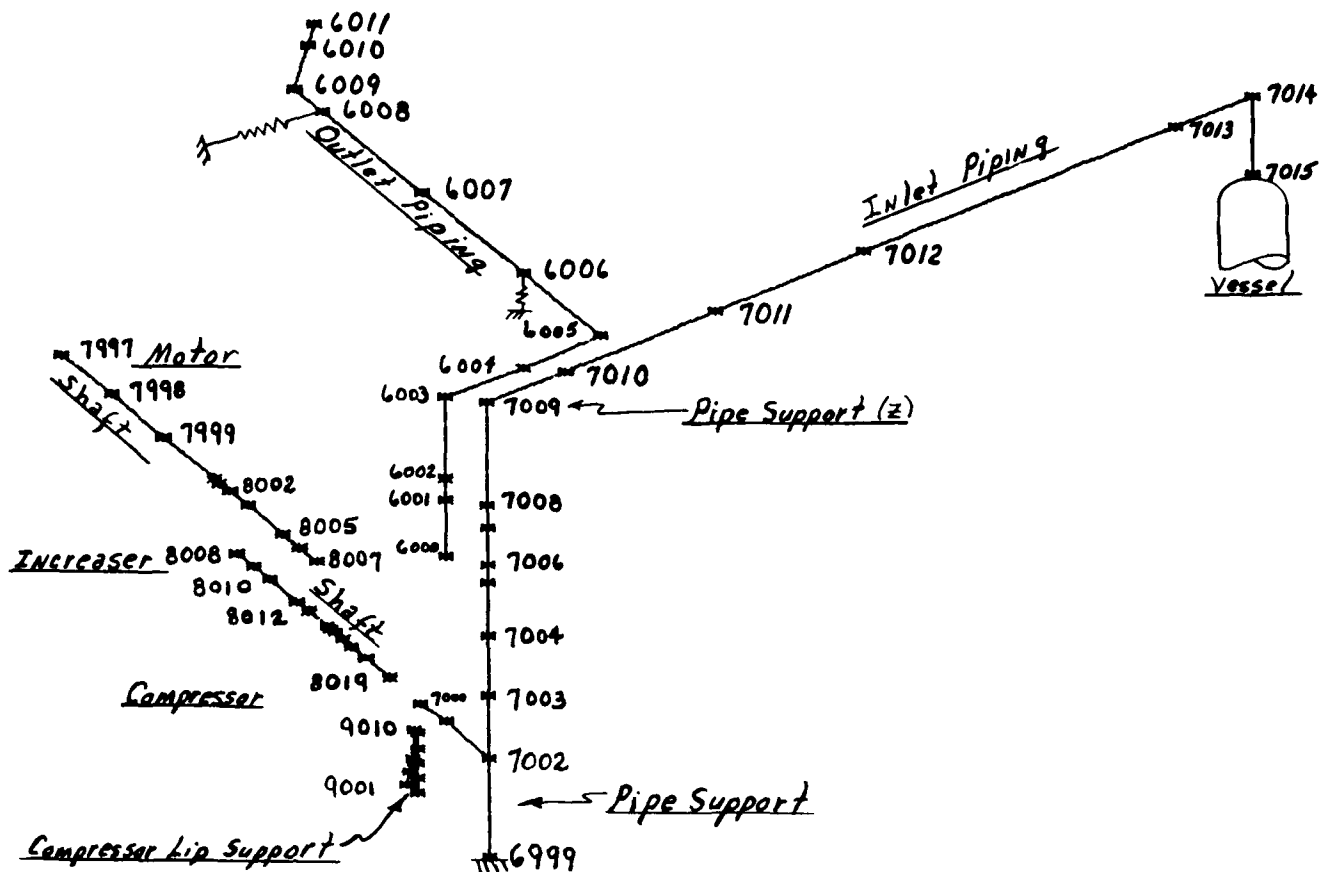
Figure A-2:   Location of Equipment on the Sole Plate
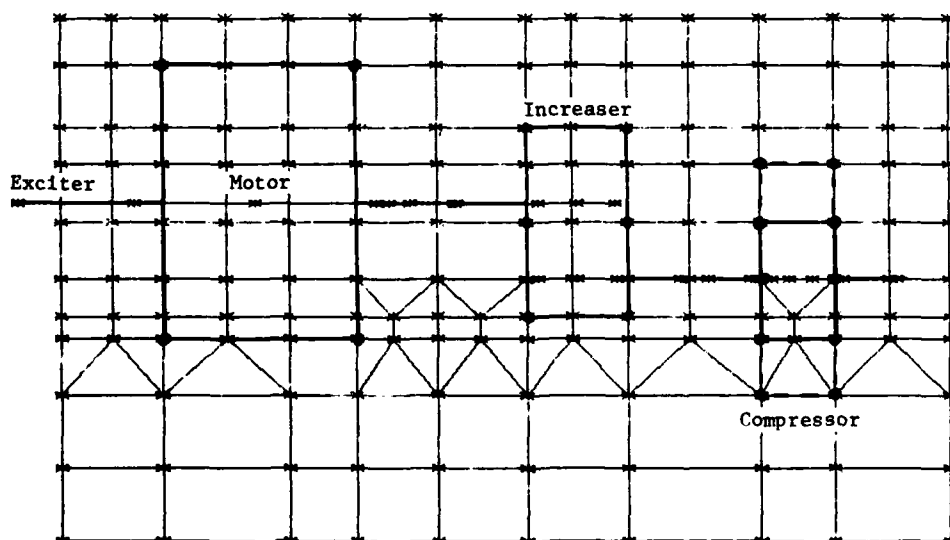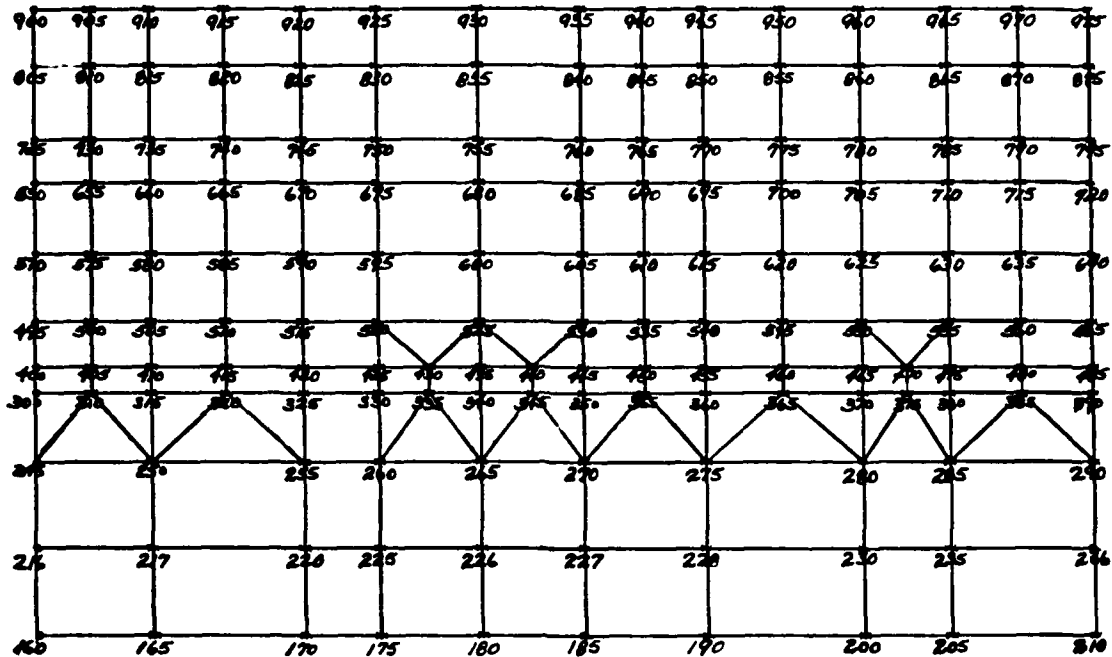
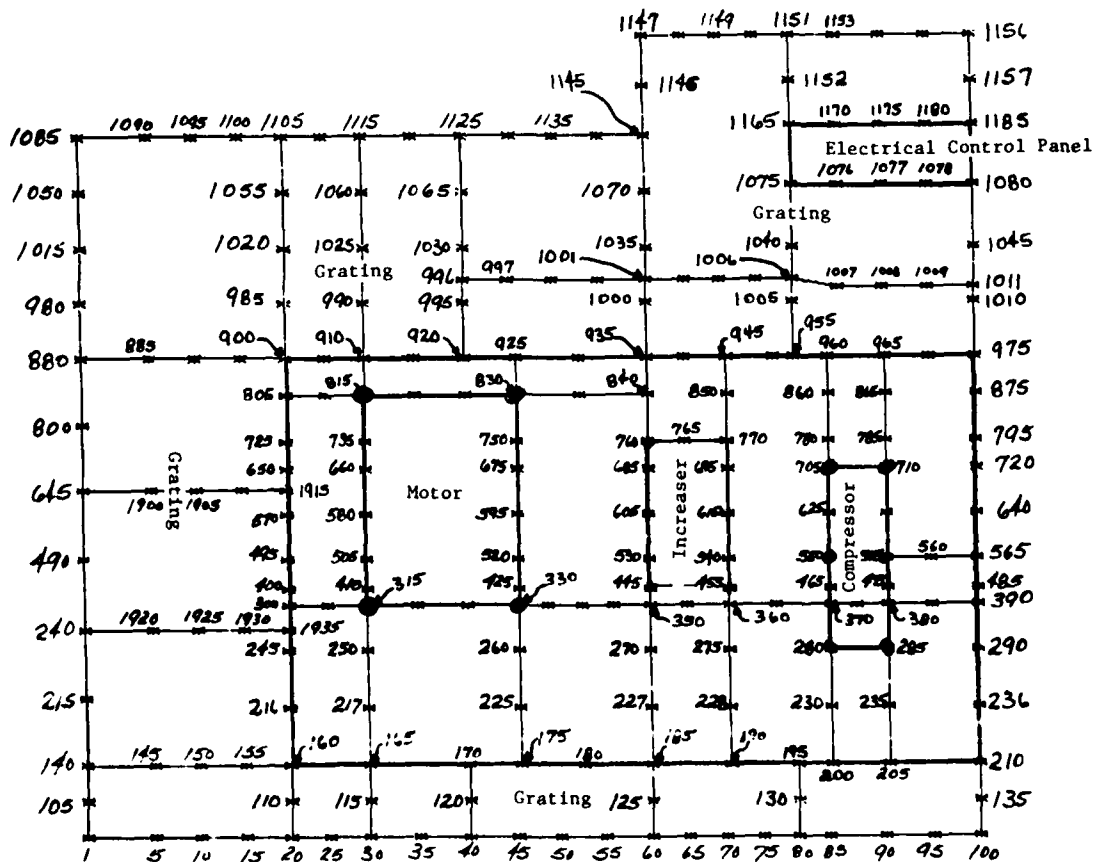Figure A-3: Grid Point Layout for Sole Plate

Figure A-4: Grid Point Layout for Sole Plate Support Structure

APPENDIX B

General References

1. The NASTRAN User's Manual, NASA SP-222.

2. Boeing Memorandum 5-9540-H-696 to NASA/MSFC entitled, "AS-503 C Prime POGO/Control System Coupled Response for Change Order 346," dated December 5, 1968.

3. Boeing Memorandum 5-9540-H-738 to NASA/MSFC entitled, "AS-504 Preliminary POGO/Control System Coupled Response for Change Order 346," dated January 16, 1969.

4. Boeing Memorandum 5-9570-H-597 to NASA/MSFC entitled, "Summary of AS-503 S-II Oscillation Assessment," dated 1969.

5. NASA CR-1539 and CR-1540 entitled, "Advancements in Structural Dynamic Technology Resulting from SATURN V Programs," Volumes I and II; dated June, 1970.

FINITE ELEMENT PREDICTION OF ACOUSTIC SCATTERING AND RADIATION FROM SUBMERGED ELASTIC STRUCTURES

G.C. Everstine, F.M. Henderson, and R.R. Lipman

David W. Taylor Naval Ship R&D Center
Bethesda, Maryland 20084 USA

ABSTRACT

A finite element formulation is derived for the scattering and radiation of acoustic waves from submerged elastic structures. The formulation uses as fundamental unknowns the displacement in the structure and a velocity potential in the fluid. Symmetric coefficient matrices result. The outer boundary of the fluid region is terminated with an approximate local wave-absorbing boundary condition which assumes that outgoing waves are locally planar. The finite element model is capable of predicting only the near-field acoustic pressures. Far-field sound pressure levels may be determined by integrating the surface pressures and velocities over the wet boundary of the structure using the Helmholtz integral. Comparison of finite element results with analytic results show excellent agreement. The coupled fluid-structure problem may be solved with general purpose finite element codes by using an analogy between the equations of elasticity and the wave equation of linear acoustics.

INTRODUCTION

There is a variety of practical engineering problems which cannot be addressed using only the separate disciplines of structural analysis and acoustics; they must instead be treated by formulating a coupled structural-acoustic problem. For example, for aircraft (Ref. 1), automobiles (Ref. 2), and railroad cars (Ref. 3), coupled analyses are being investigated to understand better the interior noise problem so that such noise can be reduced. In aerospace vehicles, the vibrations of fluid-filled tanks are of interest (Ref. 4). In aircraft hydraulic systems (Ref. 5) and shipboard piping systems (Ref. 6), the dynamic behavior of (and the transmission of sound in) fluid-filled piping systems has been analyzed. Other important naval problems involve the vibration of underwater structures such as rudders and propellers (Ref. 7-8), the shock response of submerged structures (Ref. 9-13), and the scattering of sound waves from underwater elastic structures (Ref. 14-17).

The commonality among all these problems is the mathematical model. The structure, if it can be assumed to remain elastic, behaves according to the classical theory of elasticity (Ref. 18) and the various approximate engineering theories for beams, plates, and shells. The fluid is generally treated as an acoustic medium (Ref. 19-21), a fluid whose pressure p satisfies the scalar wave equation

$$\nabla^2 p = \ddot{p}/c^2 \tag{1}$$

where c is the speed of sound in the fluid. The boundary condition at a fluid-structure interface can be obtained from momentum and continuity considerations:

$$\partial p/\partial n = -\rho \ddot{u}_n \tag{2}$$

where n is the normal at the interface, ρ is the mass density of the fluid, and $\ddot{u}_n$ is the normal component of fluid particle acceleration.

Dynamics problems involving the interaction between an elastic structure and an acoustic fluid have been formulated for finite element solution (Ref. 22) by using either pressure (Ref. 19,23,24) or fluid particle displacement (Ref. 14,25-27) as the fundamental unknown in the fluid region. In three dimensions, the pressure and displacement formulations result in, respectively, one and three degrees of freedom per finite element mesh point. Thus the pressure approach has the advantage of fewer unknowns and a smaller overall matrix profile or bandwidth. On the other hand, the displacement approach results in symmetric coefficient matrices (in contrast to the pressure formulation, for which the matrices are nonsymmetric) and a fluid-structure interface condition which is easier to implement with general purpose finite element computer programs. However, the displacement approach also suffers from the presence of spurious resonances (Ref. 27), a situation which can be bothersome in time-harmonic problems, either forced or unforced. Recently it was shown (Ref. 28) that the principal disadvantage of the pressure formulation, nonsymmetric coefficient matrices, can be removed merely by reformulating the pressure solution approach so that a velocity potential rather than pressure is used as the fundamental unknown in the fluid region. For some situations, particularly steady-state problems involving damped systems and time-dependent problems, significant computational advantages result.

The principal goal of this paper is to present in detail the symmetric velocity potential formulation for application to the specific problem of acoustic scattering from submerged elastic structures. Previously (Ref. 28), the symmetric potential formulation was described only in general terms for a wider class of fluid-structure interaction problems with no details concerning specific types of applications (such as vibrations, shock response, or acoustic scattering).

The scattering approach described here has advantages over the displacement formulations for the reasons already given. Finite element modeling of exterior fluid regions also has advantages over the use of approximate theories such as the doubly asymptotic approximation (DAA) (Ref. 15). In this case, the primary trade-off is between the large, banded matrices which finite element models generate and the smaller, densely-populated matrices which the DAA generates. This trade-off often favors the finite element approach for long structures like ships which are "naturally banded." Similar trade-offs arise if the finite element approaches are compared with T-matrix methods (Ref. 16). T-matrix approaches, however, are not yet available in general purpose codes capable of handling arbitrary three-dimensional geometries.

From an engineering point of view, it is convenient to be able to make use of existing general purpose finite element codes (such as NASTRAN, among others), because of their wide availability, versatility, reliability, consultative support, and abundance of pre- and postprocessors. Thus the next section summarizes an analogy between the equations of elasticity and the common field equations of classical mathematical physics (including the wave equation). This analogy allows the coupled structural-acoustic problem to be solved with standard finite element codes.

Subsequent sections of the paper will develop the formulation of the scattering problem for elastic obstacles with and without fluid inside. Examples will be shown for both cases.

STRUCTURAL ANALOGIES FOR SCALAR FIELD PROBLEMS

Since we wish to solve the coupled structural-acoustic problem using standard finite element codes (which were developed principally for structural analysis), we summarize here the application of such codes to various nonstructural field problems (Ref. 24,29).

Many linear problems in mathematical physics involve the solution of an equation obtained by specializing the general form

$$\nabla^2 \phi + g = a \ddot{\phi} + b \dot{\phi} \tag{3}$$

where ∇^2 is the Laplacian operator; dots denote partial time differentiation; the functions g, a, and b are, in general, position-dependent; and the unknown scalar function ϕ depends on both position and time.

Special cases of Eq. (3) arise in such diverse applications as heat conduction, acoustics, electrical and magnetic potential problems, torsion of prismatic bars, potential fluid flow, and seepage through porous media. Several common special cases are listed here:

Laplace's equation: $\qquad \nabla^2 \phi = 0 \tag{4}$

Poisson's equation: $\qquad \nabla^2 \phi + g = 0 \tag{5}$

wave equation: $\qquad \nabla^2 \phi = \ddot{\phi}/c^2 \tag{6}$

heat equation: $\qquad k\nabla^2 \phi + q = \rho c \dot{\phi} \tag{7}$

telegraph equation: $\qquad \partial^2 \phi/\partial x^2 = LC\ddot{\phi} + RC\dot{\phi} \tag{8}$

Helmholtz equation: $\qquad \nabla^2 \phi + k^2 \phi = 0 \tag{9}$

Most boundary conditions likely to be encountered in connection with Eq. (3) will probably be special cases of the general form

$$a_1 \, \partial\phi/\partial n + a_2 \, \phi + a_3 \, \dot{\phi} + a_4 \, \ddot{\phi} + a_5 = 0 \tag{10}$$

where n is the outward normal at the boundary. For example, in heat conduction problems, a boundary with a prescribed temperature function satisfies the Dirichlet condition

$$\phi = \phi_0 \tag{11}$$

and a perfectly insulated boundary has the Neumann condition

$$\partial \phi / \partial n = 0 \qquad (12)$$

In free surface flow problems, the linearized free surface condition on the velocity potential is (Ref. 30)

$$\ddot{\phi} + g_o \, \phi_{,z} = 0 \qquad (13)$$

where g_o is the acceleration due to gravity, the free surface is the plane z = constant, and commas denote partial differentiation. In one-dimensional radiation problems, the plane wave radiation condition that the velocity potential must satisfy at a non-reflecting boundary is

$$\phi_{,n} + \dot{\phi}/c = 0 \qquad (14)$$

where c is the wave speed.

An example of a boundary condition not of the general form of Eq. (10) is the condition (2) which must be satisfied at an accelerating boundary of a fluid.

According to the analogy (Ref. 29) between Eq. (3) and the Navier equations of classical elasticity, Eqs. (3) and (10) can be solved with elastic finite elements using the following procedure:

1. Select one of the three Cartesian components of displacement (or the z-component in cylindrical coordinates) to represent the scalar field variable ϕ. Constrain all other displacement components everywhere in the field.

2. Model the domain of interest (either 2-D or 3-D) with finite elements having material constants satisfying

$$E_e = \alpha \, G_e, \quad \rho_e = a \, G_e \qquad (15)$$

where "a" is the variable appearing in Eq. (3), and E_e, G_e, and ρ_e denote the Young's modulus, shear modulus, and mass density assigned on the material card to the finite elements. The subscript "e" has been added to emphasize that these constants are merely numbers assigned to the elements and may bear no resemblance to any actual material properties associated with a particular application. The dimensionless constant α in Eq. (15) should, for 3-D problems, be chosen large enough to make $\alpha+1$ numerically indistinguishable from α. For 2-D problems, α should be small, but not

so small that 1+α is numerically indistinguishable from unity. Thus, on most computers,

$$\alpha = \begin{cases} 10^{-5} & \text{(2-D)} \\ 10^{20} & \text{(3-D)} \end{cases} \qquad (16)$$

The shear modulus G_e can be selected arbitarily. The finite elements eligible for use in the model are those derived from classical elasticity theory rather than from the engineering theories involving beams, plates, or shells. Thus, for 2-D problems, the plane stress membrane elements are appropriate. For 3-D problems, the solid elements (e.g., the isoparametric or the axisymmetric solids) should be used.

3. Apply to the unconstrained degree of freedom (DOF) at each grid point in the region a "force" given by

$$F = G_e \, g \, V \qquad (17)$$

where V is the volume assigned to the point and g is the function appearing in Eq. (3). For problems for which the function g in Eq. (3) is independent of position (as, for example, in the classical St. Venant torsion problem), this load may be specified conveniently by applying to the "structure" a gravitational field for which the acceleration due to gravity g_o satisfies

$$\rho_e \, g_o = G_e \, g \qquad (18)$$

4. Connect between ground and the unconstrained DOF at each grid point in the region a scalar dashpot whose damping constant (the ratio of damping force to velocity) is $G_e bV$, where b is the function appearing in Eq. (3) and V is the volume assigned to the point.

5. Enforce the boundary condition (10) by applying to the unconstrained DOF at each grid point on the boundary of the region a "force" given by

$$F = -G_e A \, (a_2 \, \dot{\phi} + a_3 \, \dot{\phi} + a_4 \, \ddot{\phi} + a_5)/a_1, \quad a_1 \neq 0 \qquad (19)$$

where A is the area assigned to the point. (In general, the outward normal derivative $\partial\phi/\partial n$ is enforced at a boundary point by applying a "force" to the unconstrained DOF at that point equal to $G_e A \partial\phi/\partial n$. A positive force corresponds to a positive outward normal derivative.) In Eq. (19), the a_2 term is analogous to a scalar spring of constant $G_e A a_2/a_1$ connected between the point and ground. The a_3 term is analogous to a scalar dashpot of constant $G_e A a_3/a_1$ connected between the point and ground. The a_4 term is analogous to an added mass of value $G_e A a_4/a_1$ attached to the point. (Here, one should probably use a consistent, rather than lumped, formulation since Zarda and Marcus (Ref. 30) showed that the differences between the two are not

insignificant for free surface flow problems.) The a_5 term is a time-independent force given by $-G_e Aa_5/a_1$. As expected, the special case of the Neumann boundary condition ($\phi_{,n} = 0$) corresponds to the traction-free boundary in elasticity and hence is a natural boundary condition. The Dirichlet condition ($\phi=\phi_0$) is implemented merely by enforcing the desired value as a "displacement" boundary condition.

SCATTERING FROM ELASTIC BODIES

In the scattering problem (as shown in Fig. 1), a submerged elastic body is subjected to a plane wave time-harmonic acoustic incident loading of circular frequency ω. Without loss in generality, we can assume that the waves propagate in the $-x$ direction. The speed of such propagation is c, the speed of sound in the fluid (usually water).
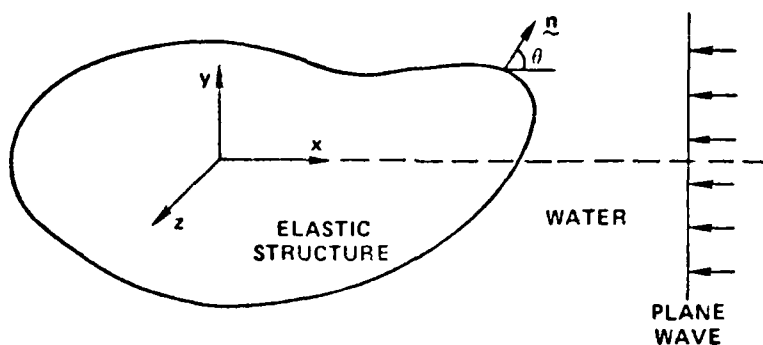
Figure 1 — The Scattering Problem

Within the fluid region, the total fluid pressure p satisfies the wave equation, Eq. (1). Since the free-field incident pressure p_i is known and is given by

$$p_i(x,t) = p_0\, e^{i(kx + \omega t)} \tag{20}$$

(where $k=\omega/c$) it is frequently convenient to decompose the total pressure p into the sum of incident and scattered pressures

$$p = p_i + p_s \tag{21}$$

each of which satisfies the wave equation.

The solution of this scattering problem has been approached in various ways, including the T-matrix method (Ref. 16), numerical approaches using approximate fluid loading schemes (Ref. 15), and finite element schemes (Ref. 14). The latter approach models with finite elements both the structure and a portion of the infinite fluid, which is terminated with a simple radiation boundary condition to absorb the outgoing waves as much as possible. Kalinowski's finite element approach (Ref. 14) uses the total fluid particle displacement as the fundamental fluid unknown.

197

The approach presented here is most similar to Kalinowski's approach (of those mentioned above), except that we use as the fundamental fluid unknown the scattered component of a fluid velocity potential rather than the total fluid displacement. Both approaches yield symmetric matrix equations, but the use of velocity potential rather than displacement as fluid unknown results, in 3-D, in fluid matrices of one-third the order and one-third the matrix bandwidth.

We now formulate the problem for finite element solution. The finite element modeling of the elastic structure results in the matrix equation

$$M \ddot{u} + B \dot{u} + K u = -A p = -A (p_i + p_s) \tag{22}$$

where u is the vector of displacement components in the structure; M, K, and B are the structural mass, stiffness, and damping matrices, respectively; p is the vector of fluid pressures at the nodes of the fluid region; and A is the area matrix which converts fluid pressures at interface points to structural loads.

A finite element model of the fluid region results in a matrix equation of the form

$$Q \ddot{p_s} + H p_s = 0 \tag{23}$$

where p_s is the vector of scattered fluid pressures at the nodes of the fluid region, and Q and H are the fluid "inertia" and "stiffness" matrices, respectively. According to the analogies described in the preceding section, the same finite element code may be used to model both the structural and fluid regions. From Eq. (15), material constants assigned to the elastic elements used to model the fluid satisfy

$$E_e = \alpha G_e, \quad \rho_e = G_e/c^2 \tag{24}$$

where α is given by Eq. (16).

As is, Eq. (23) does not account for either the fluid-structure interface condition (2) or a wave-absorbing boundary condition. As in Kalinowski's work (Ref. 14), we will use the simple plane wave absorbing condition (Ref. 31)

$$\partial p/\partial n = -\dot{p}/c \tag{25}$$

Other possibilities are discussed by, for example, Engquist and Majda (Ref. 32), Bayliss, Gunzburger, and Turkel (Ref. 33), and Israeli and Orszag (Ref. 34). However, these are not of the general form of Eq. (10). Kalinowski showed (Ref. 14, 26,35,36), and our Example 1 verifies, that the plane wave absorbing condition is satisfactory if the outer boundary is far enough away from the structure.

Both boundary conditions (2) and (25) can be handled using Eq. (19). At the fluid-structure interface, from Eqs. (2) and (21),

$$\partial p_s / \partial n = -\partial p_i / \partial n - \rho \ddot{u}_n = \rho \, (\ddot{u}_{ni} - \ddot{u}_n) \tag{26}$$

where n is the outward unit normal from the structure (into the fluid), and $\ddot{u}_n$ and $\ddot{u}_{ni}$ are, respectively, the total and incident outward components of fluid particle acceleration at the interface. Thus, using Eq. (19), we impose the condition (26) by applying a load to each interface fluid point given by

$$F^{(p)} = -G_e A \rho \, (\ddot{u}_{ni} - \ddot{u}_n) \tag{27}$$

Similarly, the radiation condition (25) is enforced by applying a load to each fluid point on the outer boundary given by

$$F^{(p)} = -(G_e A/c) \, \dot{p}_s \tag{28}$$

That is, a dashpot of constant $G_e A/c$ is connected between each boundary point and ground.

The overall matrix system describing the coupled problem is obtained by combining Eqs. (22), (23), (27), and (28):

$$\begin{bmatrix} M & 0 \\ -G_e \rho A^T & Q \end{bmatrix} \begin{Bmatrix} \ddot{u} \\ \ddot{p}_s \end{Bmatrix} + \begin{bmatrix} B & 0 \\ 0 & C \end{bmatrix} \begin{Bmatrix} \dot{u} \\ \dot{p}_s \end{Bmatrix} + \begin{bmatrix} K & A \\ 0 & H \end{bmatrix} \begin{Bmatrix} u \\ p_s \end{Bmatrix} = \begin{Bmatrix} -Ap_i \\ -G_e \rho A \ddot{u}_{ni} \end{Bmatrix} \tag{29}$$

This system, which is nonsymmetric, can be symmetrized (Ref. 28) by reformulating the problem to use a new fluid unknown q such that

$$p_s = \dot{q} \tag{30}$$

If the second partition of Eq. (29) is integrated in time, if p_s is replaced by $\dot{q}$, and if the fluid element "shear modulus" G_e is chosen as

$$G_e = -1/\rho \tag{31}$$

the system (29) is transformed into

$$\begin{bmatrix} M & 0 \\ 0 & Q \end{bmatrix} \begin{Bmatrix} \ddot{u} \\ \ddot{q} \end{Bmatrix} + \begin{bmatrix} B & A \\ A^T & C \end{bmatrix} \begin{Bmatrix} \dot{u} \\ \dot{q} \end{Bmatrix} + \begin{bmatrix} K & 0 \\ 0 & H \end{bmatrix} \begin{Bmatrix} u \\ q \end{Bmatrix} = \begin{Bmatrix} -Ap_i \\ Av_{ni} \end{Bmatrix} \tag{32}$$

199

where $v_{ni} = \dot{u}_{ni}$. This is the form of the equations which we will use to solve the scattering problem.

The new variable q is, except for a multiplicative constant, the velocity potential ϕ long used by fluid dynamicists, since

$$p = -\rho \dot{\phi} \qquad (33)$$

Eq. (32) could also be recast in terms of ϕ rather than q as the fundamental fluid unknown, but no particular advantage would result. In fact, the use of q rather than ϕ has the slight practical advantage that the fluid pressure can be recovered directly from the finite element program as the time derivative (velocity) of the unknown q.

To summarize, both structural and fluid regions are modeled with finite elements. For the fluid region, the material constants assigned to the finite elements are

$$G_e = -1/\rho, \quad E_e = \alpha \, G_e, \quad \rho_e = -1/\rho c^2 \qquad (34)$$

where α is given by Eq. (16). The dashpots making up matrix C in Eq. (32) are applied at the outer fluid boundary with damping constant $-A/\rho c$ at each grid point to which the area A has been assigned. At the fluid-structure interface, matrix A is entered using the areas (or areal direction cosines) assigned to each wet degree of freedom.

The right-hand side of Eq. (32) can be simplified further since, for plane waves propagating in the negative x-direction at speed c, the free-field incident pressure and incident fluid particle velocity in the x-direction are related by (Ref. 37)

$$p_i = -\rho c \, v_{xi} \qquad (35)$$

Then, as in Fig. 1, if we define θ as the angle between the normal n and the positive x-axis,

$$v_{ni} = v_{xi} \cos \theta \qquad (36)$$

The x-component of the free-field fluid particle velocity v_{xi} is the same at all points in space except for a phase angle, which may be introduced into the analysis by means of the time delay between two points having different x-coordinates.

EXAMPLE 1: SCATTERING FROM INFINITE CYLINDRICAL SHELL

The formulation derived in the preceding section will be illustrated first on the two-dimensional (plane strain) problem of scattering from an infinitely long

200

cylindrical steel shell (Fig. 2) of radius 0.5 m and thickness 0.01 m. The material properties of steel are E = 19.5x10^{10} N/m^2, ν = 0.28, and ρ_s = 7700 kg/m^3. The surrounding medium is seawater, for which c = 1500 m/sec and ρ = 1026 kg/m^3.
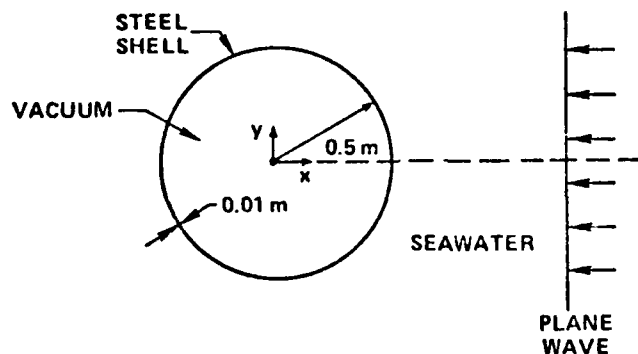

Figure 2 — Scattering from Infinite Cylindrical Shell

The shell is modeled with beam finite elements and the water with 2-D quadrilateral four-node plane stress membrane elements having properties assigned according to Eq. (34). The thickness in the z-direction for all elements is arbitrarily chosen as 1 m. By symmetry, only half of the problem (the half-plane y > 0) needs to be modeled.

For a frequency of excitation of 4100 Hz. (ka = 8.6), we modeled the region with 128 elements spanning the 180 degrees of circumference. The outer fluid boundary (a circle of radius 1.026 m) was 1.44 acoustic wavelengths away from the shell. According to Kalinowski (Ref. 14), this amount of fluid should provide excellent absorption of outgoing waves.

A typical result for this problem is shown in Fig. 3, which shows a comparison of the surface scattered pressures calculated both by finite elements and by using an analytic expression presented by Junger and Feit (Ref. 38). The agreement is clearly excellent. Although the Junger-Feit solution used for comparison is a series solution (and hence another numerical approach), it makes no approximation concerning the radiation boundary condition. The agreement in Fig. 3 thus confirms that spurious boundary reflections are not contaminating the finite element solution for this problem.

Additional results for this problem (at frequencies both above and below that shown here) have been presented by Henderson (Ref. 17).

SCATTERING FROM FREE-FLOODED ELASTIC SHELL WITH RIGID INNER CORE

Here we derive the finite element formulation for scattering from a submerged elastic thin shell which contains water on the inside (as well as on the outside) of the shell and also contains a rigid inner core (Fig. 4).

The formulation of this problem proceeds along lines similar to that of the previous problem except that the fundamental fluid unknown in the inner fluid region is the total velocity potential rather than the scattered component of velocity potential as in the outer fluid region.
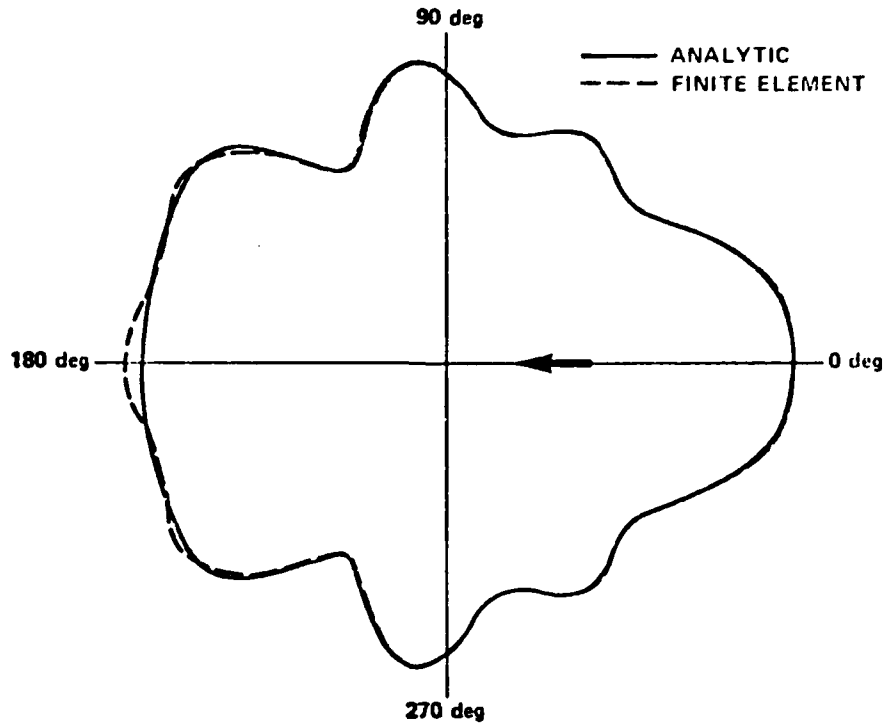
201

Figure 3 — Scattered Pressures on the Surface of an Infinite
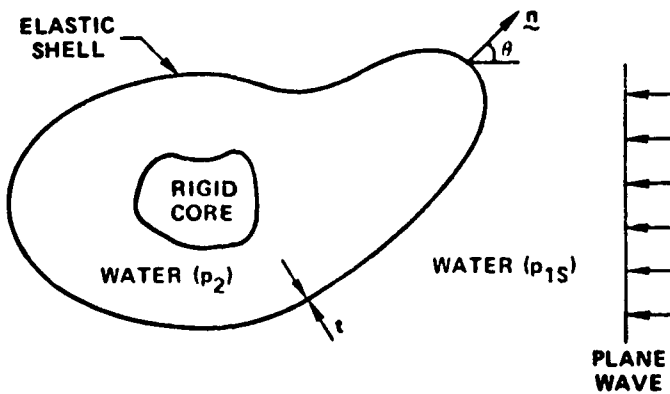Cylinder (ka = 8.6)

Figure 4 — Scattering from Free-Flooded Elastic Thin Shell
with Rigid Inner Core

Therefore, let p_{1s} denote the scattered pressure in the outer fluid region and p_2 denote the total pressure in the inner fluid region. Since the elastic shell is thin, the same shell variables interact with both inner and outer fluid regions. The main difference between the treatment of the two interfaces is that the normal n in Fig. 4 is an inward normal for the outer fluid and an outward normal for the inner fluid.

202

The generalization of Eq. (29) can then be written immediately as

$$
\begin{bmatrix} Q_2 & -A^T & 0 \\ 0 & M & 0 \\ 0 & A^T & Q_1 \end{bmatrix} \left\{ \begin{array}{c} \ddot{p}_2 \\ \ddot{u} \\ \ddot{p}_{1s} \end{array} \right\} + \begin{bmatrix} 0 & 0 & 0 \\ 0 & B & 0 \\ 0 & 0 & C \end{bmatrix} \left\{ \begin{array}{c} \dot{p}_2 \\ \dot{u} \\ \dot{p}_{1s} \end{array} \right\}
$$

$$
+ \begin{bmatrix} H_2 & 0 & 0 \\ -A & K & A \\ 0 & 0 & H_1 \end{bmatrix} \left\{ \begin{array}{c} p_2 \\ u \\ p_{1s} \end{array} \right\} = \left\{ \begin{array}{c} 0 \\ -Ap_1 \\ A\ddot{u}_{ni} \end{array} \right\} \qquad (37)
$$

where G_e has been specified as in Eq. (31), and we have assumed that the same area matrix A is used on both interfaces to convert pressures to forces.

This nonsymmetric system can also be symmetrized by reformulating the equations in terms of two new fluid variables q_1 and q_2 such that

$$
\dot{q}_1 = p_{1s}, \quad \dot{q}_2 = p_2 \qquad (38)
$$

As before, the nonsymmetric terms can be moved to the damping matrix by integrating the first and third partitions of Eq. (37) in time:

$$
\begin{bmatrix} Q_2 & 0 & 0 \\ 0 & M & 0 \\ 0 & 0 & Q_1 \end{bmatrix} \left\{ \begin{array}{c} \ddot{q}_2 \\ \ddot{u} \\ \ddot{q}_1 \end{array} \right\} + \begin{bmatrix} 0 & -A^T & 0 \\ -A & B & A \\ 0 & A^T & C \end{bmatrix} \left\{ \begin{array}{c} \dot{q}_2 \\ \dot{u} \\ \dot{q}_1 \end{array} \right\}
$$

$$
+ \begin{bmatrix} H_2 & 0 & 0 \\ 0 & K & 0 \\ 0 & 0 & H_1 \end{bmatrix} \left\{ \begin{array}{c} q_2 \\ u \\ q_1 \end{array} \right\} = \left\{ \begin{array}{c} 0 \\ -Ap_1 \\ Av_{ni} \end{array} \right\} \qquad (39)
$$

where, for both fluid regions, the material constants assigned to the finite elements are given by Eq. (34).

EXAMPLE 2:   SCATTERING FROM INFINITE CYLINDRICAL SHELL ENCLOSING A FLUID
BOUNDED BY A CONCENTRIC RIGID CYLINDER

The formulation derived in the preceding section will be illustrated on the
two-dimensional (plane strain) problem of scattering from an infinitely long cylin-
drical steel shell which contains on the inside both fluid and a concentric rigid
cylinder (Fig. 5). The rigid inner core has a radius of 0.254 m. The shell is
identical to that used in Example 1. Seawater floods the region between the shell
and the rigid inner core.
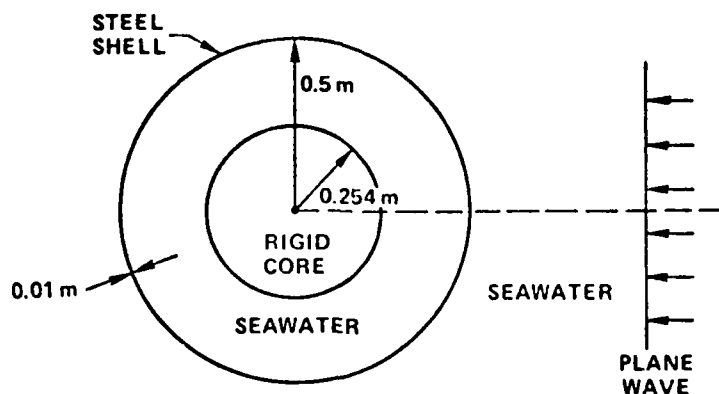
Figure 5 - Scattering from Infinite Cylindrical Shell Enclosing
a Fluid Bounded by a Concentric Rigid Cylinder

A finite element model was prepared for this problem for excitation at 2100 Hz.
(ka = 4.4). Since this frequency is lower than that used in Example 1, a coarser
mesh (having 96 elements spanning the 180 degrees of circumference) was used. Here,
the outer fluid boundary was a circle located 1.32 m away from the shell, a distance
equal to 1.85 wavelengths of the incident free-field acoustic wave.

For this problem, no analytic results were readily available for comparison, so
instead a comparison was made to the corresponding problem with the inside of the
shell evacuated (as in Example 1, but at a different frequency). See Fig. 6.
Clearly, the presence of the contained fluid and the inner core affect the solution
significantly.

Although the two cylinders in this problem were chosen to be concentric, the
formulation derived in the preceding section is clearly general enough to handle
arbitrary geometry. In addition, the formulation applies to both 2-D and 3-D prob-
lems.

RADIATED PRESSURES

A finite element model of an exterior fluid-structure interaction problem is
capable of predicting only near-field acoustic pressures because of the approximate
nature of the radiation boundary condition on the fluid. However, given fluid pres-
sures and normal velocities on the fluid-structure interface, the fluid pressure at
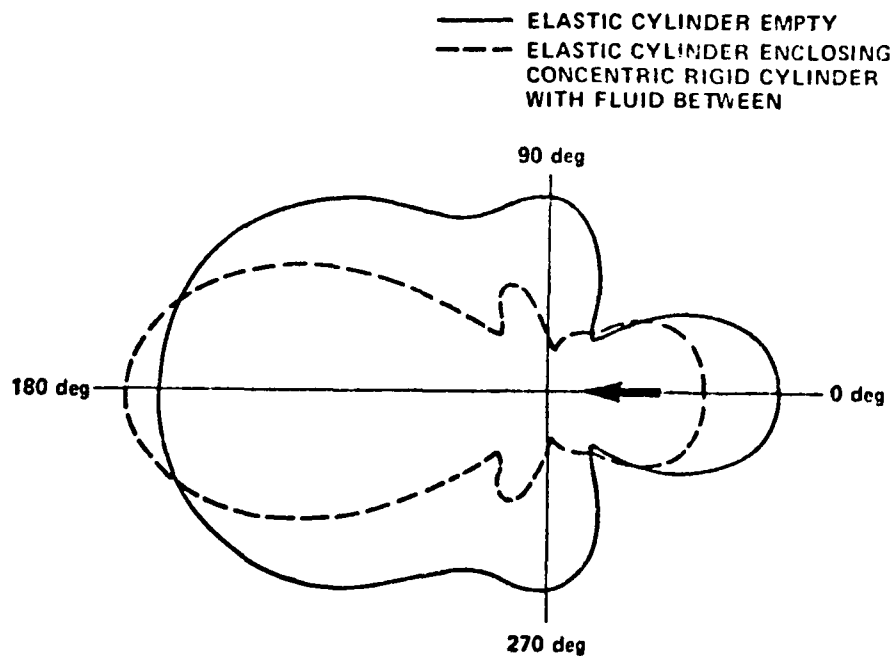any point in the exterior field can be calculated by a numerical quadrature.

204

Figure 6 — Comparison of Surface Pressures Scattered by an Evacuated
Cylinder with Pressures Scattered by a Cylinder Containing a
Fluid and a Concentric Rigid Cylinder (ka = 4.4)

In Fig. 7, let $\underline{z}$ be the position vector to an exterior field point P, and z = $|\underline{z}|$. Let $\underline{x}$ be the position vector to a point on the fluid-structure interface (with x = $|\underline{x}|$), let $\underline{r} = \underline{z} - \underline{x}$ (with r = $|\underline{r}|$), and let $\underline{n}$ be the unit outward normal at the location $\underline{x}$. The pressure at $\underline{z}$ is (Ref. 39)

$$p(\underline{z}) = - \int_S q(\underline{x})(e^{-ikr}/4\pi r)dS + \int_S p(\underline{x})\, \partial/\partial n(e^{-ikr}/4\pi r)dS \tag{40}$$

where

$$q = \partial p/\partial n = -i\omega\rho v_n \tag{41}$$

$$k = \omega/c \tag{42}$$

and it is assumed that the harmonic time-dependence of the variables is exp(iωt) rather than exp(−iωt).

Since

$$\partial/\partial n(e^{-ikr}/4\pi r) = (e^{-ikr}/4\pi r)(ik + r^{-1}) \cos \beta \tag{43}$$
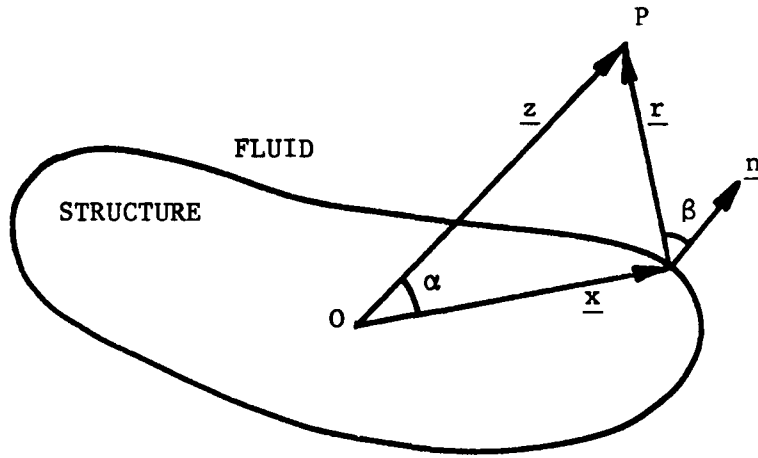
205

Figure 7 — Notation for Far-Field Radiated Pressure Calculations

it follows that

$$p(\underline{z}) = \int_S [i\omega\rho v_n(\underline{x}) + (ik + r^{-1}) p(\underline{x}) \cos \beta] (e^{-ikr}/4\pi r)dS \qquad (44)$$

This expression is valid for any point in the exterior field.

Eq. (44) can be simplified if only far-field locations are of interest. As $|\underline{z}| \to \infty$, $ik + r^{-1} \to ik$, and, from the law of cosines, $r \to z - x \cos \alpha$. Thus, at far-field locations,

$$p(\underline{z}) \cong (ik \, e^{-ikz}/4\pi z) \int_S [\rho c v_n(\underline{x}) + p(\underline{x}) \cos \beta]e^{ikx \cos \alpha} dS \qquad (45)$$

where

$$\cos \beta \cong (\underline{z}/|\underline{z}|) \cdot \underline{n} \qquad (46)$$

The numerical integrations in Eqs. (44) and (45) require, for each wet structural point, the knowledge of the location (coordinates), normal, area, pressure, and outward normal velocity. All these quantities can be obtained directly from NASTRAN using the OUTPUT2 utility module. The grid point coordinates and areas (or areal direction cosines) can be obtained from an abbreviated static analysis in which a unit outward pressure load is applied to the structure. The unit normal at a point is then the unit vector parallel to the area vector. The pressures and velocities are obtained from the frequency response analysis.

REFERENCES

1. J.T. Howlett and D.A. Morales, "Prediction of Light Aircraft Interior Noise," NASA TM X-72838, National Aeronautics and Space Administration, Washington, DC (1976).

2. D.J. Nefske, J.A. Wolf, Jr., and L.J. Howell, "Structural-Acoustic Finite Element Analysis of the Automobile Passenger Compartment: A Review of Current Practice," J. Sound and Vibration, 80(2), 247-266 (1982).

3. P.W. Eade and C.G. Stanworth, "Acoustic Aspects of Railway Vehicle Design," Proc. Inst. of Mech. Engr., Railway Div., 190, 58-76 (1976).

4. G.R. Khabbaz, "Dynamic Behavior of Liquids in Elastic Tanks," AIAA J., 9(10), 1985-1990 (1971).

5. J.T. Howlett, "Applications of NASTRAN to Coupled Structural and Hydrodynamic Responses in Aircraft Hydraulic Systems," NASTRAN: Users' Experiences, NASA TM-2378, National Aeronautics and Space Administration, Washington, DC, 407-419 (1971).

6. L.C. Davidson and D.R. Samsury, "Liquid-Structure Coupling in Curved Pipes - II," The Sound and Vibration Bulletin, 42(1), 123-136 (1972).

7. M.S. Marcus, "A Finite-Element Method Applied to the Vibration of Submerged Plates," J. Ship Research, 22(2), 94-99 (1978).

8. R.V. Raetz and G.C. Everstine, "Calculation of Natural Vibration Frequencies and Transient Response of Partially Submerged, Supercavitating Marine Propellers," DTNSRDC-81/051, David W. Taylor Naval Ship R&D Center, Bethesda, MD (1981).

9. G.C. Everstine, "A NASTRAN Implementation of the Doubly Asymptotic Approximation for Underwater Shock Response," NASTRAN: Users' Experiences, NASA TM X-3428, National Aeronautics and Space Administration, Washington, DC, 207-228 (1976).

10. T.L. Geers, "Doubly Asymptotic Approximations for Transient Motions of Submerged Structures," J. Acoust. Soc. Amer., 64(5), 1500-1508 (1978).

11. D. Ranlet, F.L. DiMaggio, H.H. Bleich, and M.L. Baron, "Elastic Response of Submerged Shells with Internally Attached Structures to Shock Loading," Computers and Structures, 7(3), 355-364 (1977).

12. H.C. Neilson, G.C. Everstine, and Y.F. Wang, "Transient Response of a Submerged Fluid-Coupled Double-Walled Shell Structure to a Pressure Pulse," J. Acoust. Soc. Amer., 70(6), 1776-1782 (1981).

13. H. Huang, G.C. Everstine, and Y.F. Wang, "Retarded Potential Techniques for the Analysis of Submerged Structures Impinged by Weak Shock Waves," in Computational Methods for Fluid-Structure Interaction, ed. by T. Belytschko and T.L. Geers, AMD-Vol. 26, American Society of Mechanical Engineers, New York, 83-93 (1977).

14. A.J. Kalinowski, "Fluid Structure Interaction," in Shock and Vibration Computer Programs: Reviews and Summaries, SVM-10, ed. by W. Pilkey and B. Pilkey, The Shock and Vibration Information Center, U.S. Naval Research Laboratory, Washington, DC, 405-452 (1975).

15. H. Huang, "Approximate Fluid-Structure Interaction Theories for Acoustic Echo Signal Prediction," NRL Memorandum Report 4661, U.S. Naval Research Laboratory, Washington, DC (1981).

16. S.K. Numrich, V.V. Varadan, and V.K. Varadan, "Scattering of Acoustic Waves by a Finite Elastic Cylinder Immersed in Water," J. Acoust. Soc. Amer., 70(5), 1407-1411 (1981).

17. F.M. Henderson, "Computation of Steady-State Scattered Sound from Submerged Infinite Cylinders by a Structural Analog Method," Report DTNSRDC-82/012, David W. Taylor Naval Ship R&D Center, Bethesda, MD (1982).

18. I.S. Sokolnikoff, Mathematical Theory of Elasticity, second ed., McGraw-Hill, New York (1956).

19. O.C. Zienkiewicz and R.E. Newton, "Coupled Vibrations of a Structure Submerged in a Compressible Fluid," in Proc. Internat. Symp. on Finite Element Techniques, Stuttgart, 359-379 (1969).

20. T.L. Geers, "Transient Response Analysis of Submerged Structures," in Finite Element Analysis of Transient Nonlinear Structural Behavior, AMD-Vol. 14, ed. by T. Belytschko, J.R. Osias, and P.V. Marcal, The American Society of Mechanical Engineers, New York, 59-84 (1975).

21. R.E. Newton, "Finite Element Analysis of Two-Dimensional Added Mass and Damping," in Finite Elements in Fluids, vol. 1, chap. 11, ed. by R.H. Gallagher, J.T. Oden, C. Taylor, and O.C. Zienkiewicz, Wiley, London, 219-232 (1975).

22. O.C. Zienkiewicz and P. Bettess, "Fluid-Structure Dynamic Interaction and Wave Forces: An Introduction to Numerical Treatment," Int. J. Num. Meth. in Engrg., 13(1), 1-16 (1978).

23. A. Craggs, "The Transient Response of a Coupled Plate-Acoustic System Using Plate and Acoustic Finite Elements," Journal of Sound and Vibration 15(4), 509-528 (1971).

24. G.C. Everstine, E.A. Schroeder, and M.S. Marcus, "The Dynamic Analysis of Submerged Structures," NASTRAN: Users' Experiences, NASA TM X-3278, National Aeronautics and Space Administration, Washington, DC, 419-429 (1975).

25. L. Kiefling and G.C. Feng, "Fluid-Structure Finite Element Vibrational Analysis," AIAA J., 14(2), 199-203 (1976).

26. A.J. Kalinowski, "Transmission of Shock Waves into Submerged Fluid Filled Vessels," in Fluid Structure Interaction Phenomena in Pressure Vessel and Piping Systems, PVP-PB-026, ed. by M.K. Au-Yang and S.J. Brown, Jr., The American Society of Mechanical Engineers, New York, 83-105 (1977).

27. M.A. Hamdi and Y. Ousset, "A Displacement Method for the Analysis of Vibrations of Coupled Fluid-Structure Systems," _Int. J. Num. Meth. in Engrg._, 13, 139-150 (1978).

28. G.C. Everstine, "A Symmetric Potential Formulation for Fluid-Structure Interaction," _J. Sound and Vibration_, 79(1), 157-160 (1981).

29. G.C. Everstine, "Structural Analogies for Scalar Field Problems," _Int. J. Num. Meth. Engrg._, 17(3), 471-476 (1981).

30. P.R. Zarda and M.S. Marcus, "Finite Element Solutions of Free Surface Flows," _Sixth NASTRAN Users' Colloquium_, NASA CP-2018, National Aeronautics and Space Administration, Washington, DC, 27-52 (1977).

31. J. Lysmer and R.L. Kuhlemeyer, "Finite Dynamic Model for Infinite Media," _J. Engrg. Mech. Div._, American Society of Civil Engineers, 95(EM4), Proc. Paper 6719, 859-877 (1969).

32. B. Engquist and A. Majda, "Radiation Boundary Conditions for Acoustic and Elastic Wave Calculations," _Comm. Pure Appl. Math._, 22, 313-357 (1979).

33. A. Bayliss, M. Gunzburger, and E. Turkel, "Boundary Conditions for the Numerical Solution of Elliptic Equations in Exterior Regions," Report No. 80-1, Institute for Computer Applications in Science and Engineering, NASA Langley Research Center, Hampton, VA (1980).

34. M. Israeli and S.A. Orszag, "Approximation of Radiation Boundary Conditions," _J. Comp. Phys._, 41, 115-135 (1981).

35. A.J. Kalinowski, "A Survey of Finite Element-Related Techniques as Applied to Acoustic Propagation in the Ocean. Part II: Transparent Boundary Simulation Techniques," _The Shock and Vibration Digest_, 11, 7-16 (1979).

36. A.J. Kalinowski and C.W. Nebelung, "Media-Structure Interaction Computations Employing Frequency Dependent Mesh Sizes with the Finite Element Method," _The Shock and Vibration Bulletin_, 51, Part 1, 173-193 (1981).

37. R.H. Cole, _Underwater Explosions_, Princeton University Press, Princeton, NJ (1948).

38. M.C. Junger and D. Feit, _Sound, Structures, and Their Interaction_, The MIT Press, Cambridge, MA (1972).

39. H. Lamb, _Hydrodynamics_, sixth edition, Dover Publications, New York (1945).

NONLINEAR ANALYSIS OF A BOLTED MARINE RISER

CONNECTOR USING NASTRAN SUBSTRUCTURING

Gary L. Fox
Hughes Offshore

Division of Hughes Tool Company

SUMMARY

Results of an investigation of the behavior of a bolted, flange type marine riser connector is reported. The method used to account for the nonlinear effect of connector separation due to bolt preload and axial tension load is described. The automated multilevel substructuring capability of COSMIC/NASTRAN was employed at considerable savings in computer run time. Simplified formulas for computer resources, i.e., computer run times for modules SDCOMP, FBS, and MPYAD, as well as disk storage space, are presented. Actual run time data on a VAX-11/780 is compared with the formulas presented.

INTRODUCTION

A marine riser is the equipment which connects an offshore drilling rig to the subsea wellhead control system on the ocean floor. The riser provides a conduit for various fluids and tools, as well as support for the control lines which run from the rig to wellhead. A riser consists of a series of lengths of pipe with connectors on each end. Axial tension load is applied to the riser by tensioners on the rig to prevent the riser from buckling and to resist ocean current. As offshore drilling depths have increased to over a mile, new riser connector designs have evolved to meet this need.

The analysis reported here is of a bolted, eliptical flange type of connector (HMF) with a rated axial load of 1.5 million pounds. The riser pipe is 18-5/8 inches outside diameter. The connector, shown in Figure 1, is characterized by 4 inch thick flanges and an outside diameter of 38-1/4 inches. The analysis must include the nonlinear effect which is introduced by the fact that the mating surfaces of the connector will support only a compressive type of loading. Bolt preload can cause the connector surface to separate at points remote from the bolt pressure area. The axial tension load will also tend to separate the connector. The solution technique reported here makes use of COSMIC/NASTRAN automated multistage substructuring. This capability provides an economical solution to very large models, such as the one described below

TECHNICAL APPROACH

The calculation of bolt preload stress and alternating stresses caused by cyclic loading of the riser connector requires an accurate understanding of how the pin/box/bolt interfaces behave under these load conditions. A solid (three-

dimensional) model of a 22.5 degree section of the connector was developed. The 22.5 degree "pie" section was taken in the region of the choke and kill line, as shown in Figure 2. The flange stiffness is lowest in this area, which provides a conservative assumption.

A practical limit is quickly approached, in terms of computer resources, when very detailed, three-dimensional solid models are required for an analysis. This restriction is relieved to some extent by using a technique called substructuring.

The substructure approach reduces the number of equations to be solved by modeling the structure as separate pieces. Each piece is modeled independently. Using matrix reduction techniques, an equivalent stiffness matrix is formulated with the degrees of freedom only of the boundaries of mating pieces. These reduced matrices are combined in the same manner as finite element stiffness matrices (hence referred to as superelements) to form a set of equations identical in form to the non-substructure case, but consisting of much fewer equations. After solution of the combined structures, the stresses in each of the individual pieces are rec vered separately.

In the case of the HMF connector, the pin, box, and bolt each make up a substructure. The boundary interfaces are the pin/box interface, the bolt/shoulder interface, and the bolt thread/box interface.

Mathematical Model Description

Separate finite element models were developed of the pin, box, and bolt. Hidden line plots of the finite element models of the pin, box, and bolt, showing the element boundaries, are presented in Figures 3, 4, and 5, respectively. Table I shows the substructure components along with the related number of elements, degrees of freedom (D.O.F.), and boundary degrees of freedom.

As can be seen from Table I, the use of substructuring reduces the number of degrees of freedom by a factor of 30 (from 23,753 to 789). It is with this reduced structure that the analysis proceeds during Phase II.

Boundary interface behavior is determined through the use of NASTRAN substructure multipoint constraints (MPC's), which is a method to impose constraints on the relative motion of grid points of different substructures. Bolt preload is applied as an equivalent thermal load. Axial load is applied as a pressure normal to box/riser pipe boundary.

Loads, Boundary Conditions, and Constraints

The loads consist of the bolt preload and the axial load applied to the coupling. Boundary conditions define the fixed end of the assembly to react the applied axial load, as well as cyclic symmetry boundary conditions. Constraints refer to the interface boundaries of the pin, box, and bolt. An axial tension load of 1.5 million pounds is applied to the connector. Results are presented for three bolt preloads; equivalent to 1.7, 2.5, and 3.3 million pounds.

Boundary conditions are applied to react the primary axial load and to provide symmetry constraints to the model. The pin/riser pipe interface (i.e., the analogues surface on the pin that the axial load is applied to on the box), is

211

constrained from moving in the axial direction only. Radial motion is allowed.

The symmetry boundary condition, for an axisymmetric load, is achieved by forcing the displacement of grid points lying on the two planes (i.e., 0 degrees and 22.5 degrees) to be zero in the direction normal to the surface. The local coordinate system used on the 22.5 degree boundary is rotated 22.5 degrees from the global coordinate system. This rotation is necessary since NASTRAN can only constrain grids along the local coordinate axes.

The interfaces between the pin, box, and bolt are controlled by substructure multipoint constraints. These constraints are defined in NASTRAN by the following equation:

$$\Sigma A_i U_i = 0 \tag{1}$$

where,

A_i = coefficient of ith degree of freedom

U_i = displacement of ith degree of freedom

For the case where two grids, numbers 1 and 2, are constrained to move together in the Z direction, equation (1) would be:

$$W_1 - W_2 = 0 \tag{2}$$

where,

$A_1 = 1$

$A_2 = -1$

W_i = displacement in the Z direction of ith grid

The finite element mesh for pin, box, and bolt are compatible in that the node points of the models along the mating surfaces are coincident in space. Each pair of nodes are coupled according to equation (2).

Solution Procedure

The substructure solution process is divided into three "phases" by NASTRAN; Phase I - Generation of each substructure, Phase II - Combining and reducing any number of times and then solving for the final substructure, and Phase III - Stress recovery of the individual substructures.

Two separate procedures are needed for the Phase II solution:

1. Determine equivalent thermal loads to achieve the desired bolt preload consistent with proper equilibrium forces, and

2. Determine the pin/box interface with both bolt preload and axial load applied consistent with proper equilibrium forces.

Both load conditions, when applied to the pin/bix/bolt assembly, cause certain portions of the surfaces to lose contact. This characteristic creates a nonlinear

212

influence in the solution. An iterative technique is adopted to solve this problem.

For each substructure, at the solution phase (i.e., Phase II of the substructure procedure), equilibrium forces (i.e., substructure single point constraint forces), are calculated by NASTRAN as

$$[F_e^{\ i}] = [K^i][X^i] - [F^i] \tag{3}$$

where,

$[F_e^{\ i}]$ = Equilibrium forces for the ith substructure

$[K^i]$ = Stiffness matrix for the ith substructure

$[X^i]$ = Solution vector for the ith substructure

$[F^i]$ = Load vector for the ith substructure

The solution for both load cases is started assuming that the mating surfaces are in complete contact and the solution for the combined substructures is obtained. The equilibrium forces are calculated according to equation (3). The equilibrium forces necessary are either tension or compression on the interface surface. Those forces that are tensile in nature are not allowed, so the constraint condition, equation (2), is removed for all degrees of freedom (D.O.F.) associated with the tensile load.

Removal of the constraints changes the stiffness matrix in equation (3). With the constraints removed from the selected D.O.F., a new Phase II solution is obtained. The process is repeated until equilibrium is obtained, i.e., all interface forces are compressive. With equilibrium established in the Phase II solution, stress recovery in Phase III can then be accomplished.

Results of Analysis

The results of the Phase II solution illustrate the nonlinear characteristics of the solution. The stress recovery in Phase III is straight forward and not included in this paper.

The equilibrium condition for bolt preload of 1.7, 2.5, and 3.3 million pounds resulted in the same contact surface of the bolt. The contact surface is shown as the shaded area in Figure 6. The effective diameter, as calculated in accordance with equations presented in Reference 1, are shown for comparison. Figure 6 graphically illustrates the effect of the proximity of the choke and kill lines. The flange stiffness, which is proportional to contact area, is less than predicted by the classical method. However, the actual alternating stresses in any of the bolts will be less than that calculated by the finite element model. This is due to the modeling assumptions. The four bolts that are next to the choke and kill lines have a stiffer flange than the model, because the model symmetry implies a choke and kill line on both sides of the bolt. The remaining four bolts have flange stiffnesses even higher since these lie between hydraulic lines which are smaller in diameter than the choke and kill lines.

213

The applied axial load of 1.5 million pounds is applied to the box while the pin was restrained. Due to the eccentric nature of the load, the head of the bolt bends and some contact is lost between the pin and the box. The solution procedure, as in the bolt-up load condition, is iterative due to this nonlinearity.

The contact areas for bolt preloads of 1.7, 2.5, and 3.3 million pounds are shown in Figures 7, 8, and 9, respectively. Note that as the bolt preload increases, the contact area increases and moves inward. This causes an increase in the effective flange stiffness and reduces the amount of bending in the bolt. Both of these effects reduce the alternating peak stress in the bolt caused by the axial load as bolt preload is increased.

RESOURCE ESTIMATES

In order to determine the most cost effective substructure method, it is necessary to calculate computer resource requirements; computer run time and disk storage. The documentation available, References 2 and 3, provide some guidance in this area. However, the timing equations presented in these documents are complex, and is some cases, are apparently in error. Simplified timing equations are presented for the operations which, in the analysis presented, Static Analysis (Solution 1), Phase I, II and III substructuring comprise the overwhelming majority of computer run time.

Computer run time, using a VAX-11/780 with a floating point accelerator (FPA), was used for the analysis. The timing equations should prove to be quite general since the TIMETEST module in NASTRAN was used to provide the timing constants. The operations discussed below are symmetric decomposition (SDCOMP module), forward-backward substitution (FBS module), and matrix multiply and add (MPYAD module).

Symmetric Decomposition

Symmetric decomposition time can be significant in both Phase I and Phase II. In Phase I, the calculation of the substructure stiffness matrix, K_{aa}, requires the decomposition of K_{oo},

$$K_{aa} = \bar{K}_{aa} + K_{oa}{}^T G_{oa} \tag{4}$$

where the Guyan transformation matrix, G_{oa};

$$G_{oa} = K_{oo}{}^{-1} K_{oa} \tag{5}$$

is formed by forward-backward substitution. This process is also performed if multipoint constraints are called for in case control.

Similar reductions are available in Phase II. The matrices are smaller, but very dense. For these calculations the average bandwidth, C, is essentially equal to N/2. The BANDIT program, Reference 4, can be used as an effective means to find C in Phase I. A more costly method is to use a small value on the TIME card that will cause NASTRAN to abort the decomposition process after SDCOMP time is calculated. A time estimate will be printed out and the solution terminated.

Time estimates for symmetric decomposition, assuming that no spill occurs, is (Reference 3, Section 14):

$$T_{sdc} = .5T_m NC^2 + T_b NC \qquad (sec) \qquad (6)$$

where,

T_b = Time/word to pack and write elements of a matrix (sec/word)

T_m = Medium loop multiply, an average of loose loop and tight loop multiply (sec/ele)

N = Order of the matrix (degrees of freedom) K_{oo}

C = Average bandwidth of matrix K_{oo}

The first item is multiplication time, usually double precision; the second item is I/O time.

Forward-Backward Substitution

Immediately after decomposition of K_{oo}, the forward-backward substitution process, (FBS), is initiated to form the G_{oa} transformation matrix. No timing checks are made by NASTRAN on this operation, however, the time involved can be substantial. The time for symmetric FBS is estimated as (Reference 3, Section 14):

$$T_{fbs} = 2T_m PNC + T_b N(2C + P/2) \quad sec. \qquad (7)$$

where,

P = degrees of freedom in the "A" set, i.e., the order of K_{aa}

The first item is multiply time (two operations forward and backward) and the second item is I/O (P is read only once, but N*C is written twice).

Matrix Multiply

Time estimates for matrix multiply and add (MPYAD) is most troublesome for a number of reasons:

1. NASTRAN will automatically pick one of three very different methods depending on the characteristics of the matrices.

2. I/O time is strongly dependent on matrix characteristics but is considered completely described by the matrix trailers. In particular, the matrix density is used to calculate how many columns must be processed; a very rough approximation. I/O time can be the dominant factor in MPYAD.

3. Each of the three matrix processing routines are quite complex. Some require multiple passes if a matrix does not fit in core. It is common for a matrix not to fit even in the very large virtual core than the VAX can provide.

In spite of these difficulties a simplified approximation is offered here. Assume that the matrix multiply and add is described by

$$[A][B] + [C] = [D] \tag{8}$$

Use the Method 1 time estimated provided in Reference 2, Section 3.5.12.4:

$$T_{mpy} = \rho_a R_a C_a C_b \qquad T_m \qquad \text{(multiply time)} \tag{9}$$

$$N_p(\rho_a R_a + 5)C_a \ T_i \qquad \text{(interpretive unpack A)}$$

$$.5(1 + \rho_b)R_b C_b \ T_u \qquad \text{(unpack B)}$$

$$.5(1 + \rho_d)R_a C_b \ T_p \qquad \text{(pack D)}$$

$$.5(1 + \rho_c)R_a C_b \ T_u \qquad \text{(unpack C - if present)}$$

where,

R_i, C_i = number of rows or columns in matrix "i"

T_i = interpretive unpack   sec/word

T_u = unpack   sec/word

T_p = pack   sec/word

T_m = multiply time   sec/operation

N_p = number of passes to interpretive unpack B

and:

$$N_p \cong \frac{(R_a + C_a) * \ C_b}{\text{OPEN CORE/WORDS PER ELEMENT}} \tag{10}$$

where open core is the number of words in open core (set diagnostic no. 13 in the executive control deck to find this number) and words per element are 1 and 2 for single precision and double precision, respectively.

Repeat the calculation for the transpose of equation (9) by interchanging R_a and C_b, C_a, and R_b, ρ_a and ρ_b pick the smallest of the two times.

The reader is cautioned that equation (9) will only provide an order of magnitude due to the complexities of the operation.

Disk Storage Space

Disk storage space, including the substructure operating file (SOF) is dominated by the G_{oa} matrix since the matrix density is 100% and the boundary D.O.F. are usually numerous. It is worthwhile to calculate ahead of time this space for planning purposes. For example, up to ten physical files may be used for the single SOF logical file. One may wish to limit each physical file such that a single tape or mountable disk pack would be adequate for back-up storage.

The G_{oa} size is simply

$$W_{Goa} = 2 * N * P \quad \text{words}$$

where double precision has been assumed.

216

COMPUTER TIME COMPARISONS

Computer time estimates are based on data obtained from the TIMETEST module with the outer loop, N, equal to 100 and the inner loop, M, equal to 1,000. The timing parameters, shown in Table II, are those which NASTRAN uses and is found in NTMXBD data block. A VAX-11/780 with a floating point accelerator (FPA) was used.

SDCOMP Module

Table III gives a comparison of actual time expended in the SDCOMP module vs. that calculated by equation (4) for various size matrices. Note that as the time increases so does the error in the estimate. This may indicate a stronger depen-- dence on C than was assumed. To be conservative one should add 50% to the estimated time.

FBS Module

Table IV gives a comparison of actual time in the FBS module vs. that calculated by equation (7) for various size matrices. Again, to be conservative, one should add 20% to the estimated time. If NASTRAN finds that all the time has been expended in FBS and SDCOMP, she terminates without checkpointing first; the time is lost.

MPYAD Module

Table V compares both estimated times (remember to pick the smallest) for the MPYAD module vs. actual times. The examples given are characteristic of Phase I, II, and III operations and include all five possible NASTRAN MPYAD options. An educated guess must be made at the densities of the matrices involved. The following densities are suggested:

Phase I: $G_{oa} = 1.0$

$\bar{K}_{aa} \cong 0.1 - 0.25$

$K_{oa} \cong 0.005 - 0.05$

Phase II: $K_{aa} = 1.0$

$H \cong R_b$ / Number of rows in H = order of K

where,

R_b = Substructure DOF / Combined DOF

Phase III: $G_{oa} = 1.0$

$U_a = 1.0$

$P_o = 0 - 1.0$

It is assumed that a program like BANDIT, Reference 4, has been used. NASTRAN internal BANDIT was not used in this analysis.

The matrix multiply times generally are within a factor of two; indicating that one would want to double the time estimate to be safe. The sole exception is

Case No. 3, which is off by nearly an order of magnitude. Comparing this time to Case No. 4, it is possible that if Method 2 had been used the time would match more closely. All five possible methods are included for comparison; Method 3 is only available for the transpose case. Table VI provides a breakdown of the preferred time estimate into the five components. Note that I/O time is often significant. Table VII provides the matrix characteristics and typical operations for the three phases.

CONCLUDING REMARKS

Use of substructure multipoint constraints provides an effective means to model contacting surfaces of separate substructures. The single point constraint forces let the analyst check for proper equilibrium conditions. Nonlinear effects can be accounted for by repeated analysis until equilibrium is satisfied. The method used converged reasonably quickly, requiring about 8 iterations for each of the 4 solutions; the bolt preload condition, 3 bolt preloads plus axial load.

The number of iterations required for each solution was 8, a total of 32 for the entire analysis. Without substructuring, approximately 30 hours per iteration or 900 hours of computing time would have been required. By using substructuring, the computer time was reduced to less than 90 hours, a factor of ten in cost reduction. This calculation assumes that SDCOMP will not use spill logic for decomposition of the combined model. Numerical error is also a concern; with a 64 bit word length, matrices over about 10,000 D.O.F. are risky (Reference 5).

It is imperative that a small model be analyzed, start to finish, and checked for correctness, not just completion. Subcase structures in particular must be compatible. With thermal loads, it was found that in Phase II, additional subcases could be added that are linear combinations of Phase I loads. In Phase III, new loads and temperature subcases, corresponding exactly to those in Phase II, must be used. This will cause NASTRAN to re-generate the proper thermal loads but not decompose the stiffness matrix. Do not change the loads in subcases defined in Phase I, NASTRAN will not re-calculate the thermal loads. The solution will complete normally but the answers will be incorrect!

The FBS module is the dominant factor in computer run time for substructuring, assuming that there is no core spill in the SDCOMP module. It is recommended that the substructures be small enough to avoid spill logic in SDCOMP since, if not – according to Reference 3, quantum increases in computer time will result.

It appears that a large number of small substructures is most cost efficient from a computer run time standpoint. This must be traded off against the loss in labor and clock time efficiency caused by additional bulk data generation and bookkeeping. For example, each substructure must have a specified boundary and, it multiple stages are used, boundary sets for each stage may be specified.

REFERENCES

1. Moyer, M.C., and Marshek, K.M., An Investigation of Stresses in Bolted Connectors for Marine Risers, Journal Energy Resources Technology, Trans ASME V104 n 1, March 1982, pp. 84-90.

2. The NASTRAN® Programmer's Manual, (Level 17.5), December 29, 1980, National Aeronautics and Space Administration, Publication NASA SP-223(05).

3. Field, E.I., Herting, D.N., and Morgan, M.J., NASTRAN® User's Guide, NASA Contractor Report 3146, June 30, 1981.

4. Everstine, Gordan C., The BANDIT Computer Program for the Reduction of Matrix Bandwidth for NASTRAN®, Naval Ship Research and Development Center, Bethesda, Maryland, Report 3827, March 1972.

5. MacNeal, R., et al., The NASTRAN® Theoretical Manual, National Aeronautics and Space Administration, Washington, D.C., Publication NASA SP-221(06), January 1981.

6. The NASTRAN® User's Manual, (Level 17.5), National Aeronautics and Space Administration, Publication NASA SP-222(05), December 29, 1980.

TABLE I

CHARACTERISTICS OF THE THREE BASIC SUBSTRUCTURES

NAME	D.O.F.*	ELEMENTS	BOUNDARY D.O.F.
Pin	10,923	4,474	235
Box	6,407	1,824	359
Bolt	6,423	1,920	159
Total	23,753	8,218	789

*After removal of symmetry boundary D.O.F.

220

TABLE II

VAX-11/780 TIMING CONSTANTS

ITEM*	TIME (micro-sec)	DESCRIPTION
1	15.6	Average of Read, Write, and Backward Read/Word
2 (T_b)	1200	Pack and Write elements of a column
3 (T_i)	1277	Read and Unpack elements of a column
4 (T_p)	49.5	Pack and Write entire column
5 (T_u)	112	Read and Unpack entire column
6	31	Read a string from buffer
7	31	Write a string to buffer
8	8	Real Single Precision (RSP)
9	13.5	Real Double Precision (RDP)
10	23	Complex Single Precision (CSP) $\Big\}$ Tight Loop Multiply (T_t)
11	42	Complex Double Precision (CDP)
12	10	RSP
13	16.5	RDP $\Big\}$ Loose Loop Multiply (T_ℓ)
14	26.5	CSP
15	44	CDP

* Position in NTMXBD data block; $T_m = \frac{1}{2}(T_t + T_\ell)$

221

TABLE III

COMPARISON OF SDCOMP TIMES

(VAX-11/780 with FPA)

N	C†	TIME (MINUTES)			
		ARITH*	I/O*	TOTAL*	ACTUAL
250	125	0.48	0.62	1.10	0.92
291	131	0.62	0.76	1.38	1.85
3139	299	35.1	18.8	53.9	54.5
3268	274	30.7	17.9	48.6	51.8
4159	372	71.9	31.0	102.9	133.1
4202	422	93.5	35.5	129.0	192.4
6270	289	65.5	36.2	101.7	100.4
9652	494	294.7	95.5	390.2	589.1

* Calculated with T_m = 15E-6, T_b = 1200 E-6;

† C is average bandwidth from NASTRAN message 3023

TABLE IV

COMPARISON OF FBS TIMES

(VAX-11/780 with FPA)

N	C[†]	P	TIME (MINUTES)			
			ARITH*	I/O*	TOTAL*	ACTUAL
250	125	4	0.06	1.26	1.32	0.12
291	131	248	4.72	2.24	6.96	6.08
3139	299	294	138.0	46.8	184.8	154.7
3268	274	323	144.6	46.4	191.0	160.8
4159	372	841	650.6	96.9	747.5	769.5
4202	422	814	721.7	105.1	826.8	868.8
6270	289	153	138.6	82.1	220.7	154.6
9662	494	235	560.8	213.6	774.4	617.5

* Calculated with $T_m = 15E-6$, $T_b = 1200 E-6$;

† C is average bandwidth from NASTRAN message 3023

223

TABLE V

COMPARISON OF MPYAD TIMES (Seconds)

(VAX-11/780 with FPA)

| CASE | TIME EST. | | METHOD* USED | ACTUAL TIME |
	AB + C	$B^T A^T + C^T$		
1	1305	154	3-T	143
2	1267	149	1-NT	289
3	20	465	1-T	135
4	699	26	2-NT	22
5	167	3303	2-T	262
6	1292	151	3-T	145

* See References 2 and 3 for a description of the methods; T means that the A matrix is to transposed; times are in seconds.

224

TABLE VI

TIME ESTIMATE COMPONENTS FOR BEST CASE (Seconds)

TERM	CASE					
	1	2	3	4	5	6
1-Multiply time	4.3	38.8	0.67	1.89	9.71	2.12
2-Interpritive Unpack Matrix A (B^T)	42.7	1.6	2.24	2.24	46.04	41.35
3-Unpack B (A^T)	107.4	107.4	9.68	12.87	107.4	107.4
4-Pack D	0.02	0.93	7.1	9.44	1.16	0.02
5-Unpack C	0.00	0	0.0	0.0	2.62	0
TOTAL	154	149	19.7	26.45	167	151

TABLE VII

MATRIX OPERATIONS AND MATRIX CHARACTERISTICS

MPYAD MODULE

PHASE	CASE	OPERATION*	R_a	C_a	ρ_a	R_b	C_b	ρ_b	ρ_c
III	1	$G_{oa}{}^T P_o + \bar{P}_a$	153	6270	1.000	6270	3	0.11	1.000
	2	$G_{oa}\ U_a + \bar{U}_o$	6270	153	1.000	153	3	1.000	1.000
II	3	$H^T K_{aa}$	488	294	0.002	294	294	1.000	0
	4	$(H^T K_{aa})\ H$	488	294	0.602	294	488	0.002	0
I	5	$K_{oa}{}^T G_{oa} + \bar{K}_{aa}$	153	6270	0.005	6270	153	1.000	0.100
	6	$G_{oa}{}^T P_o + P_a$	153	6270	1.000	6270	2	0.082	1.000

* See Reference 6 for a description of the matrix operation.

226

PIN

BOLT

BOX
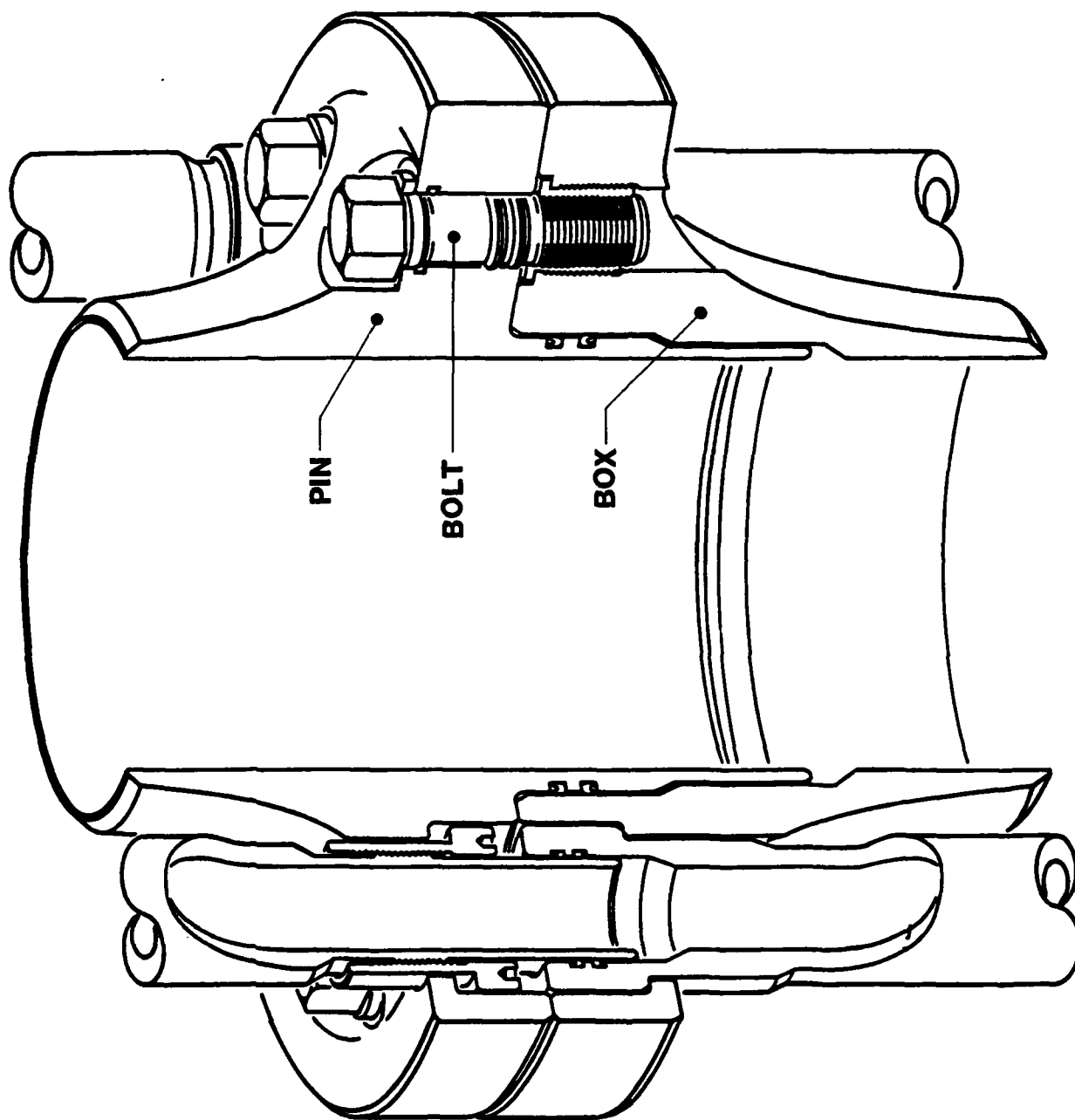
FIGURE 1 - HMF RISER CONNECTOR

227

CHOKE AND KILL LINES (2 AT 180°)

LOCKING BOLT THREADS
8 PLCS EQ SPACED

HYDRAULIC LINES
4 PLACES

22.5°
SECTION

18 5/8

TENSILE LOAD
38,717 PSI

11 WALL 16

32.625 DIA X 13.0 DIA
ELLIPSE

SECTION A—A

38.250
O.D.
REF
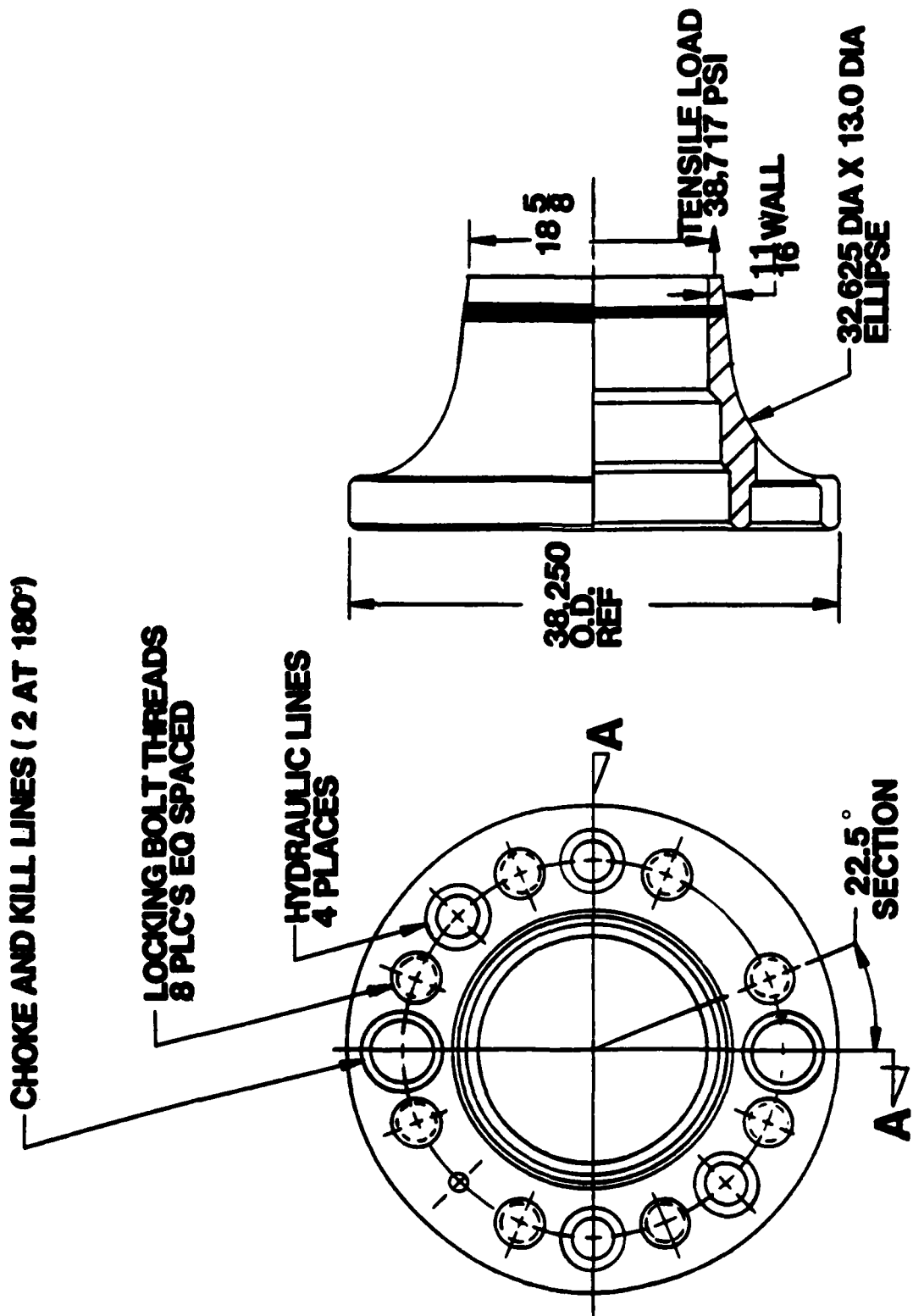
FIGURE 2 – CROSS SECTION OF HMF RISER CONNECTOR
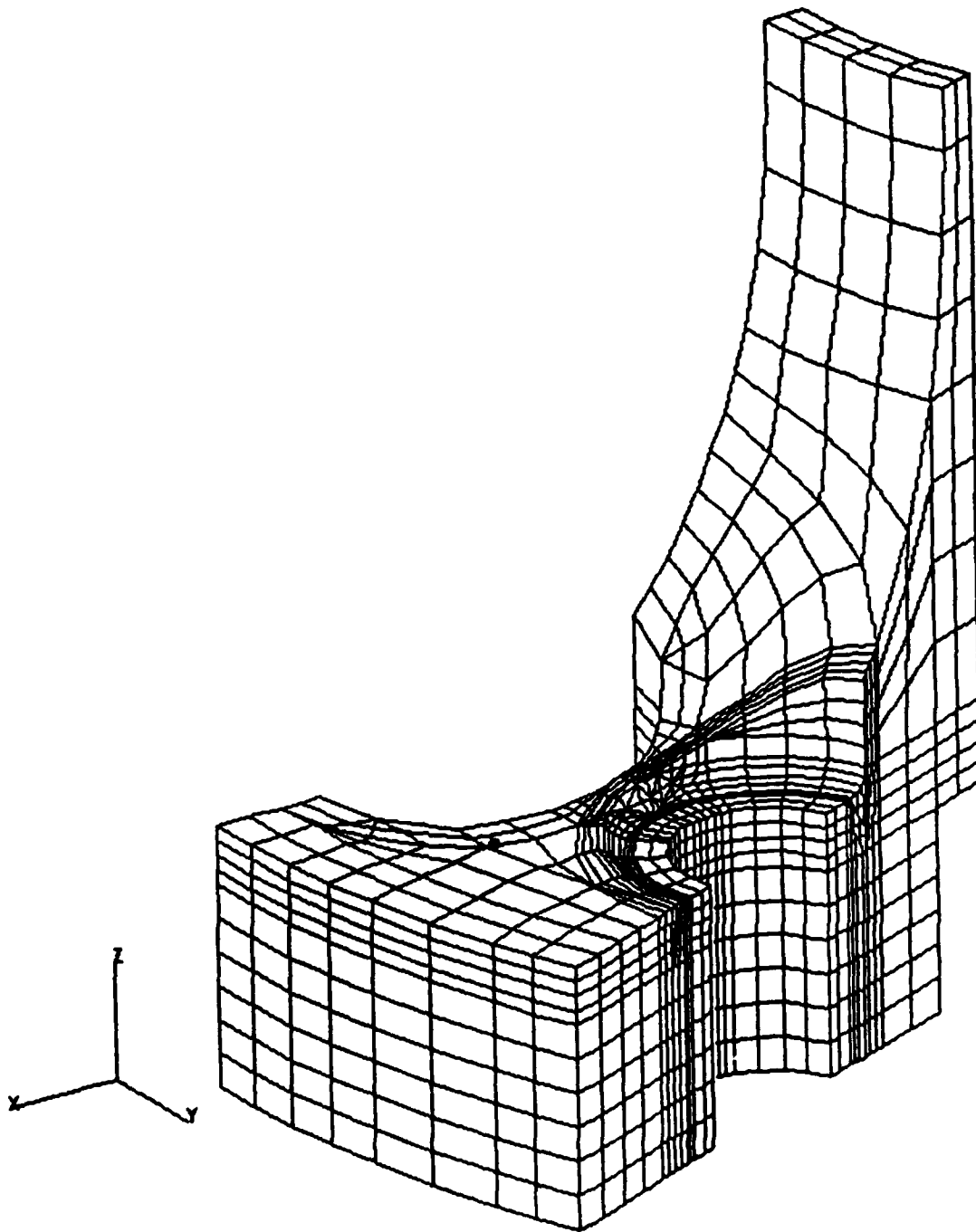
FIGURE 3 - HIDDEN LINE VIEW OF HMF PIN, 22.5° PIE SECTION

229
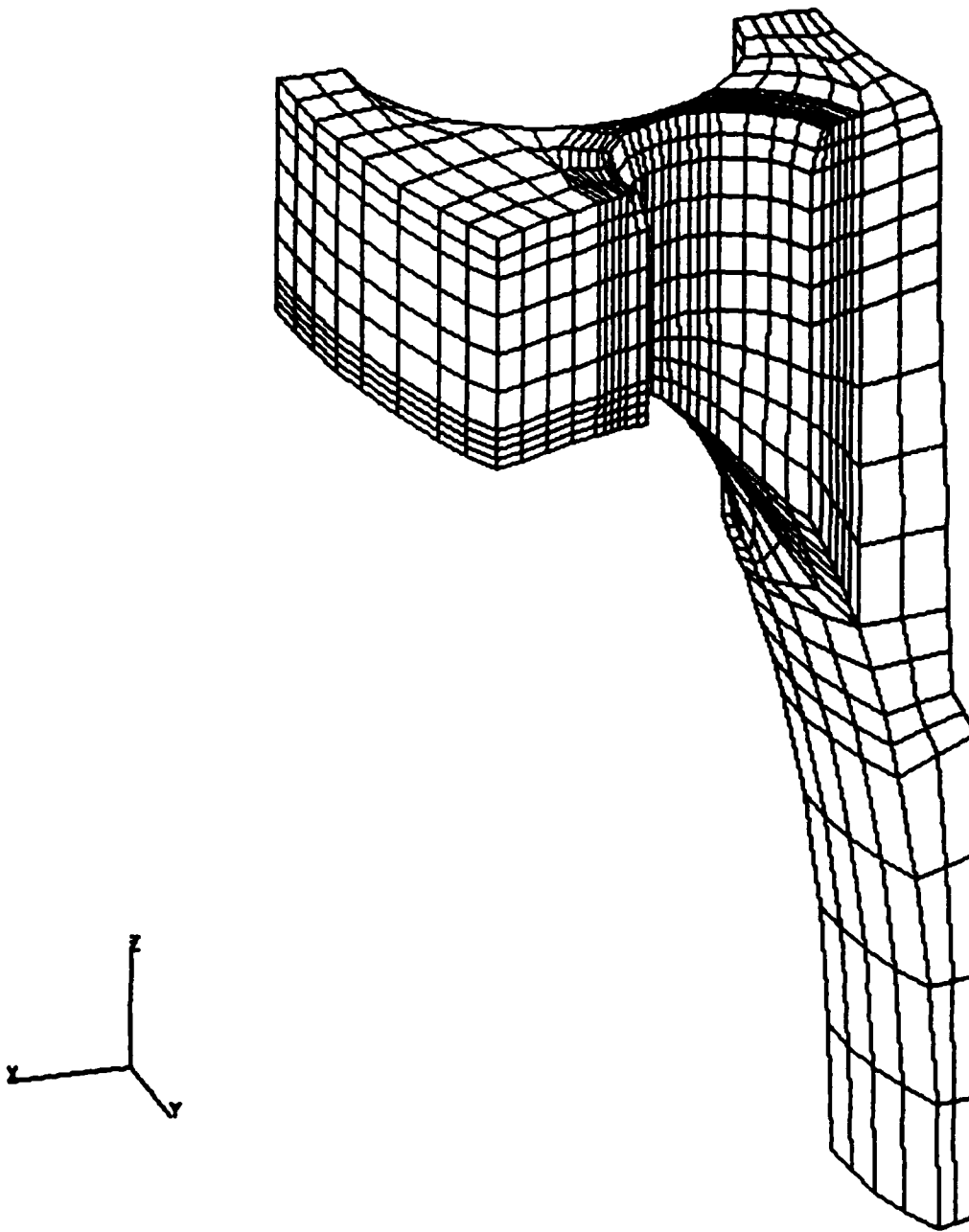
FIGURE 4 - HIDDEN LINE VIEW OF HMF BOX, 22.5° PIE SECTION
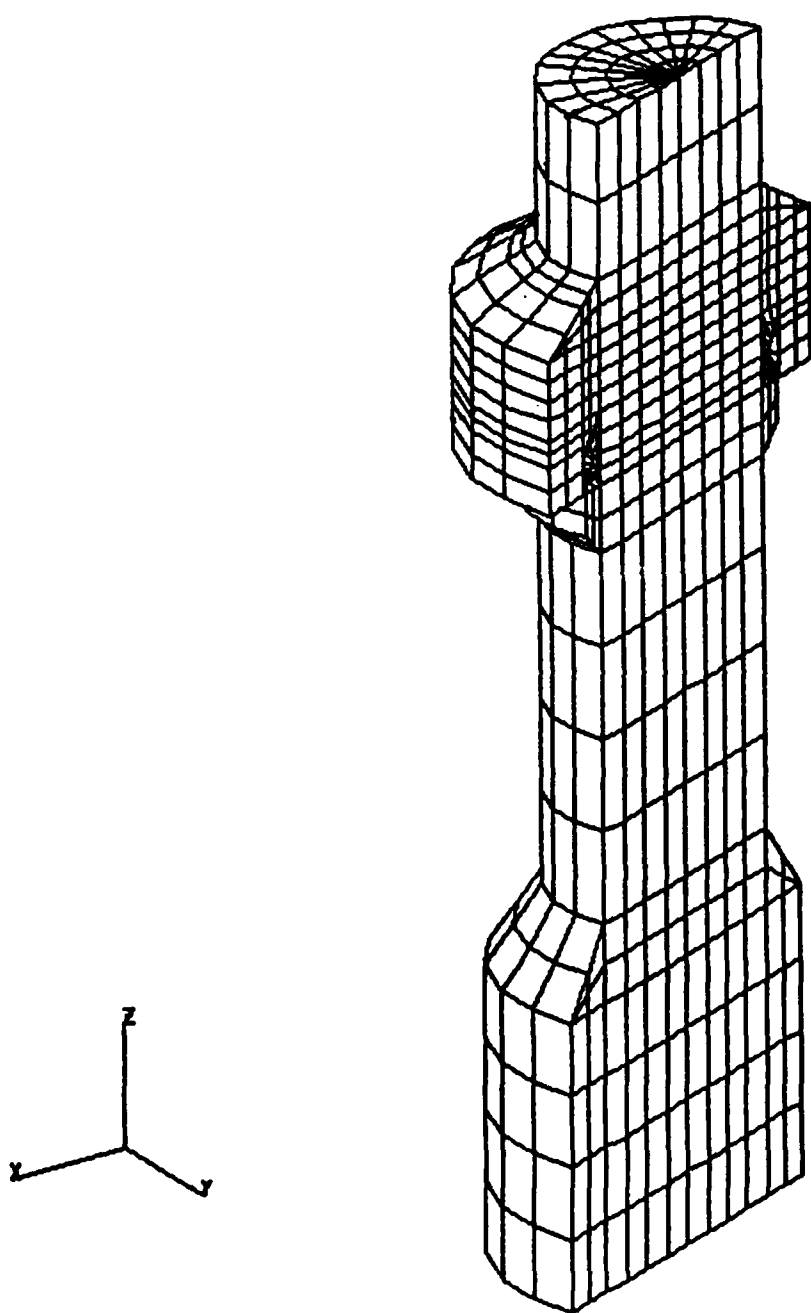
FIGURE 5 - HIDDEN LINE VIEW OF HMF BOLT, 22.5° PIE SECTION

231

$3D_H$

$\dfrac{H + C}{2}$

$H + \dfrac{L}{10}$
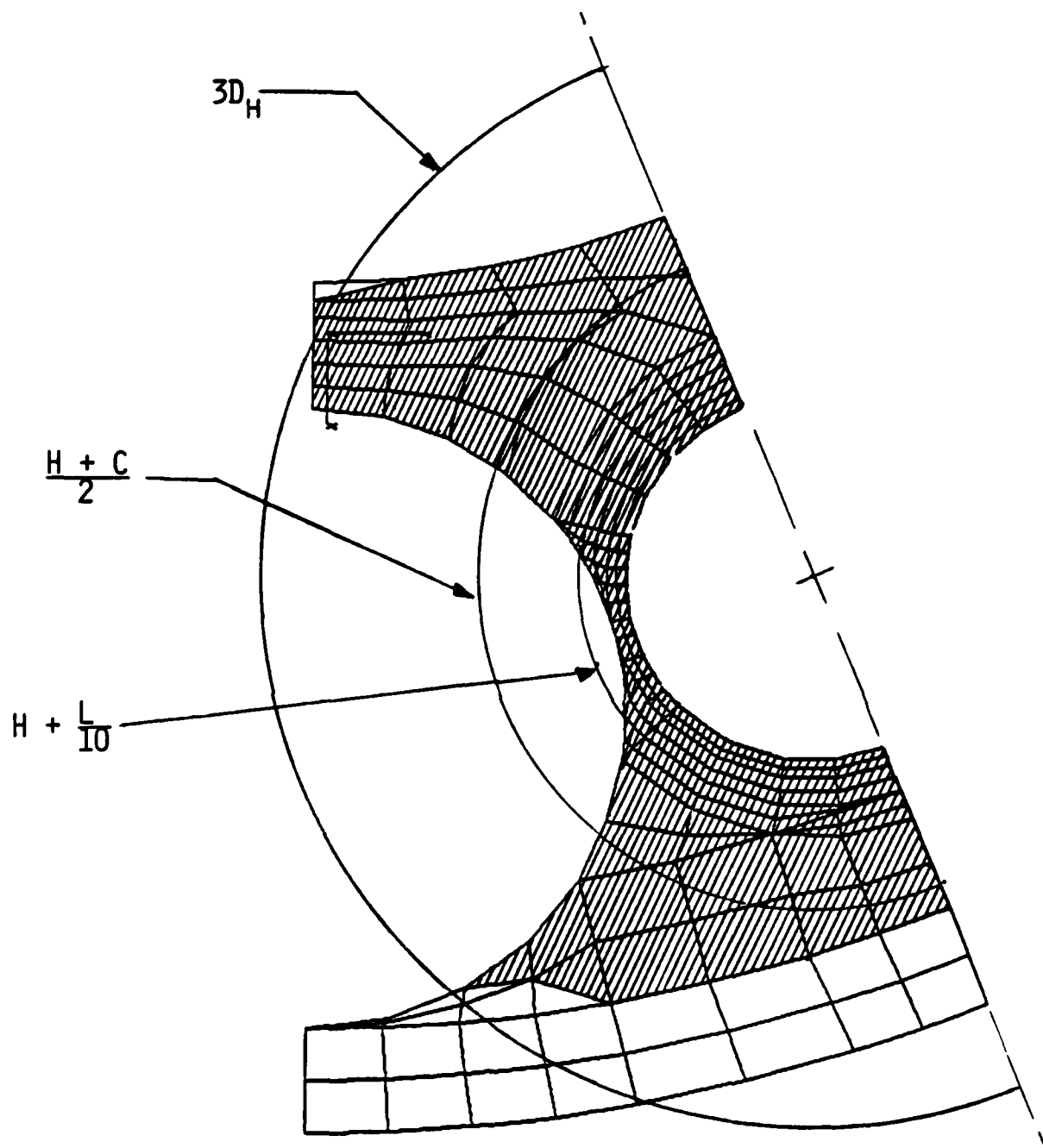
FIGURE 6 – PIN/BOX CONTACT WITH BOLT PRELOAD ONLY
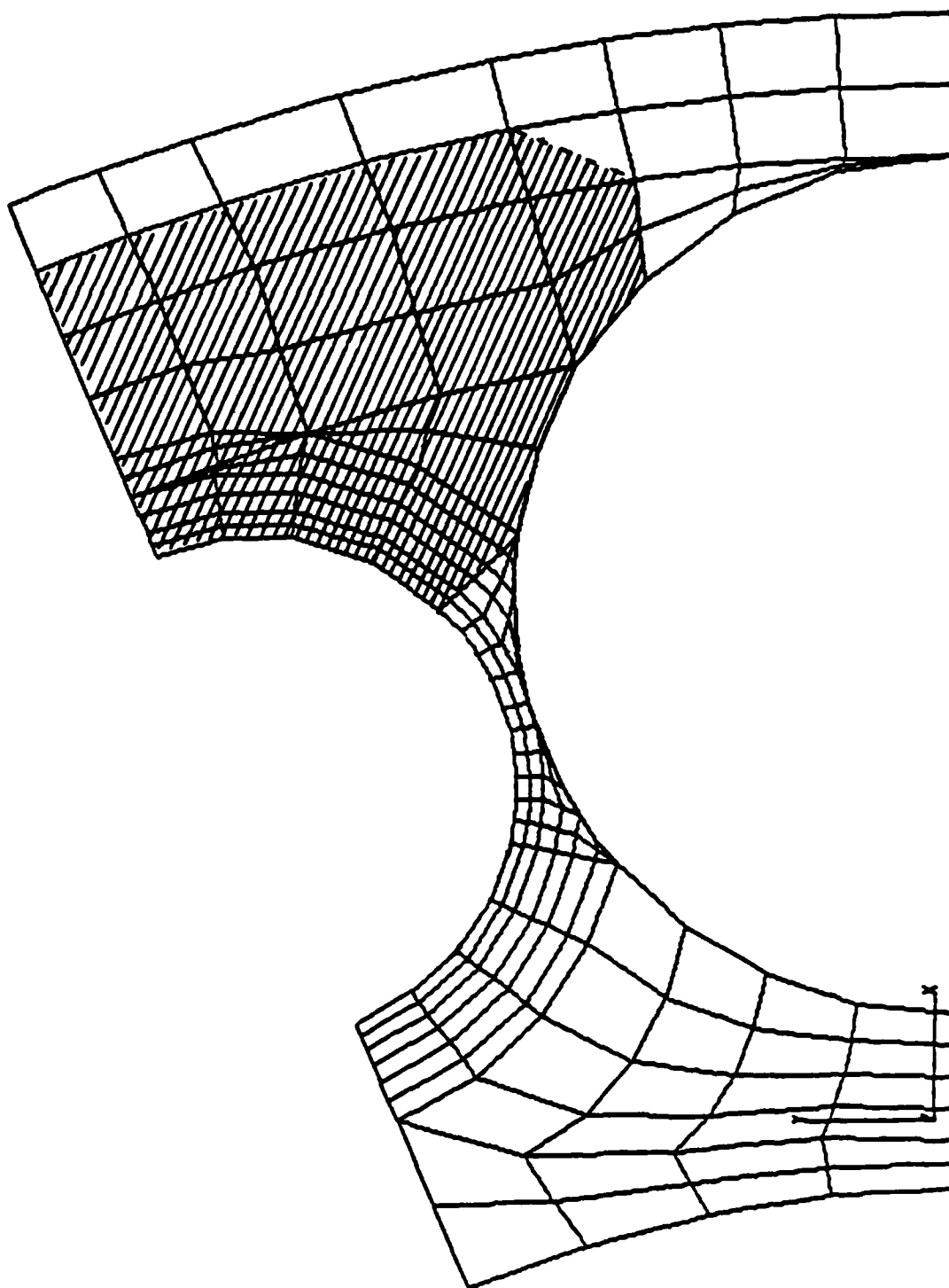
FIGURE 7 - CONTACT AREA FOR 1.7 M LBS. BOLT PRELOAD
AND 1.5 M LBS. AXIAL LOAD

233
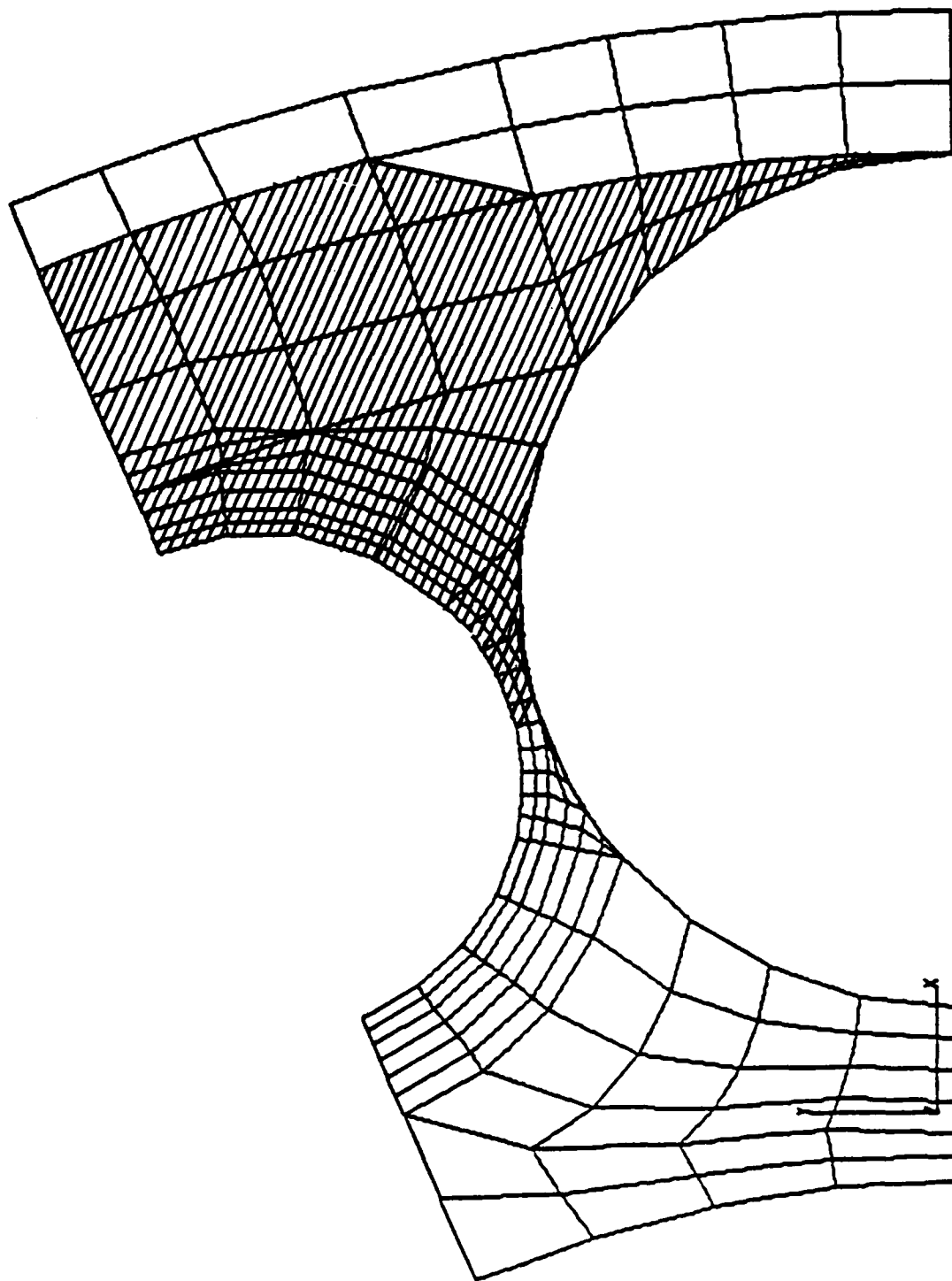
FIGURE 8 – CONTACT AREA FOR 2.5 M LBS. BOLT PRELOAD AND 1.5 M LBS. AXIAL LOAD
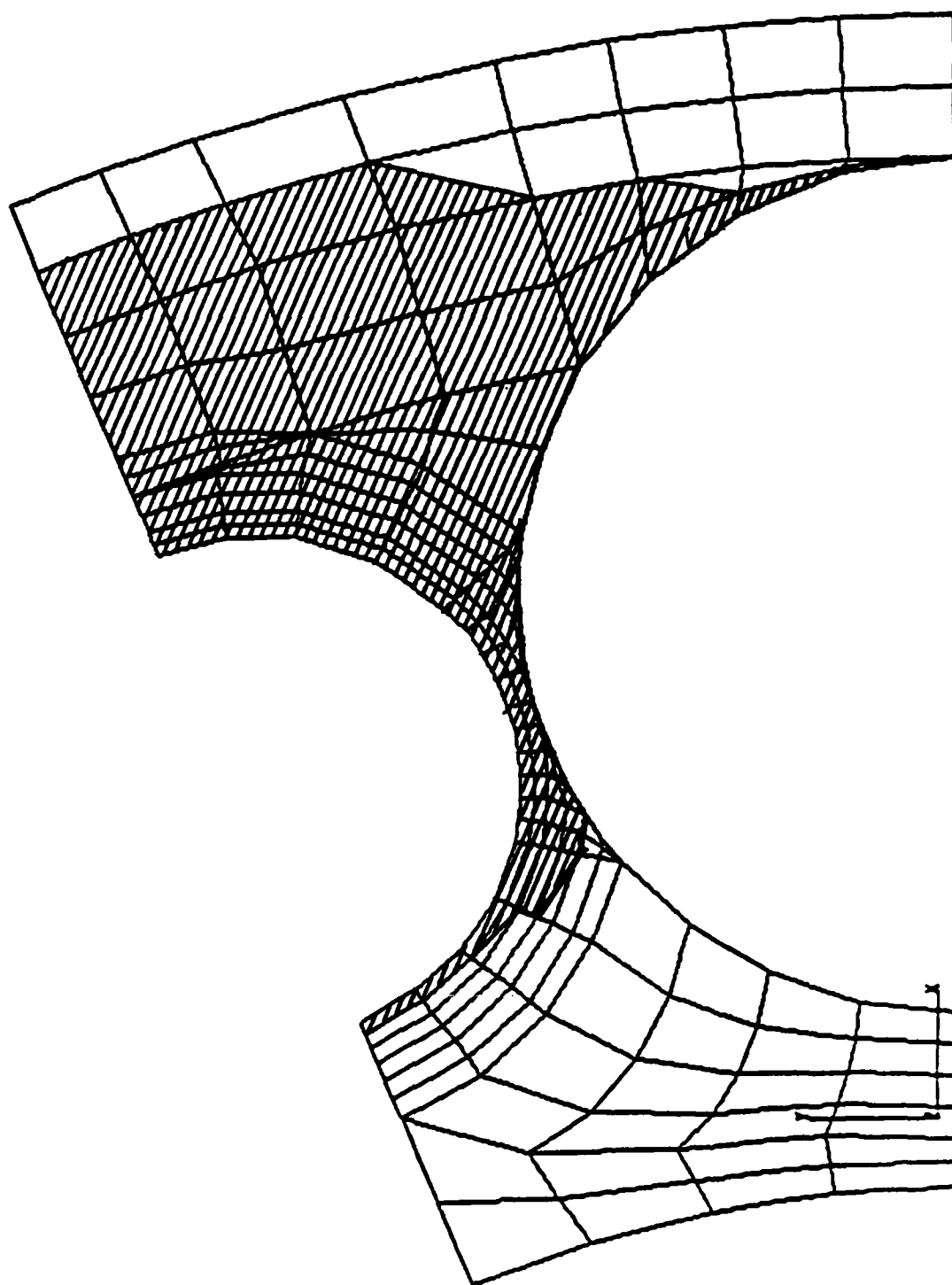
FIGURE 9 - CONTACT AREA FOR 3.3 M LBS. BOLT PRELOAD
AND 1.5 M LBS. AXIAL LOAD

236

FOUR NEW CAPABILITIES IN NASTRAN FOR

DYNAMIC AND AEROELASTIC ANALYSES OF

ROTATING CYCLIC STRUCTURES

V. Elchuri
Aerostructures, Arlington, Virginia

A. Michael Gallo
Bell Aerospace Textron, Buffalo, New York

SUMMARY

Static aerothermoelastic design/analysis of axial-flow compressors, modal flutter analysis of axial-flow turbomachines, forced vibration analysis of rotating cyclic structures and modal flutter analysis of advanced turbopropellers with highly swept blades are four new capabilities developed and implemented in NASTRAN Level 17.7. The purpose of this paper is to briefly discuss the contents, applicability and usefulness of these capabilities which were developed and documented under the sponsorship of NASA's Lewis Research Center. Overall flowcharts and selected examples are also presented.

INTRODUCTION

Impellers, propellers, fans and bladed discs of turbomachines are some examples of structures that exhibit rotational cyclic symmetry in their geometric, material and constraint properties. The problem of statics and dynamics including aeroelastic analyses of such structures can be collectively and generally stated by the following equations of motion:

$$[M^n]\{\ddot{u}^n\} + \left[[B^n] + 2\Lambda[B_1^n]\right]\{\dot{u}^n\}$$
$$+ \left[[K^e] + [K^d] - \Lambda^2[M_1^n]\right]\{u^n\} - [Q^n]\{u^n\}$$
$$= \{P^n\}^{aero.} + \{P^n\}^{non-aero.} - [M_2^n]\{\ddot{R}_0\} , \tag{1}$$

$$u^n_{side\ 2} = u^{n+1}_{side\ 1} , \tag{2}$$

where n = 1, 2, ..., N.

The retention and interpretation of the terms of the above equations vary with the specific analysis being considered, and, as such, are discussed further under appropriate sections. A generic statement of the equations of motion is used to illustrate a logical approach to the solution of the problems of rotating cyclic structures. References 1 through 7 present extensive details of all the analyses discussed in this paper.

All capabilities described in this paper address tuned cyclic structures, i.e., structures composed of cyclic sectors identical in mass, stiffness, damping and constraint properties.

SYMBOLS

B   viscous damping matrix

B_1 Coriolis acceleration coefficient matrix

K   stiffness matrix

k   circumferential harmonic index

M   mass matrix

M_1 centripetal acceleration coefficient matrix

M_2 base acceleration coefficient matrix

N   number of rotationally cyclic sectors in complete structure

P   load vector

Q   aerodynamic matrix

$\ddot{R}_0$ base acceleration vector

u   displacement vector

Ω rotational velocity

Superscripts:

d   differential

e   elastic

n   cyclic sector number

STATIC AEROTHERMOELASTIC "DESIGN/ANALYSIS"

OF AXIAL-FLOW COMPRESSORS

Problem Definition

At any operating point under steady-state conditions, the rotors and stators of axial-flow compressors are subjected to aerodynamic pressure and temperature loads. The rotors, in addition, also experience centrifugal loads. These loads result in deformation of the elastic structure, which, in turn influences the aerodynamic loads. These interactive loads and responses arise fundamentally from the elasticity of the structure and determine the performance of the "flexible" turbomachine. For a given flow rate and rotational speed, the elastic deformation implies a change in the operating point pressure ratio.

The process of arriving at an "as manufactured" blade shape to produce a desired (design point) pressure ratio (given the flow rate and rotational speed) is herein termed the "design" problem of axial-flow compressors. The subsequent process of analyzing the performance of "as manufactured" geometry at off-design operating conditions including the effects of flexibility is termed the "analysis" problem of axial-flow compressors.

The capability also determines:

1) the steady-state response of the structure (displacements, stresses, reactions, etc.), and

2) a differential stiffness matrix for use in subsequent modal, flutter and dynamic response analyses.

Formulation

Referring to equation 1, the degrees of freedom, u, are the steady-state displacements expressed in body-fixed global coordinate systems. The steady-state aerodynamic pressure and thermal loads, $P^{aero.}$, are computed using a three-dimensional aerodynamic theory for axial-flow compressors (Ref. 8). K^e , K^d and $P^{non-aero.}$ are the other terms retained in the analysis.

All cyclic sectors of the structure are assumed to respond identically, implying a zeroth circumferential harmonic distribution. Therefore only one rotationally cyclic sector is modelled and analyzed (Figure 1), with the intersegment boundary conditions (equation 2) imposed via MPC equations.

NASTRAN Implementation

A new rigid format, DISP APP RF 16, has been developed for the solution of "design/analysis" problems of axial-flow compressors. The rigid format features new functional modules, bulk data cards and parameters. The computer code of Reference 8, with minor changes, has been adapted for NASTRAN in a new functional module ALG (Aerodynamic Load Generator). The NASTRAN Static Analysis with Differential Stiffness rigid format, DISP APP RF 4, has been modified to include the interactive effects of aerodynamic loads along with the effects due to centrifugal loads.

A simplified flowchart of the rigid format is shown in Figure 2.

MODAL FLUTTER ANALYSIS OF AXIAL-FLOW TURBOMACHINES

Problem Definition

Unstalled flutter boundaries of axial-flow turbomachines (compressors and turbines) can be determined using this capability. The stability of a given operating point of a given stage of the turbomachine is investigated in terms of modal families of several circumferential harmonic indices considered one at a time.

Formulation

Considering the degrees of freedom, u, in equation 1 to represent the vibratory displacements superposed on the steady-state deformed shape of the rotor or stator, the natural modes and frequencies of the tuned cyclic structure can be grouped in terms of several uncoupled sets, with each set corresponding to a permissible circumferential harmonic index, k. Except for k = 0 and N/2 (even N), the cyclic modes can further be separated into cosine and sine component modes (Ref. 9). For tuned cyclic structures, the modal flutter problem can be posed in terms of either cosine or sine modes with identical results (Ref. 2). For k = 0 and N/2, only cosine modes are defined. In the present capability, this selection of mode type is provided as a user option.

B_1 , M_1 and the right hand side terms from equation 1 are omitted for this flutter capability.

For the computation of the generalized aerodynamic loads matrix, Q, two two-dimensional cascade unsteady subsonic and supersonic aerodynamic theories of References 10 and 11 are used in a strip theory manner from the blade root to the tip as shown in Figure 1. Based on the relative flow Mach number at a given streamline, either the subsonic or the supersonic theory is used. For the user specified transonic Mach number range, the aerodynamic matrix terms are interpolated from adjacent streamline values.

240

NASTRAN Implementation

A new rigid format, AERO APP RF 9, has been developed for the cyclic modal flutter analysis of axial-flow turbomachines. The rigid format integrates the cyclic modal computations for a given circumferential harmonic index with currently available flutter solution techniques in NASTRAN. The unsteady aerodynamic theories have been incorporated in the existing functional module AMG (Aerodynamic Matrix Generator). New bulk data cards have been designed to meet specific needs of this flutter capability.

A flowchart outlining the rigid format is shown in Figure 3.

FORCED VIBRATION ANALYSIS OF ROTATING CYCLIC STRUCTURES

Problem Definition

Figure 4 illustrates the problem by considering a 12-bladed disc as an example. The bladed disc consists of twelve identical $30°$ segments. The disc rotates about its axis of symmetry at a constant angular velocity. The axis of rotation itself is permitted to oscillate translationally in any given inertial reference, thus introducing inertial loads. In addition, the bladed disc is allowed to be loaded with sinusoidal or general periodic loads moving with the structure. Under these conditions, it is desired to determine the dynamic response (displacements, accelerations, stresses, etc.) of the bladed disc.

Formulation

The degrees of freedom, u, in equation 1 define the vibratory displacements due to the vibratory excitation provided by the directly applied loads and the inertial loads due to the acceleration of the axis of rotation ("base" acceleration). These displacements are measured from the steady-state deformed shape of the rotating structure, and are expressed in body-fixed global coordinate systems. The non-aerodynamic loads, $P^{non-aero.}$, can either be sinusoidal loads specified as functions of frequency, or general periodic loads specified as functions of time. Physical loads on various segments or their circumferential harmonic components can be specified. The base acceleration, $\ddot{R}_0$, is noted as a function of frequency. All but Q and $P^{aero.}$ terms are retained in the analysis.

Based on the circumferential harmonic content of the excitation, the user can specify a range of such harmonic indices, k_{min} to k_{max}, for solution. Although the user models only one cyclic sector, results can be obtained for the complete structure.

241

NASTRAN Implementation

The Direct Frequency and Random Response rigid format, DISP APP RF 8, and the Static Analysis with Cyclic Symmetry rigid format, DISP APP RF 14, have been suitably merged with extensive modifications, in the form of a package of ALTERs to the former rigid format. New functional modules for Coriolis, centripetal and base acceleration terms, bulk data parameters, and varied use of existing functional modules are some of the features of this alter package. Figure 5 presents a schematic flowchart of this forced vibration analysis capability for rotating cyclic structures.

Illustrative Example

This example illustrates the out-of-plane displacement response of grid points 8 and 18 of the 12-bladed disc of Figure 4, when the disc, rotating at 600 rps, is simultaneously subjected to lateral base accelerations of $\ddot{Y}_{inertial} = 1000 \cos 2\pi f t$ in/sec^2 and $\ddot{Z}_{inertial} = 500 \cos 2\pi f t$ in/sec^2, $1700 \leq f \leq 1920$ Hz. Details of the bladed disc are given in Table 1. Table 2 lists the first few natural frequencies of the bladed disc for k=0,1 and 2. Although the frequency band of input base acceleration is 1700-1920 Hz., the rotation of the disc at 600 Hz. splits the input bandwidth into two effective bandwidths: (1700-600) = 1100 to (1920-600) = 1320 Hz., and (1700+600) = 2300 to (1920+600) = 2520 Hz. Since the lateral base acceleration excites only k = 1 modes, the only k = 1 mode in the effective bandwidths is the first torsional mode of the blade, with the disc practically stationary (2460 Hz., k=1, Table 2). This is shown by the out-of-plane displacement magnitudes of grid points 18 (blade) and 8 (disc) in Figure 6. For brevity, only the magnitude of the cosine component of the k = 1 response is shown.

MODAL FLUTTER ANALYSIS OF ADVANCED TURBOPROPELLERS

Problem Definition

Advanced turbopropellers are multi-bladed propellers with thin blades of low aspect ratio and varying sweep (Figure 7). The problem of determining the unstalled flutter boundaries of such propellers is identical to that discussed earlier for the axial-flow turbomachines with the exception that the effects of blade sweep and its spanwise variation are taken into account in computing the generalized unsteady aerodynamic loads. From a structural viewpoint, if the propeller hub is considered to be relatively much stiffer than the blades, the blades can be treated independently, and only the k = 0 modes need be considered for flutter analysis.

Formulation

This is the same as that for the axial-flow turbomachines, except that the subsonic unsteady aerodynamic theory of Ref. 10 has been modified to include the effects of blade sweep and its radial variability (Ref. 6).

NASTRAN Implementation

The functional module AMG has been modified to include the subsonic unsteady aerodynamic theory with sweep effects. This option can be invoked by including the NASTRAN System (76) = 1 card in front of the Executive Control Deck for the AERO APP RF 9. The STREAML2 bulk data card developed for turbomachine flutter analysis has been modified to also accept turboprop aerodynamic data.

Illustrative Example

A comparison of the predicted flutter boundary using this NASTRAN capability and that obtained from NASA Lewis Research Center's wind tunnel test results is shown in Figure 8. The first six $k = 0$ modes were included for flutter analysis of the 10-bladed advanced turboprop. The hub of the propeller was assumed to be rigid compared to its flexible blades.

CONCLUDING REMARKS

A brief account of four new capabilites developed and implemented in NASTRAN Level 17.7 has been given in terms of problem definition, formulation, NASTRAN implementation and some selected examples. Details of all of these capabilities can be found in References 1 through 7.
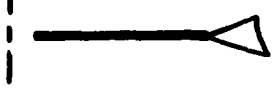
REFERENCES

1. Elchuri, V., Smith, G.C.C., Gallo, A.M., and Dale, B.J., "
   NASTRAN Level 16 Theoretical, User's, Programmer's and
   Demonstration Manual Updates for Aeroelastic Analysis of Bladed
   Discs, " NASA CRs 159823-159826, March 1980.

2. Smith, G.C.C., and Elchuri, V., " Aeroelastic and Dynamic
   Finite Element Analyses of a Bladed Shrouded Disc, " Final
   Technical Report, NASA CR 159728, March 1980.

3. Gallo, A.M., Elchuri, V., and Skalski, S.C., "
   Bladed-Shrouded-Disc Aeroelastic Analyses: Computer Program
   Updates in NASTRAN Level 17.7, " NASTRAN Manuals Updates, NASA CR
   165428, December 1981.

4. Elchuri, V., and Smith, G.C.C., " Finite Element Forced
   Vibration Analysis of Rotating Cyclic Structures, " Final
   Technical Report, NASA CR 165430, December 1981.

5. Elchuri, V., Gallo, A.M., and Skalski, S.C., " Forced
   Vibration Analysis of Rotating Cyclic Structures in NASTRAN, "
   NASTRAN Manuals, NASA CR 165429, December 1981.

6. Elchuri, V., and Smith, G.C.C., " NASTRAN Flutter Analysis of
   Advanced Turbopropellers, " Final Technical Report, NASA CR
   167926, April 1982.

7. Elchuri, V., Gallo, A.M., and Skalski, S.C., " NASTRAN
   Documentation for Flutter Analysis of Advanced Turbopropellers, "
   NASTRAN Manuals, NASA CR 167927, April 1982.

8. Hearsey, R.M., " A Revised Computer Program for Axial
   Compressor Design, " ARL-75-0001, vol.I and II, Wright-Patterson
   AFB, January 1975.

9. NASTRAN Level 17.6 Theoretical Manual, NASA SP 221 (05),
   October 1980.

10. Rao, B.M., and Jones, W.P., " Unsteady Airloads for a Cascade
    of Staggered Blades in Subsonic Flow, " 46th Propulsion
    Energetics Review Meeting, Monterey, California, September 1975.

11. Goldstein, M.E., Braun, Willis, and Adamczyk, J.J., "Unsteady
    Flow in a Supersonic Cascade with Strong In-Passage Shocks,"
    Journal of Fluid Mechanics, vol. 83, part 3, December
    1977, pp. 569-604.

TABLE 1. GEOMETRIC DETAILS OF 12-BLADED DISC

Diameter at blade tip	= 19.4 in.
Diameter at blade root	= 14.2 in.
Shaft diameter	= 4.0 in.
Disc thickness	= 0.25 in.
Blade thickness	= 0.125 in.
Young's modulus	= 30.0×10^6 lbf/in^2
Poisson's ratio	= 0.3
Material density	= 7.4×10^{-4} lbf-sec^2/in^4
Uniform structural damping (g)	= 0.02

TABLE 2: BLADED-DISC NATURAL FREQUENCIES

Frequency (Mode No.), Hz.			Mode Description
k = 0*	k = 1	k = 2	
214 (1)	208 (1)	242 (1)	
591 (2)	594 (2)	622 (2)	
1577 (3)	1633 (3)	1814 (3)	
2468 (5)**	2460 (4)	2433 (4)	

* k is the circumferential harmonic index

** Mode No. 4 for k = 0 at 1994 Hz represents an in-plane shear mode not excited by the applied forces.
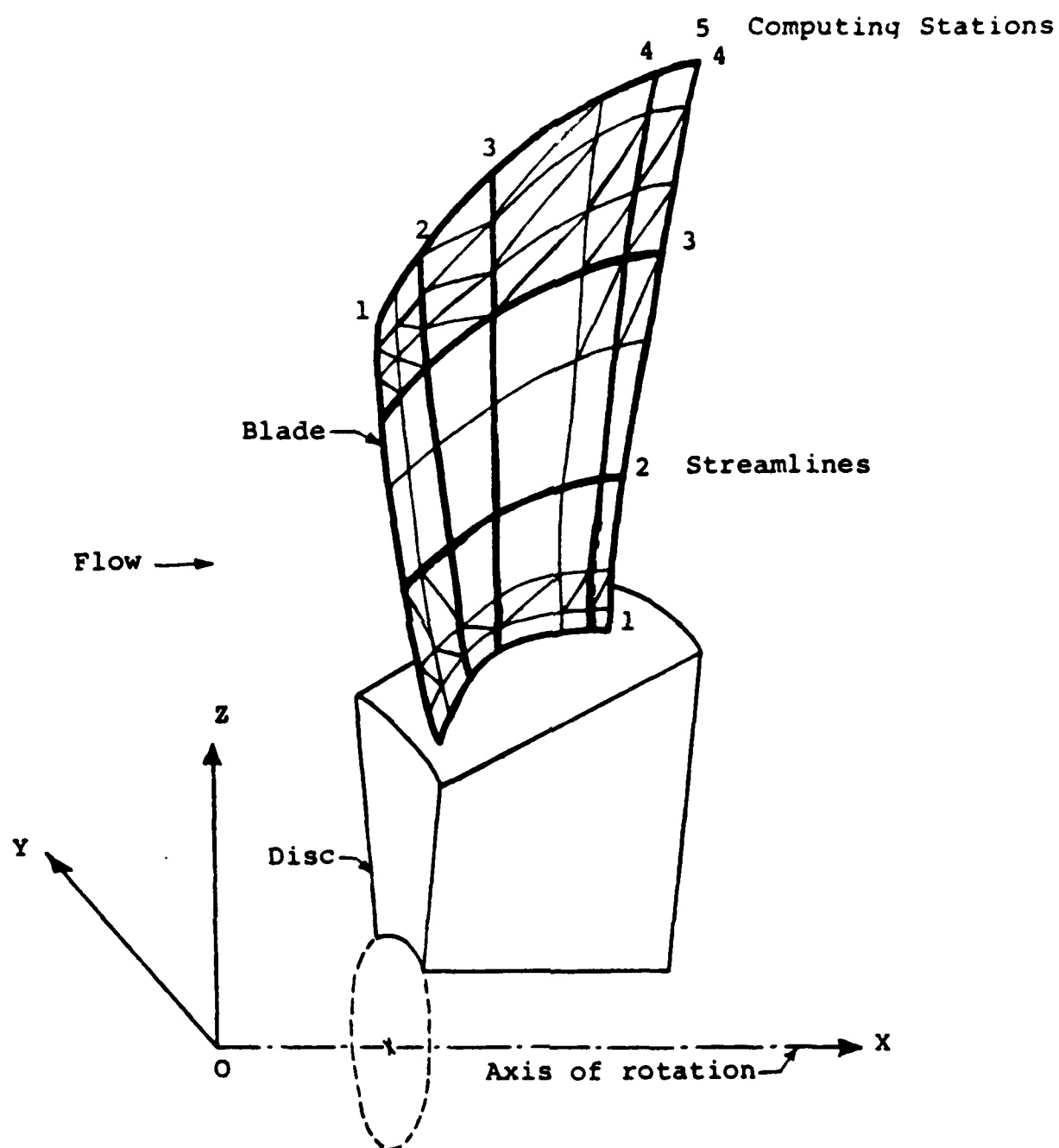
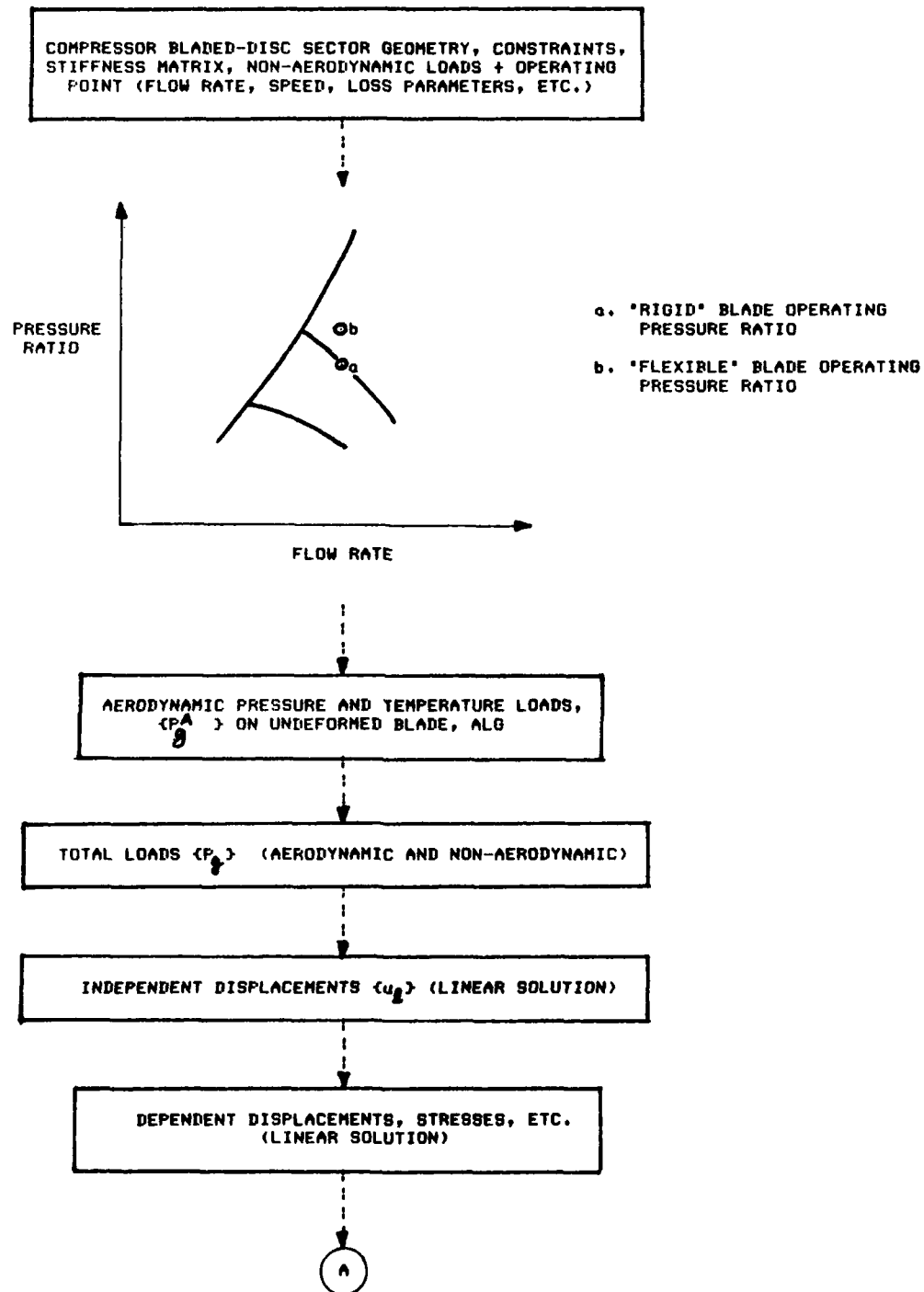FIGURE 1.   ROTATIONAL CYCLIC SECTOR OF A BLADED DISC

FIGURE 2. SIMPLIFIED PROBLEM FLOW FOR STATIC AEROTHERMOELASTIC
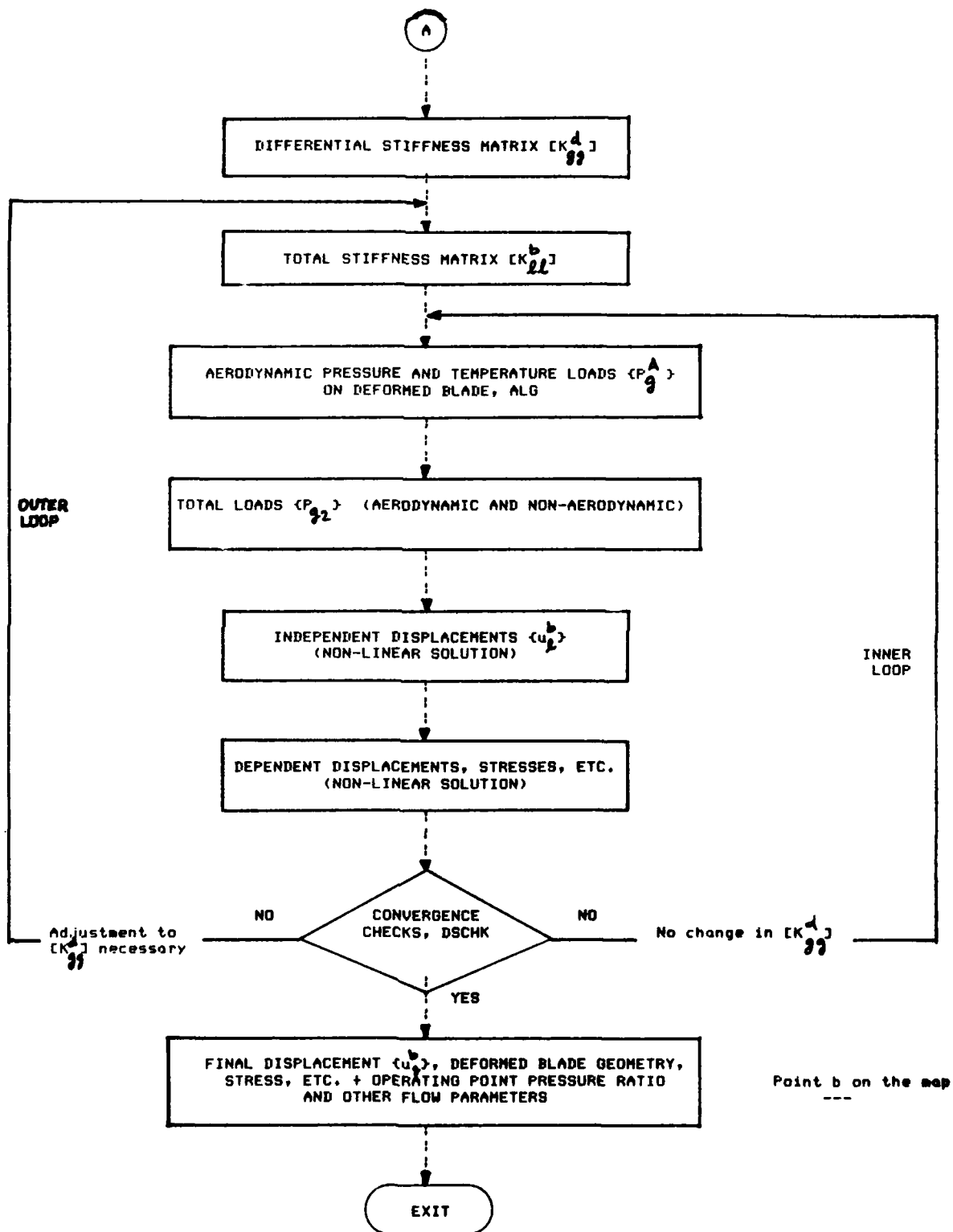'DESIGN/ANALYSIS' RIGID FORMAT FOR AXIAL FLOW COMPRESSORS
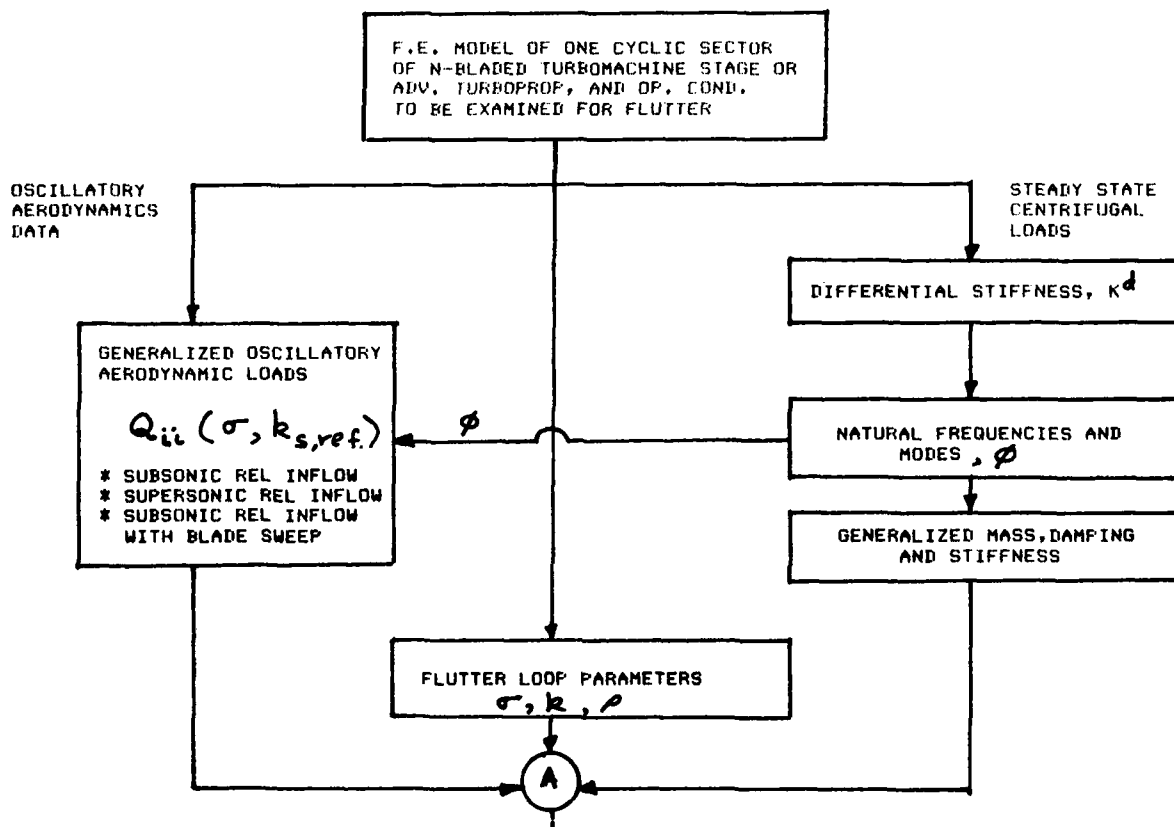
247

FIGURE 2. (Concluded)

248

FIGURE 3. OVERALL FLOWCHART OF CYCLIC MODAL FLUTTER ANALYSIS RIGID FORMAT
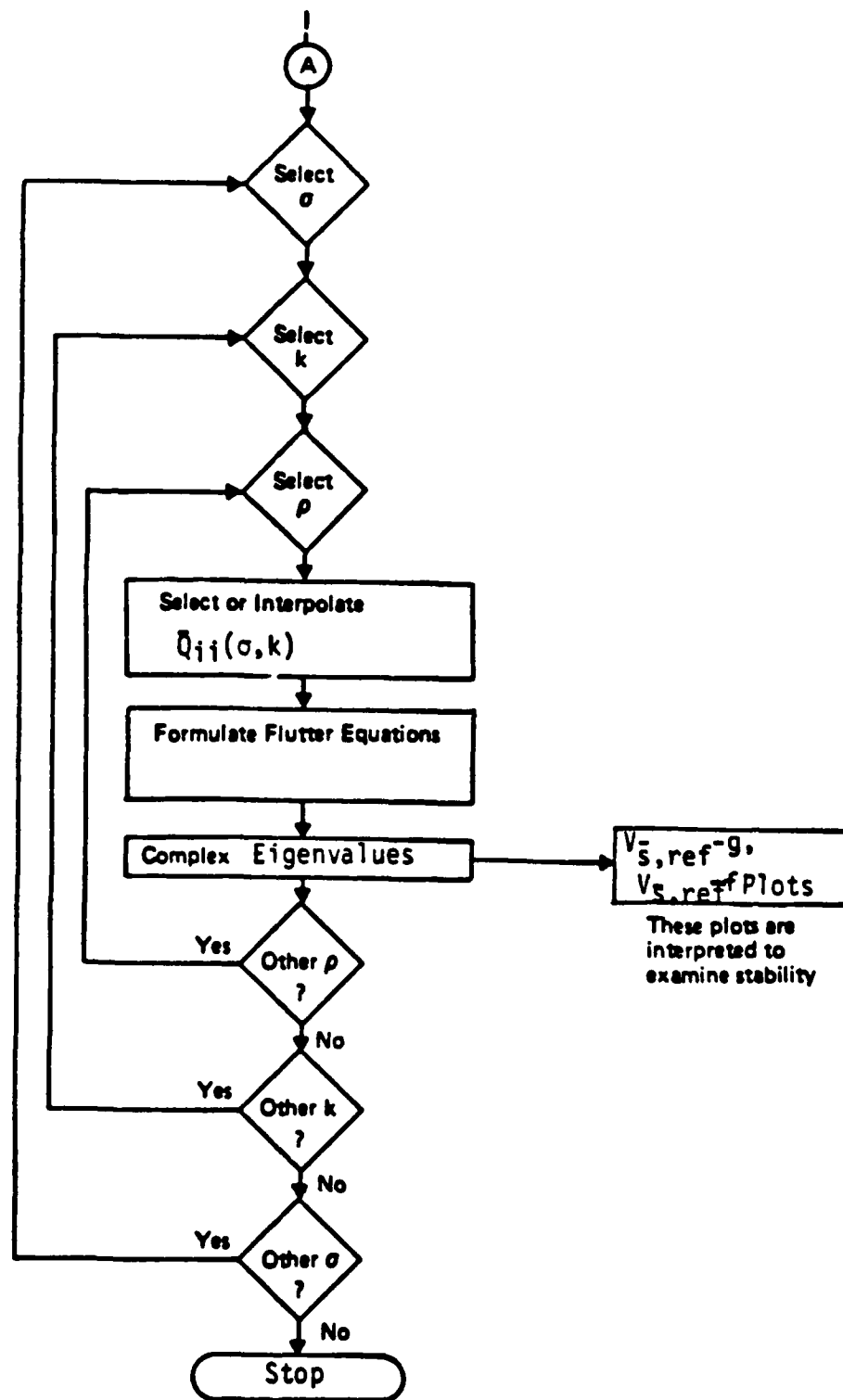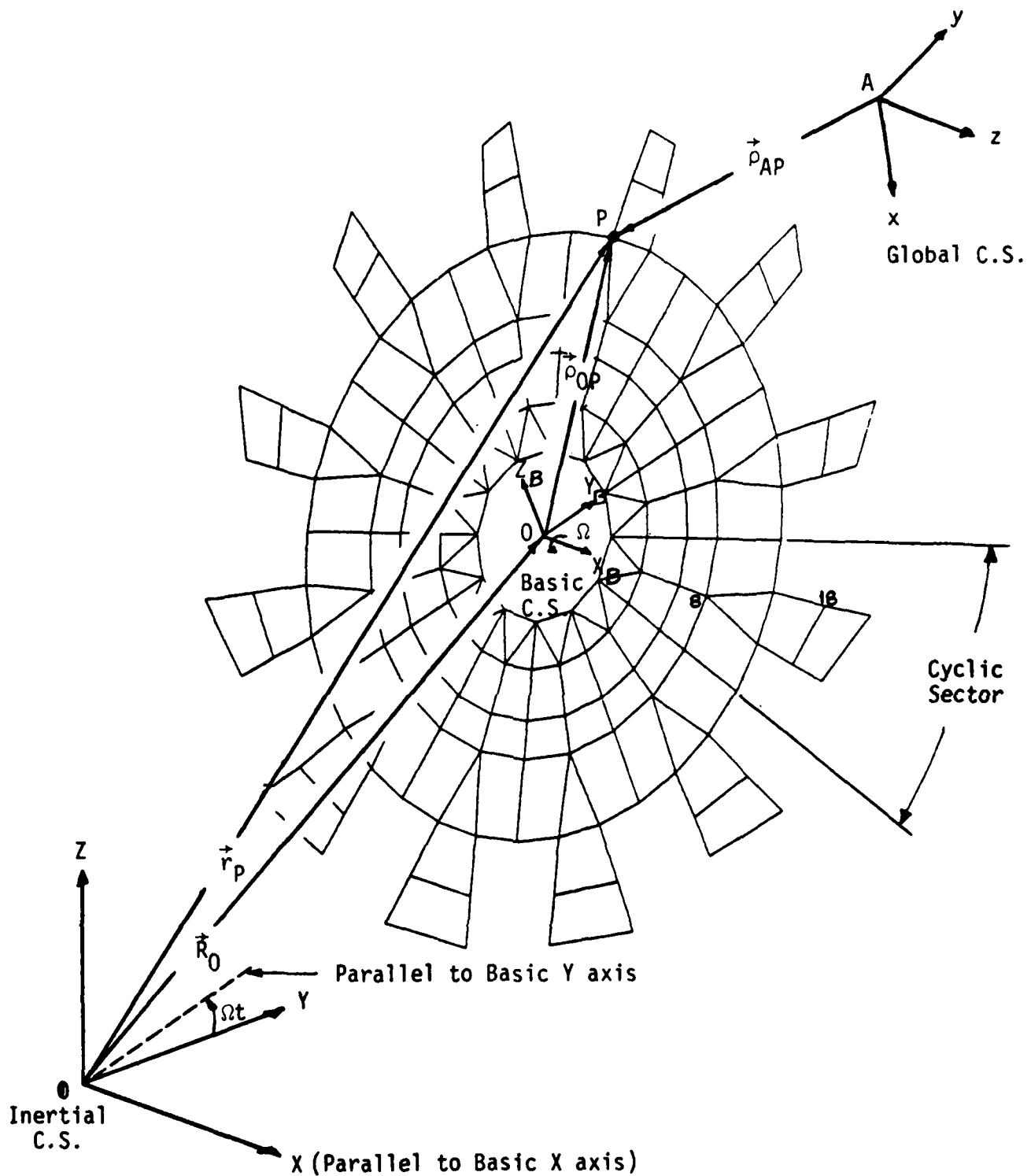FOR TURBOMACHINES AND ADVANCED TURBOPROPELLERS

FIGURE 3. (Concluded)

250

$\hat{I}, \hat{J}, \hat{K}$ Unit vectors along Inertial XYZ axes

$\hat{I}_B, \hat{J}_B, \hat{K}_B$ Unit vectors along Basic $X_B Y_B Z_B$ axes

$\hat{i}, \hat{j}, \hat{k}$ Unit vectors along Global xyz axes

**FIGURE 4.   BLADED DISC EXAMPLE FOR FORCED VIBRATION
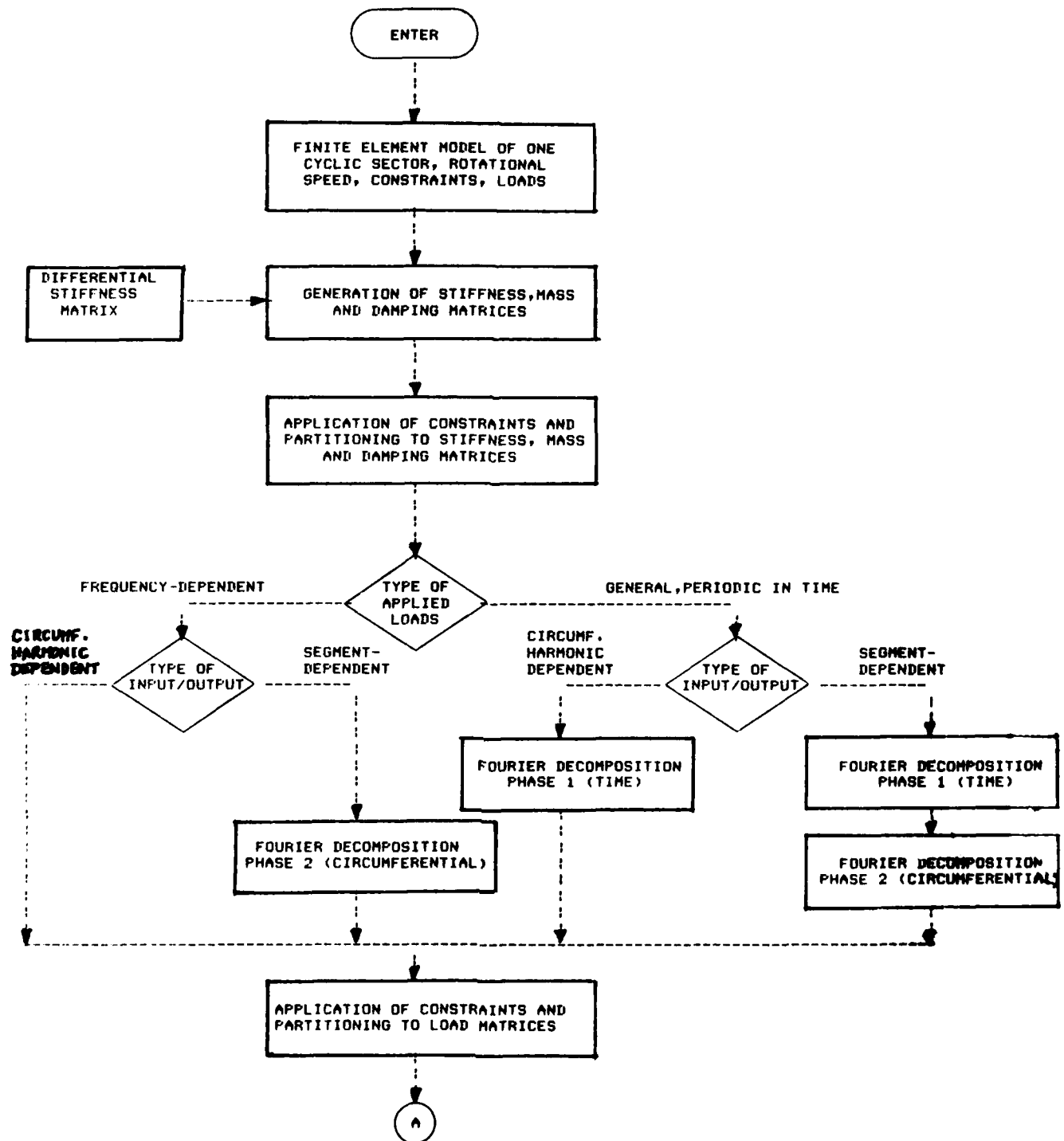ANALYSIS OF ROTATING CYCLIC STRUCTURES**

251

FIGURE 5 - OVERALL FLOWCHART OF FORCED VIBRATION ANALYSIS OF ROTATING CYCLIC STRUCTURES

252

SELECTION OF
CIRCUMF. HARMONIC
INDEX k
$k_{min} \leqslant k \leqslant k_{max}$

APPLICATION OF INTERSEGMENT COMPATIBILITY
CONSTRAINTS TO STIFFNESS, MASS, DAMPING
AND LOAD MATRICES

SOLUTION OF INDEPENDENT
HARMONIC DISPLACEMENTS

INCREMENT k BY 1
$k > k_{max}$?

NO

YES

RECOVERY OF SEGMENT-DEPENDENT INDEPENDENT
DISPLACEMENTS (INVERSE PHASE 2, IF NECESSARY)

RECOVERY OF DEPENDENT DISPLACEMENTS

OUTPUT REQUESTS FOR DISPLACEMENTS,
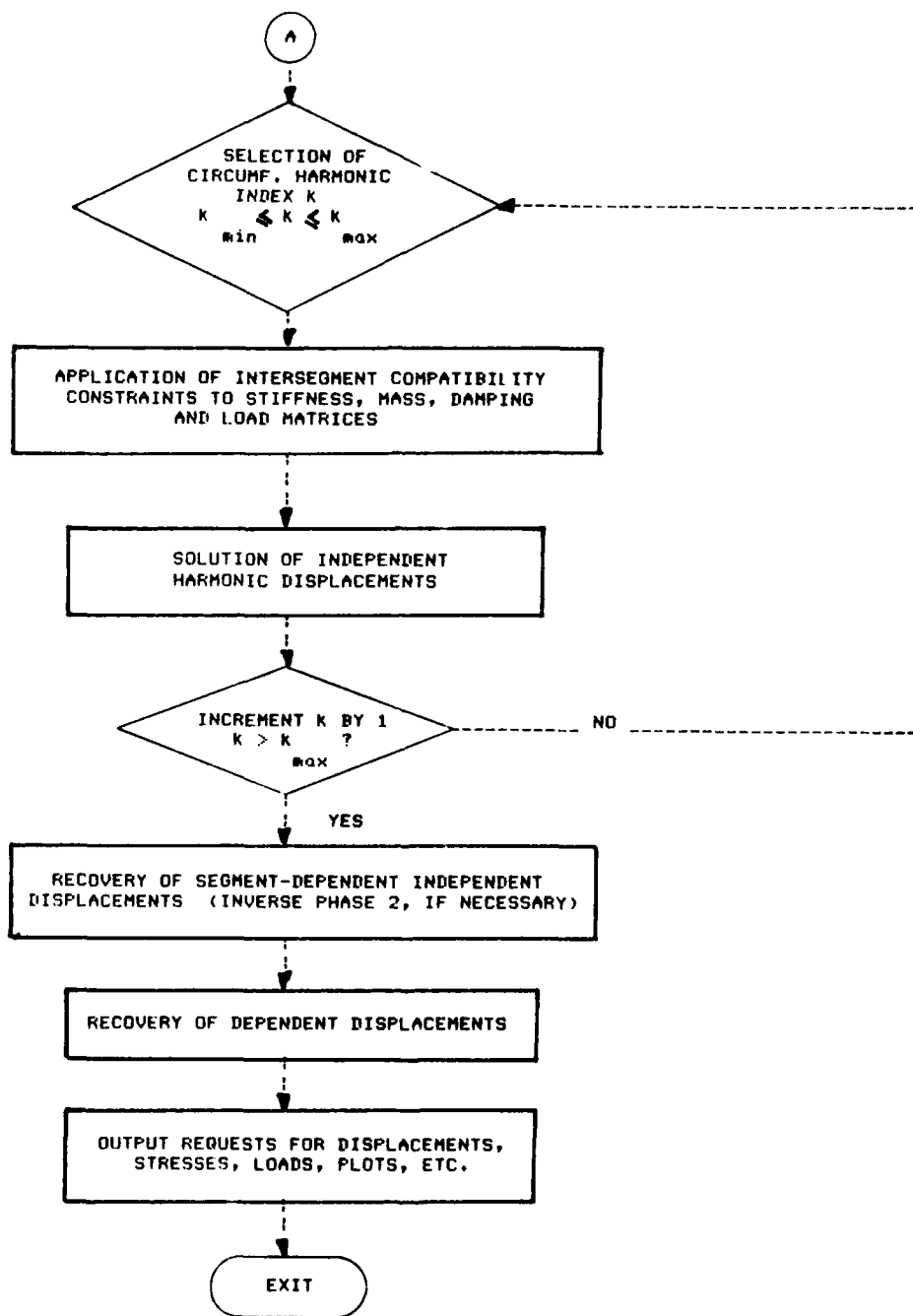STRESSES, LOADS, PLOTS, ETC.

EXIT

FIGURE 5 - (Concluded)

253

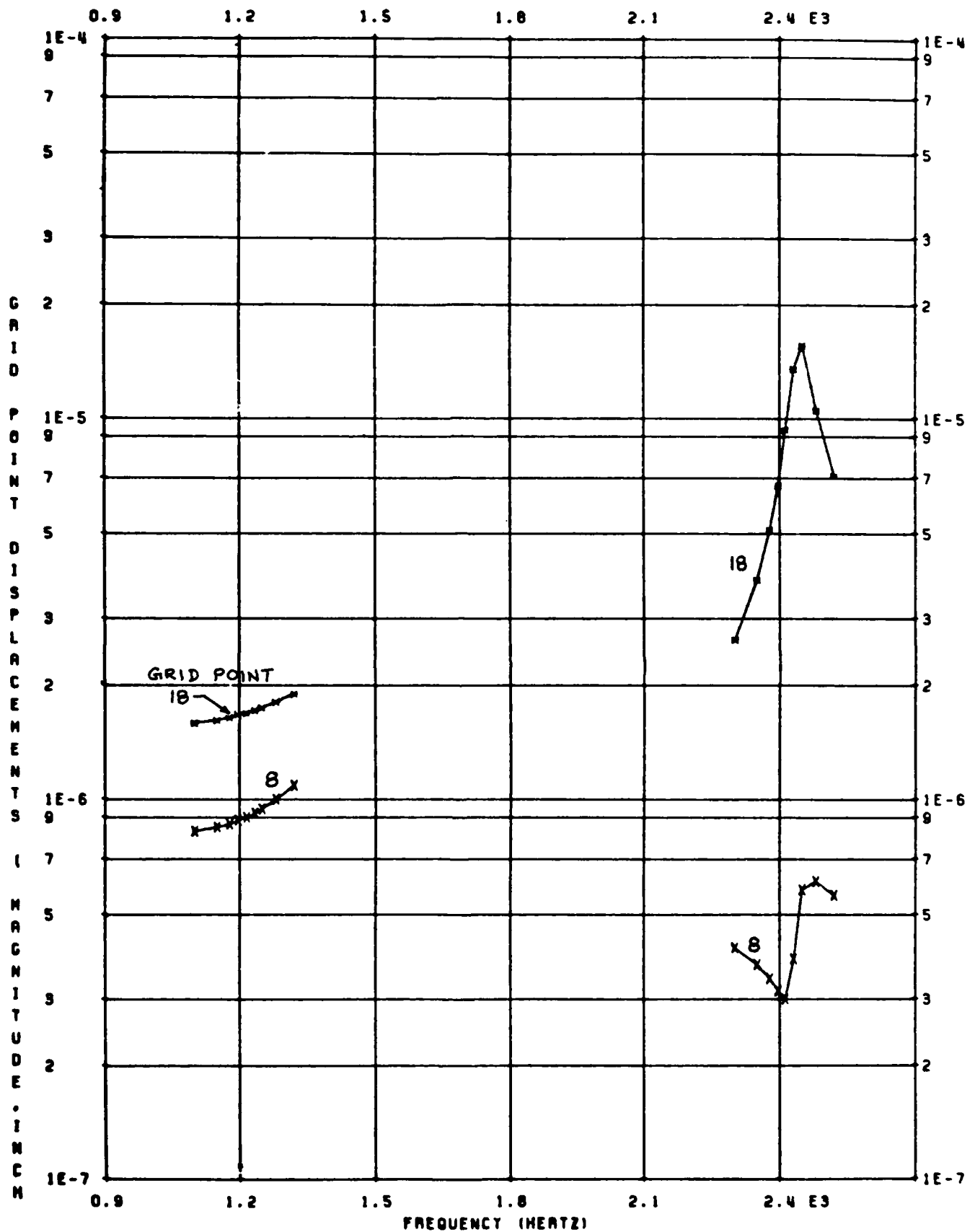·FIGURE 6.   k=1c DISPLACEMENT RESPONSE OF 12-BLADED DISC
TO LATERAL BASE ACCELERATION EXCITATION

FIGURE 7.   AN ADVANCED TURBOPROPELLER
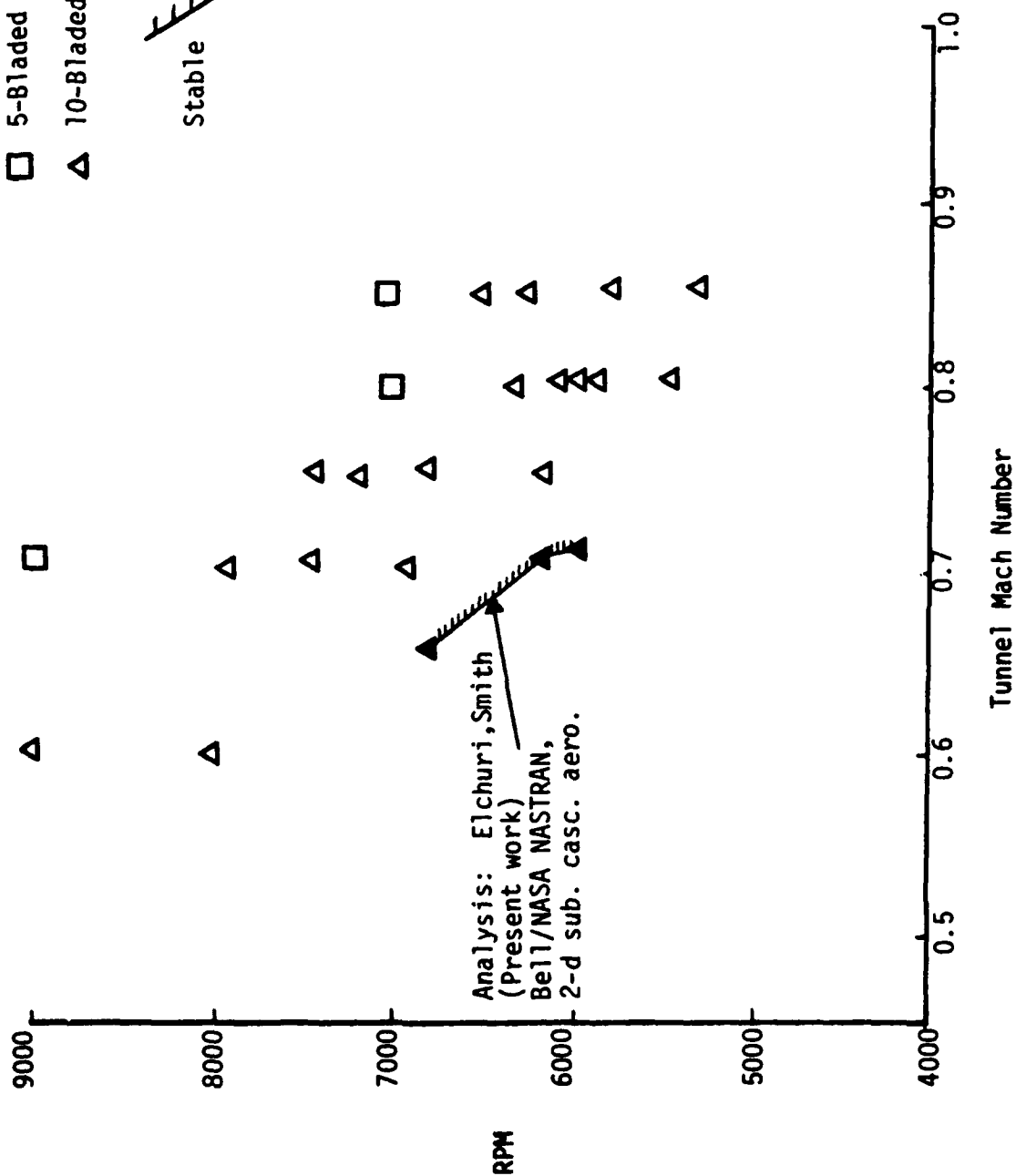
FIGURE 8.   TURBOPROP FLUTTER SUMMARY

1. Report No. NASA CP-2328	2. Government Accession No.	3. Recipient's Catalog No.
4. Title and Subtitle Twelfth NASTRAN® Users' Colloquium		5. Report Date August 1984
		6. Performing Organization Code
7. Author(s)		8. Performing Organization Report No.
9. Performing Organization Name and Address COSMIC, NASA's Computer Software Management 　　　　　　and Information Center The University of Georgia Athens, GA 30602		10. Work Unit No.
		11. Contract or Grant No.
12. Sponsoring Agency Name and Address National Aeronautics and Space Administration Washington, D.C. 20546		13. Type of Report and Period Covered Conference Publication
		14. Sponsoring Agency Code

15. Supplementary Notes

Available from COSMIC, Athens, GA   30602

16. Abstract

This publication is the proceedings of a colloquium, and it contains technical papers
contributed during the Twelfth NASTRAN® Users' Colloquium held in Orlando, Florida
on May 7-11, 1984. The authors review general application of finite element
methodology and the specific application of the NASA Structural Analysis System,
NASTRAN, to a variety of static and dynamic structural problems.

17. Key Words (Suggested by Author(s)) NASTRAN Structural Analysis Structures Finite Element Analysis Colloquium	18. Distribution Statement Unclassified – Unlimited Subject Category 39		
19. Security Classif. (of this report) Unclassified	20. Security Classif. (of this page) Unclassified	21. No. of Pages 256	22. Price -no charge-